UNIVERSITY OF CALIFORNIA, SAN DIEGO

Iron and Copper Organic Complexation in Marine Systems: Detection of Multiple Ligand Classes via Electrochemistry

A dissertation submitted in partial satisfaction of the requirements for the degree Doctor of Philosophy

in

Oceanography

by

Randelle May Bundy

Committee in charge:

Professor Katherine Barbeau, Chair
Professor Seth Cohen
Professor Mike Landry
Professor Todd Martz
Professor Brian Palenik

2014

The Dissertation of Randelle May Bundy is approved, and it is acceptable in quality and form for publication on microfilm and electronically:

Chair

University of California, San Diego

2014

Dedication

For my family;

Mom, Dad, Mallory and Michael

Epigraph

Twenty years from now you will be more disappointed by the things you didn't do than by the ones you did. So throw off the bowlines, sail away from the safe harbor, catch the trade winds in your sails. Explore. Dream. Discover.

Mark Twain

Table of Contents

List of Figures

List of Tables

Acknowledgements

I would like to acknowledge Professor Katherine Barbeau for her endless support as chair of my committee. Her guidance as a mentor has been invaluable. I would also like to thank my committee members for their support and advice while writing my dissertation: Mike Landry, Brian Palenik, Todd Martz, and Seth Cohen.

Chapter 2, in full, is a reprint of the material as it appears in Deep Sea Research II: Topical Studies in Oceanography 2013. Bundy, R.M., Barbeau, K.A., Buck, K.N., Deep Sea Research Part II: Topical Studies in Oceanography, Volume 90, Pages 134-146 2013. The dissertation author was the primary investigator and author of this paper.

Chapter 3, in full, is a reprint of the material as it appears in Limnology and Oceanography 2014. Bundy, R.M., Barbeau, K.A., Biller, D.V., Buck, K.N., Bruland, K.W., Limnology and Oceanography, Volume 59, Issue 3, Pages 769-787 2014. The dissertation author was the primary investigator and author of this paper.

Chapter 4, in full, is under review in Marine Chemistry. Bundy, R.M., Abdulla, H.A, Hatcher, P., Biller, D.V., Buck, K.N., Barbeau, K.A, Marine Chemistry 2014. The dissertation author was the primary investigator and author of this paper.

Chapter 5, in full, will be submitted to Marine Chemistry. Bundy, R.M., Barbeau, K.A., Carter, M., Jiang, M. Understanding the sources and sinks of iron-binding ligands in the southern California Current Ecosystem: A mechanistic study. The dissertation author was the primary investigator and author of this paper.

Vita

2008	Bachelor of Science, University of California, San Diego
2013	Master of Science, University of California, San Diego
2008-2014	Research Assistant, University of California, San Diego
2014	Doctor of Philosophy, University of California, San Diego

Publications

Bundy, R.M., Abdulla, H.A, Hatcher, P., Biller, D.V., Buck, K.N., Barbeau, K.A. Submitted. Iron-binding ligands and humic substances in the San Francisco Bay estuary and estuarine-influenced shelf regions of coastal California. Marine Chemistry. In review.

Bundy, R.M., Barbeau, K.A., Biller, D.V., Buck, K.N., Bruland, K.W. 2014. Distinct pools of dissolved iron-binding ligands in the surface and benthic boundary layer of the California Current. Limnology and Oceanography. Volume 59. Issue 3. Pages 769-787. doi: 10.4319/lo.2014.59.3.0769

Bundy, R.M., Barbeau, K.A., Buck, K.N. 2013. Sources of strong copper-binding ligands in Antarctic Peninsula surface waters. Deep Sea Research Part II: Topical Studies in Oceanography. Volume 90. Pages 134-146. ISSN 0967-0645. http://dx.doi.org/10.1016/j.dsr2.2012.07.023

Fields of Study

Major Field: Oceanography

Studies in Marine Chemistry
Professor Katherine Barbeau

Abstract of the Dissertation

Iron and Copper Organic Complexation in Marine Systems: Detection of Multiple Ligand Classes via Electrochemistry

by

Randelle May Bundy

Doctor of Philosophy in Oceanography

University of California, San Diego, 2014

Professor Katherine Barbeau, Chair

Iron and copper are essential bioactive elements in the marine environment, but they have a complex chemical speciation dominated by a heterogeneous mixture of organic metal-ligand complexes. Numerous analytical constraints complicate the direct chemical characterization of these species, thus this work seeks to expand upon existing indirect electrochemical methods for examining copper and iron organic complexes in seawater. A multiple analytical window (MAW) electrochemical approach, which enables the detection of a broad spectrum of ligands, is applied in new regions of the ocean for copper and, for the first time, in studies of iron speciation.

Chapter 2 describes the first application of the MAW electrochemical technique for copper speciation in the open ocean. Copper-binding ligands were measured in four surface water masses of the Antarctic Peninsula region, and each water mass was shown to contain distinct pools of ligands.

Chapters 3 and 4 focus on applying the MAW electrochemical method to iron-binding ligands. In Chapter 3, iron-binding ligands were measured in central California coastal waters in the surface and benthic boundary layer (BBL), in order to validate the MAW approach for iron speciation in contrasting chemical regimes. Iron-binding ligands in surface waters were found to be chemically distinct from the BBL ligand pool. Chapter 4 explores San Francisco Bay as a source of iron-binding ligands to coastal California waters. Scavenging in the estuary caused the concentration of weaker ligands to decrease with salinity, while the strongest ligands remained largely resistant to flocculation.

Chapter 5 applies the MAW electrochemical technique in experimental studies and water column profiles to interpret mechanisms of in-situ iron-binding ligand cycling in the southern California Current. Photochemical processes were found to dominate in near surface waters, while biological processes controlled ligand distributions in deeper waters.

Overall, the simultaneous detection of multiple ligand classes has contributed significantly to our existing knowledge of metal ligand sources and sinks, and the unique chemical environments in which phytoplankton are utilizing trace nutrients.

Chapter 1

Introduction

1. Background

Trace metals in the marine environment such as copper (Cu) and iron (Fe) are important nutrients affecting the growth of microorganisms. Both Cu and Fe are co-factors in several enzymes needed for key cellular process such as photosynthesis and nitrate reduction (Morel and Price, 2003). However, inorganic Cu and Fe are prone to scavenging in oxygenated seawater (Turner et al., 1981), and thus the dissolved forms of these metals are often scarce in large areas of the ocean. Although the inorganic forms of Cu and Fe have a propensity to precipitate in seawater, these metals are highly soluble when they are associated with organic ligands. In fact, approximately 99% of the dissolved Cu and Fe in seawater is bound to organic metal-binding ligands (Campos and van den Berg, 1994; Rue and Bruland, 1995; Wu and Luther, 1995). These ligands are part of a highly heterogeneous pool of carbon in the ocean, which has traditionally been difficult to characterize due to the wide range of size classes and reactivities (Benner et al., 1992). Isolating organic metal-binding ligands directly from this complex matrix is a daunting task; they are present in concentrations which are orders of magnitude less than the bulk organic carbon pool (nmol L^{-1} compared to μmol L^{-1}, respectively) and likely encompass a range of binding strengths and chemical compositions.

The scarcity and heterogeneity of Cu and Fe-ligand organic molecules is an interesting predicament for both bacteria and phytoplankton in the ocean. Despite the importance of Cu and Fe for growth, it is still relatively uncertain how microorganisms access trace metals from such complex molecules. It appears that some phytoplankton may reduce the metal from the organic complex prior to uptake via cell-surface reductases (Shaked et al., 2005). However, some strains of bacteria appear to be

able to take up entire metal-organic complexes (Butler, 1998). In general, many organic complexes appear to be bioavailable to microorganisms, though the degree of availability likely depends on the type of metal-ligand complex (*e.g.*, Hutchins et al., 1999). However, the chemical identity of these ligands is largely unknown (Vraspir and Butler, 2009), which complicates our ability to understand their uptake and bioavailability to phytoplankton and bacteria. It has been hypothesized that naturally-occurring Cu and Fe-binding organic ligands range from small low molecular-weight compounds to large undefined macromolecules and exhibit a continuum of binding strengths (Gledhill and Buck, 2012; Vraspir and Butler, 2009). Since solid phase extraction methods have proved challenging and may miss some portion of the metal-ligand pool (*see* review by Gledhill and Buck, 2012), the approach most commonly used to characterize metal-binding ligands in seawater is competitive equilibration with added ligands, analyzed via electrochemistry.

2. Characterizing metal-binding ligands

The most widely used electrochemical technique for studying metal-binding ligands in seawater is competitive ligand exchange-adsorptive cathodic stripping voltammetry (CLE-ACSV). This is a well-established analytical method that allows for the determination of seawater ligand concentrations and metal binding strengths, but provides no information about the chemical structure of the ligands. The concentration of metal-binding ligands is measured in CLE-ACSV by titrating the natural ligands with added Cu or Fe, until the metal-binding ligands are completely saturated. Then, a well-characterized Cu or Fe-binding ligand is added to the sample in order to compete with the natural ligands for the added Cu or Fe. The amount of metal that is bound to the well-

characterized added ligand (AL) is measured via cathodic stripping voltammetry (CSV), and the concentrations and binding strengths of the natural ligands are calculated by employing one of several traditional data processing methods (Gerringa et al., 1995; Mantoura and Riley, 1975; Scatchard, 1949).

3. The evolution of electrochemical methods: Multiple analytical windows

Electrochemical methods were first developed for measuring organic Cu speciation in the ocean (Coale and Bruland, 1988; 1990; van den Berg, 1987), and soon after several other methods evolved for both Cu and Fe which used similar electrochemical approaches but a wide variety of added ligands (Campos and van den Berg, 1994; Croot and Johansson, 2000; Gledhill and van den Berg, 1994; Moffett and Dupont, 2007; Moffett et al., 1995; 1997; Rue and Bruland, 1995; van den Berg, 1995; 2006; Wu and Luther, 1995). These were some of the first studies to indicate that the speciation of dissolved Cu and Fe in the ocean was dominated by organic complexes, drastically changing the way we think about metal cycling in the ocean. Many of these studies detected two classes of metal-binding ligands in seawater, one stronger ligand class denoted as 'L_1' and a weaker ligand class denoted as 'L_2'. These ligand classes were simply defined by their relative conditional stability constants (log $K^{cond}_{ML_x,M'}$, where 'x' denotes ligand class) in individual studies and not their absolute strength, resulting in a range of possible binding strengths for each ligand class, often spanning several orders of magnitude (*e.g.*, CuL_1 ligands defined in the literature range from log $K^{cond}_{CuL_1,Cu^{2+}}$= 13.0-16.0).

Shortly after electrochemical methods became relatively widespread for determining metal organic speciation, it was noted that the binding strength of the AL used in the analyses can have a significant effect on the results (van den Berg and Donat, 1992). This was termed the 'analytical window' of the method, and the binding strength of the ligands detected in a sample is highly dependent on the effective strength of the AL used in the titration (Bruland et al., 2000; Donat and van den Berg, 1992). The use of several different AL in previous studies has therefore lead to significant differences in the strengths of the ligands measured by individual researchers. The strength of the AL, or analytical window, can be altered by either using another AL with a different binding strength for Cu or Fe (higher or lower), or by adding a higher or lower concentration of the original AL. Several 'analytical windows' may therefore be used on a given sample, by using different concentrations of the AL in separate titrations of the sample. In this way, analysts can target different components of the Cu or Fe-binding ligand pool, from the weak to the strong end of the complexation spectrum, and thus gain a more comprehensive view of the overall quality of the ligand pool in a sample (Bruland et al., 2000). The detection of a wider range of ligand classes in a sample also allows for a more absolute definition of multiple ligand classes based on conditional stability constants rather than relative strength, avoiding some of the confusion in the literature regarding operational definitions of metal-binding ligand classes (see review by Gledhill and Buck, 2012).

The concept of using multiple analytical windows in electrochemical methods had previously only been demonstrated for organic Cu-binding ligands in coastal environments, and it was confirmed that a continuum of ligand binding strengths exists in

bays and estuaries (Buck and Bruland, 2005; Moffett et al., 1997; Ndungu, 2005; van den Berg and Donat, 1992). The same might be expected for Fe-binding ligands, but it was uncertain whether weaker organic ligands exist which can effectively compete against the strong inorganic complexation of Fe in seawater (Liu and Millero, 2002). The multiple analytical window electrochemical method has therefore, not yet been applied to studying organic Fe-binding ligands in seawater. This thesis focuses on widening the application of multiple analytical window CLE-ACSV to study Cu- and Fe-binding ligands in seawater, in a variety of coastal and open ocean environments.

4. Biogeochemical implications of copper and iron organic complexation

Constraining the sources, sinks, and overall quality of organic metal-binding ligands in the marine environment is important for understanding the biogeochemical cycling of Cu and Fe, as well as the linkages between these metals and the carbon cycle. Ligands increase the effective solubility of Cu or Fe, which has important implications for the overall inventory of that metal in the ocean. This is especially important for Fe over long timescales, since Fe availability affects primary productivity and thus carbon export in the ocean (Martin et al., 1991). For this reason, several global biogeochemical models incorporate Fe cycling, and more recently there has been an attempt to also incorporate Fe-binding ligands into carbon models (Parekh et al., 2005; Tagliabue et al., 2009; Tagliabue and Voelker, 2011). Currently, most global biogeochemical models simply include a fixed Fe-ligand concentration throughout the entire ocean equal to 0.6 nmol L^{-1}. Fe inputs from sediments, dust, or hydrothermal vents in the model up to this fixed ligand concentration will remain soluble, and any Fe inputs which exceed this ligand concentration will be scavenged. Thus, this fixed ligand value can have a large

effect on the overall ocean inventory of Fe in the model, and ultimately how much Fe is available for primary production. Gledhill and Buck (2012) recently summarized all of the studies to date which have measured Fe-binding ligands, and found that ligand concentrations, on average, range from 0.1 to 3 nmol L^{-1} in most areas of the ocean. Incorporating a range of Fe-binding ligand concentrations and/or binding strengths in global biogeochemical models could significantly change the way Fe dynamics affect carbon export. In fact, in a recent biogeochemical modeling study by Tagliabue et al. (2014), doubling the Fe ligand concentration (to 1.2 nmol L^{-1}) in the ocean changed the atmospheric carbon dioxide (CO_2) inventory by approximately 5 ppm, an effect greater than eliminating hydrothermal and/or dust inputs of Fe to the ocean in the model (Tagliabue et al., 2014). New biogeochemical models are increasingly incorporating Fe-ligand dynamics (Jiang et al., 2013; Parekh et al., 2005; Tagliabue et al., 2009; Tagliabue and Voelker, 2011), but the sources and sinks of ligands are unknown on a global scale. New international initiatives such as GEOTRACES (www.geotraces.org) are drastically increasing the number and geographic extent of oceanic metal-binding ligand measurements, but studies focusing on the mechanisms driving these distributions are only in their infancy. This thesis seeks to increase the number and quality of metal-binding ligand measurements in biologically relevant regions of the ocean, which have been well-studied previously with respect to Cu and Fe distributions. By employing a multiple analytical window electrochemical method for detecting a wide range of Cu- and Fe-binding ligands in a variety of seawater systems, this work significantly expands upon current knowledge about the sources, sinks and quality of metal-binding organic ligands in the marine environment. This work also confirms the utility of multiple

analytical window CLE-ACSV methods, first for Cu-binding ligands in open ocean waters, and then extends this type of analysis to studying the potential range of organic Fe-binding ligands in seawater for the first time.

5. Thesis organization

Chapter 2 focuses on applying multiple analytical window CLE-ACSV to describe Cu-binding ligand distributions in open ocean surface samples from the Antarctic Peninsula region and Antarctic Circumpolar Current. This chapter has been published in a special issue in *Deep Sea Research II* in 2013 (Bundy et al., 2013).

Chapter 3 applies multiple analytical window CLE-ACSV analysis for the first time to seawater Fe organic speciation, by examining the contrast between surface and benthic boundary layer samples in the central and northern California Current. This chapter was published in *Limnology and Oceanography* in 2014 (Bundy et al., 2014).

Chapter 4 combines electrochemical and geochemical approaches to look at the distributions of Fe-binding ligands across a salinity gradient in San Francisco Bay and shallow estuarine-influenced shelf regions in the central and northern California Current. This chapter was submitted as part of a special issue in *Marine Chemistry* on organic metal-binding ligands in 2014, has been revised in response to reviewer comments, and is currently under review.

Chapter 5 focuses on the southern California Current system, and includes mechanistic experiments to explore sources and sinks of Fe-binding ligands in order to interpret the distributions of ligands found in the region. This chapter will be submitted to *Marine Chemistry* in 2014.

Chapter 6 summarizes the findings of this thesis on the continuum of organic Cu- and Fe-binding ligands present in seawater after applying multiple analytical window CLE-ACSV in a variety of marine environments. In the context of these findings, a discussion of potential future research directions is also included.

6. References

Benner, R., Pakulski, J.D., McCarthy, M., Hedges, J.I. and Hatcher, P.G., 1992. Bulk chemical characteristics of dissolved organic-matter in the ocean. Science, 255(5051): 1561-1564.

Bruland, K.W., Rue, E.L., Donat, J.R., Skrabal, S.A. and Moffett, J.W., 2000. Intercomparison of voltammetric techniques to determine the chemical speciation of dissolved copper in a coastal seawater sample. Analytica Chimica Acta, 405(1-2): 99-113.

Buck, K.N. and Bruland, K.W., 2005. Copper speciation in San Francisco Bay: A novel approach using multiple analytical windows. Marine Chemistry, 96(1-2): 185-198.

Butler, A., 1998. Acquisition and utilization of transition metal ions by marine organisms. Science, 281(5374): 207-210.

Campos, M. and van den Berg, C.M.G., 1994. Determination of copper complexation in sea-water by cathodic stripping voltammetry and ligand competition with salicylaldoxime. Analytica Chimica Acta, 284(3): 481-496.

Croot, P.L. and Johansson, M., 2000. Determination of iron speciation by cathodic stripping voltammetry in seawater using the competing ligand 2-(2-thiazolylazo)-p-cresol (TAC). Electroanalysis, 12(8): 565-576.

Donat, J.R. and Van Den Berg, C.M.G., 1992. A new cathodic stripping voltammetric method for determining organic copper complexation in seawater. Marine Chemistry, 38(1-2): 69-90.

Gerringa, L.J.A., Herman, P.M.J. and Poortvliet, T.C.W., 1995. Comparison of the linear van den Berg Ruzic transformation and a nonlinear fit of the Langmuir isotherm applied to cu speciation data in the estuarine environment. Marine Chemistry, 48(2): 131-142.

Gledhill, M. and Buck, K.N., 2012. The organic complexation of iron in the marine environment: a review. Frontiers in microbiology, 3: 69.

Gledhill, M. and van den Berg, C.M.G., 1994. Determination of complexation of iron(III) with natural organic complexing ligands in seawater using cathodic stripping voltammetry. Marine Chemistry, 47(1): 41-54.

Hunter, K.A. and Boyd, P.W., 2007. Iron-binding ligands and their role in the ocean biogeochemistry of iron. Environmental Chemistry, 4(4): 221-232.

Hutchins, D.A., Witter, A.E., Butler, A. and Luther, G.W., 1999. Competition among marine phytoplankton for different chelated iron species. Nature, 400(6747): 858-861.

Jiang, M., Barbeau, K. A., Selph, K. E., Measures, C. I., Buck, K. N., Azam, F., Mitchell, B.G. and Zhou, M.2013. The role of organic ligands in iron cycling and primary productivity in the Antarctic Peninsula: A modeling study. Deep Sea Research Part II: Topical Studies in Oceanography, 90: 112-133.

Liu, X.W. and Millero, F.J., 2002. The solubility of iron in seawater. Marine Chemistry, 77(1): 43-54.

Mantoura, R.F.C. and Riley, J.P., 1975. Analytical concentration of humic substances from natural-waters. Analytica Chimica Acta, 76(1): 97-106.

Martin, J.H., Gordon, R.M. and Fitzwater, S.E., 1991. The case for iron. Limnology and Oceanography, 36(8): 1793-1802.

Moffett, J.W., 1995. Temporal and spatial variability of copper complexation by strong chelators in the Sargasso-sea. Deep-Sea Research Part I-Oceanographic Research Papers, 42(8): 1273-1295.

Moffett, J.W., Brand, L.E., Croot, P.L. and Barbeau, K.A., 1997. Cu speciation and cyanobacterial distribution in harbors subject to anthropogenic Cu inputs. Limnology and Oceanography, 42(5): 789-799.

Moffett, J.W. and Dupont, C., 2007. Cu complexation by organic ligands in the sub-arctic NW Pacific and Bering Sea. Deep-Sea Research Part I-Oceanographic Research Papers, 54(4): 586-595.

Morel, F.M.M. and Price, N.M., 2003. The biogeochemical cycles of trace metals in the oceans. Science, 300(5621): 944-947.

Ndungu, K., Hurst, M.P. and Bruland, K.W., 2005. Comparison of copper speciation in estuarine water measured using analytical voltammetry and supported liquid membrane techniques. Environmental Science & Technology, 39(9): 3166-3175.

Parekh, P., Follows, M.J. and Boyle, E.A., 2005. Decoupling of iron and phosphate in the global ocean. Global Biogeochemical Cycles, 19(2). Rue, E.L. and Bruland, K.W., 1995. Complexation of iron(III) by natural organic-ligands in the central North Pacific as determined by a new competitive ligand equilibration adsorptive cathodic stripping voltammetric method. Marine Chemistry, 50(1-4): 117-138.

Scatchard, G., 1949. The attractions of proteins for small molecules and ions. Annals of the New York Academy of Sciences, 51(4): 660-672.

Shaked, Y., Kustka, A.B. and Morel, F.M.M., 2005. A general kinetic model for iron acquisition by eukaryotic phytoplankton. Limnology and Oceanography, 50(3): 872-882.

Tagliabue, A., Aumont, O. and Bopp, L., 2014. The impact of different external sources of iron on the global carbon cycle. Geophysical Research Letters, 41(3): 920-926.

Tagliabue, A., Bopp, L. and Aumont, O., 2009. Evaluating the importance of atmospheric and sedimentary iron sources to Southern Ocean biogeochemistry. Geophysical Research Letters, 36.

Tagliabue, A. and Volker, C., 2011. Towards accounting for dissolved iron speciation in global ocean models. Biogeosciences, 8(10): 3025-3039.

Turner, D.R., Whitfield, M. and Dickson, A.G., 1981. The equilibrium speciation of dissolved components in fresh-water and seawater at 25-degrees-c and 1 atm pressure. Geochimica Et Cosmochimica Acta, 45(6): 855-881.

van den Berg, C.M.G., 1987. Organic Complexation and its Control on the Dissolved Concentrations of Copper and Zinc in the Scheldt Estuary. In: A.G.A. Merks (Editor). Elsevier, Estuarine, Coastal and Shelf Science, pp. 785-797.

van den Berg, C.M.G., 1995. Evidence for organic complexation of iron in seawater. Marine Chemistry, 50(1-4): 139-157.

van den Berg, C.M.G., 2006. Chemical speciation of iron in seawater by cathodic stripping voltammetry with dihydroxynaphthalene. Analytical Chemistry, 78(1): 156-163.

van den Berg, C.M.G. and Donat, J.R., 1992. Determination and data evaluation of copper complexation by organic-ligands in sea-water using cathodic stripping voltammetry at varying detection windows. Analytica Chimica Acta, 257(2): 281-291.

Vraspir, J.M. and Butler, A., 2009. Chemistry of Marine Ligands and Siderophores. Annual Review of Marine Science, 1: 43-63.

Wu, J.F. and Luther, G.W., 1995. Complexation of Fe(III) by natural organic-ligands in the northwest Atlantic-ocean by a competitive ligand equilibration method and a kinetic approach. Marine Chemistry, 50(1-4): 159-177.

Chapter 2

Sources of strong copper-binding ligands in Antarctic Peninsula surface waters

1. Abstract

Copper-binding organic ligands were measured during austral winter in surface waters around the Antarctic Peninsula using competitive ligand exchange- adsorptive cathodic stripping voltammetry with multiple analytical windows. Samples were collected from four distinct water masses including the Antarctic Circumpolar Current, Southern Antarctic Circumpolar Current Front, Bransfield Strait, and the shelf region of the Antarctic Peninsula. Strong copper-binding organic ligands were detected in each water mass. The strongest copper-binding ligands were detected at the highest competition strength in the Antarctic Circumpolar Current, with an average conditional stability constant of $\log K^{cond}_{CuL,Cu^{2+}}$ = 16.00±0.82. The weakest ligands were found at the lowest competition strength in the shelf region with $\log K^{cond}_{CuL,Cu^{2+}}$ = 12.68±0.48. No ligands with stability constants less than $\log K^{cond}_{CuL,Cu^{2+}} = 13.5$ were detected in the Antarctic Circumpolar Current at any competition strength, suggesting a shelf source of weaker copper-binding ligands. Free, hydrated copper ion concentrations, the biologically available form of dissolved copper, were less than 10^{-14} M in all samples, approaching levels that may be limiting for some types of inducible iron acquisition.

2. Introduction

Copper (Cu) plays an important role in phytoplankton growth. Cu can be both a micronutrient and a toxicant for phytoplankton in the ocean and this role is dependent on its speciation and concentration. The most bioavailable form of dissolved Cu is considered to be the inorganic free, hydrated Cu^{2+} ion (hereafter referred to simply as Cu^{2+}; Sunda and Lewis 1978), while the majority of dissolved Cu in the oceans is strongly chelated by a heterogeneous pool of organic ligands (van den Berg 1987; Moffett and Dupont 2007; Coale and Bruland 1988). The extent of the organic complexation of Cu causes Cu^{2+} concentrations to remain extremely low in most open ocean environments, generally less than 10^{-13} M, with elevated levels in contaminated coastal regions (Moffett 1997; Moffett and Dupont 2007; Buck and Bruland 2005). Most Cu research has, thus, focused on these anthropogenically influenced areas, since concentrations as low as 10^{-11} M can be toxic to some phytoplankton, particularly to small cells like the cyanobacteria *Synechococcus* (Brand et al. 1986). However, Cu has also been shown to be an important micronutrient, especially for diatoms such as *Thalassiosira oceanica* when using inducible iron (Fe) uptake that requires multi-Cu oxidases (Peers et al. 2005; Maldonado et al. 2006). This implies that Cu requirements may be heightened in some Fe-stressed regions of the ocean, especially high nutrient low chlorophyll regions (HNLC) such as the Southern Ocean (Maldonado et al. 2006; Annett et al. 2008; Peers et al. 2005, Peers and Price 2006).

The Antarctic Peninsula is an important ecological region in the Southern Ocean and serves as an ideal setting to study Cu along a natural gradient. The Antarctic Peninsula is a site of mixing between a low Fe, relatively low chlorophyll “blue water

zone" to the west and naturally Fe-enriched water masses influenced by the peninsula to the east. In this region, the southern portion of the mesotrophic Antarctic Circumpolar Current (ACC) sweeps south and is mixed with shelf-influenced water masses as it becomes bathymetrically constrained by the Shakelton Fracture Zone, here called the Southern ACC Front (SACCF). Water from the Bransfield Strait (BS), moving between the continent and the Shetland Islands, also mixes with the SACCF along the bathymetry. This mixing causes an input of Fe and other nutrients to the shelf and the ACC, and has been hypothesized to be the cause of numerous large-scale summer blooms that can be seen down-stream (Selph et al. this issue; Measures et al. this issue). Cu in particular may be mixed into the waters surrounding the Antarctic Peninsula from Cu-enriched sediments or upwelling of Upper Circumpolar Deep Water (UCDW) (Nolting et al. 1991; Loscher 1999). This distinct circulation and the resulting natural gradients in Fe and productivity are unique for studying sources of Cu and organic ligands to this region of the Southern Ocean.

Although Fe and its organic speciation have been studied extensively, very little Cu speciation data exists in the open ocean despite the influence of organic Cu-binding ligands on Cu^{2+} concentrations and phytoplankton growth. The Southern Ocean is relatively understudied with respect to Cu and its organic speciation (Boyle et al. 1977; Capodaglio et al. 1994; Capodaglio et al. 1998; Corami et al. 2005; Frache et al. 2001). Previous Cu speciation studies in this region have employed a common electrochemical approach to speciation analyses, competitive ligand exchange-adsorptive cathodic stripping voltammetry (CLE-ACSV). This approach involves titrating the natural organic ligands in a sample with added Cu, and then adding a well-characterized electroactive

ligand to compete with the natural ligands for the added Cu (Campos and van den Berg 1994). The concentrations as well as the conditional stability constants of naturally occurring pools of organic ligands (usually distinguished as stronger, L_1 or weaker, L_2) can then be determined. Previous studies in both the northern Pacific (Coale and Bruland 1988) and the Sargasso Sea (Moffett 1995) have hypothesized that Cu organic speciation is dominated by strong complexation in the surface ocean due to production of strong Cu-chelators by cyanobacteria and diatoms, as seen in culture studies under toxic conditions (Moffett and Brand 1996; Dupont et al. 2004). This is supported by the remarkably similar stability constants ($\log K^{cond}_{CuL,Cu^{2+}} = 14 - 16$) of Cu-binding ligands measured in culture to those measured in seawater by CLE-ACSV in field studies. These strong Cu-binding ligands observed in culture studies (Moffett and Brand 1996; Dupont et. al. 2004; Wiramanaden et. al. 2004) are thought to be the main source of strong Cu ligands in seawater. Weaker Cu ligands also exist in seawater and have been hypothesized to be comprised mostly of thiols (Dupont et al. 2006) and humics (Laglera and van den Berg 2009), and are thought to have an estuarine or sediment source (Donat et al. 1994; Skrabal et al. 1997; Chapman et al. 2009). Some weaker Cu ligands may also be degradation products (*i.e.*, photochemical) of strong Cu ligands in the euphotic zone (Laglera and van den Berg 2006). However, few of these ligand sources have been studied in the open ocean despite their importance on Cu cycling and bioavailability. Attempts to infer sources and sinks of Cu-binding ligands have also been complicated in the past due to variations in analytical approach to CLE-ACSV, which can result in marked differences in perceived conditional stability constants (Bruland et al. 2000).

The technical specifics of CLE-ACSV can have important effects on the concentration and strength of the Cu-binding ligands detected (Bruland et al. 2000). In particular, the competition strength of the added ligand is an important consideration and has been shown to have an effect on the strength and concentration of Cu-binding ligands measured in the field (Bruland et al. 2000; Buck and Bruland 2005). Thus, competition strength, or analytical window, should be considered when studying particular classes of ligands, strong or weak. Stronger ligands (operationally referred to herein as having $\log K^{cond}_{CuL,Cu^{2+}} > 13.5$) are generally detected by methods employing higher concentrations of the added ligand, while weaker ligands ($\log K^{cond}_{CuL,Cu^{2+}} \leq 13.5$, herein) are generally detected by methods using weaker competition strengths. The differences in the analytical window employed for Cu speciation studies by CLE-ACSV have generally made data interpretation difficult between laboratories and Cu complexation comparisons between sites nearly impossible. Data evaluation techniques incorporating multiple analytical windows can prove extremely insightful, but are not common in most studies (van den Berg and Donat 1992; Sander et al. 2011). A few studies have employed multiple analytical windows (MAW) to fully probe the continuum of Cu-binding ligands in seawater (Campos and van den Berg 1994; Moffett et al. 1997; Buck and Bruland 2005). The MAW approach enables a more complete view of Cu complexation and, hence, bioavailability. These studies are unique in that they elucidate the importance of detecting the full range of stronger to weaker Cu-binding ligands, which have been shown to have important effects on Cu bioavailability (Buck and Bruland 2005).

In this study, dissolved Cu and Cu organic speciation was determined in Antarctic Peninsula surface waters during austral winter. In order to probe sources of Cu and

ligands to these surface waters, CLE-ACSV was employed using the MAW approach to fully characterize the range of Cu-ligands present in these waters.

3. Experimental

3.1 CLE-ACSV Theory

CLE-ACSV is an electrochemical method that utilizes the competition between a well-characterized added ligand and the natural ligands in a sample in order to determine the thermodynamic stability of the ambient ligands. Previous studies have employed a variety of added ligands, which govern the analytical window or the competition strength of the method, and consequently the type of ligands detected, whether stronger or weaker (Campos and van den Berg 1994; Moffett et al. 1997; Buck and Bruland 2005; Moffett and Dupont 2007). The competition strength of the added ligand, in this case salicylaldoxime (SA), determines the range of binding strengths that can be detected in a given sample. The competition strength is represented by the side reaction coefficient, $\alpha_{Cu(SA)_x}$, defined as

$$\alpha_{Cu(SA)_x} = \frac{[Cu(SA)_x]}{Cu^{2+}} = \beta_2^{cond} \cdot [SA]^2 + K_1^{cond} \cdot [SA] \quad (1)$$

where β_2^{cond} and K_1^{cond} are the conditional stability constants of the $Cu(SA)_2$ and $Cu(SA)^+$ complexes (SA-labile Cu species). Both β_2^{cond} and K_1^{cond} have been experimentally determined at different salinities (Campos and van den Berg 1994) according to $log\beta_2^{cond} = 15.78 - (0.53 \cdot \log(salinity))$ and $logK_1^{cond} = 10.12 - (0.37 \cdot \log(salinity))$, and can therefore be considered as constants. All $\alpha_{Cu(SA)_x}$ determined in this study were determined using this salinity relation as described by Campos and van den Berg (1994). The competition strength, then, is simply a function of

the added ligand concentration. Only at high added ligand concentrations (> 2.5 µM SA) the $Cu(SA)^+$ species is insignificant, and equation (1) can be simplified to

$$\alpha_{Cu(SA)_2} = \beta_2^{cond} \cdot [SA]^2 \quad (2)$$

where analytical window is simply related to the square of the added ligand concentration. Equation (1) was employed in this study, using a range of concentrations of SA from 1- 25 µM and the resulting analytical window ranging from approximately 1,000-644,000. A variety of ligand stability constants can be detected when a range of competition strengths are employed (see Bruland et al. 2000, Buck and Bruland 2005, Hudson et al. 2003, Sander et al. 2011). It also allows subtle distinctions to be made between different ligand pools, and potentially ligand sources.

At each titration point, assuming inorganic complexation is negligible, the mass balance between all Cu species is given by

$$[Cu_T] = [CuL] + [Cu(SA)_x] + [Cu^{2+}] \quad (3)$$

where $[Cu_T]$ is the total dissolved Cu in the sample, $[CuL]$ is the Cu bound by organic ligands. $[Cu(SA)_x]$ is proportional to the sensitivity and the peak height at each titration point, and $[Cu^{2+}]$ is the free, hydrated form of Cu. The sensitivity is determined by internal calibration, from the linear portion at the end of the titration curve, where it is assumed that all ligands are titrated. Using the calculated sensitivity, $\alpha_{Cu(SA)_x}$, and the known $[Cu_T]$, the $[Cu(SA)_x]$, $[CuL]$, and $[Cu^{2+}]$ can be calculated at each titration point(see Buck and Bruland 2005 for a thorough explanation).

An additional term can also be defined from equation (3) which excludes the Cu bound by the artificial ligand,

$$[Cu^*] = [Cu_T] - [Cu(SA)_x] \quad (4)$$

and can be a convenient way to look at natural changes to the Cu system (Moffett et al. 1997; Buck and Bruland 2005). The effect of changing $[Cu_T]$ on $[Cu^{2+}]$ may then be predicted directly from the titration data by plotting log $[Cu^{2+}]$ versus $[Cu^*]$ and interpolating where $[Cu^*] = [Cu_T]$ of interest (Moffett et al. 1997; Buck and Bruland 2005). The concentration of $[Cu^{2+}]$ in the original sample can also be calculated in this way, by plotting log $[Cu^{2+}]$ versus $[Cu^*]$ calculated at each titration point (equation (3) and (4)) and interpolating where $[Cu^*] = [Cu_T]$ in the original sample.

3.2 Sampling Location and Hydrography

Samples were collected from water masses surrounding the Antarctic Peninsula during the austral winter in July/August 2006 aboard the *R/V/I/B* Nathaniel B. Palmer as part of a collaborative research project investigating an area of natural Fe fertilization. Surface samples were collected in four water masses surrounding the peninsula, including the Antarctic Circumpolar Current (ACC), Southern ACC Front (SACCF), Bransfield Strait (BS), and the shelf region (Figure 2.1). Water mass distinctions for each station were determined based on absolute salinity and potential temperature signatures (Figure 2.2) at the surface, in conjunction with the relative location of the station (Figure 2.1, Table 2.1). Although each station sampled was classified as ACC, SACCF, BS or shelf, several stations likely represent mixtures between the water masses. Additional samples from sea ice, glacier ice, and algal-influenced sea ice were taken in Admiralty Bay (Figure 2.1).

3.3 Sampling Methods

Surface dissolved Cu_T and Cu speciation samples were taken using a towed trace metal clean “fish” at approximately 10 m depth at each station (Vink et al. 2000).

Samples were then filtered using acid-washed 0.4 µm polycarbonate track-etched (PCTE; Whatman) filters (Buck et al. 2010). Samples taken for organic Cu complexation measurements were immediately frozen at -20°C, and samples collected for total dissolved Cu analyses were acidified to pH 1.8 using 4 mL/L of 6 N Q-HCl (Optima, Fisher Scientific) and allowed to sit for at least one year prior to analysis. Ice samples were collected with gloves and reduced in size with a hammer covered in plastic gloves. Once collected, the outer, presumably contaminated, layers of the ice samples were rinsed away with ultrapure water (Milli-Q). The remaining ice samples were allowed to thaw in acid-cleaned bottles, filtered through 0.4 µm PCTE filters and stored frozen or acidified for subsequent Cu speciation or total dissolved analyses, respectively.

3.4 Reagents

All reagents were made using ultra trace metal clean reagents and Milli-Q water unless otherwise noted. A 1.5 M borate buffer solution was prepared by diluting boric acid (> 99.99%, Alfa Aesar) in 0.4 N Q-NH_4OH (Optima, Fisher Scientific). A 4 mM salicylaldoxime (SA; > 98%, Fluka) stock solution was prepared in methanol (Optima LC/MS, Fisher Scientific), and was replaced every three months or as consumed. A 200 µM secondary stock was prepared as necessary for smaller additions of salicylaldoxime. Cu standards were diluted from an AA standard (1000 ppm, Spex CertiPrep) into pH 2 Q-HCl and were prepared in concentrations ranging from 100 nM- 10 µM. Hydrogen peroxide was made with Ultrex hydrogen peroxide (Fisher Scientific) to a final concentration of 10 µM. The 1.5 M nitric acid intemal standard was made with a 10 ppb cobalt spike.

3.5 Total Dissolved Cu Determinations

Total dissolved Cu (Cu_T) concentrations were determined using either high-resolution inductively coupled plasma-mass spectrometry (HR-ICP-MS) according to Lohan et al. (2005) or adsorptive cathodic stripping voltammetry (ACSV) following procedures of Buck and Bruland (2005). For HR-ICP-MS analyses, samples were UV-oxidized overnight following a spike with hydrogen peroxide to a final concentration of 10 µM. Samples were then loaded onto a column with a commercially available nitriloacetic acid (NTA Superflow, Qiagen) resin for 3 min, and then eluted in 1.5 M nitric acid with an internal 10 ppb cobalt standard spike. The resulting eluent was run directly on the HR ICP-MS at University of California, Santa Cruz. SAFe reference samples (Johnson et al. 2007) were run along with the field samples, and resulted in excellent agreement for S1 and slight overestimation of D2 (Buck et al. 2010) with 0.53 ± 0.03 nM for S1 and 2.83 ± 0.09 nM Cu_T (n=3) for D2, respectively (consensus values are 0.52 ± 0.05 nM for S1 and 2.31 ± 0.11 nM for D2, http://es.ucsc.edu/~kbruland/GeotracesSaFe/kwbGeotracesSaFe.html).

Total dissolved Cu determinations using ACSV were carried out on a BioAnalytical Systems (*BASi*) controlled growth mercury electrode (CGME). This was interfaced with an Epsilon 2 voltammetric analyzer connected to a laptop computer. A large mercury drop was used as the working electrode (size 14), a platinum wire as the counter electrode, and a Ag/AgCl (3 M NaCl) reference electrode, using a static mercury drop setting. Samples were measured after UV-irradiating 100 mL of the sample in 120 mL wide-mouth Teflon (FEP, Savillex) jars with quartz lids at ambient pH for 8 hours using a UVO Cleaner (Jelight Model 342). Samples were irradiated by a mercury lamp (1200 W; Hanovia, Union, NJ) from above at 10 mW/cm^2 and cooled by a fan during

irradiation (Ndungu et al. 2003). Samples warmed slightly over the irradiation period, but with minimal evaporation. 10 mL subsamples were then aliquoted into trace metal clean Teflon (FEP) vials with 25 µM SA and borate buffer (final concentration: 7.5 mM; pH 8.2). Samples were then run using ACSV as described in Buck and Bruland (2005) and Buck et al. (2010). Briefly, the sample was stirred with a trace metal clean Teflon rod at 600 rpm and the electroactive $Cu(SA)_x$ complexes were adsorbed onto the mercury drop with a -0.15 V applied potential during the 300 second deposition time. Stirring was then stopped, and a 15 second "quiet time" occurred. Samples were scanned in differential pulse mode from -0.15 V to -0.60 V using a 20 mV/s pulse rate and 50 mV pulse amplitude. The change in the cathodic stripping current was then recorded by the analyzer as Cu was reduced and stripped from the adsorbed $Cu(SA)_x$ complex. A standard addition method was used in order to determine Cu_T concentrations. Values for S1 and D2 of 0.51 $\pm$ 0.01 and 1.95 $\pm$ 0.01 nM (n=3) were obtained using this method, with good agreement to the consensus surface value and a slightly lower concentration than the consensus value for D2 (consensus values are 0.52$\pm$ 0.05 nM for S1 and 2.31$\pm$ 0.11 nM for D2).

3.6 Dissolved Cu Organic Complexation Determinations

Cu organic complexation determinations were made by gently thawing samples at 4°C over two days, and vigorously shaking before measurement. 10 mL aliquots were placed in 10 pre-conditioned Teflon (FEP) vials, and spiked with dissolved Cu ranging from 0-20 nM. Cu additions were allowed to equilibrate with the natural ligands for at least two hours, after which SA was added to all the vials at 1, 2.5, 10, or 25 µM concentration and equilibrated for at least fifteen minutes for the 2 highest detection

windows and at least 30 minutes for the 2 lower detection windows. Each vial was run separately according to the same procedure as described above for ACSV. Ligand concentrations and thermodynamic stability constants were calculated using the averages and standard deviations of both van den Berg/Ružić linearizations (Ružić 1982; van den Berg 1982) as well as Scatchard linearizations (Scatchard 1949; Mantoura and Riley 1975). If two classes of ligands were detected, they were categorized as either stronger or weaker ligands. If only one class of ligands was detected they were denoted as stronger if $\log K^{cond}_{CuL,Cu^{2+}} > 13.5$ and weaker if $\log K^{cond}_{CuL,Cu^{2+}} \leq 13.5$. More recent data processing techniques employing numerical methods with multiple analytical windows have demonstrated the ability to detect statistically robust distinct ligand classes (Hudson et al. 2003, Sander et al. 2011). This study did not employ these methods however, because they are not yet publicly available. Thus, general characteristics of the ligand pool are discussed in this study based on the relative strengths of the ligands detected at each analytical window.

4. Results

4.1 Hydrography

Conservative temperature and absolute salinity signatures (TS) from the surface layer where the towed "fish" was sampling (upper 35 m) at the stations in each water mass (ACC, SACCF, BS and shelf) are shown in Figure 2.2. Water mass signatures were relatively distinct, with some obvious mixing between regions. Bransfield Strait (BS) waters are distinct from the other water masses surrounding the Antarctic Peninsula, and are characterized by colder, saltier waters at most depths (Holm-Hansen et al. 1997; Hewes et al. 2008) which can be mixed with shelf waters in this region. Weddell Sea

water may also be influencing the cold signature of the BS stations. Shelf stations are characterized by a cold and stratified layer at the surface, while having "ACC-like" properties deeper in the water column due to influences of warmer, saltier UCDW (Hewes et al. 2008). Southern ACC Front (SACCF) stations reflect TS characteristics of ACC waters, with some potential mixing between shelf water and UCDW due to interactions with the Shakelton Fracture Zone (Holm-Hansen et al. 1997). Some CTD casts in the ACC also reflect the influence of the cold stratified shelf water from near-shore stations (Figure 2.2).

4.2 Dissolved Cu_T Concentrations

Dissolved Cu_T concentrations in seawater samples ranged from ~1.0-2.8 nM (Table S 2.1, supplementary information). The highest concentrations of Cu_T were generally found in the stations closest to the continental shelf. The Bransfield Strait (BS) and shelf regions had similar average Cu_T concentrations, of 2.39 $\pm$ 0.31 nM (n=4) and 2.26 $\pm$ 0.58 nM (n=9), respectively. Slightly higher variability in dissolved Cu_T was seen in stations sampled from the shelf, with an apparent nearshore to offshore gradient from high to low dissolved Cu_T. The lowest concentrations of Cu_T were found in the SACCF and the ACC, with 1.58 $\pm$ 0.47 nM (n=10) and 1.56 $\pm$ 0.42 nM (n=3), respectively (Table 2.1, Figure 2.3A). Cu_T concentrations were also determined in glacier, sea ice, and algal influenced sea ice. The sea ice had generally twice as much Cu_T as found in the open ocean samples, with values of 8.96$\pm$0.30 nM and 7.06$\pm$0.25 nM in the algal sea ice and the sea ice samples, respectively. Cu_T concentrations in the glacier samples were much lower, even than seawater samples, with 0.54$\pm$0.03 nM dissolved Cu_T.

4.3 Cu-binding Ligand Characteristics: Single Competition Strength

The concentrations and strengths of Cu-binding ligands were first examined using a single mid-range competition strength (10 µM added SA, α = 141,460) to probe for both strong and weak ligands in each sample. The strongest ligands measured at this competition strength were in the BS and the ACC, with $\log K^{cond}_{CuL,Cu^{2+}} = 15.0 \pm 0.54$ (n=2) and $\log K^{cond}_{CuL,Cu^{2+}} = 14.94$ (n=1) followed by the SACCF and shelf ($\log K^{cond}_{CuL,Cu^{2+}} = 14.89 \pm 0.37$ (n=3), 14.59 ± 0.30 (n=5) (Figure 2.3A). The weaker pool of ligands ($\log K^{cond}_{CuL,Cu^{2+}} \leq 13.50$) measured at this competition strength are all similar in strength, with $\log K^{cond}_{CuL,Cu^{2+}} = 13.19 \pm 0.06$ (n=2), 13.18 ± 0.45 (n=5), and 13.10 ± 0.68 (n=3) in the BS, Shelf, and SACCF. No ligands with $\log K^{cond}_{CuL,Cu^{2+}} \leq 13.5$ were detected in the ACC at this competition strength. The highest concentrations of both stronger and weaker ligands were detected in the BS at this competition strength, with 3.63 ± 0.01 nM (n=2) stronger Cu-binding ligands, and 6.00 ± 2.98 nM (n=2) of the weaker ligand class. Slightly lower concentrations of the stronger ligands were found in the other water masses, ranging from $2.48 - 2.81$ in the SACCF, shelf, and the ACC. While no weaker pool of ligands were present in the ACC at this competition strength, the shelf and SACCF regions had elevated concentrations of weaker ligands relative to stronger ligands (2.54 ± 0.81 nM and 3.62 ± 2.52 nM, respectively (Figure 2.3B), although less so than the BS (6.00 ± 2.18 nM). There was much greater variability in the weak ligand pool between samples in all water masses. In general, higher concentrations of dissolved Cu_T and weaker ligands were found at the stations over the shallow shelf in the BS.

4.4 Cu-binding Ligand Characteristics: Multiple Competition Strengths

4.4.1 Stronger Cu-binding ligands

When other competition strengths were employed, a broader range of ligands were detected. It is widely acknowledged that Fe, and likely Cu-binding ligands exist in a continuum of binding strengths in seawater (Bruland et al. 2000, Buck and Bruland 2005, Gledhill and Buck 2012 and references therein), and this study supports that finding. Figure 2.4B and D show the spectrum of binding strengths that were detected in the stronger and weaker ligand classes at various SA competition strengths (1, 2.5, 10 and 25 µM SA) in each water mass. Strong Cu-binding ligands, as defined here, were detected in all samples at the highest competition strength (Table 2.2). The strongest Cu-binding ligands were found in the ACC at an average concentration of 2.26 ± 0.01 nM (n=2) (Figure 2.4A) with $\log K^{cond}_{CuL,Cu^{2+}} = 16.00 \pm 0.82$ (Figure 2.4B), stronger than those found in all other samples (see supplementary information). Higher concentrations of slightly weaker ligands were found at this competition strength in the other samples, with average concentrations of 2.39 ± 0.77 (n=7), 3.10 ± 1.54 (n=9), and 5.14 ± 2.08 nM (n=5) in the shelf, SACCF, and BS, respectively (Figure 2.4A). Other than in the ACC, the strongest ligands were found in the SACCF ($\log K^{cond}_{CuL,Cu^{2+}} = 15.13 \pm 0.54$), followed by the shelf and the BS with similar conditional stability constants ($\log K^{cond}_{CuL,Cu^{2+}} = 14.96 \pm 0.66$ and $\log K^{cond}_{CuL,Cu^{2+}} = 14.94 \pm 0.66$). Large differences in conditional stability constants of the stronger ligand classes are apparent at the highest competition strength, but are much less apparent at lower analytical windows. Stronger ligands with similar stability constants were found in every water mass at the 10 µM SA

competition strength, ranging from 14.60±0.27 in the shelf to 15.00±0.54 in the BS. Alternatively, no strong ligands were detected at the 2.5 µM SA competition strength in the BS, while there are similar concentrations of ligands in the shelf, SACCF and ACC at this competition strength (4.25 ± 0.81 (n=6), 4.54 ± 1.12 (n=5) and 3.72 ± 1.00 (n=2)). At the 1 µM SA concentration, 8.04 nM strong ligands were detected with $\log K^{cond}_{CuL,Cu^{2+}} = 13.57$ in the only ACC sample that was measured at this competition strength (Figure 2.4A and B). There were no ligands with $\log K^{cond}_{CuL,Cu^{2+}} > 13.5$ detected at this competition strength in the other water masses.

4.4.2 Weaker Cu-binding ligands

The weakest ligands were seen at the lowest competition strengths in all of the samples. The average conditional stability constants of the weakest ligands detected in this study were found at the lowest competition strength in the shelf region, with $\log K^{cond}_{CuL,Cu^{2+}}$ of 12.68 ± 0.48 (n=7). Similarly weak ligands were found both in the Bransfield Strait and the SACCF, with log stability constants of 12.81 ± 0.27 (n=2) and 12.95 ± 0.74 (n=7) (Table 2.2). Of the two samples measured from the ACC, one was measured at the lowest competition strength (1 µM SA), and the ligands detected with this analytical window were still almost an order of magnitude stronger than in the other samples, with $\log K^{cond}_{CuL,Cu^{2+}} = 13.57$. In the BS, weak ligands were detected at all competition strengths. At the 25 µM SA competition strength, one of the two samples measured in the BS contained 7.37 nM weak ligands, with $\log K^{cond}_{CuL,Cu^{2+}} = 13.31$. No comparably weak ligands were detected in any of the other samples at this competition strength. The BS also had the greatest concentration of weak ligands at each lower

competition strength, with average concentrations of $6.00 \pm 2.98, 8.32 \pm 0.62$ and 8.28 ± 1.78 nM at 10, 2.5 and 1 µM SA, respectively (n=5) (Figure 2.4C). These ligands were all similar in strength, with $\log K^{cond}_{CuL,Cu^{2+}}$ ranging from $12.81 - 13.19$. The shelf and SACCF had similar ranges in weaker ligand strengths, with $\log K^{cond}_{L}$ ranging from $12.68 - 13.33$ at the three lowest competition strengths (Figure 2.4 D). However, the concentrations of weak ligands in the shelf and the SACCF were less than in the BS except at the lowest competition strength. The concentration of weaker ligands were approximately $2 - 4$ nM at the 10 and 2.5 µM competition strengths, and closer to the levels found in the BS waters (approximately 7 nM) at the 1 µM analytical window. No similarly weak ligands were detected at these windows in the ACC stations.

4.5 Ice Sample Analysis

Ligand concentrations and conditional stability constants were determined at the highest competition strength (25 µM SA) in each of the ice samples, and a 2.5 µM competition strength was also employed in the glacier and sea ice sample (Table 2.2). The $\alpha_{Cu(SA)_x}$determined for ice samples was determined using the Campos and van den Berg (1994) salinity relationship (see section 2.1), however this relationship has only been determined down to a salinity of 1. The differences of the calculated $\alpha_{Cu(SA)_x}$ at a salinity of 1, and a salinity less than 1 but greater than 0, however, is negligible. The calculated $\alpha_{Cu(SA)_x}$and the determined $\log K^{cond}_{CuL,Cu^{2+}}$ is likely over-estimated for the ice samples, but the difference is likely insignificant. In glacial ice, 3.18 ± 0.08 nM (n=2) Cu-binding ligands were detected with a conditional stability of $\log K^{cond}_{CuL,Cu^{2+}} = 15.59 \pm 0.02$, and 2.12±0.06 nM with $\log K^{cond}_{CuL,Cu^{2+}}$ = 14.25±0.10 at the 2.5 µM SA analytical

window. The sea ice contained ligand concentrations of 15.99 ± 0.77 nM (n=2) and $\log K^{cond}_{CuL,Cu^{2+}} = 14.42 \pm 0.04$ at the highest competition strength and 8.97 ± 0.10 nM (n=2) ligands with a conditional stability of $\log K^{cond}_{CuL,Cu^{2+}} = 13.87 \pm 0.11$ at the lower competition strength. The algal sea ice contained 26.15 ± 3.88 nM (n=2) ligands with a strength of $\log K^{cond}_{CuL,Cu^{2+}} = 15.15 \pm 0.25$ with the 25 µM window.

4.6 Cu^{2+} Concentrations

Cu^{2+} concentrations were determined at every competition strength for the samples according to Moffett et al. (1997) and equation (4). Since total dissolved Cu concentrations were less than the stronger ligand concentrations determined at the highest competition strength, these ligands are assumed to be dominant in complexing dissolved Cu (Table 2.2). Therefore, log [Cu^{2+}] levels in each sample were calculated from the highest analytical window results (equation (4) and the explanation following). The average log [Cu^{2+}] levels in the BS are -14.55 ± 0.69 (n=2), -14.78 ± 0.43 (n=6) in the shelf region, -15.15 ± 0.24 (n=2) in the ACC, and -15.18 ± 0.33 (n=10) in the SACCF (See supplementary information).

5. Discussion

5.1 Dissolved Cu Distributions

A narrow range of dissolved Cu_T concentrations was detected in all of the samples, with concentrations ranging from $1.07 - 2.84$ nM. In all of the Cu studies in the Southern Ocean, including the Ross Sea and South of New Zealand (Boyle and Edmond 1975; Capodaglio et al. 1994; Capodaglio et al. 1998; Frache et al. 2001; Corami et al. 2005), a similar range was observed (0.4-3.8 nM). A larger range in Cu_T

concentrations was seen in the sea ice and glacier samples here, with $0.54 - 8.96$ nM dissolved Cu_T. Within the small variability of observed Cu_T concentrations in the seawater samples, the lowest concentrations were found in the ACC, the water mass farthest from the shelf. Previous studies have found elevated Cu_T concentrations surrounding the Antarctic Peninsula, presumed to be from Cu-rich sediments (Nolting et al. 1991) resuspended by upwelling processes and subsequently remineralized (Corami et al. 2005). Nolting et al. (1991) found similar concentrations of dissolved Cu_T in the Scotia Sea and Weddell Sea (approximately 2 nM), which the authors noted were significantly higher than in Atlantic waters, and hypothesized a local sediment source. A sediment source of Cu is consistent with a shelf source of Fe observed in Fe: manganese ratios in this region (Measures et al. this issue). However, the dissolved Cu_T concentrations seen during this study are also similar to surface values found in the North Pacific by other researchers (Boyle et al. 1977; Moffett and Dupont 2007), attributed to upwelling processes that are also likely to strongly influence Cu distributions in the Antarctic Peninsula region during this study.

All of the previous studies in the Southern Ocean were completed during the austral summer, but deep winter mixing during this study would likely bring elevated dissolved Cu_T concentrations to the surface due to upwelling of UCDW (Capodaglio et al. 1994). Cu_T concentrations determined during this study are consistent with this observation, and similar to deep water Cu_T concentrations found in the North Pacific (Moffett and Dupont 2007), Atlantic (Bruland 1983). and Southern Ocean (Boyle and Edmond 1975). A sediment source of Cu is also likely, as other studies have similarly found sediments to be a source of both Cu and ligands (Donat et al. 1994; Skrabal et al.

1997). Although shelf sediments may be a source of Cu, the consistency in Cu distributions between sampling sites in this study probably reflects local scavenging processes and ligand concentrations (Boyle et al. 1977). In addition, both sea ice samples reflect high levels of dissolved Cu_T that were probably concentrated as the ice froze (Frache et al. 2001), and are perhaps an additional source of dissolved Cu_T in summer months when the sea ice melts. The glacial ice, on the other hand, had very low dissolved Cu_T (0.54 ± 0.03 nM), thus making it unlikely that the land mass is a considerable source of dissolved Cu_T to the surface ocean in this area. However, slightly higher particulate Cu concentrations were observed in glacier ice and sea ice compared to dissolved Cu_T (data not shown), and therefore may contribute slightly to surface dissolved Cu_T concentrations if a portion of this particulate Cu is remobilized by excess stronger ligands.

5.2 Cu-binding Ligand Distributions and Sources and Sinks

5.2.1 Strong Cu-binding ligands

The findings of this study indicate that a strong class of Cu-binding ligands is present ubiquitously throughout Antarctic Peninsula surface waters in the winter, despite the minimum in biological activity. The strongest of these ligands were found in ACC waters, which also generally contained the lowest concentrations of Cu_T. Strong ligands, as defined in this study ($\log K^{cond}_{CuL,Cu^{2+}}$ >13.5), were also only detected in the BS at the highest two analytical windows and the strongest of these ligands were weaker than those in the ACC (Table 2.2, Figure 2.4 B). There was also a narrower continuum of ligands detected in the BS, as the concentration and strength of the ligands detected at all competition strengths were remarkably similar (Figure 2.4B and D), while more

variability was seen in the ligands in the other samples. Shelf waters had similar Cu_T concentrations as the BS, but relatively fewer ligands. Strong ligands were detected in the shelf samples at all but the lowest competition strength, and were similar in concentration and strength to those in the SACCF, perhaps reflecting the influence of deep shelf water to both regions. The concentration of strong ligands in shelf samples was slightly lower than in the SACCF (2.39 versus 3.10 nM), with slightly weaker log $K^{cond}_{CuL,Cu^{2+}}$ (14.96 versus 15.13). This perhaps reflects mixing in the SACCF samples with ACC waters, with relatively stronger ligands (log$K^{cond}_{CuL,Cu^{2+}}$ =16.00). The ACC samples were distinct from the rest of the stations, especially at the highest analytical window. Although ligands detected in the ACC using 1 µM SA (log $K^{cond}_{CuL,Cu^{2+}}$ =13.57) are similar in strength to ligands detected in other samples, they are an order of magnitude stronger than any other ligands detected at this same competition strength in the other water masses (log$K^{cond}_{CuL,Cu^{2+}}$ =12.81 in the BS, 12.68 in the shelf, 12.95 in the SACCF). This likely reflects a distinct source of strong Cu-binding ligands to ACC waters.

The presence of strong ligands in this region is interesting considering the low biological activity during light-limited winter months, and the absence of *Synechococcus*, a known producer of strong Cu ligands. Strong Cu-ligands detected throughout the water column in other studies however, suggest there may be other biological ligand sources. Very few open ocean Cu-binding ligand studies have been completed, as most have focused on contaminated bays and inlets (*e.g.*, Donat et al. 1994; Moffett et al. 1997; Blake et al. 2004; Dryden et al. 2004; Buck and Bruland 2005), and the resulting potential for Cu toxicity. Some studies have been done in the open ocean such as in the

North Pacific (Coale and Bruland 1988; Coale and Bruland 1990), Sub-arctic Pacific (Moffett and Dupont 2007) and in the Sargasso Sea (Moffett et al. 1997), but have produced conflicting results. Initial profiles of Cu-binding ligands from the North Pacific measured by anodic stripping voltammetry (ASV) revealed that Cu is strongly complexed in the upper ocean, and weakly complexed at depth (Coale and Bruland 1990). This led the authors to hypothesize that upper ocean biological processes were likely responsible for the production of strong Cu chelators, and organic degradation products were dominant at depth. Similar findings were confirmed by Moffett et al. (1997) in the Sargasso Sea, although just the upper water column was examined (Moffett et al. 1997). However, in later findings Moffett and Dupont (2007) found strong Cu-binding ligands to be ubiquitous throughout the water column in the sub-arctic North Pacific (Moffett and Dupont 2007), and attributed the source of strong Cu-ligands to other *in-situ* processes, or perhaps long residence times of ligands produced in the euphotic zone. The analytical procedures of Moffett and Dupont and early studies by Coale and Bruland differed in the analytical window employed (with Moffett and Dupont employing a higher analytical window), and this may be the cause of differences seen in conditional binding strengths (Bruland et al. 2000). This stresses the importance of employing MAWs in Cu speciation studies. Only one other open ocean Cu-ligand depth profile has been reported since Moffett and Dupont 2007 (Buck et al. in press), so it is difficult to discern if the differences in ligand strengths observed between their study and Coale and Bruland are simply an artifact of analytical technique or due to differences between regions.

Although just surface samples were measured in this study, evidence from the

elevated dissolved Cu distributions and physical oceanographic observations during this study suggest that upwelled deepwaters were mixed with surface waters in this region. These surface samples should then contain similar Cu-binding ligands as found in deepwaters in both the Atlantic and Pacific Oceans (Moffett and Dupont 2007; Moffett 1995; Boyle and Edmond 1975), but the extremely weak ligands observed by Coale and Bruland were not detected in these samples at any analytical window (Coale and Bruland 1988). ACC waters only contained relatively stronger Cu-ligands despite the influence of upwelled UCPDW, suggesting that the weaker Cu-ligand complexes observed by Coale and Bruland (1988) in deep waters of the Pacific may be scavenged in this region, or the dominance of stronger ligands made them difficult to detect analytically. This may also be purely an analytical window effect as suggested by more recent data (Buck et al. in press), since the analytical windows applied here are much higher than the window used by Coale and Bruland (1988). The strong ligands observed here could have a distinct source in the Southern Ocean, or may have long residence times as suggested by Moffett and Dupont (2007), supporting the persistence of strong ligands with depth as seen in the North Pacific (Moffett and Dupont 2007).

There are several lines of evidence suggesting a distinct source of Cu-ligands to this region. Sea ice samples contained elevated concentrations of relatively strong ligands (Table 2.2), with the highest concentrations observed in the algal-influenced sea ice. Excess ligand (*e*L) concentrations (total ligand concentration – total dissolved Cu) were also much higher in the algal-influenced sea ice, with approximately 17 nM excess ligand compared to an average of 2-7 nM *e*L in all other samples (see supplementary information). This suggests that the resident phytoplankton community in the sea ice may

be a source of strong Cu-ligands. Sea ice and icebergs have been found to be a source of Fe-binding ligands (Lin et al. 2012), likely due to the resident biological communities that exist near or within the ice (Smith et al. 2007; Kaufmann et al. 2011). Pigment data measured in the algal-influenced sea ice samples using high performance liquid chromatography (HPLC, data not shown) indicate a resident community comprised mostly of diatoms. It is possible that these diatoms are a source of Cu-binding ligands to the sea ice either due to active production or cell lysis. This is supported by the much higher concentrations of excess ligands observed in the algal sea ice compared to sea ice without any algal communities (17 nM vs. 5 nM). However, publications to date on sources of strong Cu ligands have focused on *Synechococcus* and *Emiliania huxleyi* in culture (Moffett and Brand 1986; Dupont et al. 2004), with these ligands produced primarily under Cu stress conditions ($\log[Cu^{2+}] \geq -11$). Cu^{2+} levels do not generally exceed this toxicity threshold in the open ocean, nor do they exceed this level in this study. Additionally, both *Synechococcus* and *Emiliania huxleyi* are not dominant in Southern Ocean waters, and are likely not responsible for producing strong Cu ligands surrounding the Antarctic Peninsula, especially considering the minimum in biological activity observed during this sampling period (K. Selph, *pers. comm.*). There was also no correlation between stations with the highest total ligand or *e*L concentrations observed and the number or type of phytoplankton (data not shown, K. Selph *pers. comm*.). It is possible that additional organisms produce strong Cu-binding ligands in this region, such as those in sea ice, that are so far unknown. The ecological role for these ligands could be significant in the Southern Ocean and warrants further investigation.

In a related study during the same field expedition, which explored the effects of

biology on ligand production, Buck et al. (2010) simulated a spring bloom in an incubation of water collected from the Bransfield Strait (BS), and amended bottles with several Fe treatments while tracking the changes in both Fe and Cu organic speciation over the course of 15 days. A small initial biological community was observed (Buck et al. 2010) as well as similar initial strong Cu-binding ligand concentrations as observed in this study (3.71 ± 0.01 nM). Although Buck et al. (2010) employed the same detection window as the highest window used here (25 µM SA), the initial ligand pool was similar to the ligands found in the ACC ($\log K_L^{cond} = 16.1 \pm 0.3$ versus 16.00 ± 0.82 in this study) and stronger than those found in the Bransfield Strait region in this study. This could perhaps be due to some mixing of ACC and shelf waters at this particular station, as it is in the eastern BS which is known to have mixing with "ACC-like" UCDW and Antarctic surface water (Holm-Hansen et al. 1997). Buck et al. (2010) did not observe significant changes in the Cu ligand pool throughout the study despite significant changes in both the resident phytoplankton community and in Fe-binding ligands when the natural community approached Fe limiting conditions. Although recent studies have shed light on the importance of Cu requirements on the growth of open ocean phytoplankton (Peers et al. 2005; Semeniuk et al. 2009), especially under Fe-limiting conditions (Annett et al. 2008; Maldonado et al. 2006), these effects were not seen in the Buck et al. (2010) study, suggesting that the biological community may not have an effect on Cu-binding ligands in this region. Recent studies have also shown that many phytoplankton may be able to access organically-complexed Cu, despite previous assumptions that these complexes were relatively inert (Quigg et al. 2006; Semeniuk et al. 2009). If this is the case, then changes to the Cu-binding ligand pool may be extremely difficult to perceive especially

in an incubation study context. Future incubation studies examining Fe and Cu-binding ligands along with gene expression may be the most effective at determining these effects, especially in HNLC regions. Multiple analytical windows analysis for Cu organic speciation may also elucidate changes in the ambient ligands if those changes are just visible within certain detection windows

5.2.2 Weak Cu-Binding ligands

Generally weaker Cu-binding ligands were found in shelf-influenced near shore waters. Weaker ligands were detected in almost all samples, but their concentration and strength was variable and does not seem to follow any direct onshore-offshore trend, besides their absence in ACC waters. Analysis at multiple competition strengths helped to highlight relative distinctions between samples, as some of the competition strengths employed gave similar results for all water masses with regards to conditional stability constants (*i.e.* 10 µM SA analytical window), while other "extreme" competition strengths favored detection of either the strong or weaker ligand classes (*i.e.*, 25 µM versus 1 µM SA). However, according to the ratio of $\alpha_{CuL_i}/\alpha_{Cu(SA)_x}$ for each analytical window, a ratio between 1 and 10 indicates the use of proper competition strength for detecting either strong or weak ligands (van den Berg and Donat 1992; Ibisanmi et al. 2011; Sander et al. 2011). All of the $\alpha_{CuL_i}/\alpha_{Cu(SA)_x}$ for each window were close to this range (data not shown), however the average ratio for detecting weak ligands at the highest competition strength fell slightly outside of this range (~0.5), suggesting that 25 µM of the added ligand is too strong for accurately detecting weak ligands at this competition strength. However, only one sample in the BS showed the presence of a second ligand class at this window. The conditional stability constant determined at this

window may therefore be too low. Overall, the apparent differences in the quality of the ligand pool, as distinguished by the multiple competition strength analysis, gives a more thorough characterization of the continuum of ligands for determining sources and sinks.

Both the Bransfield Strait (BS) and the ACC had distinct ligand characteristics compared to shelf and SACCF waters. The BS was dominated by relatively weaker ligands overall, and had the highest concentrations of both Cu_T and ligands. This likely suggests, as mentioned above for dissolved Cu_T distributions, a source of weaker Cu ligands from shelf sediments. Several studies have observed a source of weak Cu ligands from sediments (Skrabal et al. 1997; Donat et. al. 1994; Shank et al. 2004), but this has solely been studied in estuaries where there is a large gradient between ligand and metal concentrations in pore waters and the overlying waters. The ligands determined in those environments are also much weaker than were observed here ($\log K^{cond}_{CuL,Cu^{2+}}$ = 8-10 versus 11-13.5 in this study). Capodaglio et. al. 1994 and 1998 also found weaker Cu-ligands in Terra Nova Bay and near-shore Gerlache Inlet (Capodaglio et al. 1994; Capodaglio et al. 1998), but these ligands showed a relatively homogenous distribution and were found to be much weaker and in higher concentrations than this study. Capodaglio et al. 1994 and 1998 used ASV instead of CSV with an effective analytical window much lower than the windows employed in this study, and therefore may have been able to detect ligands outside the analytical capabilities of this study. They suggested the source of weaker ligands to Terra Nova Bay were degradation products of strong Cu-ligands, which had been found to vary slightly between seasons (spring and summer) and correspond to chlorophyll concentrations (Capodaglio et al. 1998). Weaker ligands observed here may also be degradation products as has been proposed previously for humic substances and

saccharides with respect to Fe (Laglera and van den Berg 2009; Hassler et al. 2011) which are present in significant concentrations throughout the ocean. Future studies should investigate the importance of these ligands to Cu distributions in near-shore and open ocean environments. Overall, this study supports previous evidence found in estuaries that shelf environments may be an important source of weaker Cu-ligands either from shelf sediments or degradation products.

5.3 Cu Complexation and Relationship to Cu^{2+}

Although observed ligand concentrations and strengths varied between stations in the water masses surrounding the Antarctic Peninsula, Cu^{2+} concentrations remained relatively constant (-log[Cu^{2+}] ranging from 14.55 ± 0.69 in the BS to 15.18 ± 0.35 in the SACCF). The concentrations of Cu^{2+} seen here were also similar to those seen by Capodaglio et al. (1998) in a coastal Antarctic region. The lowest observed Cu^{2+} concentrations were in the samples from the ACC, and the furthest offshore stations along the SACCF. Station 96 for example, (see supplementary information) on the edge of the shelf, had lower concentrations of strong Cu-ligands than the ACC stations, but similar Cu^{2+} concentrations. Strong ligands alone are not responsible for the low observed Cu^{2+} concentrations since the strength and concentration of strong ligands varied significantly between samples. The weaker ligands are also contributing to Cu complexation, but the extent is not clear. This makes it difficult to predict the effects of ligands on log[Cu^{2+}] levels, due to the inherent variability in the ligand pool. Analysis at multiple competition strengths helps to begin to decipher this variability, but the relative influence of the ligands detected at each analytical window is difficult to interpret. Previous work on data evaluation of Cu ligands by van den Berg and Donat (1992)

modeled Cu speciation using overall α-coefficients determined in each sample as it relates to Cu^{2+} concentrations. This is a convenient way to combine organic speciation data at multiple competition strengths into one meaningful parameter that can be easily related to Cu^{2+}. The overall side reaction coefficient for Cu-ligand complexation in seawater can be calculated simply as in equation (2) from the product of the determined conditional stability constant and the ligand concentration measured by CLE-ACSV. If we assume a 1:1 complex with Cu_T and the ambient organic ligands, then

$$\alpha_{CuL} = K^{cond}_{CuL,Cu^{2+}} \cdot [L] \quad (5)$$

where $K^{cond}_{CuL,Cu^{2+}}$ and $[L]$ are both determined by CLE-ACSV. These side reaction coefficients can also be combined when more than one ligand class is detected at a given competition strength, such that $\alpha_{CuL} = 1 + \sum_i \alpha_{CuL_i}$, where i is the number of ligand classes (Turner *et al.* 1981). This allows ligand data from a single competition strength to be modeled by a side reaction coefficient and related to calculated log[Cu^{2+}] (from equation (5)) as shown in figure 2.5 A. The -log[Cu^{2+}] determined at each competition strength from every station is plotted against the logα_{CuL} calculated from the speciation data. Although the Cu^{2+} concentrations in these samples were assumed to be equal to those calculated at the highest analytical window (see section 3.6), if these ligands were to be fully titrated with added Cu from melting sea ice or another input event, Cu^{2+} concentrations would approach those seen at the lower analytical windows. The linear relationship is relatively robust, and may be a good way to model future speciation data at multiple analytical windows as it relates to free metal concentrations. It is also a convenient way to calculate log[Cu^{2+}] directly from calculated ligand concentrations and

stability constants in the literature, when raw titration data is not available (Turner et al. 1981). Modeled α_{CuL} coefficients are also effective for comparing ligand data in the literature, as can be seen from figure 2.5 B where data from a selected study (Buck and Bruland 2005, completed using the same analytical procedure and a similar range of analytical windows) is shown to compare fairly well. Although that study was done in an estuarine environment, the range of observed α's and resulting Cu^{2+} concentrations cover a similar range, suggesting that comparing the relative α coefficients, instead of ligand concentrations and stabilities, between studies could be useful in the future. These coefficients represent the complexation capacity of the system including all ligand classes, and are therefore useful in comparing ligand pools from different regions and different analytical windows. In further studies, discussing organic speciation data in terms of overall α_{CuL} coefficients may therefore be more beneficial with regards to determining Cu^{2+} metal concentrations, as well as when attempting to directly compare speciation data of different ligand pools with varying complexation capacities. Translation of measured ligand concentrations and conditional stability constants into overall α_{CuL} may also be beneficial for future large-scale speciation studies where several labs complete analyses at different analytical windows.

5.4 Cu^{2+} Concentrations and Implications for Phytoplankton

Cu^{2+} concentrations were extremely low in all samples (-log[Cu^{2+}] 14.5-15, as determined at the highest analytical window) nearing levels that may be limiting for inducible Fe uptake, a likely mechanism for Fe acquisition in this HNLC region. Variability in the ligand pool seen between regions surrounding the Antarctic Peninsula did not seem to have significant effects on log[Cu^{2+}] levels, but may be important to

consider for Cu availability in this region. Recent work has made it clear that some phytoplankton can access organic forms of Cu (Quigg et al. 2006), but the particular forms that are bioavailable are not clear. Future studies that focus on the expanded continuum of Cu-binding ligands and their bioavailability may help to elucidate this important question. It is possible that weakly complexed Cu is more bioavailable, and perhaps the absence of any clear Cu limitation in the BS region from Buck et al. (2010) is due in part to the availability of some weakly bound Cu in that area. Since strong ligands were greater than dissolved Cu_T concentrations in all samples at the highest competition strength, the log[Cu^{2+}] levels and α_{CuL} determined using 25 µM SA was assumed to be most applicable to these samples. However, if significant dissolved Cu_T is released from melting sea ice in the summer with enriched Cu levels (7.06 ± 0.25 nM), then perhaps the log[Cu^{2+}] levels determined at lower competition strengths (log[Cu^{2+}] levels < 14.5 in figure 2.5 A) will be more applicable, as weaker ligands will buffer the Cu inputs as the strong ligands become saturated. Figure 2.6A-D displays this visually, where log[Cu^{2+}] is shown versus Cu* (total Cu added to the system, excluding that bound by the added ligand, equation (4)). It is clear from Figure 2.6 that at the ambient dissolved Cu_T concentration in each representative sample from the four regions studied, the resulting log[Cu^{2+}] is similar. When Cu_T concentrations are increased in each sample however (such as from melting sea ice, Figure 2.6), the resulting *change* in log[Cu^{2+}] between each region varies significantly. Although the ligands are generally stronger in the ACC and SACCF, they are titrated quickly by the increases in total dissolved Cu. Cu inputs are buffered more in the shelf and BS due the slightly higher concentrations of weaker Cu-binding ligands, and thus the resulting change in log[Cu^{2+}] is much less (2 orders of

magnitude versus 3-4). Thus, the relevance of determining a range of log[Cu^{2+}] levels and α_{CuL} at varying competition strengths may be appropriate even for some regions of the open oceans, especially in areas where Cu inputs might be variable (areas of runoff, sea ice melt, aerosol inputs).

6. Conclusion

This study is the first to report dissolved Cu_T and Cu-binding ligand concentrations during the austral winter in the Southern Ocean. Although only surface samples were examined, this study significantly increases the number of Cu-binding ligand measurements that have been made in open ocean environments (as opposed to estuaries). Strong Cu-binding ligands were detected in all samples surrounding the Antarctic Peninsula, suggesting that strong Cu ligands have a distinct source in the Southern Ocean despite the minimal biological activity observed at the time of sampling in austral winter. Sea ice may be an important source of these ligands, and future studies exploring the ecological significance of these ligands to natural sea ice communities may prove insightful. Although Cu^{2+} concentrations observed during this study were generally less than levels thought to limit inducible Fe transport, significant changes to the Cu-binding ligand pool by the biological community were not apparent and warrant further investigation. Continued analysis of the Cu-binding ligand pool at multiple analytical windows may shed some light on important sources and sinks of Cu-binding ligands in the Southern Ocean.

7. Acknowledgements

The authors would like to thank the captain and crew of the *R/V/I/B* Nathaniel B. Palmer. We would also like to thank Dr. Chris Measures and his lab (U Hawaii) for

enabling sampling. Thank you also to Brian Seegers and Mattias Cape for CTD data and deployments. We would like to thank the Bruland lab, Maeve Lohan, Ana Aguilar-Islas, and Rob Franks at the Marine Analytical Facility at University of California Santa Cruz, for their help with HR-ICP-MS total copper analyses. Buck was funded in part by a Scripps Institution of Oceanography Earth Section postdoctoral fellowship and supported by institutional funding from the G. Unger Vetlesen Foundation at the Bermuda Institute of Ocean Sciences (BIOS). This manuscript represents BIOS contribution number 2018 for KNB. This work was supported by NSF award ANT 04-44134 and RMB was supported by NSF award ANT-0948338. Chapter 2, in full, is a reprint of the material as it appears in Deep Sea Research II: Topical Studies in Oceanography 2013. Bundy, R.M., Barbeau, K.A., Buck, K.N., Deep Sea Research Part II: Topical Studies in Oceanography, Volume 90, Pages 134-146 2013. The dissertation author was the primary investigator and author of this paper.

Table 2.1 The dissolved concentration of copper for each station (and the associated water mass and latitude and longitude) as well as the average temperature and salinity in the upper 35 m. *indicates stations where no speciation data was obtained. 'nd' indicates stations where no CTD data was collected

Station	Latitude	Longitude	Water Mass	$[Cu_T]$ nM	std dev	Temperature ˚C	Salinity (psu)
78*	-62.311	-58.065	BS	2.12	0.06	-1.69	34.18
81*	-62.229	-58.118	BS	2.33	0.08	-0.68	34.21
211	-63.783	-60.215	BS	2.84	0.21	-1.22	34.26
224	-62.817	-57.755	BS	2.25	0.07	-1.79	34.43
82*	-61.833	-57.565	Shelf	2.32	0.08	-0.70	34.07
86	-61.611	-57.730	Shelf	2.31	0.09	-0.73	34.08
90	-61.375	-57.905	Shelf	2.01	0.15	-0.43	34.02
93	-61.125	-58.093	Shelf	1.65	0.15	-0.75	33.87
96	-60.950	-58.374	Shelf	1.44	0.06	-0.81	33.89
119	-61.225	-54.411	Shelf	2.11	0.10	-1.12	34.20
215	-62.965	-61.576	Shelf	2.20	0.16	-1.04	34.18
217	-62.526	-62.456	Shelf	2.15	0.07	-1.04	34.20
219*	-62.150	-63.100	Shelf	1.86	0.06	-1.33	33.97
130	-61.749	-56.903	SACCF	1.27	0.07	nd	nd
136	-61.196	-56.238	SACCF	1.17	0.14	nd	nd
141	-60.836	-56.110	SACCF	2.58	0.07	nd	nd
145	-60.571	-56.746	SACCF	1.51	0.20	nd	nd
146	-60.276	-57.451	SACCF	1.33	0.04	-0.71	33.87
148	-60.491	-57.000	SACCF	1.33	0.05	-0.63	33.87
150	-60.666	-56.520	SACCF	1.51	0.04	-0.97	33.95
152	-60.745	-56.330	SACCF	1.07	0.10	-0.73	34.09
156	-60.835	-56.107	SACCF	1.90	0.14	-0.74	34.30
160	-60.921	-55.904	SACCF	2.10	0.05	-0.73	34.30
197*	-60.750	-58.375	ACC	1.25	0.07	-1.01	33.86
197	-60.750	-58.375	ACC	2.04	0.08	-1.02	33.51
198	-60.750	-59.250	ACC	1.41	0.07	-1.12	33.93
glacier	-62.166	-58.416		0.54	0.03	nd	nd
sea ice	-62.166	-58.416		7.06	0.25	nd	nd
algal ice	-62.166	-58.416		8.96	0.31	nd	nd

Table 2.2 Average concentrations of copper in the BS, shelf, SACCF, ACC, glacier ice, sea ice, and algal sea ice determined in all the samples. Strong ligands ($logK^{cond}_{CuL,Cu^{2+}} \geq 13.5$, L_1) and weak ligands ($logK^{cond}_{CuL,Cu^{2+}} \leq 13.5$, L_2) at each competition strength (25, 10, 2.5, 1 µM SA).

Water Mass	[SA] µM	[Cu_T] nM	+/-	[L_1] nM	+/-	logK_1	+/-	[L_2] nM	+/-	logK_2	+/-
			0.3								
Bransfield	25	2.39	1	5.14	2.08	14.94	0.66	7.37	na	13.31	na
	10			3.63	0.01	15.00	0.54	6.00	2.98	13.19	0.06
	2.5							8.32	0.62	12.73	0.58
	1							8.28	1.78	12.81	0.27
			0.5								
Shelf	25	2.26	2	2.39	0.77	14.96	0.66				
	10			2.66	1.21	14.60	0.27	2.54	0.81	13.27	0.41
	2.5			4.25	0.81	14.06	0.66	4.68	2.15	13.33	0.83
	1							6.57	2.59	12.68	0.48
			0.4								
SACCF	25	1.58	7	3.10	1.54	15.13	0.54				
	10			2.48	0.30	14.89	0.37	3.62	2.52	13.10	0.68
	2.5			4.54	1.12	13.85	0.27	5.51	3.12	13.18	0.74
	1							7.50	2.94	12.95	0.74
			0.4								
ACC	25	1.56	2	2.26	0.01	16.00	0.82				
	10			2.81	na	14.94	na				
	2.5			3.72	1.00	13.63	0.29				
	1			8.04	na	13.57	na				
			0.0								
Glacier	25	0.54	3	3.18	0.08	15.59	0.02				
	2.5			2.12	0.06	14.25	0.10				
			0.2								
Sea ice	25	7.06	5	15.99	0.77	14.42	0.04				
	2.5			8.97	0.10	13.87	0.11				
Algal sea ice	25	8.96	0.3 1	26.15	3.88	15.15	0.25				

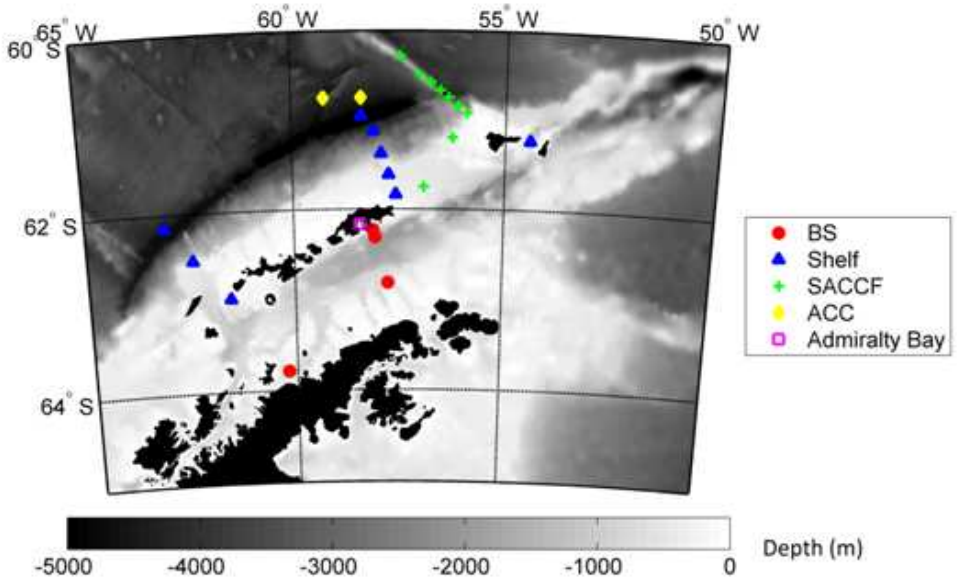

Figure 2.1 Sampling map of the Antarctic Peninsula region with stations in the BS (○), Shelf (Δ), SACCF (+), ACC (◊), and one station for ice samples in Admiralty Bay (□). Bathymetry is shown from 0-5000 m.

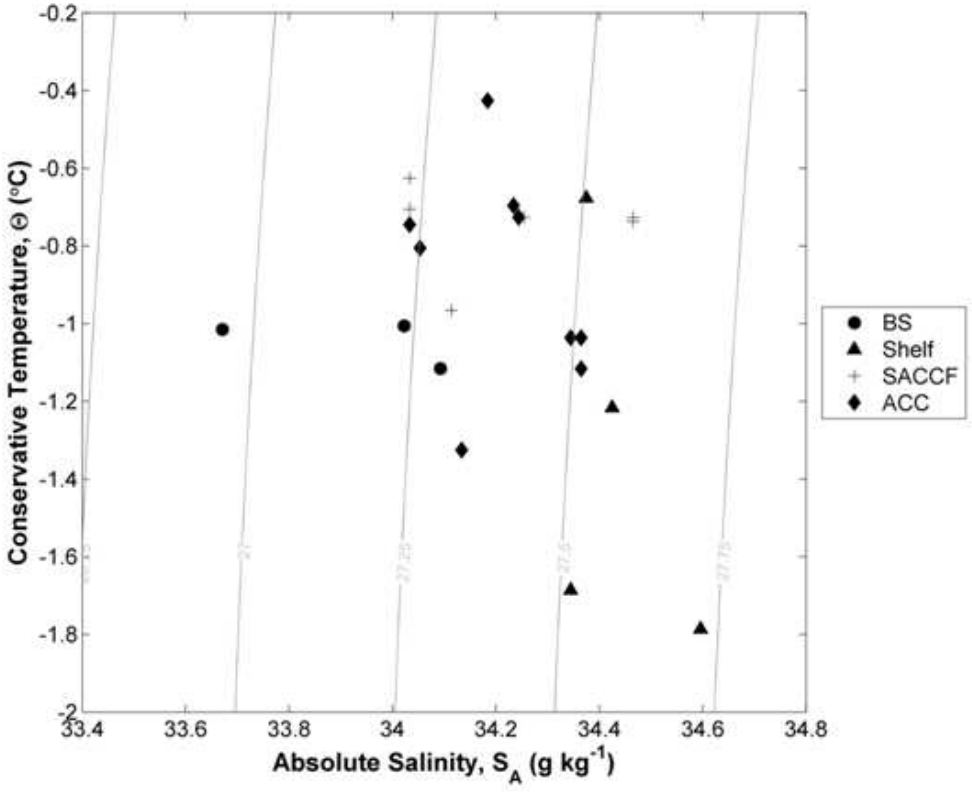

Figure 2.2 Conservative temperature (Θ, ˚C) versus absolute salinity (S_A, g/kg) with density contours (ρ_{ref} = 0 dbar) for the surface at each station from each of the four water masses sampled, BS (○), shelf (Δ), SACCF (+), and ACC (◊).

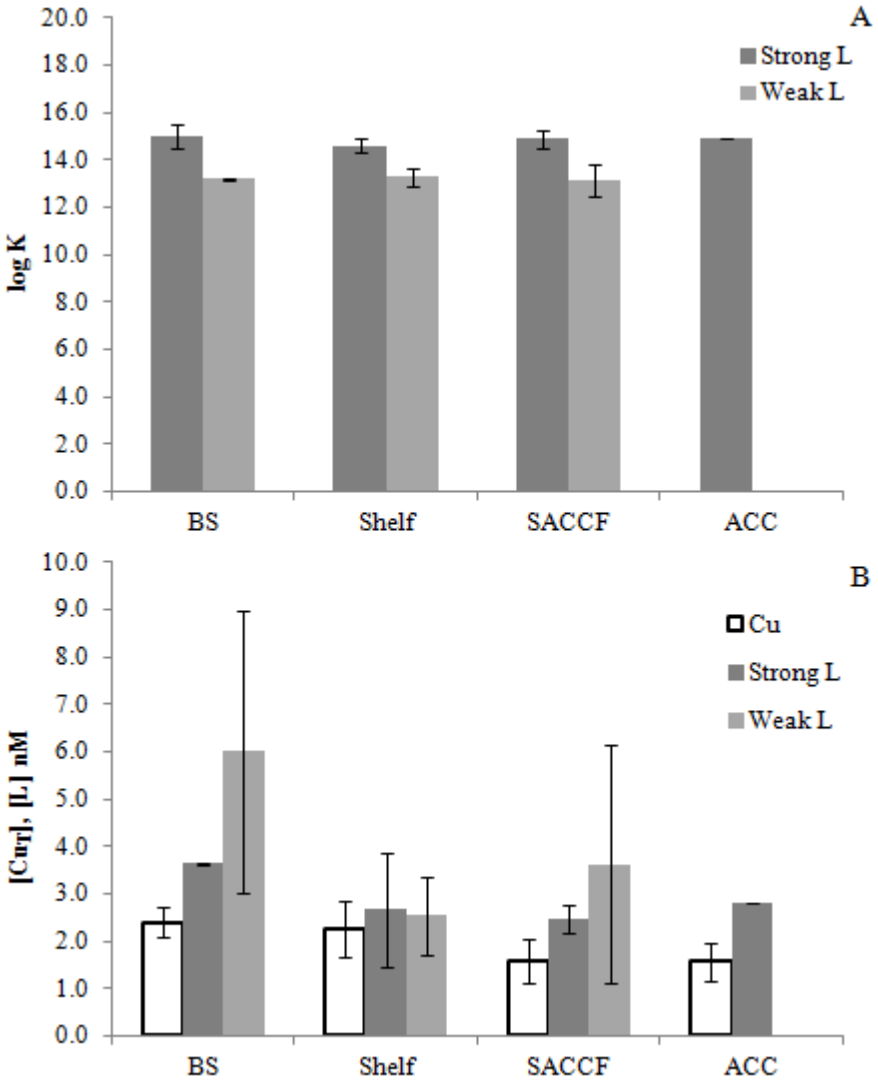

Figure 2.3 (A) The conditional stability constants of strong and weak ligands determined in each water mass using 10 µM added SA. (B) The average concentration of copper determined in each water mass, as well as the concentration of strong and weak ligands determined using 10 µM added SA.

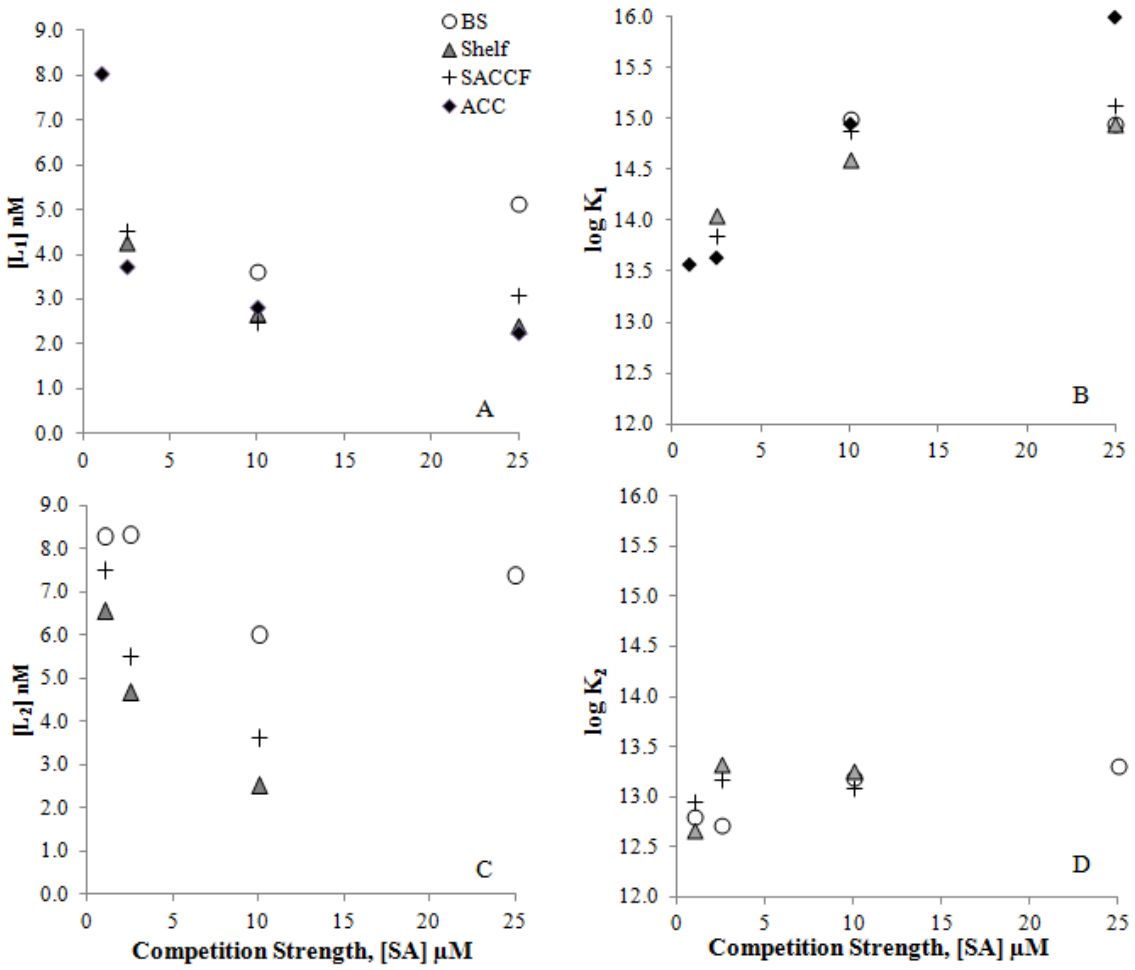

Figure 2.4 Concentrations of strong ligands (A) and conditional stability constants of strong ligands (B), determined in each water mass at several competition strengths (1, 2.5, 10, and 25 µM SA). Concentrations of weak ligands (C) and conditional stability constants of weak ligands (D) determined at each competition strength of added SA (1, 2.5, 10, 25 µM) in the BS, shelf, SACCF and the ACC.

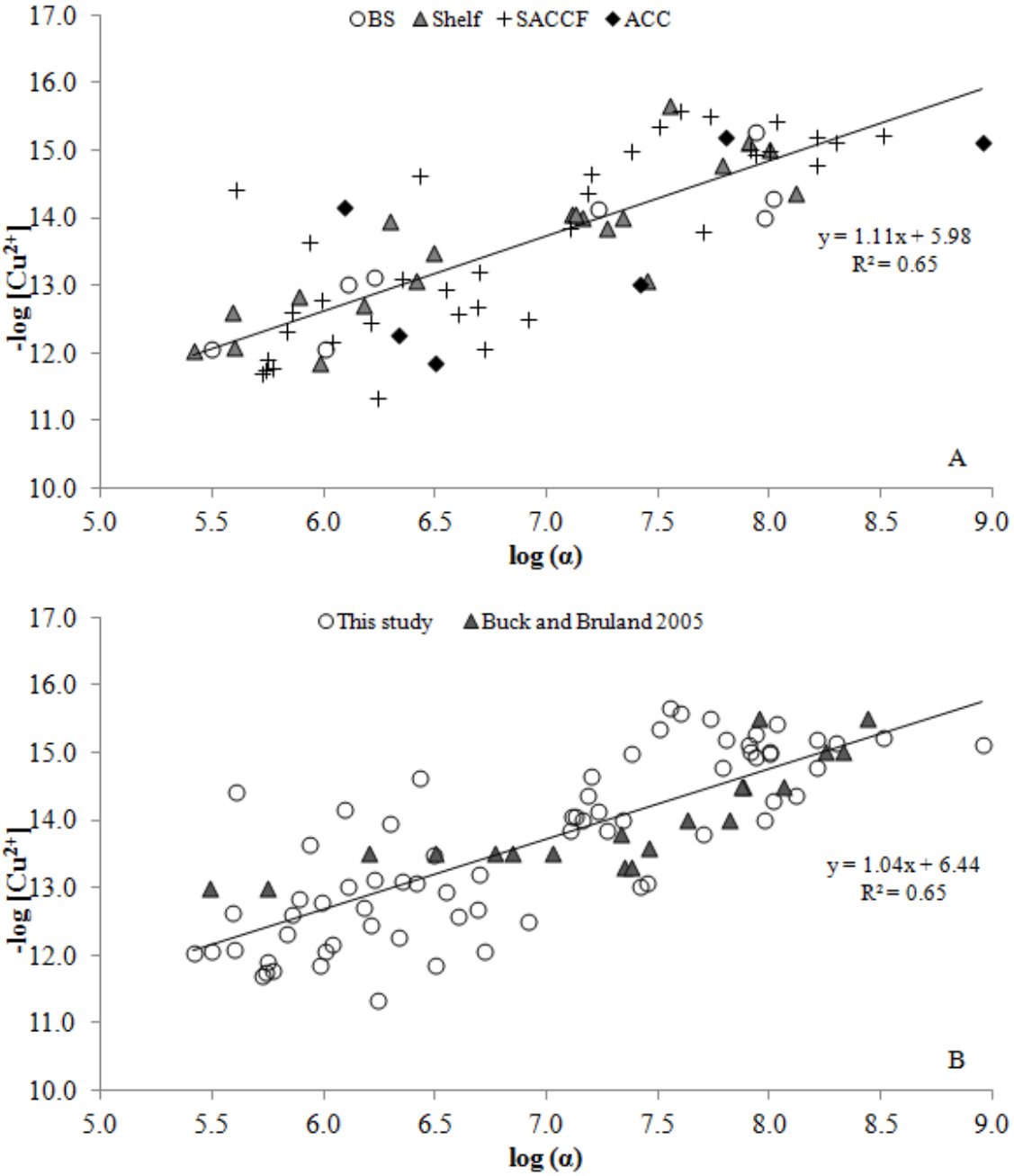

Figure 2.5 (A) The calculated log[Cu^{2+}] levels versus calculated log α_{CuL} in every sample at every competition strength from this study alone (A) and in comparison with Buck and Bruland (2005) (B).

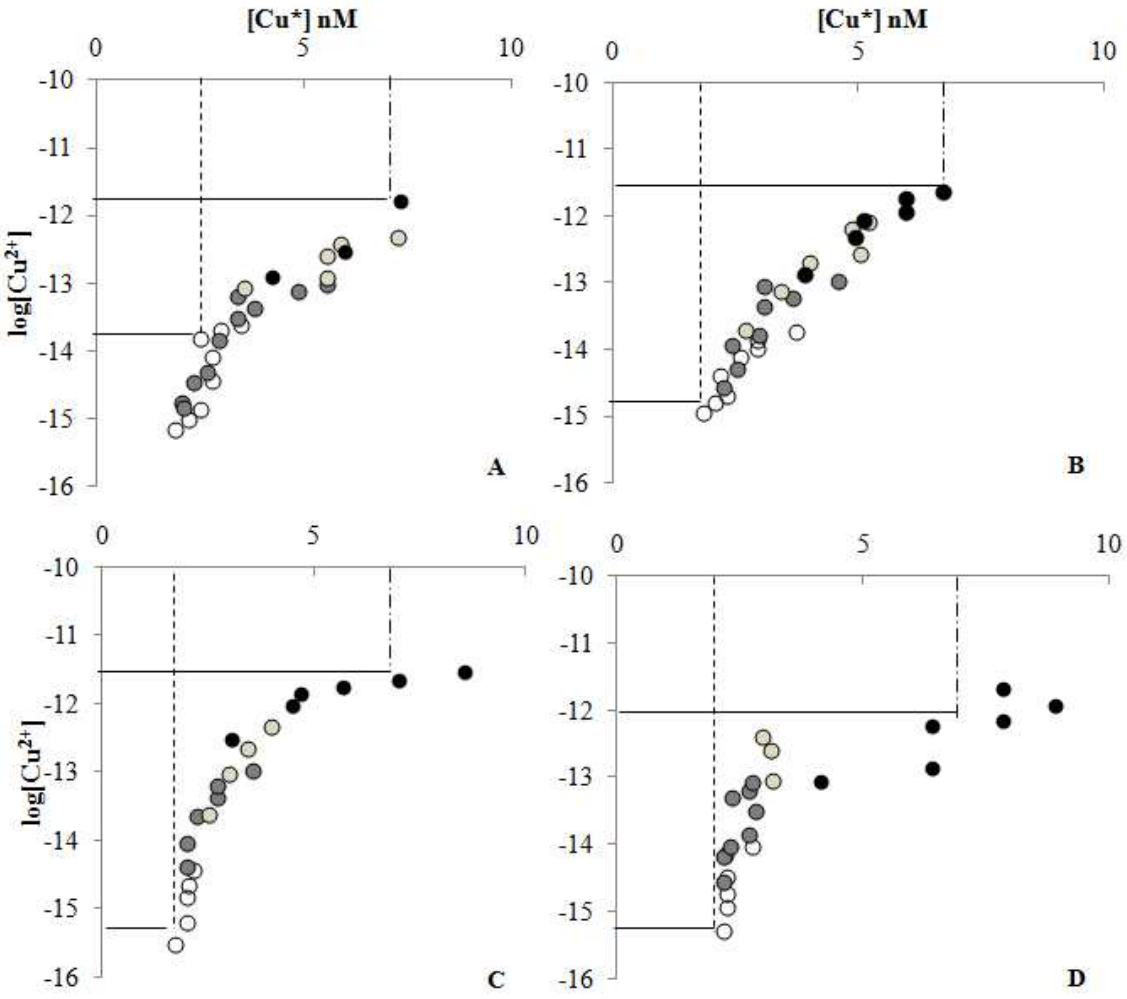

Figure 2.6 Log[Cu^{2+}] versus [Cu*] (nM) for station 224 in the Bransfield Strait (A), station 90 in the shelf (B), station 156 in the SACCF (C), and station 197 in the ACC (D). Vertical dashed lines '---' represent the ambient total dissolved Cu concentration in each sample, while the horizontal line represents the resulting log[Cu^{2+}]. The second vertical dashed line '-•-' represents the ambient total dissolved Cu concentration determined in sea ice.

Table S2.1 Stronger and weaker ligand concentrations determined in each sample with reported standard deviations from the average of Scatchard and Ružić/Langmuir linearizations (see methods). Log[Cu^{2+}] were determined from raw titration data based on Moffett *et al.* (1997). The determination of α was calculated based on the description in section 4.4 in the text.

Station	Water Mass	[Cu] nM	std dev	[SA] µM	[Ls] nM	std dev	log Ks	std dev	[Lw] nM	std dev	log Kw	std dev	*e*L	[Cu^{2+}]	-log[Cu^{2+}]	α combined
211	BS	2.84	0.21	25	6.13	0.17	15.06	0.05	6.54	1.24	14.23	0.09	9.83	5.38E-16	15.27	87316320.27
		2.84		10	3.64	0.00	15.38	0.03	3.89	0.14	13.23	0.00	4.69	9.89E-15	14.00	94270271.13
		2.84		2.5					8.75	0.08	13.14	0.02	5.91	9.60E-14	13.02	1294220.84
		2.84		1					9.54	0.01	13.00	0.11	6.70	8.64E-13	12.06	1022230.42
224	BS	2.25	0.07	25	2.75	0.26	15.54	0.14	7.37	0.29	13.31	0.02	7.87	5.06E-15	14.30	103784569.32
		2.25		10	3.62	0.36	14.61	0.24	8.11	3.58	13.15	0.22	9.48	7.59E-15	14.12	17029372.30
		2.25		2.5	6.95	0.43	13.31	0.22	7.88	1.80	12.32	0.02	12.58	7.47E-14	13.13	1696906.55
		2.25		1					7.02	0.83	12.62	0.10	4.77	8.74E-13	12.06	313572.88
86	Shelf	2.31	0.09	25	3.44	0.04	15.55	0.19					1.13	4.43E-15	14.35	130785153.33
		2.31		10	4.18	0.05	14.46	0.08					1.87	8.73E-15	14.06	12917435.91
		2.31		2.5	4.43	0.06	13.74	0.12					2.12	8.76E-14	13.06	2608578.39
		2.31		1	4.67	1.80	13.19	0.62					2.36	1.43E-13	12.84	775028.09
90	Shelf	2.01	0.15	25	2.85	0.19	15.49	0.23	2.62	0.75	14.31	0.07	3.46	9.84E-16	15.01	100104306.08
		2.01		10	2.76	0.37	14.68	0.08	3.44	0.57	13.04	0.20	4.19	9.68E-15	14.01	14559139.96
		2.01		2.5	5.27	0.25	13.37	0.22	6.22	1.62	12.48	0.19	9.48	1.98E-13	12.70	1525040.40
		2.01		1	4.71	1.01	13.27	0.37	3.36	1.01	11.82	0.61	6.06	1.39E-12	11.86	963556.53
93	Shelf	1.65	0.15	25	2.21	0.06	15.41	0.25	2.04	0.02	13.61	0.01	2.60	1.64E-15	14.79	61758947.64
		1.65		10	2.42	0.06	14.85	0.05	2.78	1.03	12.81	0.41	3.55	1.42E-14	13.85	18549907.33
		1.65		2.5	3.34	0.32	14.90	0.30	4.81	0.32	12.20	0.00	6.50	8.41E-14	13.08	28509697.00
		1.65		1					7.98	0.57	12.67	0.18	6.33	8.42E-13	12.07	399948.41
96	Shelf	1.44	0.06	25	1.99	0.01	15.14	0.68	1.78	0.13	14.52	0.14	2.33	2.18E-16	15.66	35749936.25
		1.44		10	2.03	0.26	14.98	0.00	2.42	0.37	13.68	0.04	3.01	1.02E-14	13.99	22013973.29
		1.44		2.5					4.42	0.12	13.82	0.17	2.98	3.36E-14	13.47	3129121.37
		1.44		1					10.99	0.16	12.52	0.04	9.55	2.42E-13	12.62	389940.91
119	Shelf	2.11	0.10	25	2.94	0.00	15.41	0.08					0.83	7.75E-16	15.11	80974324.88
		2.11		10	2.66	0.03	14.66	0.11	1.50	0.03	13.54	0.00	2.05	8.78E-15	14.06	13585420.44
		2.11		2.5					6.46	0.15	13.46	0.05	4.35	1.11E-14	13.95	1996331.85
		2.11		1					6.55	0.32	12.57	0.13	4.44	9.15E-13	12.04	260761.20
215	Shelf	2.20	0.16	25	3.13	0.20	15.38	0.10	0.69	0.00	14.50	0.00	1.62	9.75E-16	15.01	82791413.68
		2.20		2.5	3.97	0.12	14.21	0.08	0.60	0.00	14.35	0.00	2.37	3.16E-13	12.50	8338370.04
217	Shelf	2.15	0.07	25	2.64	0.02	15.74	0.15	2.71	0.10	14.41	0.08	3.20	1.64E-15	14.79	161839435.15
		2.15		10					3.41	0.46	14.64	0.41	1.26	2.22E-15	14.65	15812346.96
		2.15		2.5					5.56	0.19	13.66	0.21	3.41	2.39E-15	14.62	2723171.24
		2.15		1					7.71	0.38	12.69	0.19	5.56	3.92E-15	14.41	404627.55
130	SACCF	1.27	0.07	25	2.47	0.08	15.48	0.04	2.19	0.04	14.45	0.16	3.39	1.16E-15	14.94	86541328.53
		1.27		2.5					2.35	0.09	14.20	0.46	1.08	2.58E-13	12.59	3990873.58
		1.27		1					4.39	0.12	13.08	0.2	3.12	1.27E-12	11.90	565542.55
136	SACCF	1.17	0.14	25	2.71	0.06	15.70	0.06	4.96	1.79	14.51	0.22	6.50	6.37E-16	15.20	162733765.60
		1.17		2.5					3.77	0.01	13.25	0.01	2.60	2.44E-13	12.61	718359.69

Table S2.1 Continued. Stronger and weaker ligand concentrations determined in each sample with reported standard deviations from the average of Scatchard and Ružić/Langmuir linearizations (see methods). Log[Cu^{2+}] were determined from raw titration data based on Moffett *et al.* (1997). The determination of α was calculated based on the description in section 4.4 in the text.

Station	Water Mass	[Cu] nM	std dev	[SA] µM	[Ls] nM	std dev	log Ks	std dev	[Lw] nM	std dev	log Kw	std dev	*e* L	[Cu^{2+}]	-log[Cu^{2+}]	α combined
		1.17		1					4.12	0.04	13.60	0.20	2.95	4.68E-12	11.33	1757508.62
141	SACCF	2.58	0.07	25	3.99	0.04	15.67	0.17					1.41	7.43E-16	15.13	199973707.22
		2.58		2.5					6.49	0.04	13.51	0.02	3.91	8.03E-14	13.10	2250323.16
		2.58		1					10.12	0.26	13.69	0.24	7.54	8.86E-13	12.05	5311052.50
145	SACCF	1.51	0.20	25	7.44	0.09	14.83	0.01					5.93	3.20E-16	15.49	53898036.43
		1.51		2.5	6.12	0.75	13.73	0.13					4.61	1.15E-13	12.94	3521693.42
		1.51		1	4.73	0.08	13.13	0.09					3.22	4.81E-13	12.32	683694.01
146	SACCF	1.33	0.04	25	2.79	0.05	15.50	0.04	2.80	0.44	14.68	0.11	4.26	3.76E-16	15.42	107928949.00
		1.33		2.5					8.46	0.03	13.08	0.01	7.13	7.03E-13	12.15	1097674.10
148	SACCF	1.33	0.05	25	3.20	0.12	15.07	0.11					1.87	2.58E-16	15.59	40150644.25
		1.33		10	2.37	0.06	14.74	0.07	1.84	0.05	13.83	0.02	2.88	4.22E-15	14.37	15294446.24
		1.33		2.5					6.09	0.18	13.12	0.05	4.76	2.34E-14	13.63	860095.11
		1.33		1					8.78	0.29	12.75	0.14	7.45	1.98E-12	11.70	529048.32
150	SACCF	1.51	0.04	25	0.71	0.13	15.50	0.04					-0.80	1.04E-15	14.98	24057936.09
		1.51		2.5	4.47	0.05	13.53	0.04					2.96	3.60E-13	12.44	1622959.90
152	SACCF	1.07	0.10	25	3.80	0.13	14.90	0.15					2.73	4.41E-16	15.36	32343246.45
		1.07		2.5					2.81	0.85	13.29	0.44	1.74	1.72E-12	11.76	587093.21
156	SACCF	1.90	0.14	25	2.45	0.32	15.54	0.14	2.16	0.78	14.62	0.13	2.71	1.02E-15	14.99	100674497.72
		1.90		10	2.82	0.10	14.61	0.22	12.97	2.56	12.50	0.18	13.89	1.39E-14	13.86	12749228.34
		1.90		2.5	3.54	0.32	14.10	0.67	2.67	0.97	12.62	0.05	4.31	2.04E-13	12.69	4894594.12
		1.90		1	4.51	0.09	13.03	0.08	10.27	0.12	11.45	0.00	12.88	1.77E-12	11.75	548833.19
160	SACCF	2.10	0.05	25	2.47	0.03	16.08	0.07	2.31	0.02	14.38	0.07	2.68	5.87E-16	15.23	324135254.53
		2.10		10	2.26	0.17	15.31	0.22	5.40	0.55	12.96	0.06	5.56	1.63E-14	13.79	49971121.80
		2.10		2.5	4.04	0.10	14.04	0.11	9.41	2.12	12.32	0.12	11.35	6.42E-14	13.19	4957250.78
		2.10		1					10.10	1.14	12.96	0.26	8.00	1.61E-13	12.79	987010.59
197	ACC	2.04	0.08	25	2.25	0.05	16.57	0.11					0.21	7.80E-16	15.11	903627534.60
		2.04		10	2.81	0.06	14.94	0.10					0.78	9.61E-14	13.02	26382995.87
		2.04		2.5	3.01	0.25	13.83	0.26					0.97	5.57E-13	12.25	2180553.24
		2.04		1	8.04	0.11	13.57	0.14					6.00	1.39E-12	11.86	3200782.65
198	ACC	1.41	0.07	25	2.27	0.01	15.42	0.08					0.86	6.38E-16	15.20	63977293.54
		1.41		2.5	4.43	0.14	13.42	0.06					3.02	7.13E-15	14.15	1248544.64
	glacier	0.54	0.03	25	3.18	0.08	15.59	0.02					2.64	1.21E-16	15.92	132564464.94
		0.54		2.5	2.12	0.06	14.25	0.10					1.58	3.67E-14	13.44	4039577.72
	sea ice	7.06	0.25	25	15.99	0.77	14.42	0.04					8.93	2.46E-15	14.61	45065944.07
		7.06		2.5	8.97	0.10	13.87	0.11					1.91	1.12E-14	13.95	7125125.27
	dirty ice algae	8.96	0.31	25	26.15	3.88	15.15	0.25					17.19	8.23E-16	15.08	395796267.47

8. References

Annett, A.L., Lapi, S., Ruth, T.J., Maldonado, M.T., 2008. The effects of Cu and Fe availability on the growth and Cu : C ratios of marine diatoms. Limnology and Oceanography 53 (6), 2451-2461.

Blake, A.C., Chadwick, D.B., Zirino, A., Rivera-Duarte, I., 2004. Spatial and temporal variations in copper speciation in San Diego Bay. Estuaries 27 (3), 437-447.

Boyle, E.A., Edmond, J.M., 1975. Copper in surface waters south of New-Zealand. Nature 253 (5487), 107-109.

Boyle, E.A., Sclater, F.R., Edmond, J.M., 1977. Distribution of dissolved copper in Pacific. Earth and Planetary Science Letters 37 (1), 38-54.

Brand, L.E., Sunda, W.G., Guillard, R.R.L., 1986. Reduction of marine-phytoplankton reproductive rates by copper and cadmium. Journal of Experimental Marine Biology and Ecology 96 (3), 225-250.

Bruland, K.W., 1983. Trace elements in seawater. in: Chemical Oceanography (J.P. Riley and R. Chester, eds. Academic Press, London, 1983), vol 8. chpt. 45.

Bruland, K.W., Rue, E.L., Donat, J.R., Skrabal, S.A., Moffett, J.W., 2000. Intercomparison of voltammetric techniques to determine the chemical speciation of dissolved copper in a coastal seawater sample. Analytica Chimica Acta 405 (1-2), 99-113.

Buck, K.N., Bruland, K.W., 2005. Copper speciation in San Francisco Bay: A novel approach using multiple analytical windows. Marine Chemistry 96 (1-2), 185-198.

Buck, K.N., Selph, K.E., Barbeau, K.A., 2010. Iron-binding ligand production and copper speciation in an incubation experiment of Antarctic Peninsula shelf waters from the Bransfield Strait, Southern Ocean. Marine Chemistry 122 (1-4), 148-159.

Buck, K.N., Moffett, J., Barbeau, K.A., Bundy, R.M., Kondo, Y., Wu, J., 2011. The organic complexation of iron and copper: an intercomparison of competitive ligand exchange-adsorptive cathodic stripping voltammetry (CLE-ACSV) techniques. Liminology and Oceanography Methods. In press.

Campos, M., van den Berg, C.M.G., 1994. Determination of copper complexation in sea-water by cathodic stripping voltammetry and ligand competition with Salicylaldoxime. Analytica Chimica Acta 284 (3), 481-496.

Capodaglio, G., Toscano, G., Scarponi, G., Cescon, P., 1994. Copper complexation in the surface seawater of Terra-Nova Bay (Antarctica). International Journal of Environmental Analytical Chemistry 55 (1-4), 129-148.

Capodaglio, G., Turetta, C., Toscano, G., Gambaro, A., Scarponi, G., Cescon, P., 1998. Cadmium, lead and copper complexation in antarctic coastal seawater. Evolution during the austral summer. International Journal of Environmental Analytical Chemistry 71 (3-4), 195-226.

Chapman, C.S., Capodaglio, G., Turetta, C., van den Berg, C.M.G., 2009. Benthic Fluxes of copper, complexing ligands and thiol compounds in shallow lagoon waters. Marine Environmental Research 67 (1), 17-24.

Coale, K.H., Bruland, K.W., 1988. Copper complexation in the northeast pacific. Limnology and Oceanography 33 (5), 1084-1101.

Coale, K. H., and K. W. Bruland. 1990. Spatial and temporal variability in copper complexation in the North Pacific. Deep-Sea Research I 37, 317-336.

Corami, F., Capodaglio, G., Turetta, C., Soggia, F., Magi, E., Grotti, M., 2005. Summer distribution of trace metals in the western sector of the Ross Sea, Antarctica. Journal of Environmental Monitoring 7 (12), 1256-1264.

Donat, J.R., Lao, K.A., Bruland, K.W., 1994. Speciation of dissolved copper and nickel in south San-Francisco Bay - a multimethod approach. Analytica Chimica Acta 284 (3), 547-571.

Dryden, C.L., Gordon, A.S., Donat, J.R., 2004. Interactive regulation of dissolved copper toxicity by an estuarine microbial community. Limnology and Oceanography 49 (4), 1115-1122.

Dupont, C.L., Nelson, R.K., Bashir, S., Moffett, J.W., Ahner, B.A., 2004. Novel copper-binding and nitrogen-rich thiols produced and exuded by Emiliania huxleyi. Limnology and Oceanography 49 (5), 1754-1762.

Dupont, C.L., Moffett, J.W., Bidigare, R.R., Ahner, B.A., 2006. Distributions of dissolved and particulate biogenic thiols in the subartic Pacific Ocean. Deep-Sea Research Part I-Oceanographic Research Papers 53 (12), 1961-1974.

Frache, R., Abelmoschi, M.L., Grotti, M., Ianni, C., Magi, E., Soggia, F., Capodaglio, G., Turetta, C., Barbante, C., 2001. Effects of ice melting on Cu, Cd and Pb profiles in Ross Sea waters (Antarctica). International Journal of Environmental Analytical Chemistry 79 (4), 301-313.

Gledhill, M., Buck, K.N., 2012. The organic complexation of iron in the marine

environment: A review. Frontiers in Microbiology 3, 69.

Hassler, C.S., Schoemann, V., Nichols, C.M., Butler, E.C.V., Boyd, P.W., 2011. Saccharides enhance iron bioavailability to Southern Ocean phytoplankton. Proceedings of the National Academy of Sciences of the United States of America 108 (3), 1076-1081.

Hewes, C.D., Reiss, C.S., Kahru, M., Mitchell, B.G., Holm-Hansen, O., 2008. Control of phytoplankton biomass by dilution and mixed layer depth in the western Weddell-Scotia Confluence. Marine Ecology-Progress Series 366, 15-29.

Holm-Hansen, O., Hewes, C.D., Villafane, V.E., Helbling, E.W., Silva, N., Amos, T., 1997. Distribution of phytoplankton and nutrients in relation to different water masses in the area around Elephant island, Antarctica. Polar Biology 18 (2), 145-153.

Hudson, R.J.M., Rue, E.L., Bruland, K.W., 2003. Modeling complexometric titrations of natural water samples. Environmental Science and Technology 37 (8), 1553-1562.

Ibisanmi, E., Sander, S.G., Boyd, P.W., Bowie, A.R., Hunter, K.A., 2011. Vertical distributions of iron-(III) complexing ligands in the Southern Ocean. Deep Sea Research Part II: Topical Studies in Oceanography 58 (21-22), 2113-2125.

Johnson, K.S., Elrod, V., Fitzwater, S., Plant, J., Boyle, E., Bergquist, B., Bruland, K., Aguilar-Islas, A., Buck, K., Lohan, M., Smith, G.J., Sohst, B., Coale, K., Gordon, M., Tanner, S., Measures, C., Moffett, J., Barbeau, K., King, A., Bowie, A., Chase, Z., Cullen, J., Laan, P., Landing, W., Mendez, J., Milne, A., Obata, H., Doi, T., Ossiander, L., Sarthou, G., Sedwick, P., Van den Berg, S., Laglera-Baquer, L., Wu, J.-f., Cai, Y., 2007. Developing standards for dissolved iron in seawater. Eos Trans. AGU 88 (11).

Kaufmann, R.S., Robison, B.H., Reisenbichler, K.R., Osborn, K.J., 2011. Composition and structure of macrozooplankton and micronekton communities in the vicinity of free-drifting Antarctic icebergs. Deep Sea Research Part II 58, 1469-1484.

Laglera, L.M., van den Berg, C.M.G., 2006. Photochemical oxidation of thiols and copper complexing ligands in estuarine waters. Marine Chemistry 101 (1-2), 130-140.

Laglera, L.M., van den Berg, C.M.G., 2009. Evidence for geochemical control of iron by humic substances in seawater. Limnology and Oceanography 54 (2), 610-619.

Lin, H., Rauschenberg, S., Hexel, C.R., Shaw, T.J., Twining, B.S., 2012. Chemical

speciation of iron in Antartic water surroudning free-drifting icebergs. Marine Chemistry 128-129, 81-91.

Lohan, M.C., Aguilar-Islas, A.M., Franks, R.P., Bruland, K.W., 2005. Determination of iron and copper in seawater at pH 1.7 with a new commercially available chelating resin, NTA Superflow. Analytica Chimica Acta 530 (1), 121-129.

Loscher, B.M., 1999. Relationships among Ni, Cu, Zn, and major nutrients in the Southern Ocean. Marine Chemistry 67 (1-2), 67-102.

Maldonado, M.T., Allen, A.E., Chong, J.S., Lin, K., Leus, D., Karpenko, N., Harris, S.L., 2006. Copper-dependent iron transport in coastal and oceanic diatoms. Limnology and Oceanography 51 (4), 1729-1743.

Mantoura, R.F.C., Riley, J.P., 1975. Analytical concentration of humic substances from natural-waters. Analytica Chimica Acta 76 (1), 97-106.

Measures, C.I., Hatta, M., 2012. Iron Distributions in the Antartic Peninsula. Deep Sea Research II. This issue.

Moffett, J.W., 1995. Temporal and spatial variability of copper complexation by strong chelators in the Sargasso-sea. Deep-Sea Research Part I-Oceanographic Research Papers 42 (8), 1273-1295.

Moffett, J.W., Brand, L.E., 1996. Production of strong, extracellular Cu chelators by marine cyanobacteria in response to Cu stress. Limnology and Oceanography 41 (3), 388-395.

Moffett, J.W., Brand, L.E., Croot, P.L., Barbeau, K.A., 1997. Cu speciation and cyanobacterial distribution in harbors subject to anthropogenic Cu inputs. Limnology and Oceanography 42 (5), 789-799.

Moffett, J.W., Dupont, C., 2007. Cu complexation by organic ligands in the sub-arctic NW Pacific and Bering Sea. Deep-Sea Research Part I-Oceanographic Research Papers 54 (4), 586-595.

Ndungu, K., Franks, R.P., Bruland, K.W., Flegal, A.R., 2003. Organic complexation and total dissolved trace metal analysis in estuarine waters:comparison of solvent extraction graphite furnace atomic absorption spectrometric and chelating resin flow injection inductively coupled plasma-mass spectrometric analysis.

Nolting, R.F., Debaar, H.J.W., Vanbennekom, A.J., Masson, A., 1991. Cadmium, copper and iron in the Scotia Sea, Weddel Sea and Weddel Scotia confluence (Antarctica). Marine Chemistry 35 (1-4), 219-243.

Peers, G., Quesnel, S.A., Price, N.M., 2005. Copper requirements for iron acquisition and growth of coastal and oceanic diatoms. Limnology and Oceanography 50 (4), 1149-1158.

Peers, G., Price, N.M., 2006. Copper-containing plastocyanin used for electron transport by an oceanic diatom. Nature (441), 341-344.

Quigg, A., Reinfelder, J.R., Fisher, N.S., 2006. Copper uptake kinetics in diverse marine phytoplankton. Limnology and Oceanography 51 (2), 893-899.

Ružić, I., 1982. Theoretical aspects of the direct titration of natural-waters and its information yield for trace-metal speciation. Analytica Chimica Acta 140 (1), 99-113.

Sander, S.G., Hunter, K.A., Harms, H., Wells, M., 2011. Numerical Approach to Speciation and Estimation of Parameters Used in Modeling Trace Metal Bioavailability. Environmental Science & Technology 45 (15), 6388-6395.

Scatchard, G., 1949. The attractions of proteins for small molecules and ions. Annals of the New York Academy of Sciences (51), 660-672.

Selph, K.E., Apprill, A., Measures, C.I., Brown, M.T., 2012. Phytoplankton distributions in the Shackleton Tranverse Ridge/Elephant Island region of the Drake Passage in February-March 2004. This issue.

Semeniuk, D.M., Cullen, J.T., Johnson, W.K., Gagnon, K., Ruth, T.J., Maldonado, M.T., 2009. Plankton copper requirements and uptake in the subarctic Northeast Pacific Ocean. Deep-Sea Research Part I-Oceanographic Research Papers 56 (7), 1130-1142.

Shank, G.C., Skrabal, S.A., Whitehead, R.F., Kieber, R.J., 2004. Strong copper complexation in an organic-rich estuary: the importance of allochthonous dissolved organic matter. Marine Chemistry 88 (1-2), 21-39.

Skrabal, S.A., Donat, J.R., Burdige, D.J., 1997. Fluxes of copper-complexing ligands from estuarine sediments. Limnology and Oceanography 42 (5), 992-996.

Smith, K.L., Robison, B.H., Helly, J.J., Kaufmann, R.S., Ruhl, H.A., Shaw, T.J., Twining, B.S., Vernet, M., 2007. Free-drifting icebergs: hot spots of chemical and biological enrichment in the Weddell Sea. Science 317, 478-482.

Sunda, W.G., Lewis, J.A.M. 1978. Effect of Complexation by Natural Organic-Ligands on Toxicity of Copper to a Unicellular Alga, Monochrysis-Lutheri. Limnology and Oceanography 23 (5), 870-876.

Turner, D.R., Whitfield, M., Dickson, A.G., 1981. The equilibrium speciation of dissolved components in fresh-water and seawater at 25-degrees-C and 1 atm pressure. Geochimica Et Cosmochimica Acta 45 (6), 855-881.

van den Berg, C. M. G., 1982. Determination of copper complexation with natural organic ligands in seawater by equilibrium with MnO_2: I. Theory. Analytica Chimica Acta (11), 307-312.

van den Berg, C.M.G., 1987. Organic Complexation and its Control on the Dissolved Concentrations of Copper and Zinc in the Scheldt Estuary. Estuarine, Coastal and Shelf Science 24 (6), 785-797.

van den Berg, C.M.G., Donat, J.R., 1992. Determination and data evaluation of copper complexation by organic ligands in sea water using cathodic stripping voltammetry at varying detection windows. Analytica Chimica Acta 257 (2), 281-291.

Vink, S., Boyle, E.A., Measures, C.I., Yuan, J., 2000. Automated high resolution determination of the trace elements iron and aluminum in the surface ocean using a towed Fish coupled to flo injection analysis. Deep Sea Research Part I 47 (6), 1141-1156.

Wiramanaden, C.I.E., Cullen, J.T., Ross, A.R.S., Orians, K.J., 2008. Cyanobacterial copper-binding ligands isolated from artificial seawater cultures. Marine Chemistry 110 (1-2), 28-41.

Chapter 3

Distinct pools of dissolved iron-binding ligands in the surface and benthic boundary layer of the California Current

1. Abstract

Organic dissolved iron-binding (dFe) ligands were measured by competitive ligand exchange-adsorptive cathodic stripping voltammetry (CLE-ACSV) at multiple analytical windows (side reaction coefficient of salicylaldoxime, $\alpha_{\mathrm{Fe(SA)_2}}$ = 30, 60, and 100) in surface and benthic boundary layer (BBL) samples along the central California coast during spring and summer. The weakest ligands were detected in the BBL at the lowest analytical window with average log $K^{\mathrm{cond}}_{\mathrm{FeL,Fe'}}$ = 10.2$\pm$0.4 in the summer and 10.8$\pm$0.2 in the spring. Between 3% and 18% of the dissolved iron complexation in the BBL was accounted for by humic-like substances, which were measured separately in samples by ACSV and may indicate a source of dFe-binding ligands from San Francisco Bay. The strongest ligands were found in nearshore spring surface waters at the highest analytical window with average log $K^{\mathrm{cond}}_{\mathrm{FeL,Fe'}}$ = 11.9$\pm$0.3, and the concentrations of these ligands declined rapidly offshore. The ligand pools in the surface and BBL waters were distinct from each other based on principal components analysis, with variances in the BBL ligand pool explained by sample location and variance in surface waters explained by water mass. The use of multiple analytical window analysis elucidated several distinct iron-binding ligand pools, each with unique distributions in the central California Current system.

2. Introduction

Dissolved iron (dFe) concentrations in coastal oceanic surface waters are relatively low (generally < 0.5 nmol L^{-1}, Johnson et al. 1997; Biller et al. 2013). This is due to biological uptake (Johnson et al. 2007) and the low solubility of dFe in seawater (Hudson et al. 1992). The presence of organic dFe-binding ligands has been shown to increase the solubility of dFe in seawater (Rue and Bruland 1995; Wu and Luther 1995), but their sources and sinks are still not well known (*see* reviews by Hunter and Boyd 2007; Gledhill and Buck 2012). In general, strong dFe-binding ligands (L_1, log $K^{\mathrm{cond}}_{\mathrm{FeL,Fe'}} \geq 12.0$) measured in the surface ocean are thought to be biologically produced (Hunter and Boyd 2007; Gledhill and Buck 2012) and may play an important role in the biologically labile pool of dFe, although weaker dFe-ligand complexes (L_2, log $K^{\mathrm{cond}}_{\mathrm{FeL,Fe'}} < 12.0$) may be more bioavailable (Hutchins and Bruland 1994; Poorvin et al. 2011).

Weak ligand sources may include photochemical degradation of strong ligands in the surface ocean (Barbeau 2006), biological products (Hutchins and Bruland 1994; Boyd et al. 2010; Hassler et al. 2011), humic-like substances (HS) (Laglera and van den Berg 2009), and diffusive fluxes from sediment pore waters and resuspended sediment material (Skrabal et al. 1997; Jones et al. 2011). However, dFe complexation is thought to be governed by stronger ligands in surface waters (Rue and Bruland 1995; *see* review by Hunter and Boyd 2007) while weaker complexes dominate the deep ocean 'ligand soup' (Hunter and Boyd 2007).

The central and northern California Current (CC) has been well studied with

respect to seasonal dFe dynamics (Johnson et al. 1999; Elrod et al. 2004, 2008; Biller et al. 2013). The CC is an eastern boundary upwelling system, with high primary productivity along the coast generally coinciding with seasonal upwelling events (Bruland et al. 2001). These periodic upwelling events may bring elevated concentrations of macronutrients (nitrate, phosphate, silicate) without a corresponding adequate increase in dFe (Bruland et al. 2001; Johnson et al. 2001; Biller et al. 2013), leading to varying degrees of iron stress in the phytoplankton community (Hutchins et al. 1998; King and Barbeau 2011).

In previous studies, the highest dFe and dissolvable Fe (weak acid labile) were found just after the onset of upwelling (Elrod et al. 2004, 2008; Chase et al. 2005; Biller et al. 2013), with fine grained sediments deposited from rivers during winter storms as a significant source of the dissolved and particulate Fe (Elrod et al. 2008). These mud-belt shelf sediments are rich in organic carbon and Fe (Homoky et al. 2012) and data from flux chambers (Berelson et al. 2003; Elrod et al. 2004) show a correlation between dFe fluxes and organic matter degradation suggesting the Fe-rich deposits underlying the benthic boundary layer (BBL; Johnson et al. 1999) are organic in nature. Buck et al. (2007) found high concentrations of dFe-binding ligands in one BBL sample near San Francisco Bay, and it has subsequently been shown in a study of the Satilla River Estuary in the southeastern US that sediment pore waters can be a source of dFe and ligands to the water column (Jones et al. 2011). Organic ligands may, thus, play a significant role in remobilizing upwelled dFe-rich BBL material in the CC region and in determining its availability to phytoplankton in the surface ocean. Several studies have also characterized the distribution and in situ dynamics of dFe-binding organic ligands in the surface waters

of the CC (Macrellis et al. 2001; Buck et al. 2007, King et al. 2012).

The purpose of this study was to investigate seasonal characteristics of both stronger and weaker dFe-binding ligands in the northern and central CC, with emphasis on surface waters vs. the BBL over the mid-shelf mud-belts (50 to 90 m deep). DFe-binding ligands were measured by competitive ligand exchange-adsorptive cathodic stripping voltammetry (CLE-ACSV) using multiple concentrations of the added ligand salicylaldoxime (SA), to create a range of competition strengths of the added ligand, defined as multiple analytical windows (MAWs). This methodology allows the detection of a wider range of dFe-binding ligand classes than is determined in a single window. This MAW CLE-ACSV approach has been employed for copper (Cu) speciation studies (Bruland et al. 2000) in estuarine (Moffett et al. 1997; Buck and Bruland 2005; Ndungu 2012) and coastal environments (van den Berg et al. 1990; van den Berg and Donat 1992; Bundy et al. 2013), though it has not yet been applied to Fe speciation studies. Recently, 'reverse' titrations have been employed in one study to assess tightly bound dFe fractions not typically exchangeable with SA (Hawkes et al. 2013).

Previous studies report an overlapping range of conditional stability constants ($\log K^{\mathrm{cond}}_{\mathrm{FeL_x,Fe'}}$) of dFe-binding ligands detected by CLE-ACSV in the marine environment (9.6-13.9; *see* review by Gledhill and Buck 2012, their table 1), confounding the distinction between the stronger 'L_1' and weaker 'L_2' ligand classes. This makes the interpretation of the sources and sinks of dFe-binding organic ligands in the environment difficult. The overlapping range also suggests that there may be additional ligand classes present in seawater. This study aimed to detect a wider range of dFe-binding ligand classes in surface and BBL waters using MAW analyses in the spring and summer off

northern and central California. Surface waters, hypothesized to contain the strongest dFe-binding ligands, and BBL waters suspected to contain organic degradation products and/or terrestrial humic-like substances, were intended to represent two end-members in ligand composition for which to verify MAW analyses for dFe-binding ligands.

3. Methods

3.1 Sampling

Surface and BBL samples for this study were collected on the R/V *Point Sur* in May 2010 (spring) and August and September 2011 (summer) off the coast of northern and central California (Fig. 3.1). All BBL stations during the August and September 2011 cruise were also sampled in the surface, while only a subset of BBL stations were sampled in surface waters during the May 2010 cruise (Fig. 3.1). Trace metal clean samples from the BBL in May 2010 and August 2011 were collected using Teflon-coated 8 liter GO-Flo bottles (General Oceanics) suspended on a Kevlar line and triggered with Teflon messengers. Hydrographic data was collected using the ship's rosette system, which contained a conductivity, temperature and depth (CTD) sensor as well as a fluorometer, dissolved oxygen sensor and transmissometer. The BBL sampling locations were determined based on the local maximum in beam attenuation within 10 meters of the ocean bottom along with a higher salinity and lower temperature feature, obtained from a CTD cast immediately preceding the GO-Flo cast. An attempt was made to obtain the GO-Flo sample approximately 5 meters off the bottom within the BBL. Nitrate and silicic acid data for the GO-Flo sample was also used to compare with the preceding CTD cast to ensure the sample was within the BBL. For additional details on hydrographic and trace metal sampling, *see* Biller et al. (2013). Surface samples on both

cruises were obtained from a trace metal clean towed 'fish' (Bruland et al. 2005) plumbed through clean Teflon tubing into a clean van for sample collection. All dissolved samples were filtered through Acropak 200 capsule filters (0.2 μm, VWR International) into bottles that had been cleaned by both nitric acid (HNO_3^-; trace metal grade, Fisher Scientific) and hydrochloric acid (HCl; trace metal grade, Fisher Scientific). Samples for total dFe were filtered into 125 mL low density polyethylene bottles (LDPE, Nalgene) and subsequently acidified to pH 2 (Johnson et al. 2007; Lohan et al. 2006). Samples collected for dFe speciation were filtered into 500 mL fluorinated polyethylene bottles (FLPE, Nalgene) and either kept at 4°C for 'fresh' analyses shipboard (within 1-3 days) or frozen at -20°C for later analysis (1-2 months) in the lab.

3.2 Chlorophyll a and nutrient analyses

Nutrients were analyzed shipboard using a Lachat QuickChem 800 Flow Injection Analysis System following standard colorimetric methods (*see* Biller et al. 2013). Samples were analyzed for nitrate + nitrite (herein referred to as nitrate, NO_3^-), phosphate (PO_4^{3-}), and silicic acid ($Si(OH)_4$) on surface transects as well as from GO-Flo bottles (*see* Biller et al. 2013). Chlorophyll *a* was calculated from in situ fluorescence based on a calibrated underway data acquisition (UDAS) fluorometer (SeaBird Electronics).

3.3 Dissolved Fe totals

DFe totals were determined shipboard using flow injection analysis (FIA) as described previously by Lohan et al. (2006) and in detail for this study by Biller et al. (2013). Samples were acidified to pH 2 immediately after collection using quartz-distilled HCl (Optima, Fisher Scientific) and were allowed to sit for two hours prior to analysis. Blank measurements using this method were 0.048 ± 0.009 nmol kg^{-1} (n=18),

and the detection limit (three times the standard deviation of the blank) was 0.026 nmol kg^{-1}. As quality control, the analysis of Sampling and Analysis of Fe (SAFe) standards (Johnson et al. 2007) were completed during the cruise. The results for dFe during the May 2010 cruise were surface (S): 0.095 ± 0.006, deep (D2): 0.93±0.07 (*n*=11) and for the August 2011 cruise were S: 0.094 ± 0.008 nmol kg^{-1}, D2: 0.94 ± 0.06 nmol kg^{-1} (*n*=18) (Biller et al. 2013). These values are in the range of the current consensus values as of May 2013 of S: 0.093 ± 0.008 nmol kg^{-1} and D2: 0.93 ± 0.02 nmol kg^{-1} (http://www.geotraces.org/science/intercalibration/322-standards-and-reference-materials). A subset of samples were also analyzed using a new multi-element method developed by Biller and Bruland (2012) to compare with FIA results, and good agreement was seen between methods (Biller et al. 2013).

3.4 Dissolved Fe speciation

Dissolved Fe organic speciation was measured using CLE-ACSV with salicylaldoxime (SA) as the competing ligand (Rue and Bruland 1995; Buck et al. 2007), using multiple analytical windows (MAWs, *see* description below). All summer samples and a subset of spring samples were analyzed with MAWs ($\alpha_{\mathrm{Fe(SA)_2}}$= 30, 60, 100) with a single titration at each window; remaining spring samples were analyzed in triplicate at $\alpha_{\mathrm{Fe(SA)_2}}$= 60 only. For the titrations, 10 mL aliquots of each dissolved Fe speciation sample were pipetted into 10 separate Teflon vials that had been pre-conditioned with the added dFe concentrations used in this study. A 1.5 mol L^{-1} boric acid (> 99.99%, Alfa Aeasar) buffer was prepared in 0.4 mol L^{-1} NH_4OH (Optima, Fisher Scientific) and 50 μl was added to each vial (7.5 mmol L^{-1} final concentration, pH 8.2). Eight of the 10 aliquots were then spiked with Fe from a 100 nmol L^{-1}, 200 nmol L^{-1}, 1 μmol L^{-1}, 2 μmol

L^{-1}, or 10 μmol L^{-1} secondary standard that had been diluted from an AA standard (CertiPrep) into pH 1.8 ultra clean water (Milli-Q water, >18 mol L^{-1} Ω cm) to obtain a final concentration ranging from 0.25-100 nmol L^{-1}. The added Fe was then left to equilibrate with the natural ligands for at least 2 hours, and up to 8 hours. The appropriate concentration of the competing ligand was added ($\alpha_{Fe(SA)_2}$ of 30, 60, or 100) following the 2 hour equilibration period with the added iron, and left to equilibrate an additional 15 minutes for the highest analytical window ($\alpha_{Fe(SA)_2}$=100), and t 30 minutes for the lower analytical windows ($\alpha_{Fe(SA)_2}$=30, 60). Each Teflon cup was then run separately using a controlled growth mercury electrode (CGME, BAS*i*) interfaced with an analyzer (E2, Epsilon) and a laptop computer using adsorptive cathodic stripping voltammetry (ACSV) as described in detail elsewhere (Rue and Bruland 1995; Buck et al. 2007, 2010). The calibration of the side reaction coefficient ($\alpha_{Fe(SA)_2}$) for SA has been completed previously according to Rue and Bruland (1995) with corrections for salinity as described in Buck et al. (2007).

3.5 Sensitivity determination

The sensitivity (defined as nA nmol L^{-1} s^{-1}) for all samples was determined by internal calibration from the linear portion of the titration curve at the end of the titration, where it is assumed all ligands are saturated with added dFe. The internally calibrated sensitivity was compared to the sensitivity determined by 'overload titration' (Kogut and Voelker 2001) for BBL samples to ensure an accurate sensitivity due to the high organic matter content and potential presence of HS in BBL samples. 'Overload titrations,' as described by Kogut and Voelker (2001) are an additional method for determining the sensitivity in coastal seawater samples. These titrations are completed at high analytical

windows (high $\alpha_{\mathrm{Fe(SA)_2}}$) in order to completely outcompete the natural ligands present in the sample. This method also uses an internally calibrated sensitivity, but ensures that the ligands are fully titrated by outcompeting them (Kogut and Voelker 2001). This is a concern in coastal samples, because HS have been shown to have measured effects on the sensitivity in CSV analyses using SA (Laglera and van den Berg 2011), and could lower the internal sensitivity. The internal calibrations and overload titrations were also compared to the sensitivity determined in ultra violet (UV)-irradiated seawater (UVSW, made from UV-irradiating BBL sample at Sta. 10 in the summer 2011) with 22 μg L^{-1} HS subsequently added (Suwannee River fulvic acid standard; SRFA International Humic Substances Society, IHSS) to determine the effect of HS on the sensitivity determinations (Laglera and van den Berg 2011). First, 22 μg L^{-1} HS were added to UVSW and titrated with 0, 1, 5 and 10 nmol L^{-1} of added Fe and the sensitivity determined from the linear portion of the titration curve, as in the internal sensitivity calculation. Iterative sensitivity determinations have also been used in recent studies to address the issues associated with high organic content samples (Hudson et al. 2003; Wu and Jin 2009), but they may over-estimate the sensitivity in some cases (Laglera et al. 2013). This study chose to compare internal calibrations, overload titrations and UVSW titrations with HS for determining the most accurate sensitivity for the seawater matrix in this coastal region.

3.6 Multiple analytical window analysis

DFe speciation samples were analyzed using CLE-ACSV with MAWs of the added competing ligand (SA). The analytical windows employed were determined based on the estimated side reaction coefficients (i.e., carrying capacity) of the ambient ligand pool (α_L) and that of the competing ligand ($\alpha_{Fe(SA)_2}$). When the ratio of these two side

reaction coefficients ($\log\alpha_{\mathrm{L}}/\log\alpha_{\mathrm{Fe(SA)_2}}$) is between 1-10, then the chosen analytical window is appropriate for detecting that ligand class (van den Berg and Donat 1992; Ibisanmi et al. 2011). The side reaction coefficient, α, is determined by:

$$\alpha_{\mathrm{L}} = 1 + \sum_{\mathrm{i}}^{\mathrm{n}}([\mathrm{L}]^{\mathrm{n}} \times K^{\mathrm{cond}}_{\mathrm{FeL_n,Fe'}}) \quad (1)$$

where [L] is the concentration of the ligand (natural or competing) and $K^{\mathrm{cond}}_{\mathrm{FeL_n,Fe'}}$ is the conditional stability constant. For SA, the $K^{\mathrm{cond}}_{\mathrm{FeL_n,Fe'}}$ is noted as $\beta^{\mathrm{cond}}_{\mathrm{SA_2,Fe'}}$ since SA is thought to form an electroactive bis complex with Fe as experimentally determined by Rue and Bruland (1995) and Buck et al. (2007) at a concentration of 25-27.5 μmol L^{-1} SA ($\alpha_{\mathrm{Fe(SA)_2}}$ = 60-75). A separate calibration of SA was completed here for the relevant concentrations of SA (17-32 μmol L^{-1}), and was not found to differ substantially from Buck et al. (2007). The $\beta^{\mathrm{cond}}_{\mathrm{SA_2,Fe'}}$ determined by the Buck et al. (2007) calibration was therefore used for all determinations of $\alpha_{\mathrm{Fe(SA)_2}}$ in this study. This work aimed to detect both strong and weak dFe-binding ligands, and thus a range of detection windows were used in the surface and BBL. The $\alpha_{\mathrm{Fe(SA)_2}}$range of 30-100 was chosen to ensure the competing ligand would still outcompete the strong inorganic side reactions for Fe ($\alpha_{\mathrm{Fe'}}$=10) on the low [SA] end, but not too strong to completely outcompete all natural ligands at the high end (Rue and Bruland 1995). A $\log\alpha_{\mathrm{L}}/\log\alpha_{\mathrm{Fe(SA)_2}}$ from 1-10 was determined in all titrations except one (ratio equal to 10.15, data not shown), ensuring that the analytical windows chosen were appropriate for the ambient ligand pool present in the samples (van den Berg and Donat 1992; Ibisanmi et al. 2011).

3.7 Dissolved humic-like substance analyses

Determination of dissolved humic-like substances (HS) was completed by ACSV analysis as described above for dFe speciation titrations but fine-tuned for HS determination with the modifications described by Laglera and van den Berg (2007). Briefly, boric acid buffer (pH 8.2, NBS) and dFe was added to each 10 mL aliquot of the sample to sufficiently saturate the excess Fe-binding HS (20-50 nmol L^{-1} Fe). Several concentrations (5-300 μg L^{-1}) of Suwannee River Fulvic Acid Standard (SRFA, 20 mg L^{-1} stock solution) were then added to five of the aliquots and 3 aliquots had no added HS. The Fe and HS additions were then equilibrated for at least 2 hours. Immediately before analysis, 400 μl of 0.4 mol L^{-1} potassium bromate (> 99%, VWR) was added as an oxidative catalyst for the reaction, and each aliquot was analyzed as described by Laglera and van den Berg (2007) at a -0.1 V deposition potential, with a 50 mV s^{-1} scan rate in linear sweep mode. The concentration of HS in samples was determined by the standard addition method, and the resulting concentrations determined in each sample represent humic-like substances that contribute to the observed electrochemical peak at -0.6 V.

3.8 Dissolved Fe speciation data processing

Several advanced numerical methods exist for processing complex ligand data (Hudson et al. 2003; Garnier et al. 2004; Wu and Jin 2009) and one using MAWs (Sander et al. 2011), but to date none of these methods are publicly available. An intercomparison of data processing methods is currently underway (S. G. Sander unpubl.), but another recent intercomparison effort found reasonable agreement in open ocean samples between the method used here and the Gerringa et al. (1995) non-linear method (Buck et al. 2012). Recent numerical methods have used only simulated titration data (Garnier et al. 2004; Wu and Jin 2009) or data from estuaries, which likely contain a much larger

continuum of binding capacities (Hudson et al. 2003; Sander et al. 2011). Most methods agree in the detection of L_1 (log $K^{cond}_{FeL,Fe'} \geq 12.0$), although some discrepancy exists in the detection of L_2 due to underestimations of the sensitivity (Wu and Jin 2009; Ibisanmi et al. 2011). Extra care was taken in this study to determine an accurate sensitivity in BBL samples, where sensitivity underestimation is likely to be a problem. Ligand concentrations and conditional stability constants were determined using averages and standard deviations of both van den Berg-Ružić linearizations (Ružić 1982; van den Berg 1982) and Scatchard linearizations (Scatchard 1949; Mantoura and Riley 1975; Buck et al. 2012). Ligand classes were then characterized simply by their log $K^{cond}_{FeL,Fe'}$, in order to avoid ambiguity in the literature between ligand classes defined by relative as opposed to absolute binding strengths (Gledhill and Buck 2012). 'Stronger' ligands in this study are presented as L_1 (log $K^{cond}_{FeL,Fe'} \geq 12.0$) and L_2 ($12.0 > \log K^{cond}_{FeL,Fe'} \geq 11.0$), while the 'weaker' ligand pool is represented as L_3 ($11.0 > \log K^{cond}_{FeL,Fe'} \geq 10.0$) and L_4 (log $K^{cond}_{FeL,Fe'} \leq 10.0$) ligands. These L_1 and L_2 ligand classes represent the pool of stronger dFe-binding ligands in the literature while our L_3 and L_4 represent the weaker ligand pool (Table 3.1; following the convention of Gledhill and Buck 2012). The distinction between ligand classes is operationally defined by the conditional stability constant values, so the concentration of excess ligand (*e*L, [L_x]- [dFe]) and overall complexing capacity (α_s, or the side reaction coefficient of the sample) were also determined in order to compare across analytical windows and ligand classes.

3.9 Statistical analyses

To examine relationships between all collected variables, Pearson's correlation analysis was used on the data (non-normalized). To specifically address the ligand data, a contingency table was made of the average ligand concentrations from each season and sampling location (surface and BBL at all analytical windows), based on the presence or absence of each class of ligand during that season. A ligand class was considered to be present if it was measured in at least one sample ($n \geq 1$, Table 3.3) and considered not present if it was not measured ('nd' or not detected in Table 3.3). Statistical differences in the presence or absence of ligands between seasons and sampling locations (surface and BBL) were then assessed in this contingency table using chi-squared analysis. Multivariate statistical analyses were used in order to compare associations between physical and chemical parameters. A standard principal component analysis (PCA) was used to reduce the dimensionality (number of variables) of the dataset and investigate interactions between the measured variables. For the PCA, the dataset was first scaled by the standard deviation of each variable to equally weight the contribution of each variable to the dataset. PCA was then performed on the data matrix comprised of 18 variables (latitude, longitude, depth, temperature, salinity, nitrate, phosphate, silicate, [dFe], [L_1], log K_1, [L_2], log K_2, [L_3], log K_3, [L_4], log K_4, and distance from shore) and 82 samples. Missing values in the dataset were filled using the average value for that variable at that depth and season, except for the ligand concentrations which were noted as zero if they were not detected. For example, a missing surface nutrient data point was filled with the average concentration that was determined in the surface during that season from the current dataset. There were anywhere from 0-12 missing values for a given variable within the dataset. If more than 12 data points were missing, then the variable was

excluded from the statistical analyses (i.e., chlorophyll *a*, and dissolved manganese). All statistics were deemed significant at probabilities less than 0.05 ($p < 0.05$), and were calculated using the Matlab statistics and bioinformatics toolbox.

4. Results

4.1 Hydrography and dissolved Fe distributions

In-depth dFe and hydrographic results are reported elsewhere (Biller et al. 2013). Temperature, salinity, chlorophyll *a* and nutrient concentrations for all stations sampled for dFe speciation are presented in Table 3.2. Macronutrient, chlorophyll *a*, and dFe data for the remaining stations can be found in Biller et al. (2013); only a subset of that data is presented here. Surface samples taken during the spring cruise had lower average temperatures (10.4±1.5 $^{\circ}$C, n=20) and higher average macronutrient concentrations (17.1±10.1 μmol L^{-1} NO_3^-, 1.3±0.6 μmol L^{-1} PO_4^{3-} and 25.4±14.9 μmol L^{-1} $Si(OH)_4$, n=20) than those sampled during the summer cruise (12.5±1.8 $^{\circ}$C, 13.5±8.0 μmol L^{-1} NO_3^-, 1.3±0.6 μmol L^{-1} PO_4^{3-} and 17.9±14.9 μmol L^{-1} $Si(OH)_4$, n=33), likely due to intense upwelling conditions during the spring cruise (Fig. 3.1 and National Oceanic and Atmospheric Association, NOAA upwelling index, http://www.pfeg.noaa.gov/products/las.html, data not shown). Surface samples in the spring also contained relatively higher chlorophyll *a* concentrations, with 5.9±9.2 μg L^{-1} (n=20) on average in the surface waters sampled for dFe speciation compared to the summer (3.5±3.6, n=33). Chlorophyll *a* concentrations were not determined in the BBL samples. BBL conditions were similar during both cruises, with similar average NO_3^- (29.8±1.1, n=12 and 30.0±3.7 μmol L^{-1} NO_3^-, n=17) and temperatures (8.3±0.3, n=12 and 9.4±1.0°C, n=17) in the spring and summer, respectively. The PO_4^{3-} and $Si(OH)_4$

concentrations were similar for BBL samples during the spring and summer cruise, but BBL samples on average contained higher concentrations of both PO_4^{3-} (2.3±0.1 μmol L^{-1}, n=12; 2.6±0.3 μmol L^{-1}, n=17) and $Si(OH)_4$ (47.6±3.4 μmol L^{-1}, n=12; 44.7±10.0 μmol L^{-1}, n=17) relative to surface samples in the spring and summer, respectively.

The highest NO_3^- concentrations measured in the surface waters during both cruises were observed north of San Francisco Bay off Point Reyes, Point Arena, and Cape Mendocino (Fig. 3.2C, D). This region generally correlated with higher chlorophyll *a* concentrations as observed from satellite (Fig. 3.1C, D, CoastWatch Aqua MODIS), and from underway measurements (Table 3.2). These areas also corresponded to the some of the highest dFe concentrations ([dFe], Fig. 3.2A, B) and lowest temperatures (Fig. 3.1, Table 3.2) observed. Higher [dFe] were measured on average in the surface during the spring (Biller et al. 2013). Similar [dFe] were found between seasons in the BBL, with higher concentrations observed in some repeat sampling locations in the spring and vice versa in the summer (Biller et al. 2013). In the BBL, the highest dFe and NO_3^- concentrations were also observed north of San Francisco Bay (Fig. 3.3) during both cruises. Relatively lower [dFe] and NO_3^- were observed south of Monterey Bay, along the narrow Big Sur coastline (Wheatcroft et al. 1997), also corresponding to lower average chlorophyll *a* concentrations (Fig. 3.1C, D).

4.2 Sensitivity determinations for ACSV measurements

The sensitivities (nA nmol L^{-1} s^{-1}) in all surface samples were determined by internal calibration (Rue and Bruland 1995) from the linear portion of the titration curve, where it is assumed that all ligands have been titrated by the excess dFe additions. Internally measured sensitivities in BBL samples were then compared to two other

methods to ensure accurate determination of the sensitivity. An $\alpha_{Fe(SA)_2}$ of 251 and 500 were employed in 'overload' titrations (Kogut and Voelker 2001; Table 3.3), and these $\alpha_{Fe(SA)_2}$ were estimated to be outside the analytical window for the ligand pool in the BBL based on the ratio of $\log\alpha_L/\log\alpha_{Fe(SA)_2}$. The sensitivities determined by 'overload' titration were less than the average sensitivity determined by internal calibration at all analytical windows employed in the sample analyses, but the differences were not statistically significant ($\alpha_{Fe(SA)_2}$ of 30, 60, and 100; *t*-test, *t*= 0.16, degrees of freedom (df) = 28 , $p > 0.05$). The average sensitivity determined by internal calibration at $\alpha_{Fe(SA)_2}$ =30, 60, and 100 was 1.27$\pm$0.88 (*n*=29), 1.28$\pm$0.80 (*n*=45), and 0.82$\pm$0.39 (*n*=28), respectively. Using an $\alpha_{Fe(SA)_2}$= 500 (*n*=1) the sensitivity determined by 'overload' titration was 0.21 nA nmol L^{-1} s^{-1} and with an $\alpha_{Fe(SA)_2}$ = 251 (*n*=4) the sensitivity was 0.66$\pm$0.20 nA nmol L^{-1} s^{-1}. These differences in sensitivity, with a lower average sensitivity at higher analytical windows, included considerable variability and were not significant ($p>0.05$).

With no statistical differences observed between internal and 'overload' sensitivities, additional sensitivity tests were performed using UVSW (a UV-irradiated sample from BBL Sta. 10 in the summer) with added HS (22 μg L^{-1}) to confirm the validity of internal calibration in the presence of HS in BBL samples, since high variability was observed. Sensitivities determined at each analytical window using UVSW and added HS were also found to be statistically indistinct from those internally calibrated in the BBL sample analyses (*t*-test; *t*=0.29, 0.27, 0.96; df=28, 44, 27; p = 0.78, 0.79, and 0.36 for $\alpha_{Fe(SA)_2}$= 100, 60, and 30 respectively).

4.3 Dissolved Fe-binding ligand distributions in surface waters

Averaged dFe speciation results, of all samples at each analytical window are presented in Table 3.3. Although the average ligand concentrations and conditional stability constants are presented for every analytical window, the detection of each ligand class was found to be optimal at specific windows based on the ratio of $\log\alpha_{L}$/ $\log\alpha_{Fe(SA)_2}$. Therefore, the distributions of each ligand class are only presented at their optimized window ($\alpha_{Fe(SA)_2}$= 100 for L_1, 60 for L_2, and 30 for L_3 and L_4; Fig. 3.4, 3.5) Similar concentrations and strengths of ligands were observed in the spring and summer in the surface waters. Chi-squared analysis based on a contingency table of the ligand data revealed there was no significant difference between the ligands observed in the spring and the summer ($p > 0.05$). Fig. 3.4 presents the distribution of average concentrations of each ligand class across both seasons in the study area.

4.3.1 Stronger ligand pool (L_1 and L_2)

Spatial distributions of the stronger ligand classes in surface waters are shown together for both cruises in Fig. 3.4 (A and B), with L_1 presented from the highest analytical window ($\alpha_{Fe(SA)_2}$=100) and L_2 presented from the middle analytical window ($\alpha_{Fe(SA)_2}$= 60). Stronger ligand concentrations were generally highest closest to shore and decreased offshore. Excess ligand concentrations ([L_x]-[dFe], *e*L) also followed this trend (data not shown). Elevated concentrations of strong dFe-binding ligands were observed just outside the mouth of San Francisco Bay (4.8 and 7.5 nmol L^{-1}), near Point Reyes (10.2 nmol L^{-1}), and south of Cape Mendocino (7.3 nmol L^{-1}). These ligand concentrations were among the highest observed in surface waters. The strongest ligands

(L_1) were not observed in any of the offshore stations (Fig. 3.4A), though L_2 ligands were detected at almost all stations and in fact were the most common ligand class detected in surface waters. The complexation capacity generally decreased offshore as the concentrations of the strongest ligands declined (Table 3.3). Although the observations were patchy between cruises, in general the highest concentrations and strongest ligands were found closest to shore in the northern part of the study region, and near the mouth of San Francisco Bay.

4.3.2 Weaker ligand pool (L_3 and L_4)

The highest concentrations of weaker ligands (L_3 and L_4) in surface waters were measured at the lowest analytical window ($\alpha_{Fe(SA)_2}$=30), the window optimized for weaker ligand detection. The average concentrations of L_3 ligands were similar between the spring and summer (4.6±2.9 nmol L^{-1}, *n*=10 in spring and 5.0±2.4 nmol L^{-1}, *n*=13 in summer; Table 3.3) and chi-squared analysis based on the frequency of L_3 detections in both seasons showed there was no significant difference between the two seasons ($p > 0.05$). The L_3 ligands in the weaker ligand pool showed a distinct spatial distribution (Fig. 3.4C) compared to the stronger ligand pool (L_1 and L_2, Fig. 3.4A and B). While the stronger ligands generally declined offshore, higher concentrations of L_3 ligands were detected in the furthest offshore stations. The L_4 ligands, or the weakest ligands in the observed ligand pool, were not detected at all in surface waters during the spring, and only 3 surface samples contained L_4 ligands during the summer cruise (Table 3.3). Their concentrations were highly variable (ranging from 6-140 nmol L^{-1}), and were only found in two stations near the mouth of San Francisco Bay (Fig. 3.1B), and north of Cape

Mendocino (Fig. 3.1, 4D). No L_4 ligands were detected in surface waters offshore from the continental shelf.

4.4 Dissolved Fe-binding ligand distributions in the BBL

4.4.1 Stronger ligand pool (L_1 and L_2)

The strongest ligands (L_1) were only detected at the two highest analytical windows ($\alpha_{Fe(SA)_2}$ = 100, 60) in the BBL and were detected less frequently in the BBL compared to the surface waters. The concentrations of L_1 were higher in spring (16.2±1.1 nmol L^{-1}, *n*=3; Table 3.3) than in the summer (13.6±9.6 nmol L^{-1}, *n*=4 at $\alpha_{Fe(SA)_2}$=100 and 7.2±2.5 nmol L^{-1}, *n*=2 at $\alpha_{Fe(SA)_2}$=60; Table 3.3) though not significantly so (chi-squared, $p > 0.05$). The strongest ligands were not detected in all BBL samples, and were found most frequently in samples surrounding San Francisco Bay and Point Arena (Fig. 3.5, $\alpha_{Fe(SA)_2}$ = 100). The L_2 ligands were detected much more frequently in the BBL compared to L_1 ligands (*n*=9 in spring and summer for L_1 vs. *n*=55 for L_2), and were found at every analytical window during both seasons (Table 3.3). In general, higher concentrations of L_2 ligands were measured in the spring than in the summer, but not significantly so (chi-squared, $p > 0.05$). The concentrations of L_2 ligands were highest in the areas with the highest [dFe] in the BBL (Fig. 3.5, $\alpha_{Fe(SA)_2}$ = 60), but were present in all of the sampling regions. Relatively high concentrations of stronger ligands in the BBL lead to higher complexation capacities in these samples than in surface waters (Table 3.3).

4.4.2 Weaker ligand pool (L_3 and L_4)

While weaker ligands were most commonly detected at the lower analytical windows during the spring and summer within the BBL (Table 3.3), two samples had detectable L_3 ligands at even the highest analytical window. High variability was seen during both seasons in the concentrations of L_3 and L_4 ligands in the BBL (standard deviations up to 67%, Table 3.3). The L_3 ligand class was detected in BBL samples from all regions of the study area, including the shelf areas outside of San Francisco Bay, Point Arena, Cape Mendocino, and Big Sur (Fig. 3.5, $\alpha_{\mathrm{Fe(SA)_2}}$ = 30). Higher [L_3] generally coincided with higher [dFe], and [L_3] was always in excess of [dFe]. The L_4 ligand class showed a distinct distribution compared to all the other ligand classes. L_4 ligands were only detected in 5 samples in the BBL (Table 3.3), and all of these samples were within the San Francisco Bay region or the Cape Mendocino region (Fig. 3.5, $\alpha_{\mathrm{Fe(SA)_2}}$ = 30). The [L_4] were within the range observed for L_3 ligands in the BBL (14-21 nmol L^{-1}) and showed similar variability (50-70% standard deviations), but were detected less frequently in BBL samples.

4.4.3 Dissolved humic-like substances

Dissolved HS were measured in two BBL samples during the summer cruise in 2011 at Sta. 10 and 37 (10: 40.767° N, 124.386°W; 37: 37.418°N, 122.611°W) in order to determine the influence of HS on the Fe-binding ligand pool in the BBL. Sta. 10 was located on the continental shelf near Cape Mendocino at 64 m depth and Sta. 37 was sampled just south of San Francisco Bay at the same depth. Sta. 10 contained higher concentrations of dFe (20.5±0.3 nmol L^{-1}) than Sta. 37 (6.8±0.1 nmol L^{-1}), but less HS. There was 22.6 μg L^{-1} HS measured at Sta. 10, and 39.2 μg L^{-1} HS at Sta. 37 outside of San Francisco Bay. The concentration of HS was related to the Fe complexation by

assuming all the measured HS was complexed to dFe. Previous researchers have shown that HS can bind approximately 32 nmol L^{-1} Fe per 1 mg of HS (Laglera and van den Berg 2009), though this can be variable depending on the type and batch of HS (Laglera and van den Berg 2009). Using the approximation of 32 nmol L^{-1} Fe:1 mg HS, approximately 3.5% of the dFe at Sta. 10 can be bound by HS and 18.5% at Sta. 37 outside of San Francisco Bay. This would also amount to 4.3% and 11.1% of the total ligand pool (only L_2 was detected in these samples), respectively.

4.5 Statistical analyses

Pearson's correlation analysis revealed that very few of the ligand parameters correlated linearly with any other variable examined in the dataset (data not shown). To examine these relationships further, several additional statistical techniques were examined. No significant differences in ligands were found between seasons based on chi-squared analysis, but there was a significant difference between the presence of ligands in the surface and BBL based on the contingency table (chi-squared, $p < 0.025$). PCA was applied to quantify the differences seen between samples in the chi-squared analysis. The 18 variables used in the PCA are shown in Table 3.4, along with their principal component (PC) loadings (eigenvectors) for the first three PCs (Table 3.4). The PCs are linear combinations of the variables that explain the greatest variance in the dataset (with the first PC explaining the most variance). The first three PCs explained 57% of the variance in the dataset, and the first two explained 46% (data not shown). The first PC was dominated by loadings from temperature, [dFe], NO_3^-, PO_4^{3-} and $Si(OH)_4$, as can be seen by the magnitude of their eigenvectors (suggesting greater influence on the first PC) in Table 3.4 and also their distance to the right or left of the vertical '0' axes in

Fig. 3.6A. The variables depth, distance from shore, and salinity contributed to the first PC as well, but to a lesser extent (Fig. 3.6A). In the first PC, the temperature and distance from shore were inversely related to the [dFe], nutrients and salinity. The second PC consisted of strong loadings from several of the ligand parameters. The strongest loadings were from L_1, log K_1, L_4, and log K_4, and inversely related to these but also with strong loadings were L_3, log K_3, and latitude. The contribution of L_2, log K_2, and longitude were similar in magnitude for each PC but opposite in sign, with all three variables showing positive loadings for the second component and negative loadings for the first PC. The third PC was similar to the second, but had strong loadings from latitude that were negatively correlated with L_3 and log K_3, as well as longitude and L_1 and logK_1 (Fig. 3.6B).

When all of the data (surface and BBL, n=82) are plotted in the PC space, there is a clear grouping of surface and BBL samples (Fig. 3.6C, D). Surface samples group along the positive axis of the first PC, where the variance is strongly related to temperature and distance from shore (Fig. 3.6C). BBL samples group more along the second PC in the lower left quadrant, where the variance is related to depth, salinity, nutrients (macronutrients and dFe), and L_3 (Fig. 3.6C). The addition of the third PC does not change the position of the surface samples in the PC space, but does shift more of the BBL samples to the upper left quadrant. The variances of samples in this quadrant are also explained by L_2 and log K_2 in addition to those variables strongly related to the second PC.

5. Discussion

5.1 Multiple analytical window analysis

Current electrochemical methodology in detecting dFe-binding ligands constrains the analyst to measuring only one (or sometimes two) ligand classes. This study expands the scope of current electrochemical methods (CLE-ACSV) for detecting a wide range of dFe-binding ligands in seawater. Of the few studies that have used MAW in CLE-ACSV, all have focused on Cu speciation in estuaries (Moffett et al. 1997; Buck and Bruland 2005; Ndungu 2012), coastal environments (Bundy et al. 2013) or using numerical modeling (Sander et al. 2011). This study has extended MAW analysis to dFe speciation. Although a smaller range of ligands is generally thought to be present in seawater for Fe than for Cu (due to the propensity of Fe in seawater to form insoluble (oxy)hydroxides; Liu and Millero 2002), the detection of both weaker and stronger ligands gives insight into the quality of the ligand pool in the surface and BBL in this study. MAW analysis enabled the detection of ligands with a wide range of conditional stability constants (log $\square^{cond}_{FeL,Fe'}$ ranging from 9-13), similar to the use of MAWs in Cu organic speciation analysis (Bruland et al. 2000), though an even larger range of ligand strengths may be possible as a relatively narrow range in MAWs was employed here.

Although there was no clear pattern in the concentrations of ligands detected at each analytical window, the use of MAW highlighted the distinctions between the ligand pools in the surface and BBL. If only the $\alpha_{Fe(SA)_2}$= 60 window was used (as in most of the current electrochemical methods), subtleties in the patterns of L_1, L_3, and L_4 ligands may have been masked by not using an optimal analytical window. The contingency table produced for the chi-squared analysis revealed that certain analytical windows were indeed optimized for the detection of a given ligand class based on the frequency of detections for that ligand class. These were also the same optimal windows predicted by

using the ratio of $\log\alpha_L / \log\alpha_{Fe(SA)_2}$ for determining the proper competition strength of the added ligand in CLE-ACSV titrations. The use of MAWs may therefore be most beneficial in dFe-binding ligand analysis with the use of targeted analytical windows depending on the ligand class of interest. Overall, MAW analysis enabled the detection of several distinct ligand classes, compared to previous studies.

5.2 Distributions of DFe-binding ligands

5.2.1 L_1 ligands

The strongest ligands measured in this study (L_1) were dominant in surface waters, and along the continental shelf (Fig. 3.4A). L_1 detected in this study is similar in strength to the L_1 defined by Rue and Bruland (1995) in the North Pacific to be a siderophore-like ligand, where a similar analytical window was employed ($\alpha_{Fe(SA)_2}$ = 73). The highest [L_1] and excess L_1 (eL_1; [L]-[Fe])) were observed in the regions influenced by riverine or estuarine input (San Francisco Bay, Eel River near Cape Mendocino), suggesting these areas are sources of strong dFe-binding ligands. Few studies have examined dFe-binding ligands in estuaries and rivers (Buck et al. 2007; Jones et al. 2011), but both detected high concentrations of dFe-binding ligands in freshwater-influenced systems. Buck et al. (2007) found elevated [L_1] in waters influenced both by the Columbia River Plume (north of this study) and San Francisco Bay. Buck et al. (2007) found a strong correlation between [L_1] and [dFe], and attributed this to the stronger ligand pool 'capping' [dFe] in this region despite high concentrations of leachable particulate Fe which could otherwise contribute to the dFe inventory. [L_1] was in excess of [dFe] in almost all of the surface samples in this study, supporting the finding from Buck et al. (2007) that L_1 is largely responsible for limiting [dFe] in the

region, at least in steady state conditions. [L_1] and eL_1 also decline markedly offshore (Fig. 3.7), suggesting a coastal source of these ligands.

Bacteria in both marine and freshwater systems are known to produce siderophores (Haygood et al. 1993; Butler 1998; Macrellis et al. 2001), with similar log $K^{cond}_{FeL_1,Fe'}$ as the L_1 class observed here. It is probable that terrestrial or in situ strong ligands from San Francisco Bay may be a source of stronger ligands to CC coastal waters. This is an interesting finding, considering previous studies have suggested that L_1 is likely produced in situ (Rue and Bruland 1995). Buck et al. (2010) and King et al. (2012) found excess L_1 production in bottle incubations when NO_3^-:dFe (μmol L^{-1}: nmol L^{-1}) were high (> 10), indicating potential Fe stress relative to NO_3^- (Bruland et al. 1991; King and Barbeau 2007; Biller et al. 2013). Coastal samples in this study had very high NO_3^-:dFe ratios (up to 92 μmol L^{-1}: nmol L^{-1}) due to elevated NO_3^- during upwelling conditions and relatively low dFe. In fact, some of the samples with the highest NO_3^- :dFe ratios were associated with high eL_1 concentrations (data not shown). Macrellis et al. (2001) isolated strong dFe-binding ligands with known siderophore-like functional groups from this region, thus supporting their presence in the CC. L_1 ligands were also detected in some of the BBL samples (Table 3.3), though much less frequently than in the surface (7% of the BBL samples vs. 29% of the surface samples). This implies L_1 may also have a sediment source (Jones et al. 2011), or may reach the BBL without degradation. The presence of stronger ligands in the BBL may therefore play an important role in stabilizing dFe in this high Fe environment.

Although L_1 might have a coastal source, it may also have an offshore sink. The decline in L_1 offshore could be due to degradation processes as coastal waters are

advected offshore, resulting in the disappearance of L_1 and an increase in other ligand classes. The photochemical and biological degradation of L_1 has been hypothesized by several authors (Hutchins et al. 1994; Barbeau et al. 1996; *see* photochemical review by Barbeau 2006) but has only been documented in a few field studies (Powell and Wilson-Finelli 2003*a*,*b*; Rijkenberg et al. 2006). When L_1 ligand concentrations in surface nearshore waters (on the continental shelf) were compared to surface offshore waters from both cruises in this study, the samples were shown to be significantly different (chi squared, $p < 0.025$). This study presents indirect evidence that L_1 has a coastal source and is degraded as water masses move offshore.

5.2.2 L_2 ligands

L_2 ligands showed a similar spatial distribution to L_1, though L_2 was detected more often in offshore waters and in the BBL (Fig. 3.4B, 3.5). While L_2 concentrations (and excess L_2; eL_2) declined offshore, they were still detected in the furthest offshore stations (Fig. 3.7). L_2, as defined in this study, is still part of the stronger ligand pool, and, as such, may have similar sources as L_1. Few studies examining dFe-binding ligands in the marine environment have detected stronger ligands than the L_2 measured in this study, but most studies detect L_2 throughout the water column (*see* review by Gledhill and Buck 2012). This may be related to the analytical window used in the analyses, since a higher window was used in this study and also in Rue and Bruland (1995), who first suggested the presence of a stronger L_1 ligand class limited to surface waters in offshore environments. The L_2 ligand class defined here agrees with the majority of previous work, in that it was the most ubiquitous ligand class measured in this region. L_2 was

found both in surface waters and the BBL, and has elevated concentrations over the wide continental shelf dominated by mud-flats (Wheatcroft et al. 1997).

Although CLE-ACSV gives no information on the structure of the ligands detected, additional analyses for HS in this study give some evidence that the L_2 class is partly comprised of humic-like substances. The log $K^{cond}_{FeL_{HS},Fe'}$ of HS has been determined to be 11.1 (Laglera and van den Berg 2007), and would make it part of the L_2 ligand class in this work. HS analyses on selected samples from the BBL indicate that HS are one of the components of the BBL ligand pool, with 22.6 and 39.2 μg L^{-1} HS amounting to 3-18% of the complexation in the BBL in these samples (where only L_2 was detected). Terrestrial derived HS have been found in coastal and deep waters to contribute to the pool of dFe-binding ligands (up to 4% of the deep dissolved organic matter pool; Laglera and van den Berg 2009), and these results are in the range found by Laglera and van den Berg (2009) in deep waters of the Pacific (36 µg L^{-1}). Lower [HS] were observed in this study than those reported for the Irish Sea by Laglera and van den Berg (2009) (70-400 µg L^{-1}), yet HS still represented a portion of the dFe-binding ligand pool. Calculations for the percentage of the ligand pool comprised of HS were completed using a binding capacity for HS of 32 nmol L^{-1} Fe mg^{-1} HS determined by Laglera and van den Berg (2009). The binding capacity of HS may vary widely; preliminary results in this study showed that different batches of Suwannee River fulvic acid standard can bind anywhere from 12-32 nmol L^{-1} Fe mg^{-1} HS (data not shown). Thus, 3-18% of the dFe-binding in the BBL likely represents a lower bound on the binding capacity of HS in this system. These results represent some of the first definitive evidence that coastal margin sediments may be a source of HS and L_2 ligands.

5.2.3 L_3 and L_4 ligands

The distribution of weaker dFe-binding ligands is not well understood in the marine environment. This is partially due to analytical constraints, because studies to date have focused on siderophore-like ligands using stronger analytical windows (Rue and Bruland 1995) and the detection of weaker ligands is not as statistically robust as the stronger ligand class (Wu and Jin 2009). A lower analytical window was employed in this study in order to gain insight into the spatial distribution of weaker ligands in the surface and BBL, since they are hypothesized to play an important role in dFe cycling (Boyd et al. 2010) and phytoplankton iron acquisition (Hassler et al. 2011). Samples with the lowest temperatures in the surface and BBL tended to have the highest concentrations of weaker ligands, suggesting the source of most of the weaker ligands is the BBL or deeper waters. These samples also corresponded to stations with high [NO_3^-] and manganese (Mn) concentrations (Ana Aguilar-Islas pers. Comm.; Biller and Bruland 2013), which supports the BBL as a source of weaker ligands since Mn concentrations are higher in areas influenced by reducing processes in margin sediments (Johnson et al. 1992; Biller and Bruland 2013). Diffusive fluxes of Cu-binding ligands have been found in estuary environments (Skrabal et al. 1997), implying a similar process could be occurring for dFe-binding ligands (Jones et al. 2011).

The highest concentrations of L_3 and L_4 ligands were detected in BBL samples in the mud-belt regions of the continental margin (Fig. 3.5), known to be areas of high organic matter content and particulate Fe (Homoky et al. 2012). These L_3 and L_4 may thus represent organic by-products associated with organic matter degradation in margin sediments. Although it is not entirely clear what comprises this weaker ligand pool, it is

likely a combination of degraded cellular material from surface waters (Hunter and Boyd 2007) like polysaccharides (Hassler et al. 2011), thiols (Dupont et al. 2006), or heme (Hopkinson et al. 2008). Evidence from surface waters supports the hypothesis that the weaker ligand pool is comprised of terrestrial and in situ degradation products as well. The L_3 and L_4 ligand classes both show distinct patterns offshore compared to L_1 and L_2 (Fig. 3.7). L_4 is only present in the stations closest to shore (< 25 km, Fig. 3.7B) and then quickly disappears offshore, suggesting scavenging of dFe and L_4 offshore and a nearshore source. The samples collected in the mouth of San Francisco Bay have the highest concentrations of L_4 ligands, indicating San Francisco Bay is likely a dominant source. On the other hand, L_3 ligands are the only class of ligands in this study that increase in concentration offshore (Fig. 3.7) despite the decline in dFe, strongly suggesting L_3 is related to degradation processes, perhaps of the L_1 and L_2 classes (Fig. 3.7). Stronger ligands may be degraded in surface waters by photochemistry (Barbeau 2006), or bacterial particle regeneration (Boyd et al. 2010) which have both been shown to produce weaker dFe-binding ligands best described by the L_3 class in this study.

5.3 Characteristics of the Fe-binding ligand pool in surface and BBL waters

The surface waters in this study were shown to contain a continuum of ligand classes, likely from terrestrial sources (HS from San Francisco Bay), the BBL (L_2, L_3, and L_4 ligands), and in situ production (L_1, L_2). This leads to heterogeneity of the surface ligand pool between samples that was difficult to explain by linear correlations alone (Pearson's correlation, data not shown) supporting results from the PCA that the variance in surface ligand distributions must be explained by several factors (Fig. 3.6). This finding is consistent with the hypothesis that a continuum of dFe-binding ligands likely

exists in seawater, as part of a heterogeneous dissolved organic carbon pool. Although the ligand classes are operationally defined in this study (based on the ligand strengths) and not necessarily ligands with different chemical structures, this analysis represents an initial step in determining the relevant processes governing complex ligand distributions in coastal waters.

The grouping of surface samples along the first PC in the PCA suggests a strong relationship with water masses in the CC, since the variance in the first PC is primarily explained by nutrient distributions. This result is supported by the onshore to offshore gradients in the ligand pool (Fig. 3.7) with the variance in surface waters explained predominantly by temperature, distance from shore, and nutrient concentrations (Fig. 3.7A, C). This result is not surprising, since previous evidence suggests numerous processes affect the dFe-binding ligand pool in surface waters (Gledhill and Buck 2012). The greater variance seen among surface samples is evidence that water mass-specific in situ processes are more important in surface samples than in the BBL, which exhibited relatively little variance between stations and seasons (Fig. 3.6, 3.7). Further evidence to suggest that the surface ligand pool is influenced by several sources and sinks is the different scale lengths of dFe and each ligand class as water masses advect offshore. Scale length can be defined as the distance at which the concentration has reached 1/e (37%) of its original concentration (here, concentration on the shelf; Johnson et al. 1997). The calculated scale length of dFe in surface waters from this study is 75 km, suggesting dFe is rapidly removed offshore. Each ligand class has different scale lengths from dFe, suggesting distinct processes influence their distributions and simple water mass mixing is not responsible for the patterns observed. Interestingly, L_1 and L_2 ligands have similar

scale lengths of 133 and 187 km, respectively, while L_4 has a scale length of 6 km, and L_3 has a much longer scale length of 2000 km since it increases in concentration in many of the offshore stations. These scale lengths provide evidence that the excess ligand pools and dFe are largely decoupled in the CC, and complex patterns control their distributions. The longer persistence of ligands with distance from shore compared to dFe may in part explain the higher deep water dFe concentrations observed in the Pacific compared to the Atlantic (Johnson et al. 1997), if Pacific continental margin sediments are sources of both high [dFe] and ligands.

BBL samples show less variance than surface waters between samples, and are predominantly grouped along the second and third PC. The low variance between BBL samples and their relationship to spatial parameters (latitude and longitude) suggest that ligands in the BBL are primarily related to their location on the shelf. The distribution of ligands on the shelf shows coherence with shelf width and dFe concentrations (Fig. 3.5), which have also been shown to be related to organic matter degradation processes (Homoky et al. 2012) as well as sediment type (Wheatcroft et al. 1997; Biller et al. 2013). The L_2 ligands were shown to be dominant in the BBL, and were positively related to nutrient concentrations and L_1 (Pearson's correlation, data not shown). If the BBL ligand pool was directly related to degradation of the surface ligand pool, we would expect to see a negative trend between stronger (L_1 and L_2) and weaker ligands (L_3 and L_4) and a similar grouping of BBL and surface samples in the PC space. However, surface waters have much higher variance between samples and the variance is explained by different factors than BBL samples. This is strong indirect evidence that the BBL ligand pool is

comprised of material that has both been deposited on the shelf from rivers and estuaries (Fig. 3.5), and from degradation processes in the sediments.

The surface and BBL are two very distinct biogeochemical regimes in the coastal ocean and provided good contrast for which to explore the use of MAW analysis for dFe speciation. The highest analytical window was optimal for characterizing the strongest Fe-binding ligands, while lower windows facilitated the detection of weaker ligands whose nature is poorly understood and often go undetected by current single-window methods. The MAW approach to dFe speciation in this study helped to determine the full spectrum of iron ligands, and may be an important tool in future studies looking at the cycling of ligands in the marine environment. The ability to define a wider range of ligands with this analysis may also be helpful for future modeling efforts, where ligands are often poorly defined but important to overall dFe dynamics (Moore et al. 2004; Tagliabue and Volker 2011; Jiang et al. 2013). Future studies looking at mechanistic and temporal variations in the ligand pool will provide essential new information regarding the important role of dFe-binding ligands in Fe supply to productive coastal waters.

6. Acknowledgements

We thank Geoffrey Smith for help with sampling, and the captain and crew of the R/V *Point Sur*. We thank Tyler Coale for nutrient analyses, Ana Aguilar-Islas for manganese analyses, and Melissa Peacock for chlorophyll *a* analyses. R.M. Bundy was supported by National Science Foundation grant Division of Ocean Sciences 10-26607 for the California Current Ecosystem Long Term Ecological Research program. This project was funded by National Science Foundation grant Division of Ocean Sciences 0849943 to K.W. Bruland and for D.V. Biller. K.N. Buck was supported by institutional

funding from the Walwyn Hughes Fund for Innovation and the Ray Moore Endowment Fund at the Bermuda Institute of Ocean Sciences (BIOS); this manuscript is BIOS contribution number 2027. Chapter 3, in full, is a reprint of the material as it appears in Limnology and Oceanography 2014. Bundy, R.M., Barbeau, K.A., Biller, D.V., Buck, K.N., Bruland, K.W., Limnology and Oceanography, Volume 59, Issue 3, Pages 769-787 2014. The dissertation author was the primary investigator and author of this paper.

Table 3.1 Classes of ligands used in this study where the stronger ligand classes are represented by L_1 and L_2, and the weaker ligands are represented by L_3 and L_4. Literature range represents the range of conditional stability constants reported for that ligand class in the literature, as reported by Gledhill and Buck (2012)[1].

Ligand Category	L_i	$\log K^{cond}_{FeL,Fe'}$	Literature Range
Strong	L_1	≥ 12.0	9.6-13.90[1]
	L_2	11.0-11.9	9.6-11.95[1]
Weak	L_3	10.0-10.9	
	L_4	≤10.0	

Table 3.2 Hydrographic (temp. and salinity), chlorophyll *a*, and macronutrient (nitrite+nitrate: 'nitrate', phosphate, silicate) data for all stations sampled for organic Fe-binding ligands during May 2010 and August and September 2011 in the surface and benthic boundary layer. The notation 'nd' notes a parameter for which there is no data.

Date Sampled	Transect	Sta.	Latitude (°N)	Longitude (°W)	Depth (m)	Temp. (°C)	Salinity	Chl *a* (μg L^{-1})	Nitrate (μmol L^{-1})	Phosphate (μmol L^{-1})	Silicate (μmol L^{-1})
May 2010	1	2	39.1830	-123.8267	2	9.34	33.38	1.27	27.4	2.0	43.5
May 2010	1	3	39.4512	-123.8869	2	9.71	33.56	0.00	24.7	1.8	33.9
May 2010	1	4	39.7025	-123.8817	2	11.18	33.33	0.00	25.4	1.9	34.6
May 2010	1	5	39.9421	-124.0867	2	9.82	34.01	0.00	29.6	2.2	44.8
May 2010	1	6	40.1510	-124.3092	2	15.57	35.48	0.00	29.9	2.2	51.2
May 2010	1	7	40.3781	-124.5318	2	11.29	33.00	0.00	13.9	1.2	24.4
May 2010	2	1	40.1917	-125.1827	2	12.22	32.28	0.00	0.0	0.3	3.7
May 2010	2	2	39.8687	-124.9036	2	11.71	32.11	1.92	1.0	0.3	5.0
May 2010	2	3	38.9608	-124.4121	2	10.26	32.69	1.99	19.0	1.4	26.8
May 2010	6	1	38.2712	-123.1036	2	8.58	33.99	1.01	29.3	2.1	41.4
May 2010	6	2	38.5350	-123.8423	2	9.72	33.33	0.37	21.1	1.5	25.1
May 2010	6	3	38.5747	-123.9531	2	10.27	33.36	6.86	12.1	1.0	13.6
May 2010	8	1	38.7817	-124.4115	2	10.83	32.28	14.01	5.1	0.6	8.2
May 2010	8	2	38.9321	-123.9908	2	11.36	32.27	3.58	2.3	0.5	2.3
May 2010	8	3	39.0100	-123.7887	2	9.92	32.54	1.36	21.5	1.6	30.1
May 2010	8	4	39.3341	-123.8415	2	9.18	33.94	30.69	17.2	1.2	28.5
May 2010	9	1	39.5342	-123.8333	2	9.11	33.12	14.86	21.0	1.4	30.4
May 2010	9	2	39.6638	-124.0785	2	9.35	33.04	12.65	16.6	1.3	22.8
May 2010	9	3	39.8516	-123.9394	2	9.49	33.11	28.74	6.3	0.6	13.4
May 2010	9	4	39.9199	-124.2714	2	10.63	33.27	4.07	7.1	0.9	8.0
May 2010	10	1	38.6430	-123.4439	2	9.03	33.89	0.17	28.5	2.1	41.9
May 2010	11	1	37.9411	-122.9649	58	8.28	34.03	nd	29.3	2.2	49.5
May 2010	11	2	37.9063	-122.8802	53	8.50	34.01	nd	28.8	2.1	45.3
May 2010	11	3	37.7817	-122.9515	62	8.37	34.03	nd	29.4	2.2	42.9
May 2010	11	4	37.8706	-123.0930	86	8.61	33.98	nd	28.6	2.1	41.2
May 2010	11	5	38.1120	-123.1234	74	8.19	34.04	nd	29.6	2.2	48.3
May 2010	11	6	38.1108	-123.0256	61	8.37	34.01	nd	28.8	2.2	43.9
May 2010	11	7	38.2553	-123.0805	69	8.14	34.04	nd	29.6	2.3	50.8
May 2010	11	8	38.4600	-123.2448	67	8.06	34.04	nd	29.1	2.2	51.2
May 2010	11	9	38.6386	-123.4310	69	7.78	34.05	nd	30.0	2.3	51.2
May 2010	11	10	38.7849	-123.6212	65	7.80	34.05	nd	30.4	2.3	50.3
May 2010	11	17	39.0301	-123.7690	68	7.77	34.05	nd	31.9	2.4	49.5
May 2010	11	19	39.3341	-123.8415	78	7.87	34.03	nd	31.9	2.4	46.4
May 2010	11	23	38.6390	-123.4369	72	8.02	34.04	nd	29.7	2.4	48.7
Aug 2011	1	1	38.0233	-123.0889	2	11.81	33.65	5.86	18.1	1.7	27.9
Aug 2011	1	2	38.2004	-123.1060	2	12.06	33.61	1.76	17.5	1.8	24.5
Aug 2011	1	3	38.6353	-123.4926	2	10.75	33.82	0.08	26.8	2.3	33.6
Aug 2011	1	4	38.9050	-123.7876	2	11.40	33.49	2.41	17.2	1.4	19.8
Aug 2011	1	5	39.3911	-123.8968	2	10.81	33.53	10.13	15.7	1.3	13.1
Aug 2011	2	1	39.7127	-124.6647	2	16.09	32.66	0.08	0.0	0.3	2.8
Aug 2011	2	2	39.1683	-124.2509	2	11.83	32.89	0.00	6.8	0.8	8.2
Aug 2011	5	1	37.7793	-126.2642	2	17.16	33.15	0.00	3.8	0.6	2.5
Aug 2011	5	2	38.0066	-125.7003	2	15.26	33.14	0.00	5.4	0.6	3.8
Aug 2011	5	3	38.0181	-124.9463	2	13.31	33.38	3.09	nd	nd	nd
Aug 2011	7	1	38.0684	-124.4368	2	14.51	33.18	0.14	6.6	0.7	5.5
Aug 2011	7	2	38.2556	-124.1933	2	13.25	33.31	1.30	11.7	1.0	9.8
Aug 2011	7	3	38.3498	-124.0705	2	12.42	32.89	1.50	5.3	nd	7.1
Aug 2011	7	4	38.6132	-123.7229	2	12.39	32.86	1.18	7.4	0.8	8.0
Aug 2011	17	2	38.7832	-123.6176	2	10.38	33.70	3.18	25.5	2.1	32.5
Aug 2011	17	3	38.8247	-123.6500	2	10.08	33.76	1.56	25.5	2.1	34.2
Aug 2011	17	4	38.8183	-123.6602	2	10.13	33.75	1.96	25.0	2.1	33.8
Aug 2011	17	5	38.7998	-123.6887	2	10.92	33.52	3.96	19.0	1.6	23.0
Aug 2011	17	6	39.1725	-123.7926	2	10.86	33.74	2.56	22.5	1.8	33.3

Table 3.2 Continued. Hydrographic (temp. and salinity), chlorophyll *a*, and macronutrient (nitrite+nitrate: 'nitrate', phosphate, silicate) data for all stations sampled for organic Fe-binding ligands during May 2010 and August and September 2011 in the surface and benthic boundary layer. The notation 'nd' notes a parameter for which there is no data.

Date Sampled	Transect	Sta.	Latitude (°N)	Longitude (°W)	Depth (m)	Temp (°C)	Salinity	Chl *a* (μg L^{-1})	Nitrate (μmol L^{-1})	Phosphate (μmol L^{-1})	Silicate (μmol L^{-1})
Aug 2011	17	7	39.3333	-123.8426	2	10.44	33.85	2.35	26.6	2.2	39.6
Aug 2011	17	8	39.5356	-123.8295	2	11.42	33.62	9.81	0.5	0.4	5.9
Aug 2011	17	9	40.7374	-124.3291	2	11.64	33.62	4.05	13.5	1.0	13.3
Aug 2011	17	10	40.7672	-124.3858	2	10.81	33.57	2.84	18.6	1.4	19.2
Aug 2011	17	11	40.7885	-124.4169	2	11.94	33.38	1.31	16.6	1.3	16.6
Aug 2011	17	12	40.8169	-124.4664	2	12.93	33.38	1.45	13.4	1.0	12.6
Aug 2011	17	23	37.2802	-122.5273	2	13.54	33.54	15.95	0.2	0.3	1.7
Aug 2011	17	31	35.6452	-121.3041	2	12.18	33.58	7.21	10.5	0.9	7.7
Aug 2011	17	33	36.0606	-121.6140	2	12.27	33.52	nd	15.6	1.5	17.6
Aug 2011	17	35	36.2169	-121.8065	2	11.71	33.65	6.95	14.5	1.3	15.9
Aug 2011	17	37	37.4180	-122.6109	2	14.45	33.36	6.62	3.3	0.4	8.7
Aug 2011	17	38	37.6034	-122.8299	2	12.88	33.28	nd	10.5	1.2	21.7
Aug 2011	17	39	37.7583	-123.0007	2	13.17	33.31	nd	8.8	0.9	14.8
Aug 2011	17	2	38.7832	-123.6176	64	9.18	33.94	nd	31.1	2.8	51.9
Aug 2011	17	3	38.8247	-123.6500	48	9.18	33.94	nd	31.8	2.9	50.5
Aug 2011	17	4	38.8183	-123.6602	61	9.12	33.95	nd	31.4	2.8	52.8
Aug 2011	17	5	38.7998	-123.6887	90	9.04	33.96	nd	31.2	2.6	48.6
Aug 2011	17	6	39.1725	-123.7926	70	9.34	33.92	nd	31.3	2.6	50.3
Aug 2011	17	7	39.3333	-123.8426	81	9.17	33.94	nd	31.6	2.7	49.6
Aug 2011	17	8	39.5356	-123.8295	68	9.13	33.94	nd	31.4	2.6	47.8
Aug 2011	17	9	40.7374	-124.3291	40.3	8.72	33.90	nd	30.5	2.7	47.2
Aug 2011	17	10	40.7672	-124.3858	64	8.60	33.93	nd	30.5	2.6	45.4
Aug 2011	17	11	40.7885	-124.4169	100	8.36	34.00	nd	31.8	2.6	46.1
Aug 2011	17	12	40.8169	-124.4664	339	6.95	34.12	nd	37.2	2.9	60.6
Aug 2011	17	23	37.2802	-122.5273	75	9.98	33.86	nd	27.5	2.3	36.8
Aug 2011	17	31	35.6452	-121.3041	56	11.60	33.61	nd	22.1	1.8	23.3
Aug 2011	17	33	36.0606	-121.6140	49	10.61	33.72	nd	21.4	1.9	24.7
Aug 2011	17	35	36.2169	-121.8065	79	10.11	33.78	nd	25.9	2.2	28.6
Aug 2011	17	37	37.4180	-122.6109	64	9.95	33.86	nd	31.0	2.7	48.0
Aug 2011	17	38	37.6034	-122.8299	67	9.88	33.87	nd	30.9	2.8	49.9
Aug 2011	17	39	37.7583	-123.0007	62	9.90	33.84	nd	30.9	2.6	42.5
Sep 2011	16	1	37.8264	-122.4663	2	15.62	30.88	3.96	17.8	2.4	42.1
Sep 2011	16	2	37.7722	-122.5769	2	14.65	31.92	5.55	13.7	1.6	29.6

Table 3.3 Average ligand (L_1, L_2, L_3, L_4) concentrations and conditional stability constants (log K_1, log K_2, log K_3, log K_4) for each analytical window ($\alpha_{Fe(SA)_2}$) during the May 2010 (spring) and August and September 2011 (summer) sampling periods. Averages and standard deviations are shown for surface and benthic boundary layer samples from each season, where *n* represents the number of titrations. Ligand concentrations are also shown from 'overload' titrations in the spring samples ($\alpha_{Fe(SA)_2}$ = 500, 251).

Season	Location	α	*n*	[L_1]	+/-	log K_1	+/-	*n*	[L_2]	+/-	log K_2	+/-	*n*	[L_3]	+/-	log K_3	+/-	*n*	[L_4]	+/-	log K_4	+/-	log α_L	+/-
Spring	surface	100	6	5.2	2.9	12.1	0.1	7	4.4	1.6	11.6	0.3	1	2.0	nd	10.9	nd	0	nd	nd	nd	nd	14.5	0.4
10		60	8	3.4	1.9	12.2	0.2	16	4.2	3.2	11.5	0.2	3	3.3	1.6	10.6	0.3	0	nd	nd	nd	nd	14.2	0.4
		30	3	4.1	1.0	12.1	0.2	5	2.6	1.2	11.6	0.3	10	4.6	2.9	10.7	0.4	0	nd	nd	nd	nd	14.1	0.5
	BBL	500	1	12.9	nd	12.2	nd	0	nd	nd	nd	nd	0	nd	nd	nd	nd	0	nd	nd	nd	nd	15.3	nd
		251	3	10.1	5.1	12.4	0.5	2	11.9	4.4	11.9	0.0	0	nd	nd	nd	nd	0	nd	nd	nd	nd	15.2	0.5
		100	3	16.2	1.1	12.2	0.2	10	15.2	4.8	11.4	0.3	0	nd	nd	nd	nd	0	nd	nd	nd	nd	14.8	0.5
		60	0	nd	nd	nd	nd	8	15.8	4.4	11.3	0.2	5	15.0	5.7	10.8	0.1	1	14.0	nd	10.0	nd	14.4	0.4
		30	0	nd	nd	nd	nd	7	14.4	3.4	11.2	0.3	4	17.0	7.4	10.7	0.2	0	nd	nd	nd	nd	14.2	0.3
Summer	surface	100	13	4.4	2.7	12.3	0.3	15	4.3	2.2	11.6	0.3	3	6.0	2.8	11.0	0.2	1	21.8	nd	9.7	nd	14.4	0.5
11		60	10	3.6	1.9	12.3	0.3	17	3.6	1.8	11.4	0.3	11	4.5	1.8	10.6	0.3	3	13.9	13.6	9.8	0.1	14.1	0.6
		30	3	4.0	3.2	12.2	0.0	13	3.8	2.1	11.4	0.3	13	5.0	2.4	10.7	0.3	3	68.8	66.1	9.3	0.8	13.6	0.6
	BBL	100	4	13.6	9.6	12.2	0.1	12	11.4	5.5	11.5	0.3	2	24.5	16.3	10.7	0.4	0	nd	nd	nd	nd	14.7	0.5
		60	2	7.2	2.5	12.1	0.0	11	12.9	7.4	11.5	0.2	5	19.6	7.8	10.4	0.2	0	nd	nd	nd	nd	14.4	0.5
		30	0	nd	nd	nd	nd	7	10.0	3.8	11.5	0.3	6	15.2	14.2	10.5	0.2	4	21.3	15.9	9.8	0.1	13.8	0.7

Table 3.4 Eigenvectors for the first three principal components (PC) for each of the variables used in the principal component analysis. The first three PCs explain 57% of the variance. Larger magnitude numbers indicate a stronger contribution to that PC, with positive and negative numbers contributing positively and negatively to that PC, respectively.

Variables	PC1	PC2	PC3
Latitude	0.0084	-0.2053	0.4581
Longitude	-0.1578	0.2290	-0.4632
Depth (m)	-0.2743	-0.1017	0.1394
Temperature ($^{\circ}$C)	0.3196	0.1823	-0.0450
Salinity	-0.2773	-0.2415	-0.0894
Nitrate (μmol L^{-1})	-0.3855	-0.0812	0.0178
Phosphate (μmol L^{-1})	-0.3900	-0.0021	0.0222
Silicate (μmol L^{-1})	-0.3846	-0.0196	0.0701
dFe (nmol L^{-1})	-0.3266	0.0328	0.0791
L_1 (nmol L^{-1})	-0.1571	0.3693	-0.0988
log K_1	-0.0169	0.3878	-0.2708
L_2 (nmol L^{-1})	-0.2587	0.1738	0.1421
log K_2	-0.0541	0.1276	0.1969
L_3 (nmol L^{-1})	-0.1053	-0.2424	-0.3381
log K_3	0.0340	-0.2340	-0.4392
L_4 (nmol L^{-1})	-0.0101	0.4633	0.0980
log K_4	-0.0637	0.3579	0.2125
distance (km)	0.2328	-0.0769	0.1735

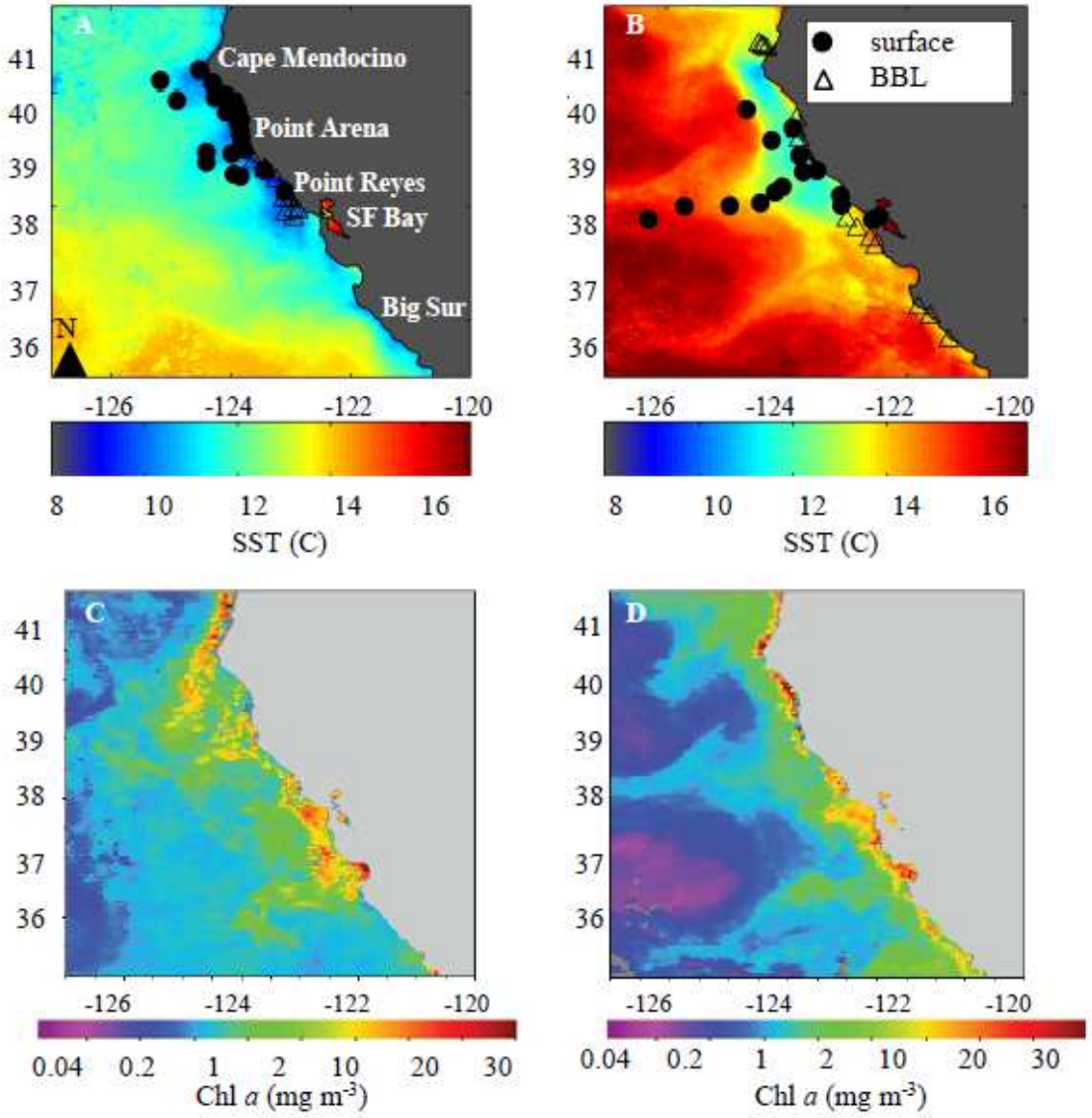

Figure 3.1 Sampling stations in the surface and benthic boundary layer (BBL) during the (A) spring and (B) summer. (B) BBL stations in the summer were also sampled in the surface waters. Stations are overlaid on a one-month average (A,B) sea surface temperature (NOAA Coast Watch, ˚C) and (C,D) chlorophyll *a* (NOAA Coast Watch, mg L^{-1}) for (A,C) spring and (B,D) summer cruises (May and August for spring and summer, respectively).

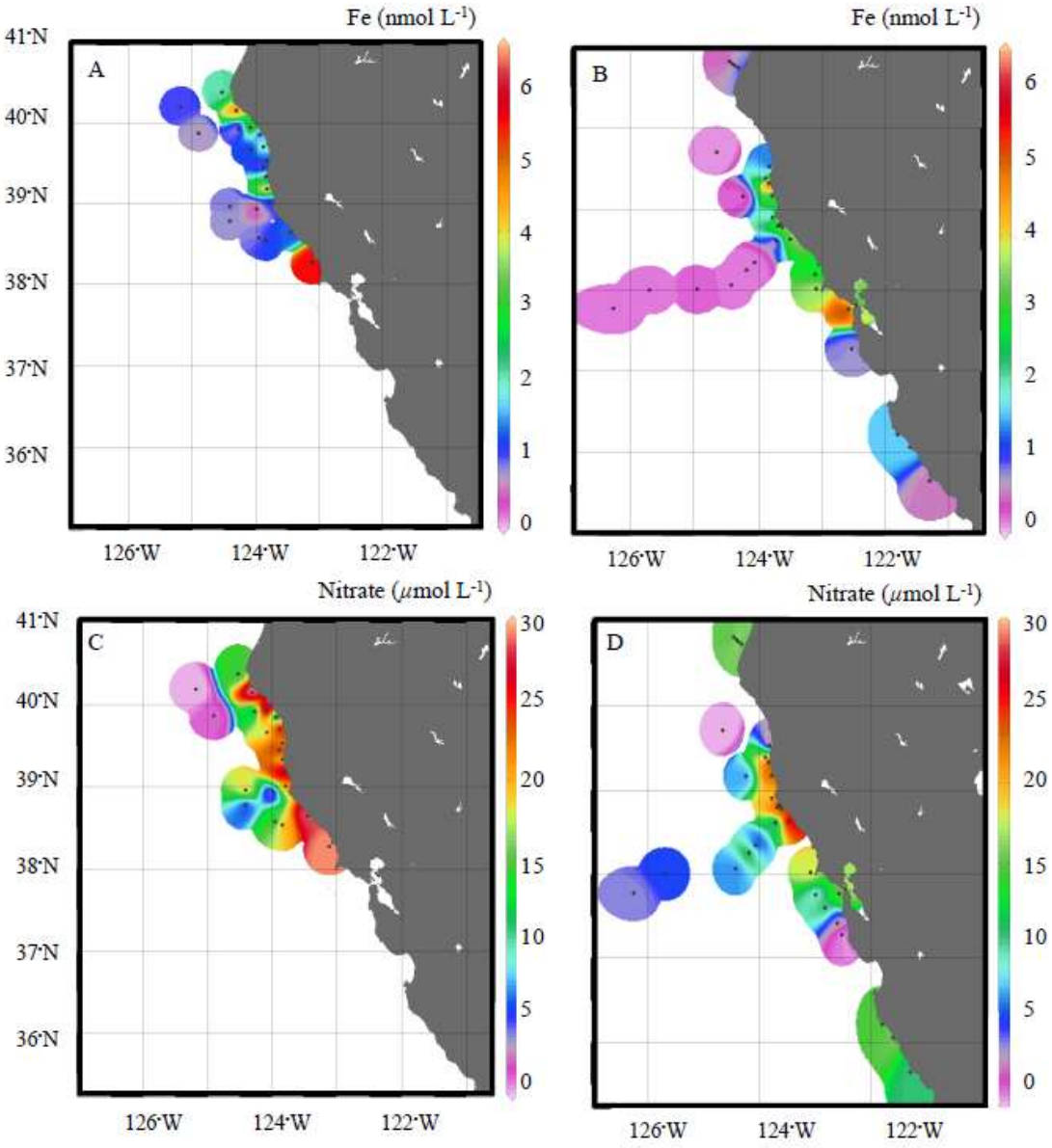

Figure 3.2 Surface dissolved Fe concentrations in the (A) spring and (B) summer at stations with accompanying Fe-organic speciation data. Surface nitrate (nitrate+nitrite) concentrations are also shown in the (C) spring and (D) summer for each station.

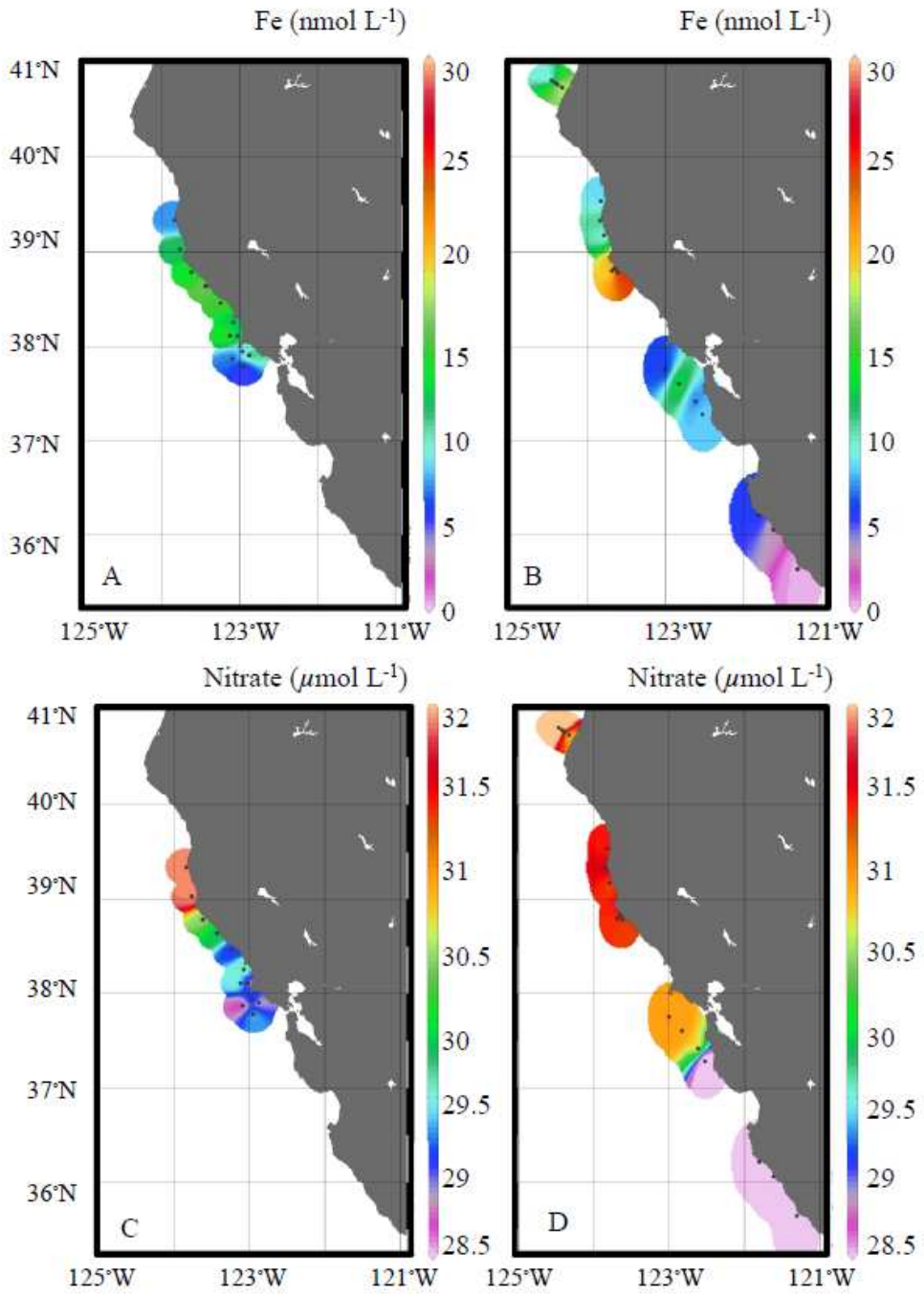

Figure 3.3 Dissolved Fe concentrations sampled in the benthic boundary layer (BBL) during (A) spring and (B) summer at stations with accompanying Fe-organic speciation data. BBL nitrate (nitrate+nitrite) concentrations are also shown in the (C) spring and (D) summer for each station.

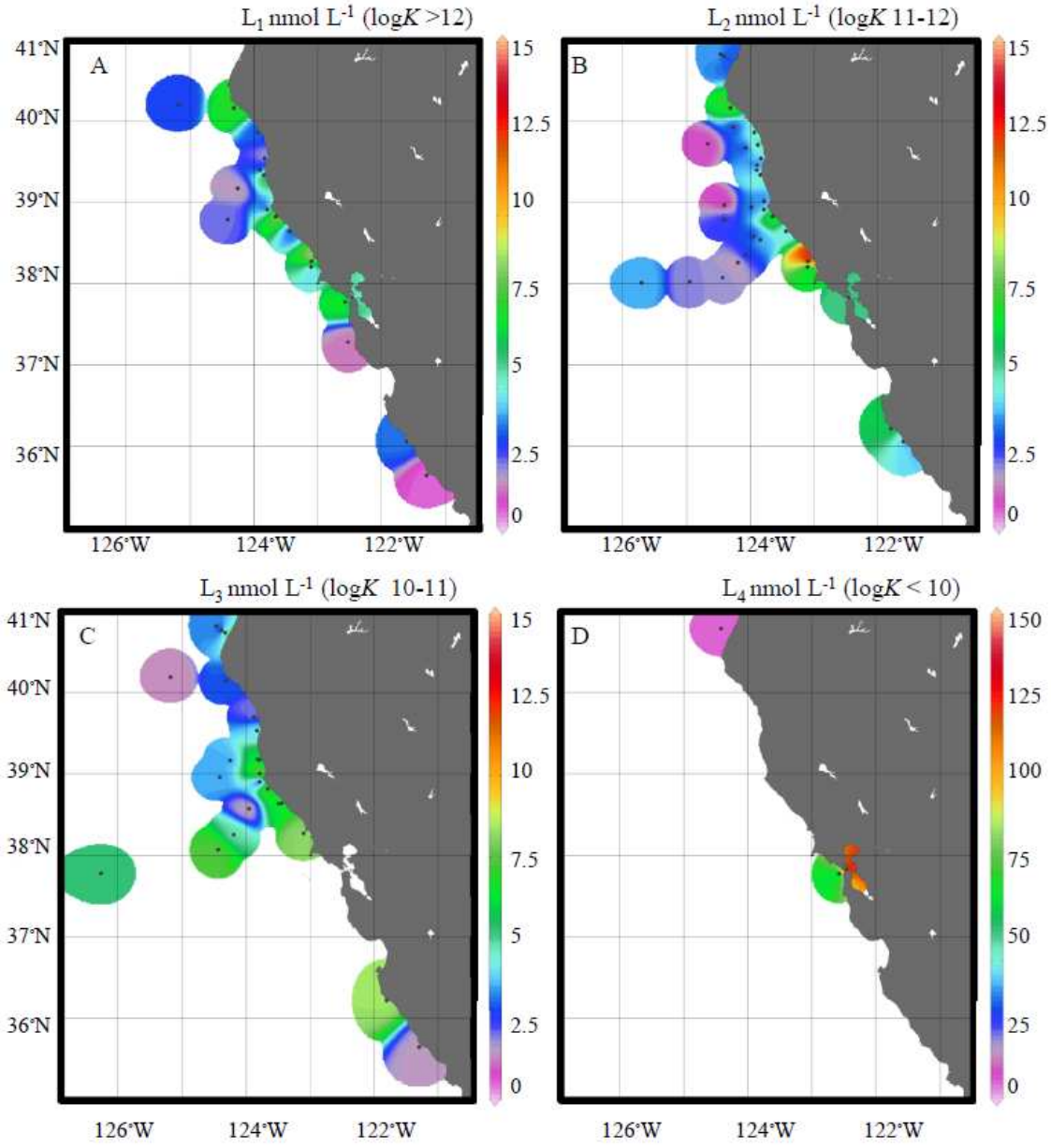

Figure 3.4 Ligand concentrations determined in both spring and summer surface waters. (A) The strongest ligands (L_1) measured at an $\alpha_{Fe(SA)_2}$=100, (B) L_2 ligand concentrations measured at an $\alpha_{Fe(SA)_2}$=60, (C) L_3 concentrations at an $\alpha_{Fe(SA)_2}$=30, and (D) L_4 concentrations measured at $\alpha_{Fe(SA)_2}$=30.

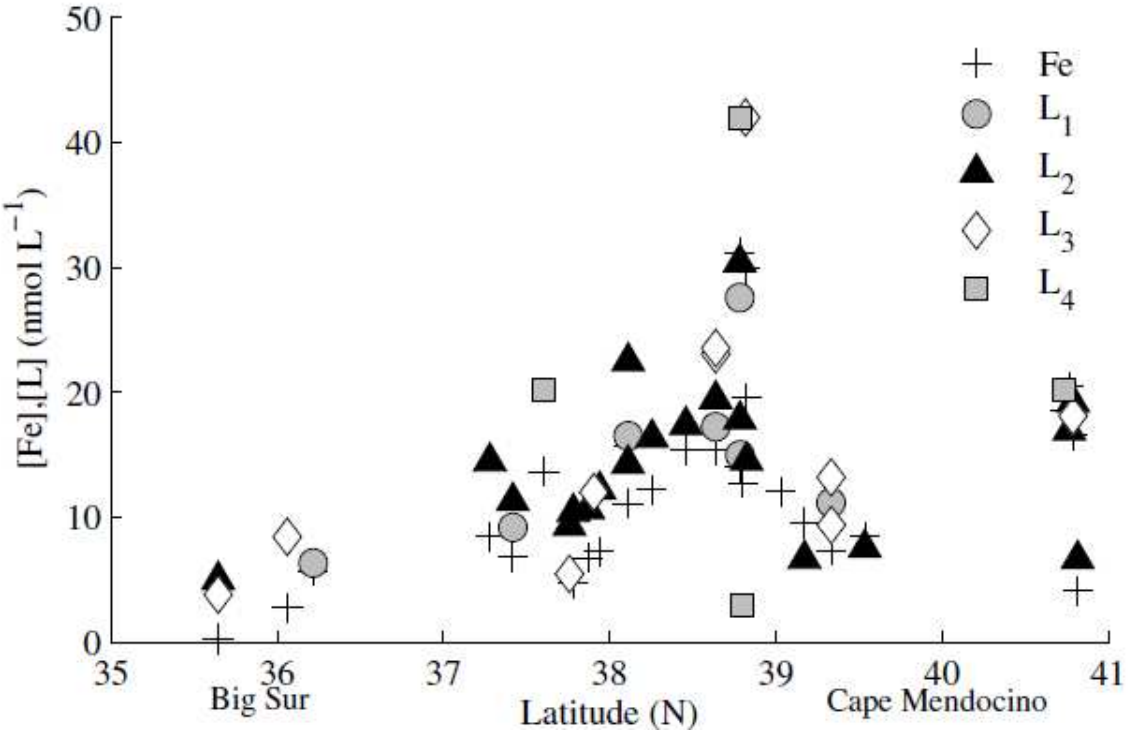

Figure 3.5 Dissolved Fe and benthic boundary layer (BBL) ligand concentrations (L_1, L_2, L_3, and L_4) measured in both the spring and summer.

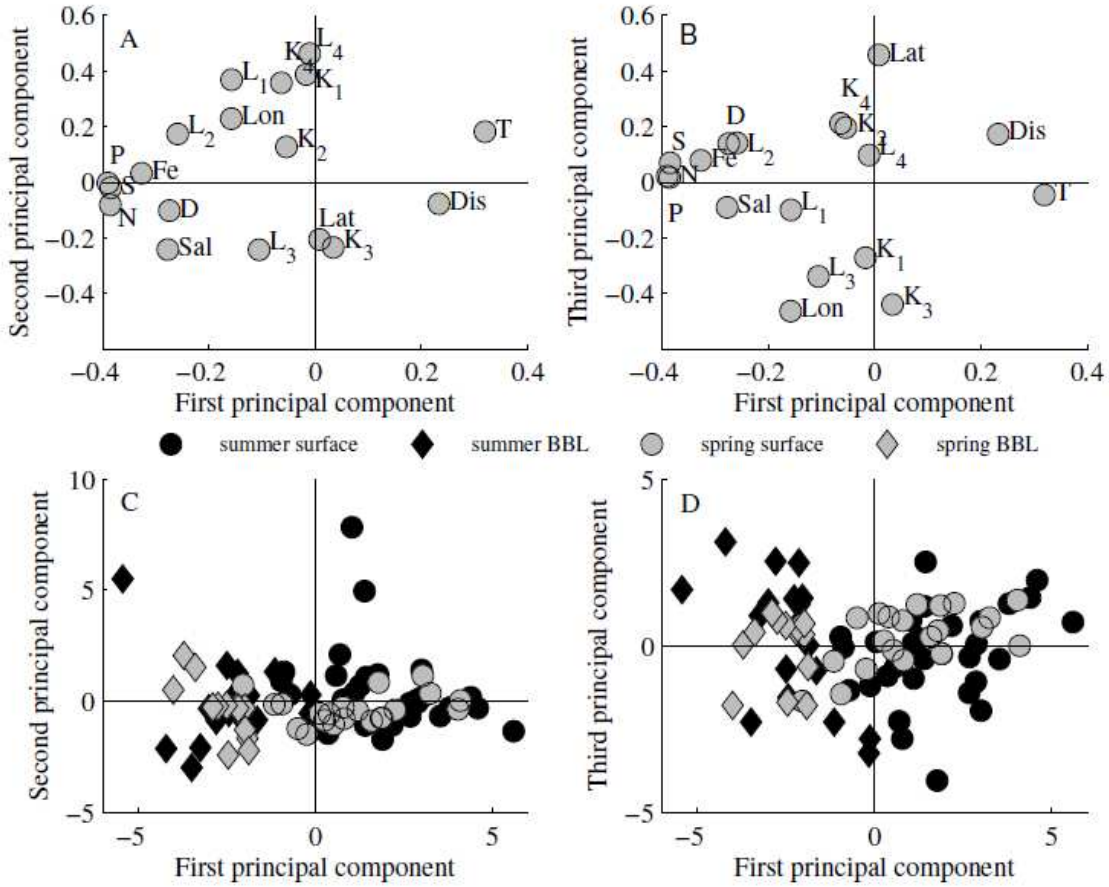

Figure 3.6 The results of the principal component analysis (PCA) shown as scatter plots in the PC space. (A) PC loadings for the 18 variables used in PCA shown in the PCA space along the first PC (x-axis) and the second PC (y-axis). Variable labels are 'Lat' (latitude), 'Lon' (longitude), 'D' (depth), 'T' (temperature), 'Sal' (salinity), 'N' (nitrate), 'P' (phosphate), 'S' (silicate), 'Fe' (dissolved Fe), 'L_1' ([L_1]), 'K_1' (log K_1), 'L_2' ([L_2]), 'K_2' (log K_2), 'L_3' ([L_3]), 'K_3' (log K_3), 'L_4' ([L_4]), 'K_4' (log K_4), and 'Dis' (distance from shore). (B) PC loadings for the 18 variables used in the PCA along the first (x-axis) and third (y-axis) PCs. (C) The PCA scores of all of the data from each sample (82 samples) along the first and second PCs. (D) The PCA scores of all of the data from each sample along the first and third PCs.

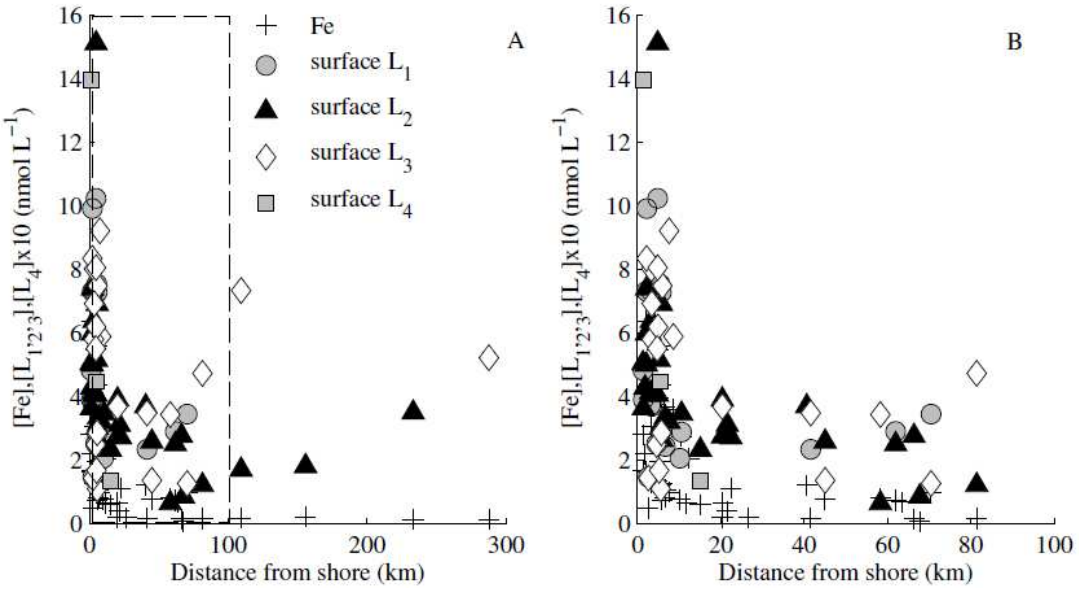

Figure 3.7 The concentrations of Fe, $L_{1,}$ $L_{2,}$ L_3, and L_4 (x10) with distance from shore in all surface samples from the (A) spring and summer, and zoomed in to (B) 0-100 km offshore.

7. References

Barbeau, K. 2006. Photochemistry of organic iron(III) complexing ligands in oceanic systems. Photochemistry and Photobiology **82:** 1505-1516.

Barbeau, K., J. W. Moffett, D. A. Caron, P. L. Croot, and D. L. Erdner. 1996. Role of protozoan grazing in relieving iron limitation of phytoplankton. Nature **380**: 61-64.

Berelson, W., J. McManus, K.H. Coale, K.S. Johnson, D. Burdige, T. Kilgore, D. Colodner, F. Chavez, R. Kudela, J. Boucher. 2003. A time series of benthic flux measurements from Monterey Bay, CA. Continental Shelf Research **23:** 457-481.

Biller, D. V., and K. W. Bruland. 2012. Analysis of Mn, Fe, Co, Ni, Cu, Zn, Cd, and Pb in seawater using the Nobias-chelate PA1 resin and magnetic sector inductively coupled plasma mass spectrometry (ICP-MS). Marine Chemistry **130**: 50-70.

Biller, D.V. and K.W. Bruland. 2013. Sources and distributions of Mn, Fe, Co, Ni, Cu, Zn, and Cd relative to macronutrients along the central California coast during the spring and summer upwelling season. Marine Chemistry **155**: 50-70.

Biller, D. V., T. H. Coale, G. J. Smith, and K. W. Bruland. 2013. Coastal iron and nitrate distributions during the spring and summer upwelling season in the central California Current upwelling regime. Continental Shelf Research **66**. 58-72.

Boyd, P. W., E. Ibisanmi, S. G. Sander, K. A. Hunter, and G. A. Jackson. 2010. Remineralization of upper ocean particles: Implications for iron biogeochemistry. Limnology and Oceanography **55:** 1271-1288.

Bruland, K. W., J. R. Donat, and D. A. Hutchins. 1991. Interactive influences of bioactive trace-metals on biological production in oceanic waters. Limnology and Oceanography **36:** 1555-1577.

Bruland, K. W., E. L. Rue, J. R. Donat, S. A. Skrabal, and J. W. Moffett. 2000. Intercomparison of voltammetric techniques to determine the chemical speciation of dissolved copper in a coastal seawater sample. Analytica Chimica Acta **405:** 99-113.

Bruland, K. W., E. L. Rue, and G. J. Smith. 2001. Iron and macronutrients in California coastal upwelling regimes: Implications for diatom blooms. Limnology and Oceanography **46**: 1661-1674.

Bruland, K.W., E. L. Rue, G. J. Smith, G.R. DiTullio. 2005. Iron, macronutrients and diatom blooms in the Peru upwelling regime: brown and blue waters of Peru. Marine Chemistry **93:** 81-103.

Buck, K. N., and K. W. Bruland. 2005. Copper speciation in San Francisco Bay: A novel approach using multiple analytical windows. Marine Chemistry **96:** 185-198.

Buck, K. N., M. C. Lohan, C. J. M. Berger, and K. W. Bruland. 2007. Dissolved iron speciation in two distinct river plumes and an estuary: Implications for riverine iron supply. Limnology and Oceanography **52:** 843-855.

Buck, K. N., J. Moffett, K. A. Barbeau, R. M. Bundy, Y. Kondo, and J. Wu. 2012. The organic complexation of iron and copper: an intercomparison of competitive ligand exchange-adsorptive cathodic stripping voltammetry (CLE-ACSV) techniques. Limnology and Oceanography: Methods **10**: 496-515.

Buck, K. N., K. E. Selph, and K. A. Barbeau. 2010. Iron-binding ligand production and copper speciation in an incubation experiment of Antarctic Peninsula shelf waters from the Bransfield Strait, Southern Ocean. Marine Chemistry **122:** 148-159.

Bundy, R. M., K. Barbeau, and K. N. Buck. 2013. Sources of strong copper-binding ligands in Antarctic Peninsula surface waters. Deep Sea Research Part II **90:** 134-146.

Butler, A. 1998. Acquisition and utilization of transition metal ions by marine organisms. Science **281:** 207-210.

Chase, Z., K.S. Johnson, V.A. Elrod, J.N. Plant, S.E. Fitzwater, L. Pickell, C.M. Sakamoto. 2005. Manganese and iron distributions off central California influenced by upwelling and shelf width. Marine Chemistry **95**: 235-254.

Dupont, C. L., J. W. Moffett, R. R. Bidigare, and B. A. Ahner. 2006. Distributions of dissolved and particulate biogenic thiols in the subarctic Pacific Ocean. Deep Sea Research Part I **53:** 1961-1974.

Elrod, V. A., W. M. Berelson, K. H. Coale, and K. S. Johnson. 2004. The flux of iron from continental shelf sediments: A missing source for global budgets. Geophysical Research Letters **31**: *L12307*, doi:10.1029/2004GL020216

Elrod, V. A., K. S. Johnson, S. E. Fitzwater, and J. N. Plant. 2008. A long-term, high-resolution record of surface water iron concentrations in the upwelling-driven central California region. Journal of Geophysical Research Part C Oceans **113***: C11021*, doi:10.1029/2007jc004610

Garnier, C., I. Pizeta, S. Mounier, J. Y. Benaim, and M. Branica. 2004. Influence of the type of titration and of data treatment methods on metal complexing parameters determination of single and multi-ligand systems measured by stripping voltammetry. Analytica Chimica Acta **505:** 263-275.

Gerringa, L. J. A., P. M. J. Herman, and T. C. W. Poortvliet. 1995. Comparison of the linear van den Berg Ružić transformation and a nonlinear fit of the Langmuir isotherm applied to Cu speciation data in the estuarine environment. Marine Chemistry **48:** 131-142.

Gledhill, M., and K. N. Buck. 2012. The organic complexation of iron in the marine environment: A review. Frontiers in Microbiology **3:** 69-86.

Hassler, C. S., E. Alasonati, C. A. M. Nichols, and V. I. Slaveykova. 2011. Exopolysaccharides produced by bacteria isolated from the pelagic Southern Ocean - Role in Fe binding, chemical reactivity, and bioavailability. Marine Chemistry **123:** 88-98.

Hawkes, J. A., M. Gledhill, D. P. Connelly, and E. P. Achterberg. 2013. Characterisation of iron binding ligands in seawater by reverse titration. Analytica Chimica Acta **766:** 53-60.

Haygood, M. G., P. D. Holt, and A. Butler. 1993. Aerobactin production by a planktonic marine *Vibrio* sp. Limnology and Oceanography **38:** 1091-1097.

Homoky, W. B., S. Severmann, J. McManus, W.M. Berelson, T.E. Riedel, P.J. Statham, R.A. Mills. 2012. Dissolved oxygen and suspended particles regulate the benthic flux of iron from continental margins. Marine Chemistry **134:** 59-70.

Hopkinson, B. M., K. L. Roe, and K. A. Barbeau. 2008. Heme uptake by Microscilla marina and evidence for heme uptake systems in the genomes of diverse marine bacteria. Applied and Environmental Microbiology **74:** 6263-6270.

Hudson, R. J. M., D. T. Covault, and F. M. M. Morel. 1992. Investigations of iron coordination and redox reactions in seawater using Fe-59 radiometry and ion-pair solvent-extraction of amphiphilic iron complexes. Marine Chemistry **38:** 209-235.

Hudson, R. J. M., E. L. Rue, and K. W. Bruland. 2003. Modeling complexometric titrations of natural water samples. Environmental Science & Technology **37:** 1553-1562.

Hunter, K. A., and P. W. Boyd. 2007. Iron-binding ligands and their role in the ocean biogeochemistry of iron. Environmental Chemistry **4:** 221-232.

Hutchins, D. A., and K. W. Bruland. 1994. Grazer-mediated regeneration and assimilation of Fe, Zn and Mn from planktonic prey. Marine Ecology-Progress Series **110:** 259-269.

Hutchins, D. A., G. R. Ditullio, Y. Zhang, and K. W. Bruland. 1998. An iron limitation mosaic in the California upwelling regime. Limnology and Oceanography **43:** 1037-1054.

Ibisanmi, E., S. G. Sander, P. W. Boyd, A. R. Bowie, and K. A. Hunter. 2011. Vertical distributions of iron-(III) complexing ligands in the Southern Ocean. Deep Sea Research Part II **58:** 2113-2125.

Jiang, M., K.A. Barbeau, K.E. Selph, K.N. Buck, F. Azam, B. Mitchell, M. Zhou. 2013. The role of organic ligands in iron cycling and primary productivity in the Antarctic Peninsula: A modeling study. Deep Sea Research Part II **90**: 112-133.

Johnson, K. S., W.M. Berelson, K.H. Coale, T.L. Coley, V.A. Elrod, W. R. Fairey, H.D. Iams, T.E. Kilgore, J.L. Nowicki. 1992. Manganese flux from continental-margin sediments in a transect through the oxygen minimum. Science **257**: 1242-1245.

Johnson, K.S., F.P. Chavez, V.A. Elrod, S.E. Fitzwater, J.T. Pennington, K.R. Buck, P.M. Walz. 2001. The annual cycle of iron and the biological response in central California coastal waters. Geophysical Research Letters **28:** 1247-1250.

Johnson, K. S., F. P. Chavez, and G. E. Friederich. 1999. Continental-shelf sediment as a primary source of iron for coastal phytoplankton. Nature **398:** 697-700.

Johnson, K. S., V.A. Elrod, S.E. Fitzwater, J. Plant, E. Boyle, B. Bergquist, K. Bruland, A. Aguilar-Islas, K.N. Buck, M. Lohan, G.J. Smith, B. Sohst, K.H. Coale, M. Gordon, S. Tanner, C. Measures, J. Moffett, K.A. Barbeau, A. King, A. Bowie, Z. Chase, J. Cullen, P. Laan, W. Landing, J. Mendez, A. Milne, H. Obata, T. Doi, L. Ossiander, G. Sarthou, P. Sedwick, C.M.G. van den Berg, L. Laglera, J. Wu, Y. Cai. 2007. Developing standards for dissolved iron in seawater. Eos Trans. AGU **88**: 131-132.

Johnson, K. S., R. M. Gordon, and K. H. Coale. 1997. What controls dissolved iron concentrations in the world ocean? Marine Chemistry **57:** 137-161.

Jones, M. E., J. S. Beckler, and M. Taillefert. 2011. The flux of soluble organic-iron(III) complexes from sediments represents a source of stable iron(III) to estuarine waters and to the continental shelf. Limnology and Oceanography **56:** 1811-1823.

King, A. L., and K. Barbeau. 2007. Evidence for phytoplankton iron limitation in the southern California Current System. Marine Ecology-Progress Series **342:** 91-103.

King, A. L., K. N. Buck, and K. A. Barbeau. 2012. Quasi-Lagrangian drifter studies of iron speciation and cycling off Point Conception, California. Marine Chemistry **128:** 1-12.

Kogut, M. B., and B. M. Voelker. 2001. Strong copper-binding behavior of terrestrial humic substances in seawater. Environmental Science & Technology **35:** 1149-1156.

Kondo, Y., S. Takeda, J. Nishoika, H. Obata, K. Furuya, W.K. Johnson, C.S. Wong. 2008. Organic iron(III) complexing ligands during an iron enrichment experiment in the western subarctic North Pacific. Geophysical Research Letters **35**: *L12601,* doi: 10.1029/2008GL033354

Laglera, L. M., G. Battaglia, and C. M. G. van den Berg. 2007. Determination of humic substances in natural waters by cathodic stripping voltammetry of their complexes with iron. Analytica Chimica Acta **599:** 58-66.

Laglera, L.M., G. Battaglia, C.M.G. van den Berg. 2011. Effect of humic substances on the iron speciation in natural waters by CLE/CSV. Marine Chemistry **127:** 134-143.

Laglera, L. M., J. Downes, and J. Santos-Echeandía. 2013. Comparison and combined use of linear and non-linear fitting for the estimation of complexing parameters from metal titrations of estuarine samples. Marine Chemistry **155:** 102-112.

Laglera, L. M., and C. M. G. van den Berg. 2009. Evidence for geochemical control of iron by humic substances in seawater. Limnology and Oceanography **54:** 610-619.

Liu, X. W., and F. J. Millero. 2002. The solubility of iron in seawater. Marine Chemistry **77:** 43-54.

Lohan, M. C., A. M. Aguilar-Islas, and K. W. Bruland. 2006. Direct determination of iron in acidified (pH 1.7) seawater samples by flow injection analysis with catalytic spectrophotometric detection: Application and intercomparison. Limnology and Oceanography: Methods **4:** 164-171.

Macrellis, H. M., C. G. Trick, E. L. Rue, G. Smith, and K. W. Bruland. 2001. Collection and detection of natural iron-binding ligands from seawater. Marine Chemistry **76:** 175-187.

Mantoura, R. F. C., and J. P. Riley. 1975. Analytical concentration of humic substances from natural-waters. Analytica Chimica Acta **76:** 97-106.

Moffett, J. W., L. E. Brand, P. L. Croot, and K. A. Barbeau. 1997. Cu speciation and cyanobacterial distribution in harbors subject to anthropogenic Cu inputs. Limnology and Oceanography **42:** 789-799.

Moore, J. K., S. C. Doney, and K. Lindsay. 2004. Upper ocean ecosystem dynamics and iron cycling in a global three-dimensional model. Global Biogeochemical Cycles **18**: Gb4028, doi:10.1029/2004gb002220

Ndungu, K. 2012. Model predictions of copper speciation in coastal water compared to measurements by analytical voltammetry. Environmental Science & Technology **46**: 7644-7652.

Poorvin, L., S. G. Sander, I. Velasquez, E. Ibisanmi, G. R. Lecleir, and S. W. Wilhelm. 2011. A comparison of Fe bioavailability and binding of a catecholate siderophore with virus-mediated lysates from the marine bacterium Vibrio alginolyticus PWH3a. Journal of Experimental Marine Biology and Ecology **399:** 43-47.

Powell, R. T., and A. Wilson-Finelli. 2003*a*. Importance of organic Fe complexing ligands in the Mississippi River plume. Estuarine Coastal and Shelf Science **58:** 757-763.

Powell, R.T., A. Wilson-Finelli. 2003*b*. Photochemical degradation of organic iron complexing ligands in seawater. Aquatic Sciences **65:** 367-374.

Rijkenberg, M. J. A., L. J. A. Gerringa, I. Velzeboer, K. R. Timmermans, A. G. J. Buma, and H. J. W. De Baar. 2006. Iron-binding ligands in Dutch estuaries are not affected by UV induced photochemical degradation. Marine Chemistry **100:** 11-23.

Rue, E. L., and K. W. Bruland. 1995. Complexation of iron(III) by natural organic-ligands in the central north pacific as determined by a new competitive ligand equilibration adsorptive cathodic stripping voltammetric method. Marine Chemistry **50:** 117-138.

Ružić, I. 1982. Theoretical aspects of the direct titration of natural-waters and its information yield for trace-metal speciation. Analytica Chimica Acta **140:** 99-113.

Sander, S. G., K. A. Hunter, H. Harms, and M. Wells. 2011. Numerical approach to speciation and estimation of parameters used in modeling trace metal bioavailability. Environmental Science & Technology **45:** 6388-6395.

Scatchard, G. 1949. The attractions of proteins for small molecules and ions. Annals of the New York Academy of Sciences **51:** 660-672.

Skrabal, S. A., J. R. Donat, and D. J. Burdige. 1997. Fluxes of copper-complexing ligands from estuarine sediments. Limnology and Oceanography **42:** 992-996.

Tagliabue, A., and C. Volker. 2011. Towards accounting for dissolved iron speciation in global ocean models. Biogeosciences **8:** 3025-3039.

van den Berg, C. M. G. 1982. Determination of copper complexation with natural organic ligands in sea water by equilibration with manganese dioxide 1. Theory. Marine Chemistry **11:** 307-322.

van den Berg. 1995. Evidence for organic complexation of iron in seawater. Marine Chemistry **50:** 139-157.

van den Berg, C. M. G., and J. R. Donat. 1992. Determination and data evaluation of copper complexation by organic ligands in sea water using cathodic stripping voltammetry at varying detection windows. Analytica Chimica Acta **257:** 281-291.

van den Berg, C. M. G., M. Nimmo, P. Daly, and D. R. Turner. 1990. Effects of the detection window on the determination of organic copper speciation in estuarine waters. Analytica Chimica Acta **232:** 149-159.

Wheatcroft, R. A., C. K. Sommerfield, D. E. Drake, J. C. Borgeld, and C. A. Nittrouer. 1997. Rapid and widespread dispersal of flood sediment on the northern California margin. Geology **25**: 163-165.

Wu, J. F., and M. B. Jin. 2009. Competitive ligand exchange voltammetric determination of iron organic complexation in seawater in two-ligand case: Examination of accuracy using computer simulation and elimination of artifacts using iterative non-linear multiple regression. Marine Chemistry **114:** 1-10.

Chapter 4

Iron-binding ligands and humic substances in the San Francisco Bay estuary and estuarine-influenced shelf regions of coastal California

1. Abstract

Dissolved iron (dFe) and organic dFe-binding ligands were determined in San Francisco Bay, California by competitive ligand exchange adsorptive cathodic stripping voltammetry (CLE-ACSV) along a salinity gradient from the freshwater endmember of the Sacramento River (salinity < 2) to the mouth of the estuary (salinity > 26). A range of dFe-binding ligand classes were simultaneously determined using multiple analytical window analysis, involving titrations with multiple concentrations of the added ligand, salicylaldoxime. The highest dFe and ligand concentrations were determined in the low salinity end of the estuary, with dFe equal to 131.5 nmol L^{-1} and strong ligand (log $K^{cond}_{FeL,Fe'}$ ≥12.0) concentrations equal to 139.5 nmol L^{-1}. The weakest ligands (log $K^{cond}_{FeL,Fe'} < 10.0$) were always in excess of dFe in low salinity waters, but were rapidly flocculated within the estuary and were not detected at salinities greater than 7. The strongest ligands (log $K^{cond}_{FeL,Fe'} > 11.0$) were tightly coupled to dFe throughout the estuary, with average excess ligand concentrations ([L]-[dFe]) equal to 0.5 nmol L^{-1}. Humic-like substances analyzed via both CLE-ACSV and proton nuclear magnetic resonance in several samples were found to be a significant portion of the dFe-binding ligand pool in San Francisco Bay, with concentrations ranging from 559.5 μg L^{-1} to 67.5 μg L^{-1} in the lowest and highest salinity samples, respectively. DFe-binding ligands and humic-like substances were also found in benthic boundary layer samples taken from the shelf near the mouths of San Francisco Bay and Eel River, suggesting estuaries are an important source of dFe-binding ligands to California coastal shelf waters.

2. Introduction

Iron (Fe) is a growth-limiting micronutrient for phytoplankton in many regions of the oceans, including even some coastal upwelling regions (Biller and Bruland, 2014; Bruland et al., 2001, 2005; King and Barbeau, 2007). This is especially true in the California Current System (CCS), a highly productive coastal region dominated by diatom growth during the spring upwelling season (Bruland et al., 2001; Hutchins et al., 1998). Although dissolved Fe (dFe) is widely recognized as a limiting nutrient, less is understood about its chemical speciation in seawater, which affects its reactivity and availability to the biological community. It is known that dFe-binding ligands are essential for maintaining dFe in solution above its thermodynamic inorganic solubility limit (Liu and Millero, 2002) and they bind the majority of the dFe in seawater (Gledhill and van den Berg, 1994; Rue and Bruland, 1995; van den berg, 1995). Organic compounds that bind dFe appear to be ubiquitous and are likely a heterogeneous mixture of complexes (Gledhill and Buck, 2012). The types of dFe-binding organic ligands present in seawater are thought to range from relatively weak macromolecules and cellular byproducts such as polysaccharides (Hassler et al., 2011*a*) and humics (Laglera and van den Berg, 2009), to low-molecular weight siderophore-like complexes such as hydroxamates (Mawji et al., 2011; Velasquez et al., 2011), and catecholates (Poorvin et al., 2011). Although only hydroxamates have thus far been directly isolated from seawater, indirect methods for detecting metal-binding ligands such as competitive ligand exchange-adsorptive cathodic stripping voltammetry (CLE-ACSV) can provide important insight on the characteristics of the ligand pool in seawater (*see* review by Gledhill and Buck, 2012).

Identifying the sources of dFe-binding ligands in seawater is an active area of research, and ligands are important in the mechanism of dFe delivery to many marine ecosystems. One such ecosystem may be the CCS, where the majority of the dFe supply is hypothesized to come from Fe-rich sediment sources along the continental shelf, ranging in character from narrow rocky shelves with low dFe to wide-shelf mudflats with high dFe near San Francisco Bay and Eel River (Biller et al., 2013; Elrod et al., 2004). High dFe concentrations have been observed in surface waters over the wide region of the shelf in the spring during the onset of upwelling (Biller et al., 2013; Elrod et al., 2008). Concentrations of dFe have been reported to increase during the initial upwelling period and decrease slowly thereafter, despite continued intensification of the upwelling (Elrod et al., 2008). This has led to the suggestion that the wide shelf regions act as 'capacitors' for dFe, charging with riverine-derived Fe during the winter flood season and discharging Fe when the Fe-rich sediments are resuspended during the initial spring upwelling phase (Bruland et al., 2001; Chase et al., 2007). Mudflats in the wide shelf region may also be a source of organic ligands, and high concentrations of strong dFe-binding ligands have been observed in the benthic boundary layer (BBL) in this region (Buck et al., 2007; Bundy et al., 2014). If these organic ligands, like the dFe with which they are associated, are primarily from terrestrial sources, then we would expect that the organic Fe-complexes in the BBL should be similar to those in local freshwater and estuarine sources such as San Francisco Bay. Previous studies have examined the binding strengths of dFe-ligand complexes in the high salinity end of the San Francisco Bay plume (Buck et al., 2007; Bundy et al. 2014), but there have been no studies of dFe-binding ligands in lower salinity waters in the San Francisco Bay estuary.

In early classic work on Fe across salinity gradients in estuarine systems, Boyle et al. (1977) found that up to 90% of the dFe in estuaries is lost to scavenging, mostly due to flocculation of humic-like substances (HS) and dFe at low salinities. Sholkovitz et al. (1978) expanded these observations to add that most of the lost dFe occurred in the colloidal size fraction. The chemical form of the small amount of dFe that survives flocculation is still unclear, however, and it is possible that organic complexation of dFe by HS plays a role in stabilizing dFe concentrations across salinity gradients. Some studies have examined the role of HS in dFe speciation in estuarine and coastal environments, using combined information about dFe binding strengths and HS distributions in the Irish Sea (Laglera and van den Berg, 2009) and Thurso Bay (Batchelli et al., 2010). Characterization of the HS pool in some studies has also shown that the high concentration of oxygen-containing functional groups in terrestrial HS is largely responsible for terrestrial dissolved organic matter (tDOM) reactivity (Stevenson, 1994), and of these functional groups, carboxyl groups are the most abundant (Cabaniss, 1991; Hatcher et al., 1981; Leenheer et al., 1995; Stevenson, 1994) and have the ability to complex dFe. In this study we examined multiple classes of dFe-binding ligands and HS using CLE-ACSV, in samples collected along a salinity gradient in San Francisco Bay. Two BBL samples were also examined, from the adjacent continental shelf in the San Francisco Bay region and from the Eel River shelf system further north. In several samples we applied proton nuclear magnetic resonance (^{1}H-NMR) to complement our CLE-ACSV analysis and provide insight into the possible chemical character of organic Fe binding groups.

This work follows on a recently published study of dFe-binding ligands in the CCS (Bundy et al. 2014), in which a multiple analytical window (MAW) CLE-ACSV approach was applied to dFe-binding ligands in order to detect several ligand classes. The method used by Bundy et al. (2014) enabled the simultaneous detection of a wide range of dFe-binding ligands (L_1-L_4), each with distinct distributions in the CCS. The authors hypothesized these ligand classes to be composed of siderophore-like ligands (L_1, log $K^{cond}_{FeL_1,Fe'}$ ≥ 12.0), HS (L_2, log $K^{cond}_{FeL_2,Fe'}$ 11-12), degradation products of the stronger ligand classes (L_3, log $K^{cond}_{FeL_3,Fe'}$ 10-11) and relatively weak macromolecules with incidental Fe binding (L_4, log $K^{cond}_{FeL_4,Fe'}$ < 10). HS was also measured directly by Bundy et al. (2014) using cathodic stripping voltammetry (CSV) (Laglera et al., 2007), which confirmed the presence of HS-like material in the BBL of mudflat regions of the California continental shelf (Bundy et al., 2014). The source of these compounds is unknown, but is thought to originate from estuarine regions such as San Francisco Bay. It is apparent from recent work (Batchelli et al., 2010; Bundy et al., 2014; Laglera and van den Berg, 2009) that some portion of terrestrial-derived HS material is resistant to flocculation in coastal estuaries, but how much is delivered to the shelf in the CCS region is an open question. This study seeks to identify the source of dFe-binding ligand complexes to the broad, estuarine-influenced shelf areas of coastal California, and characterize changes in the dFe ligand pool across an estuarine salinity gradient by employing MAW CLE-ACSV, in combination with ^{1}H-NMR and HS analysis for some samples.

3. Methods

3.1 Sampling

Samples were collected in partnership with the United States Geological Survey (USGS) on board the R/V *Polaris* on April 19, 2011 as part of the regular USGS San Francisco Bay Water Quality Measurement Program (http://sfbay.wr.usgs.gov/access/wqdata/index.html). Hydrographic data was collected for all 24 regular stations in the North Bay and Central Bay, and a subset of eight stations were sampled for dFe, organic dFe-binding ligands, and humic-like substance (HS) analyses (Figure 4.1). Hydrographic data in San Francisco Bay was obtained using a conductivity, temperature and depth (CTD) sensor outfitted with an oxygen electrode (Sea-bird Electronics), optical backscatter sensor (D&A Instruments), and a fluorometer (Turner Designs). Discrete samples were also taken for nitrate measurements (nitrate+nitrite) and other inorganic nutrients and analyzed by colorimetric methods (http://sfbay.wr.usgs.gov/access/wqdata/overview/measure/index.html). Two additional samples were also obtained for HS analyses (*see* section 2.4) from a previous cruise (Bundy et al., 2014) in the benthic boundary layer (BBL, stations 25, 26) outside of San Francisco Bay and Eel River, the two main freshwater influences on the CCS. Details about the hydrographic and ligand data of the BBL samples collected in August/September 2011 on board the R/V *Point Sur* (*see* Biller et al., 2013) can be found in Bundy et al. (2014).

DFe and dFe-binding ligand samples were collected using trace metal clean Teflon tubing and a Teflon diaphragm pump (Cole Parmer) connected to an air compressor. A small Teflon coated weight was fixed to the end of the pump tubing, and the tubing was lowered approximately 2 m below the surface off the starboard side of the

ship. A fiberglass pole was used to extend tubing approximately 2 m away from the starboard side and samples were collected while the ship was moving forward at approximately 1 knot. Samples were filtered in-line with an acid-cleaned 0.45 μm Osmonics cartridge filters (GE Osmonics) after 1 L of water had been passed through the tubing and filter. DFe samples were stored at room temperature in 250 mL acid-cleaned low density polyethylene (LDPE) bottles (Nalgene) at pH 1.8 (Optima HCl, Fisher Scientific). DFe-binding ligand and HS samples were placed in two 500 mL fluorinated polyethylene (FPE) bottles (Nalgene) and immediately frozen (-20°C) until analysis.

3.2 Dissolved iron

DFe samples were analyzed according to Biller and Bruland (2012), building on earlier work of Sohrin et al (2008). This multi-elemental analysis method utilizes an offline pre-concentration step after pH adjustment (pH=6.2) of acidified samples onto the Nobias-chelate PA1 resin (Hitachi High-Technologies; Sohrin et al., 2008). After pre-concentration in a closed-column manifold, the columns are rinsed with ammonium acetate and the trace metals are subsequently eluted using 1 N quartz distilled nitric acid (Fisher Scientific). Samples were measured using magnetic sector inductively coupled plasma- mass spectrometry (ICP-MS). For dFe, the recovery from the column was greater than 98%, with an average blank equal to 0.030 nmol kg^{-1} and a detection limit of 0.014 nmol kg^{-1}. This method had excellent agreement with reported consensus values for SAFe (Johnson et al., 2007) and GEOTRACES reference samples (www.geotraces.org), yielding values for S1 of 0.091±0.001 nmol kg^{-1} (0.093±0.008 nmol kg^{-1} consensus value as of May 2013) and 0.98±0.009 nmol kg^{-1} for D2 (0.933±0.023 nmol kg^{-1} consensus value).

3.3 Dissolved iron-binding ligands

Organic dFe-binding ligands were analyzed using a multiple analytical window (MAW) adaptation (Bundy et al., 2014) of traditional competitive ligand exchange-adsorptive cathodic stripping voltammetry (CLE-ACSV) methods (*see* Buck et al., 2012 for an intercomparison of these methods). Competitive ligand approaches utilize a well-characterized added ligand to set up a competition between the added ligand and the natural ligands present in the sample. The added ligand, in this case salicylaldoxime (SA), makes an electro-active complex with the dFe in the sample and the $Fe(SA)_x$ complex adsorbs to the mercury drop of a controlled growth mercury electrode (CGME, Bioanalytical Systems Incorporated). The dFe is then reduced and stripped from the $Fe(SA)_x$ complex (cathodic stripping) and the change in current is recorded by the analyzer (Epsilon 2, Bioanalytical Systems Incorporated) connected to a laptop computer. The peak height at each titration point can then be related to the amount of $Fe(SA)_x$ formed, and the remaining speciation can be calculated via the sensitivity and mass balance.

3.3.1 Ligand titrations

In order to set-up each titration, individual acid-cleaned Teflon vials were first conditioned to the expected dFe addition for 24 hours. Then, 10 mL aliquots of the sample were placed in 10 different vials along with 50 µl of a 1.5 M boric acid buffer (pH 8.2, NBS scale) made in 0.4 mol L^{-1} ammonium hydroxide (Optima, Fisher Scientific). The buffer and added dFe (0-100 nmol L^{-1}) were left to equilibrate for at least two hours. The competitive ligand SA was then added to each vial (9-33 µmol L^{-1}) and

was equilibrated for 15 minutes. The contents from each vial were placed into a Teflon cell and were analyzed consecutively via ACSV.

3.3.2 Multiple analytical window approach

The MAW approach used by Bundy et al. (2014) involves doing multiple titrations for each sample with a different concentration of the added ligand, yielding different competition strengths of SA. Five analytical windows were employed in this study, ranging in [SA] from 9-33 µmol L^{-1}. The highest analytical window (33 µmol L^{-1} SA, window 1) was the same in every sample, and this titration was used as an 'overload' titration to determine only the sensitivity in each sample (*see* section 2.3.3); no ligand concentrations were determined from these titrations. The other four analytical windows (windows 2-5) were used for determining four separate ligand classes (L_1-L_4). The analytical window is expressed as the side reaction coefficient, $\alpha_{Fe(SA)_x}$, of the added ligand, determined by

$$\alpha_{Fe(SA)_x} = K^{cond}_{Fe(SA)} \times [SA] + \beta^{cond}_{Fe(SA)_2} \times [SA]^2 \quad (1)$$

where $K^{cond}_{Fe(SA)}$ and $\beta^{cond}_{Fe(SA)_2}$ are the conditional stability constants of the mono and bis-SA complex with dFe. The strength of SA has been carefully characterized in previous studies under marine (Abualhaija and van den Berg, 2014) and estuarine (Buck et al., 2007) conditions. All $\alpha_{Fe(SA)_x}$ constants used in this study were determined based on the most recent calibration of SA (Abualhaija and van den Berg, 2014) and corrected for salinity effects on $\alpha_{Fe(SA)_x}$ (Buck et al., 2007). Slightly different concentrations of SA were used in each sample (with the exception of the overload titration) at each analytical window in order to have a similar $\alpha_{Fe(SA)_x}$ in each sample because of the effect of

salinity on $\alpha_{Fe(SA)_x}$. Although salinities were determined at each station using the CTD, salinities were also measured in individual speciation samples to account for any differences in salinity due to different collection depths with the trace metal pump and the ship's CTD. The salinity in speciation samples was measured using an aliquot from the speciation bottles and a hand-held digital refractometer. The salinity was found to vary by up to 2 salinity units (psu) between the salinity measured in the field by the CTD vs. the refractometer in the lab, and thus the salinity determined in each bottle was used to calculate the $\alpha_{Fe(SA)_x}$and these salinity values are also presented with the speciation data.

3.3.3 Determination of the sensitivity

The sensitivity of the method is often determined by internal calibration of the linear portion of the titration curve, where the majority of ligands in the sample have been titrated by added dFe (Rue and Bruland, 1995). However, it has been shown recently that HS may interfere slightly with the sensitivity determination in CLE-ACSV when SA is the added ligand (Laglera et al., 2011). High ligand and surfactant concentrations in estuarine samples also make the determination of the 'true' sensitivity difficult in these samples, especially in lower salinity samples where low sensitivities were particularly apparent. 'Overload' titrations were therefore employed at the highest analytical window (33 µmol L^{-1} SA) in order to outcompete all ligands in the sample and ensure an accurate determination of the sensitivity, while still accounting for any surfactant effects in the sample (Bundy et al., 2014; Kogut and Voelker, 2001). This 'overload' sensitivity was then corrected by a ratio in order to obtain the sensitivities at lower concentrations of SA (windows 2-5; Hudson et al., 2003). 'Overload' sensitivities

in each sample are presented in the supplementary information (S 4.1). The ratio used to correct the 'overload' sensitivity for lower concentrations of SA was calculated by comparing the internal sensitivities in each sample (slope of the last three titration points) at every [SA], and using the average ratio from all samples between the 'overload' sensitivity and the internal sensitivities. The average ratio (R_{AL}) used to correct the sensitivities at each [SA] is shown in the supplementary information (S 4.2) for the corresponding analytical window. As noted above however, the [SA] used in each sample for the four analytical windows (windows 2-5) varied slightly due to the effects of salinity on $\alpha_{Fe(SA)_x}$(*see* section 2.3.2), but the corresponding R_{AL} was not found to vary significantly with only these small changes in [SA] (from 1-2.7 μmol L^{-1}). A constant R_{AL} was used for each window, corresponding to a value of 0.7, 0.5, 0.4, and 0.2 for windows 2-5, respectively.

3.3.4 Data processing

Ligand concentrations and strengths were determined based on the averages of van den berg/Ružić and Scatchard linearizations at each analytical window (Buck et al., 2012; Mantoura and Riley, 1975; Scatchard, 1949). This method gives only a graphical estimate of the error, so data was also fit using a publicly available multiple detection window analytical tool for comparison (*see* section 2.3.5). Only one ligand class was determined at each analytical window, and characterized as L_1-L_4 based on the absolute strength of the ligand according to recommendations from Gledhill and Buck (2012). This study defines L_1 as ligands with log $K'^{cond}_{FeL,Fe} \geq 12.0$, L_2 with $12.0 >$ log $K'^{cond}_{FeL,Fe} \geq 11.0$, L_3 with a log $K'^{cond}_{FeL,Fe}$ range of $11.0 >$ log $K'^{cond}_{FeL,Fe} \geq 10.0$ and L_4 with a log

$K'^{cond}_{FeL,Fe}$< 10.0. L_1 ligands were determined at the highest analytical window, just below the 'overload' titration window and each subsequent ligand class was determined at progressively lower analytical windows, using the optimal analytical window for that particular ligand class (Bundy et al., 2014). A ligand was 'not detected' if the conditional stability constant of a ligand class determined at one analytical window was identical to that at a higher analytical window. For example, if a ligand with a log $K'^{cond}_{FeL,Fe}$= 10.0 was determined at both windows 4 and 5, then that sample would be deemed to contain no L_4 ligands since no ligands were measured with a log $K'^{cond}_{FeL,Fe}$< 10.0.

3.3.5 Data processing comparison

Several methods are in the intercalibration stages for processing multiple analytical window CLE-ACSV data (Giambalvo, 1997; Hudson et al., 2003; Omanović et al., in review; Pižeta et al., in review; Sander et al., 2011). None of these methods have been tested yet for dFe organic speciation, but two of the methods are currently available for download from the website of Scientific Committee on Oceanic Research (SCOR) working group 139: 'Organic Ligands-A key Control on Trace Metal Biogeochemistry in the Ocean' (http://neon.otago.ac.nz/research/scor/links.html). To ensure there was no overlap in our ligand detection and that our ligand parameters could accurately fit the titration data, the data from each detection window was fit using a modification of the Hudson (unpubl.; Pižeta et al., in review) simultaneous multi-window approach for copper speciation data interpretation adapted for dFe organic speciation. This tool is available online (https://sites.google.com/site/kineteql/home/about-kineteql) and incorporates a KINETEQL equilibrium solver add-in for Microsoft Excel (Giambalvo,

1997) to the approach developed by Hudson et al. (2003) and Sander et al. (2011). This method for titration interpretation will be further referred to as the 'Hudson' protocol throughout the manuscript. This method only allows for the detection of three ligand classes, so a comparison was made between the L_3 determined by the Hudson multi-window tool and L_3+L_4 found in this study (S 4.3).

3.4 Humic-like substance analysis by CSV

Humic-like substances (HS) were measured in five San Francisco Bay samples (stations 2, 13, 24, 25 and 26) in order to assess the potential contribution of HS to the dFe-binding ligand pool. The [HS] at stations 25 and 26 were presented previously in Bundy et al. (2014), and this study expands those measurements to include proton nuclear magnetic resonance (^{1}H-NMR) data. Four of the five stations where HS was measured by CSV were analyzed using ^{1}H-NMR (stations 13, 24, 25 and 26), as described in section 2.6. HS by CSV were measured according to the methods described in Laglera et al. (2007). Briefly, a 20 mg L^{-1} stock solution of Suwannee River Fulvic Acid Standard (International Humic Substance Society) was prepared in purified water (MilliQ water, 18 mol L^{-1} Ω cm) and added to 10 mL sample aliquots along with boric acid-ammonia buffer (pH 8.2, NBS scale) and dFe (100 nmol L^{-1}, secondary stock solutions made from an AA standard). Three vials contained no added HS, while the rest of the vials contained 5-150 μg L^{-1} HS and were left to equilibrate for at least 2 hours. Immediately before analysis by CSV, 400 μl of 0.4 mol L^{-1} potassium bromate was added in order to catalyze the reaction without oxidizing the HS. Each aliquot was analyzed separately using CSV as described by Laglera et al. (2007) using the standard

addition method. This method measures all organic substances that bind dFe and are shown to be ‘humic-like’, or contributing to the electrochemical peak at -0.6 V.

3.5 Dissolved organic carbon (DOC)

Samples for dissolved organic carbon (DOC) were taken from stations 13, 24, 25 and 26 and run in triplicate. Aliquots from the speciation bottles were taken and placed in 60 mL glass bottles and acidified to pH 2 with 6 M phosphoric acid before analysis. DOC concentrations were measured on a Shimadzu TOC-V Combustion Analyzer using high temperature (680°C) platinum (Pt)-catalyzed oxidation coupled to non-dispersive infrared gas detection of carbon dioxide (CO_2). Calibration standards were prepared using a potassium hydrogen phthalate (KHP) standard.

3.6 Proton nuclear magnetic resonance (^{1}H-NMR) analysis

The dissolved organic matter (DOM) from four stations (13, 24, 25, and 26) was characterized by ^{1}H-NMR at its natural DOM concentration without prior pretreatment. All the ^{1}H-NMR experiments were acquired using a Bruker Avance III 400 spectrometer. D_2O (> 99.9%, Aldrich Chemical Company, Milwaukee, WI) was added to 0.5 mL of the sample at a ratio of 10:90 in 5-mm glass NMR tubes (Wilmad Glass Co., NJ). Solution state ^{1}H-NMR spectra were acquired using a water suppression technique originally described by Lam and Simpson (2008) with modification. A recycle delay of 2 s was used along with a 119 ms acquisition time. Using the water suppression techniques slightly attenuates the carbohydrate signal around 3.5 ppm (Lam and Simpson, 2008); however, by using this technique we insured a complete suppression of the water peak. The ^{1}H-NMR spectra were then normalized to their total area (0.20- 10.00 ppm) and

vertically scaled by a factor of 1000. Using this technique allows for characterization the entire DOM pool without any fractionation, isolation or sample pre-treatment.

4. Results

4.1 Hydrographic data

All hydrographic data was collected by the USGS San Francisco Bay Water Quality Measuring Program and can be found in their database (http://sfbay.wr.usgs.gov/access/wqdata/index.html). The stations sampled ranged from the freshwater endmember of the Sacramento River (salinity, $S < 2$), past the mouth of San Francisco Bay ($S > 21$), and into the northern third of South Bay ($18 < S < 21$; Figures 4.1 and 4.2). The maximum salinity was measured in Central Bay at station 18, with lower salinities in South Bay (station 24) and closer to the Sacramento River (station 2). The temperature ranged from 13-15°C, with higher temperatures in the low salinity region of North Bay (Figure 4.2). Nitrate (nitrite+nitrate) ranged from 7.6 μmol L^{-1} at station 3 to a maximum of 15.6 μmol L^{-1} at station 15 in Central Bay. Elevated chlorophyll *a* concentrations were observed at stations 21 and 22 in the upper region of South Bay (15.3 and 13.4 μg L^{-1}, respectively; Figure 4.2).

4.2 Dissolved iron

DFe concentrations were highest at station 2, in the low salinity end of the bay, and decreased towards the mouth of San Francisco Bay (Figure 4.3A), as observed in many other estuarine studies (e.g. Boyle et al., 1997; Buck et al., 2007; Murray and Gill, 1978; Sholkovitz et al., 1978). The non-conservative behavior in [dFe] with increasing salinities indicates either (1) there is a net sink of dFe due to flocculation; (2) the time scale of variation in [dFe] for the marine and freshwater endmembers is shorter than the

flushing time of San Francisco Bay; or (3) there is mixing from multiple freshwater endmembers that have different [dFe]. The highest [dFe] was measured at station 8 in Suisun Bay (Figure 4.1), and was 131.5 nmol L^{-1}. This likely reflects the additional freshwater [dFe] and ligand sources from the Suisun Slough. The lowest [dFe] in San Francisco Bay was 7.0 nmol L^{-1}at station 21 in Central Bay. The highest [dFe] were found at the lower salinities in general, although the lowest salinity sample (station 2) did not have the highest [dFe] (station 8) and higher variability was seen in low salinity samples (Figure 4.3A).

4.3 Ligand data comparison

The dFe-binding ligand results from this study were compared between two different interpretation approaches: the conventional discrete linearizations approach and the unified Hudson protocol (Giambalvo, 1997; Hudson et al., 2003; Sander et al., 2011), modified for dFe organic speciation. Although the Hudson method has not been tested yet for dFe speciation, a unified approach to analyzing multiple analytical window datasets has been shown for copper speciation to yield better results than interpreting single window data alone (Pižeta et al., in review; Sander et al., 2011). Updated constants for SA were used for the interpretations, and R_{AL} was set to the values calculated in this work (1.0, 0.7, 0.5, 0.4, 0.2; S 4.2). The initial guess for the sensitivity and ligand parameters in the Hudson protocol were set to the overload sensitivity determined in that sample and the ligand concentrations determined by the linearization techniques for this work. Since only three ligands can be currently calculated in the Hudson protocol regardless of number of analytical windows employed, we compared [L_3] from the Hudson method to [L_3+L_4] from the linearization output. A comparison of the results

between both approaches is shown in S 4.3, with good agreement seen between the two methods (r^2= 0.87), particularly with the ligand concentrations. Poorer agreement was seen with the log $K'^{cond}_{FeL,Fe}$, where the log K was systematically higher in the Hudson protocol results (S 4.3). Overall, the good agreement between methods ensured we were not getting overlapping ligand concentrations in our different analytical windows, and that linearization techniques compare relatively well with unified analytical window data processing approaches currently under development.

4.4 Dissolved iron organic speciation

DFe-binding organic ligands are expressed as operationally defined ligand classes, distinguished simply by their conditional stability constants (Bundy et al., 2014). Traditionally, in the literature 'L_1' and 'L_2' ligands are determined based on their relative strengths, while the classification in this paper is based on absolute strengths. Multiple analytical window (MAW) analysis enables the detection a much broader range of ligand strengths than have been observed in the literature by any one study (Gledhill and Buck, 2012). However, in general, the stronger ligands (L_1 and L_2 in this study) are comparable to ligand classes denoted as 'L_1' in the literature, and weaker ligands (L_3 and L_4) are comparable to 'L_2' in the literature (Bundy et al., 2014; Gledhill and Buck, 2012).

The strongest ligands were inversely related to salinity in San Francisco Bay (Figure 4.3A). The highest [L_1] were found at station 8, where [dFe] was also the highest (Table 4.1). In order to examine patterns in the ligands that might be de-coupled from the [dFe], 'excess' ligand concentrations are also shown in Figure 4.3B. 'Excess' ligand is defined in this study simply as [L_x]-[dFe], where *x* denotes the ligand class. Excess L_1 ligand concentrations (*e*L_1; [L_1]-[dFe]) ranged from -12.3 to 7.9 nmol L^{-1} (Figure 4.3B),

and were relatively tightly coupled to [dFe] compared to the other ligand classes. L_2 ligands showed a similar pattern to L_1, though with higher concentrations and a slightly larger range in [eL_2] (-10.4 to 9.6 nmol L^{-1}).

The weaker ligands (L_3 and L_4) showed a similar pattern with increasing salinity as the stronger ligands and dFe, but with subtle differences (Figure 4.3). The highest concentration of L_3 ligands was at station 4, and the lowest at station 21 with 88.8 $\pm$ 9.4 nmol L^{-1} and 16.0 $\pm$ 0.03 nmol L^{-1}, respectively. Although every station contained detectable stronger ligands, station 8 and 13 did not have detectable L_3 ligands (Table 4.1) though they were detectable again at higher salinities. The range of [eL_3] was also wider than for the stronger ligands, with a range of -8.2 to 13.3 nmol L^{-1} (Figure 4.3B).

L_4 ligands were the most distinct in terms of the patterns within the estuary, and showed de-coupling from the [dFe] (Figure 4.3). [L_4] were extremely high within the low salinity end of the estuary (163.3 $\pm$ 3.7 nmol L^{-1} at station 8) and were no longer detectable in any samples with salinities above 7. In the stations where L_4 ligands were detected, they were always in excess of the [dFe], leading to large excess ligand concentrations (up to 65.9 nmol L^{-1}). Low salinity samples also had a higher overall complexation capacity (log α_{L_T}; data not shown) based on the potential of contribution of all ligand classes to bind dFe, suggesting the weaker ligands may also effectively compete with stronger ligands for dFe in low salinity waters.

4.5 Humic-like substances

Humic-like substances (HS) were determined by CSV (Laglera et al., 2007) and also inferred from ^{1}H-NMR (Abdulla et al., 2013) in samples in San Francisco Bay and California coastal waters (Figure 4.1). HS determined by CSV were found to range from

67.5 μg L^{-1} to 559.5 μg L^{-1} in San Francisco Bay, with the highest concentrations found at station 2, and lower concentrations found at station 24 (Table 4.1). In general, HS behaved non-conservatively in the estuary like dFe and ligands (Figure 4.4). HS were measured by CSV in the two California shelf BBL samples (Bundy et al., 2014), and are also shown in Table 4.1 for comparison. HS were determined to be part of the L_2 ligand pool in previous work (Bundy et al., 2014) based on the log $K'^{cond}_{FeL,Fe}$, determined by Laglera et al. (2007), which was found to be equal to 11.1-11.6 (Abualhaija and van den Berg, 2014). There was also a direct relationship in this study (r^2=0.95, $p < 0.05$, $n = 4$) between HS concentrations and the concentration of L_2 ligands (data not shown), suggesting HS may be predominantly part of the L_2 ligand pool. Some of this relationship is likely driven by a similar relationship between HS and [dFe], though a similarly robust relationship does not hold for the concentration of other ligand classes vs. [HS] (data not shown).

The amount of potential dFe binding capacity by HS can be calculated according to the binding capacity of HS measured by Laglera and van den Berg (2009). They reported that HS could bind 32 nmol Fe per mg of HS on average, which results in a range of binding capacities for dFe in San Francisco Bay samples (Figure 4.4). Based on this calculation, the concentration of dFe binding that could be accounted for by HS ranges from 0.72 nmol L^{-1} at station 25 in the BBL to 17.9 nmol L^{-1} at station 2 in San Francisco Bay (Figure 4.4). The percentage of dFe complexation by HS, in the absence of competition from any other ligands, decreased from 23% at station 2 to 3% at station 26, though there was still a significant percentage of the dFe complexed by HS at station 25 because of the much lower dFe concentrations (Table 4.1).

The presence of HS was additionally inferred from ^{1}H-NMR in four samples where HS was also determined by CSV (stations 13, 24, 25, and 26) as described in section 3.6 below.

4.6 DOC and ^{1}H-NMR analysis

Four samples were analyzed for both DOC and ^{1}H-NMR measurements as a first step in trying to understand the chemical components of the ligand pool coupled to detailed electrochemical measurements (Table 4.2). Station 13 showed the highest DOC concentrations compared to the other stations (106 μmol L^{-1}, Table 4.2), which was followed by the other surface station (Station 24, 83 μmol L^{-1}). The two BBL stations (25 and 26) had a very similar DOC concentration, with 79 and 76 μmol L^{-1}, respectively (Table 4.2).

All ^{1}H-NMR spectra of the DOM from the four stations (Figure 4.5) had several bands in common. They all illustrate an intense methyl band ($C\underline{H_3}$-C) centered on 1.2 ppm, which could be derived from either the lipids' CH_2 group or the CH_3 group of deoxy-sugars. Based on some recent studies, the assignment of these signals is mostly to deoxy-sugars. For example, Panagiotopoulos et al. (2007) used both correlation spectroscopy (COSY) and heteronuclear single quantum coherence (HSQC) NMR analysis to verify that this band is mostly from methyl group of deoxy-sugars in oceanic water samples isolated by ultrafiltration. Also, Abdulla et al. (2013) also showed that this band in ultrafiltration-isolated DOM has a positive correlation with the changes in carbohydrate signatures and a negative correlation with the terminal methyl groups along a salinity transect. Ultrafiltration was not used in the current study, so there is a possibility that lipid-like components are contributing to the DOM and the peak at 1.2

ppm may have some contribution from lipids. A band around 2.0 ppm is attributed mainly to methyl protons of the acetate functional group ($CH_3C=O$) (Aluwihare et al., 1997; Repeta et al., 2002), and a broad band centered at 3.5 ppm was assigned to protons from carbohydrate compounds (CHOH; Aluwihare et al., 1997). Interestingly, all four stations show an absence of unsaturated and aromatic signatures as indicated by missing the very broad band between 6.0 and 9.0 ppm. To estimate the contribution of the major chemical functional groups, each spectrum was divided into seven defined bands according to Abdulla et al. (2013): (1) CH_3–C (0.25–1.02 ppm), (2) CH_3-deoxy sugar (1.02–1.39 ppm), (3) CH_x–C–COO/CH_x–C–Ar (1.39–1.82 ppm), (4) CH_3–C=O (1.82–2.08 ppm), (5) CH_x–COO/CH_x –Ar (2.08–3.25 ppm), (6) CHOH (3.25–5.80 ppm), and (7) H–Ar/H–C=C (5.8–9.00 ppm). The area percentage of each of these functional groups is presented in Table 4.2. These seven functional groups are classified into two major chemical components: a) Carboxylic Rich Alicyclic Molecules (CRAM), which includes band numbers 1, 3, 5 and 7; and b) Heteropolysaccharides (HPS), which consists of band numbers 2, 4 and 6 (Hertkorn et al., 2006; Abdulla et al., 2013). The surface stations in San Francisco Bay (13 and 24) had a significantly higher CRAM percentage compared to the BBL stations (25 and 26, Table 4.2), and the BBL stations had a higher HPS component compared to the two San Francisco Bay stations (Table 4.2).

In order to account for the differences in the DOC concentrations between the stations, the area percentage of CRAM of each station was multiplied by its DOC concentration (%CRAM*DOC, Table 4.2). This normalized CRAM component (%CRAM*DOC) was plotted against [HS] determined by CSV (Figure 4.6), and resulted in a strong positive correlation ($r^2 = 0.96$, $p < 0.05$) between the two parameters.

5. Discussion

5.1 The coupling of stronger ligands (L_1 and L_2) and dissolved Fe

The two strongest ligand classes measured in San Francisco Bay have very similar distributions within the estuary (Figure 4.3). The excess ligand concentrations (Figure 4.3B) reveal that dFe in San Francisco Bay is relatively tightly coupled to the stronger ligand classes, especially in the higher salinity samples where eL_1 and eL_2 approach zero. Buck et al. (2007) was the first to note this close correlation in the San Francisco Bay plume, and suggested the stronger ligands were the most important in stabilizing the [dFe]. This was supported by the fact that leachable particulate Fe concentrations remained high in the plume, while dFe was 'capped' at the stronger ligand concentrations (Buck et al., 2007). The same phenomenon was observed in additional samples in the CCS in a follow-up study by Biller et al. (2013) and Bundy et al. (2014), especially within the BBL.

Additional evidence for the tight coupling between dFe and the strongest ligands is apparent when the internal fluxes of each constituent are calculated within the estuary. These fluxes can be estimated according to the methods of Flegal et al. (1991), where the internal flux is defined as $F_{int} = R(C_* - C_0)$, and F_{int} is the flux of the constituent within the estuary (nmol day^{-1}), R is the river discharge (L day^{-1}), C_* is the hypothetical riverine endmember given conservative mixing (nmol L^{-1}), and C_0 is the actual riverine endmember measured at station 2 (nmol L^{-1}). The river discharge (R) was estimated based on a 19 day average of the Sacramento River on the days immediately preceding sample collection in April (http://waterdata.usgs.gov/ca/nwis/current/?type=flow&group_key=basin_cd), and was

equal to 7.43 x $10^9 \pm$ 1.88 x 10^9 L day^{-1}. The value of C_* was estimated according to Flegal et al. (1991) by extrapolating the linear best-fit line from the linear portion of the mixing curve at the highest salinities to the zero salinity endmember, if conservative mixing from seawater alone were considered. When the value of C_* is less than the measured riverine endmember at station 2, then the constituent has an internal sink. These calculations all assume steady state conditions in San Francisco Bay, and that the variation in the freshwater endmember is small compared to the inventory of the constituent (Officer, 1979). Very similar dFe concentrations were obtained in this study compared to others (Flegal et al., 1991; Sañudo-Wilhelmy et al., 1996) despite the differences in sampling seasons. Thus, for the purposes of these approximations, steady state conditions are taken as a valid assumption. Based on this calculation, dFe and the strongest ligands have internal sinks in San Francisco Bay of a similar magnitude (Figure 4.7). The magnitude of F_{int} for dFe, L_1 and L_2 were calculated to be -323.5 $\pm$ 58.9, -370.3 $\pm$ 55.0, and -324.6 $\pm$ 59.1 nmol day^{-1}, respectively. These fluxes are statistically indistinct (*t-test*, $p > 0.05$), and represent very similar processes effecting both dFe and stronger ligands in San Francisco Bay. This is also apparent from the residual analysis in Figure 4.8, where residuals are shown as deviations from the best-fit polynomial line through each of the datasets (dFe and ligands). The stronger ligands (L_1 and L_2) and dFe have relatively similar residuals when compared to the weaker ligands, confirming the trends observed in stronger ligands are correlated with those in dFe.

Although there are high concentrations of stronger ligands in the low salinity end of the estuary (Table 4.1) they are almost completely titrated with dFe, which is made apparent by the low, and sometimes negative, excess ligand concentrations (Figure 4.3B).

The excess stronger ligands remain fully titrated at the higher salinities and perhaps even slightly increase in the highest salinity sample (Figure 4.3B). This suggests that the strongest ligand complexes are the most resistant to flocculation in the estuary, and that dFe is perhaps even further stabilized at high salinities by a source of stronger ligands from the seawater endmember. Elevated concentrations of strong ligands have been observed in CCS coastal waters (Bundy et al., 2014) so coastal waters may provide a small but significant source of strong ligands to San Francisco Bay and vice versa. In Bundy et al. (2014), two samples were taken from the mouth of San Francisco Bay (on an ebb tide) and those stations contained very high strong ligand concentrations (Bundy et al., 2014; transect 16). Thus, it is not entirely clear whether low salinity waters are the sole source of the stronger ligands observed in San Francisco Bay. Regardless, the stronger ligands appear to prevent some portion of the dFe from precipitating at higher salinities. This was also noted in the Satilla River Estuary, where Jones et al. (2011) observed a strong correlation between dFe-ligand complexes and [dFe] in the estuary, which they hypothesized was accounted for by a portion of the dFe pool bound to strong ligands (Jones et al., 2011).

Krachler et al. (2012) observed a portion of the DOM pool to be completely resistant to flocculation in mixing experiments at high salinities, which they hypothesized to be comprised at least in part by HS (Batchelli et al., 2010). They also found that approximately 16% of the dFe in their study area was bound to small (0.5-3.0 nm) organic molecules which comprised the portion of dFe that was resistant to scavenging (Krachler et al., 2012). These dFe-containing complexes were found to be identical to terrigenous lignin phenols that have been found in many areas of the oceans (Benner et

al., 2005; Hernes and Benner, 2002, 2006; Louchouarn et al., 2010; Opsahl and Benner, 1997). Abdulla et al. (2013) showed that the terrestrial CRAM component consists mainly of two different classes of compounds (aliphatic polycarboxyl compounds and lignin-like compounds) and these two classes share similar biogeochemical reactivity along the estuary. Based on this finding, it is expected that the Fe-rich nanoparticles detected by Krachler et al. (2012) are also enriched with aliphatic polycarboxyl compounds as well as lignin-like compounds. In the current study, there was a significant percentage of CRAM in all four samples analyzed by ^{1}H-NMR, suggesting that the CRAM component is relatively consistent across the sampled salinity gradient, although there were only four samples measured. It is likely that the complexation of these compounds with dFe represents at least some portion of the stronger ligand pool seen in this study to be resistant to scavenging.

Many of the siderophores that have been identified in aquatic systems appear to originate from freshwater cyanobacteria (Ito et al., 2004; Simpson and Neilands, 1976; Wilhelm and Trick, 1994) and heterotrophic bacteria (Gledhill et al., 2004; Mawji et al., 2011). Although diatoms clearly dominate in San Francisco Bay (Cloern 1996; Cloern and Dufford, 2005), cyanobacteria and heterotrophic bacteria are present across large gradients in salinity and appear to be ubiquitous (Cloern and Dufford, 2005). It is, therefore, likely that bacteria may be largely responsible for production of siderophores in San Francisco Bay, which then contribute to the measured strong ligand pool in low salinity waters. The percentage of the CRAM component in the surface samples from San Francisco Bay is slightly higher than the marine BBL samples, and the CRAM component has been linked to dFe binding in other studies (*e.g.*, Abdulla et al., 2010).

Isolated siderophores in culture are known to contain carboxylate functional groups (Vraspir and Butler 2009), but these types of siderophores have not been directly isolated from seawater. Based on the presence of strong ligands and high CRAM components in samples from San Francisco Bay, this study suggests the presence of carboxylate-containing dFe-binding ligands in the estuary, though the extent of their presence is unclear since not all stations were sampled. Although it is not certain how strong the carboxylate-containing organic complexes are with dFe, it is possible that CRAM components may be present in the stronger ligand pools (L_1 and L_2).

5.2 Flocculation of weaker ligands and dissolved iron

The distributions of weaker ligands in San Francisco Bay are distinct from those of the stronger ligand pool (Figure 4.3). The L_3 ligands (log $K^{cond}_{FeL,Fe'}$= 10-11) are high in stations 2-6 (Table 4.1), but were not detected in mid-salinity samples. They are detected in higher salinity samples again, with slightly elevated [eL_3] over the stronger ligands at these salinities (Figure 4.3B). The [eL_3] in the low salinity samples are comparable to [eL_2], though slightly lower than the [eL_4]. The concentrations of L_4 ligands are extremely high in the low salinity end of the North Bay, and are not detectable at salinities higher than 7 (Figure 4.3). The fact that L_4 ligands are no longer detectable at higher salinities, and [eL_3] generally declines through the estuary, suggests that most of the dFe lost to flocculation occurs in the portion of dFe bound to weaker ligands.

Internal fluxes of the weaker ligands are also statistically distinct (*t-test, $p < 0.005$)* from the flux of dFe and stronger ligands in San Francisco Bay (Figure 4.7). The internal flux of dFe and strong ligands were all approximately -300 mol day^{-1}, while for L_3 ligands it is -476.6 $\pm$ 95.8 mol day^{-1} and -599.2 $\pm$ 105.9 for L_4 ligands. This likely

reflects the different processes and chemical characteristics of the weaker ligand pool compared to the stronger ligand pool in San Francisco Bay. Although no size-fractioned ligand data is available for this study, it is possible that the majority of the weaker ligand pool is in the colloidal size fraction which has been shown to flocculate more rapidly compared to the soluble fraction (Batchelli et al., 2010; Moore et al, 1979; Murray et al. 1978; Sañudo-Wilhelmy et al., 1996; Sholkovitz et al., 1978).

There are a variety of possible sources for weaker ligands in San Francisco Bay, based on evidence from previous studies done on ligands and DOM in this estuary. In the Buck et al. (2007) study of the Columbia River and San Francisco Bay plumes, the authors identified strong ligands in both areas but only detected weaker ligands in the San Francisco Bay plume. This was attributed to the different residence times of the two estuaries, with North San Francisco Bay having a longer residence time (1-60 days; Flegal et al., 1991) than the Columbia River. The authors suggested that weaker ligands might be degradation products of the stronger ligand pool based on the longer flushing time (Buck et al., 2007). Although some weaker ligands were probably undetected in the Columbia River due to the use of a relatively high analytical window ($\alpha_{Fe(SA)_x}$= 60), it is possible that residence time plays a role in the dFe-binding ligand pool. It is also likely that the composition of DOM is important. This is supported by observations of high concentrations of detrital DOM and particulate organic matter (POM) in the low salinity endmember of San Francisco Bay (Murrell et al., 2000) and organic matter fluxes from sediments in Suisun Bay (Murrell et al., 2000). Indeed, higher weaker ligand concentrations are observed in Suisun Bay in this study (stations 4-8) and are likely contributed from sediment resuspension in that area similar to what has been observed in

other estuaries with high organic content (Jones et al., 2011). Additional sources of ligands beyond those derived from the San Joaquin and Sacramento Rivers, such as sediment resuspension, are apparent from the residual analysis (Figure 4.8), where ligands are elevated at salinities 3-7 in Suisun Bay. It is also possible that adjacent marsh lands are a source of ligands, as elevated copper-binding ligands were also seen in this area in another study (Buck and Bruland, 2005). Besides organic matter from sediments and marsh lands in Suisun Bay, Murrell et al. (2000) also found that a large portion of the organic matter in low salinity samples was from remineralization of algal POC, which has been shown in other studies to be a source of weaker ligands and dFe (Boyd et al., 2010).

The ^{1}H-NMR data also provides a first step towards identifying the weaker ligands in San Francisco Bay and in the BBL. The observed flocculation of metals and HS at low salinities in estuaries (Boyle et al., 1977; Sholkovitz et al., 1978) and the loss of weaker ligands at high salinities indicate that some portion of HS is likely also part of the weaker ligand pool, despite its relatively elevated conditional stability constant (Laglera and van den berg, 2009). This is also supported by the decline in dFe complexation by HS at higher salinities (Figure 4.4). In addition to HS, Table 4.2 indicates a high percentage of heteropolysaccharide (HPS) components were found in all four samples analyzed. Although polysaccharides were not measured in this study and have not been measured directly in San Francisco Bay, high concentrations of carbohydrates have been observed in estuaries (Abdulla et al., 2013; Wang et al. 2010) and shown to decline non-conservatively with salinity (Wang et al., 2010). Polysaccharides have the potential to transfer carbon from the dissolved to particulate

pools (Santschi et al., 2003), which could, in turn, lead to flocculation of polysaccharides and associated trace metals in the estuary. Wang et al. (2010) observed a 5-10% loss of carbohydrates in the Bay of Saint Louis in the northern Gulf of Mexico due to physical mixing alone. Terrestrial polysaccharides contain galacturonic acid, which can bind Fe. It is therefore possible that these terrestrial polysaccharides represent a portion of the dFe-binding ligand pool in San Francisco Bay. Polysaccharides have been observed in coastal waters and in the open ocean in other studies (Abdulla et al., 2013; Aluwihare et al., 1997, 2002; Benner et al., 1992; Repeta et al., 2002), and they have been previously implicated as an important component of the weaker dFe-binding ligand pool (Hassler et al., 2011*a*), but this has not been tested directly in estuaries. DFe bound to polysaccharides has been found to have enhanced reactivity and bioavailability to eukaryotic phytoplankton in the Southern Ocean (Hassler et al., 2011*b*), and thus may render the dFe bound to weaker ligands in the BBL and San Francisco Bay relatively bioavailable to coastal and estuarine phytoplankton.

5.3 Contribution of humic-like substances to the iron-binding ligand pool

Humic-like substances (HS) were found to be an important component of the dFe-binding ligand pool in this study, potentially complexing 23% of the dFe in San Francisco Bay. HS, like dFe and ligands, appear to behave non-conservatively within the estuary (Figure 4.4). This observation supports the finding that HS likely contribute to the pool of dFe-binding ligands that are flocculated in the estuary (Boyle et al., 1977; Sholkovitz et al., 1978). However, there is also some evidence that HS are not only components of the weaker ligand pool that are scavenged, but part of the stronger ligand classes less prone to flocculation as well. HS measurements made by CSV in our study

(Table 4.1) and previous work (Abualhaija and van den Berg, 2014; Bundy et al., 2014; Laglera and van den Berg, 2009) have found that HS is likely part of the L_2 ligand pool since the log $K^{cond}_{FeL,Fe'}$ for HS (11.1-11.6) falls in the L2 range (log K = 11-12), although there may be an even larger range of binding strengths for HS. The estimation of the CRAM component by ^{1}H-NMR provides supporting evidence for the presence of HS in these samples, where CRAM components show a positive correlation with [HS] measured by the CSV method (Figure 4.6). However, the positive *y*-intercept in Figure 4.6 may indicate either that the CSV method underestimates the concentration of aliphatic carboxyl ligand (in HS) or that there are wide variations in the degree of carboxylation among the compounds within the CRAM component, and only the compounds with a high degree of carboxylation (polycarboxyl compounds) will act as strong ligands for Fe while the compounds with a lower degree of carboxylation (e.g. one or two carboxyl functional group per compound) will act as weaker ligands. This is an important aspect of HS and dFe interactions that requires further investigation, and might explain the apparent presence of HS in several ligand classes.

The strong correlation between CRAM and HS measured by CSV here, as well as data from other studies (e.g., Abdulla et al., 2010), supports the concept that aliphatic polycarboxyl compounds act as strong ligands for dFe. From a theoretical point of view according to the Hard and Soft Acids and Bases (HSAB) concept (Pearson, 1963), the high negative charge density of the carboxyl group makes it an ideal strong Lewis base group to bind with strong Lewis acids like Fe^{3+} (Bertini, 2007; Kaim and Schwederski, 1994). Many studies have shown that carboxyl groups of HS are major binding sites of complexed dFe (Byler et al., 1987; Karlsson and Persson, 2010; Kung and Mcbride,

1989; Schnitzer and Skinner, 1963). In addition, based on Fourier transform infrared spectroscopy (FTIR) analysis, Abdulla et al. (2010) found that ~60 % of the carboxyl groups in high molecular weight (HMW) DOM isolated from the Great Dismal Swamp (Virginia) appeared to be bound to dFe. Based on this evidence, it appears that HS varies widely in terms of its ability to complex dFe, likely related to its size fraction and the degree of carboxylation of HS compounds.

The potential partitioning of HS into several dFe-binding ligand groups is not surprising, given previous observations from other coastal environments. Batchelli et al. (2010) saw HS in both the soluble and colloidal fractions in Thurso Bay, with the colloidal fraction behaving non-conservatively and the soluble fraction mixing conservatively. Previous studies suggested that the soluble strong ligand pool observed may be comprised of siderophores that can effectively compete for dFe bound to HS because of reversible binding to HS (Batchelli et al., 2010; Laglera et al., 2007). HS measured by CSV can also capture a wide range of complexes, including humic and fulvic acids (Laglera et al., 2007). The HS may also not be only terrestrially-derived; Guo et al. (2000) noted that a significant portion of the colloidal HS material found outside of Galveston Bay may have derived from phytoplankton, based on the metal to organic carbon ratios (Guo et al., 2000). Several studies on organic matter cycling in estuaries have noted a gradient in the size distribution of organic matter complexes through an estuary, ranging from high molecular weight complexes at the low salinity end to low molecular weight complexes at the marine endmember (Moore et al., 1979; Murray et al., 1978; Murrell et al., 2000; Sholkovitz et al., 1978), supporting the transition from weaker to strong ligands observed in this study and the potential presence of HS in more than one

ligand class in San Francisco Bay. Collectively, these observations suggest that the HS pool in estuaries is heterogeneous and dynamic, and likely plays an important role in the cycling and transport of dFe in San Francisco Bay and surrounding coastal waters.

5.4 Freshwater influences on coastal California Current waters

San Francisco Bay appears to influence California Current shelf waters as a source of both dFe and strong dFe-binding ligands. Although almost 90% of the dFe from the Sacramento and San Joaquin rivers is lost in the estuary before reaching the shelf, the remaining dFe is strongly bound by organic ligands resistant to flocculation. The scavenged Fe is likely deposited on the shelf or in the estuary and transported to the shelf, associated with weaker ligands and HS, and may be further processed in the surface sediments. The presence of HS both in the estuary and on the shelf outside of San Francisco Bay and Eel River (Table 4.1), and the similarity in CRAM components between low salinity samples to BBL samples (Figure 4.5), also suggest that some of the BBL ligand pool is comprised of HS derived from estuarine sources. It is therefore likely that this pool of dFe and ligands are responsible for the pulse of upwelled dFe from the shelf in early spring upwelling events in the coastal CCS, as the ‘capacitor’ hypothesis suggests. Due to reversible binding of dFe by strong dFe-binding ligands in surface waters in the CCS (Bundy et al., 2014), much of this upwelled dFe is likely available to phytoplankton and helps to fuel primary productivity along the California coast.

6. Acknowledgements

We thank the Captain and crew of the R/V *Polaris* for their sampling support. We would also like to thank Tara Schraga, Jessica Dyke, and Valerie Greene and the rest of the USGS San Francisco Bay water monitoring team for logistical support. RMB and

KAB were supported by NSF grant OCE 10-26607 for the California Current Ecosystem Long Term Ecological Research (LTER) program. HA and P.G.H were supported by Batten Endowment, DB was supported by NSF grant OCE 0849943 to Ken Bruland, and KNB and San Francisco bay sampling activities were supported by CALFED Bay-Delta Science Fellowship U-04-SC-005 for Sea Grant Project #R/SF-32. We thank two anonymous reviewers and Maeve Lohan for their helpful comments and insights. Chapter 4, in full, is under review in Marine Chemistry. Bundy, R.M., Abdulla, H.A, Hatcher, P., Biller, D.V., Buck, K.N., Barbeau, K.A, Marine Chemistry 2014. The dissertation author was the primary investigator and author of this paper.

Table 4.1 Hydrographic and ligand data for all stations sampled in San Francisco Bay (SF Bay) and in the California Current Ecosystem (CCE). Longitude (Lon., °W), latitude (Lat., °N), sampling depth (Depth, m), temperature (Temp., °C), and chlorophyll *a* concentrations (Chl *a*, μg L^{-1}) were obtained from the USGS San Francisco Bay Water Quality Measuring program (http://sfbay.wr.usgs.gov/access/wqdata/index.html). Salinity (S) measurements were taken from individual dFe-binding ligand samples. Ligand classes (L_1-L_4) represent dFe-binding ligands characterized by their log $K'^{cond}_{FeL_i,Fe}$ (log K_1 – log K_4) as described in section 2.3.4. The concentration of humic substances (HS, μg L^{-1}) were determined according to Laglera et al. (2007) described in section 2.4. The notation 'nd' means not detected, and (*) indicates ligand data that was previously published in Bundy et al. (2014).

Region	Sta.	Lon. (°W)	Lat. (°N)	Depth (m)	Temp. (°C)	S (psu)	Chl *a* (μg L^{-1})	dFe (nmol L^{-1})	L_1 (nmol L^{-1})	logK_1	L_2 (nmol L^{-1})	logK_2	L_3 (nmol L^{-1})	logK_3	L_4 (nmol L^{-1})	logK_4	HS (μg L^{-1})
SF Bay	2	121.855	38.063	2.0	15.9	4.2	4.2	77.1	82.3	12.9	84.0	11.7	68.9	10.3	143.0	9.9	559.5
SF Bay	4	121.935	38.048	2.0	16.0	2.3	4.3	86.9	78.5	12.4	90.7	11.7	88.8	10.9	126.2	9.2	nd
SF Bay	6	122.035	38.065	2.0	15.5	3.0	4.6	54.5	42.2	12.8	55.3	11.3	67.7	10.8	45.3	9.6	nd
SF Bay	8	122.152	38.030	2.0	15.5	3.1	5.6	131.5	139.5	12.5	121.2	12.0	nd	nd	163.3	9.2	nd
SF Bay	13	122.370	38.028	2.0	14.7	7.2	5.8	26.0	28.1	13.1	35.6	11.3	nd	nd	67.0	9.9	111.2
SF Bay	18	122.422	37.847	2.0	13.1	14.4	7.9	23.2	19.0	12.3	17.3	11.4	21.7	10.4	nd	nd	nd
SF Bay	21	122.358	37.788	2.0	14.0	22.3	15.3	7.0	10.3	12.2	12.1	11.4	16.0	11.0	nd	nd	nd
SF Bay	24	122.338	37.698	2.0	14.4	20.0	9.3	10.3	10.6	13.2	13.8	11.8	23.6	10.4	nd	nd	67.5
CCE	25*	122.611	37.418	64.0	10.0	33.9	nd	6.8	9.2	12.2	11.3	11.5	nd	nd	nd	nd	39.2
CCE	26*	124.386	40.767	64.0	8.6	33.9	nd	20.5	nd	nd	16.9	11.0	nd	nd	nd	nd	22.6

Table 4.2 Dissolved organic carbon (DOC) concentrations and ^{1}H-NMR integrated area percentages of the major chemical functional groups from stations 13, 24, 25 and 26.

Sta.	DOC µmol L^{-1}	CH_3-C	CH_3-Deoxy Sugar	CH_x-C-COO/ CH_x-C-Ar	CH_3-C=O	CH_x-COO/ CH_x-Ar	CHOH	H-Ar/ H-C=C	% CRAM	% HPS	% CRAM x DOC
13	106	13	20	15	9	29	12	1	58	42	6148
24	83	14	23	11	7	29	13	3	57	43	4765
25	79	14	19	11	7	23	22	4	52	48	4094
26	76	8	20	13	8	30	19	2	53	47	4028

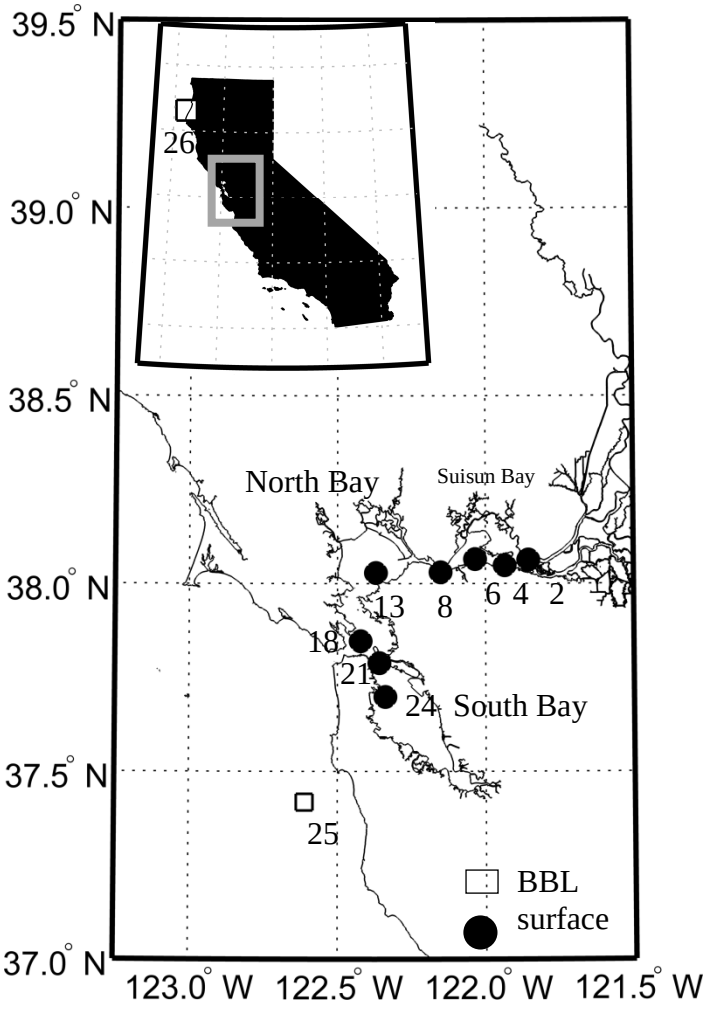

Figure 4.1 Dissolved Fe (dFe) and dFe-binding ligand surface sampling locations in San Francisco Bay (filled circles; stations 2, 4, 6, 8, 13, 18, 21, 24) and the California continental shelf benthic boundary layer (BBL, open squares; stations 25, 26).

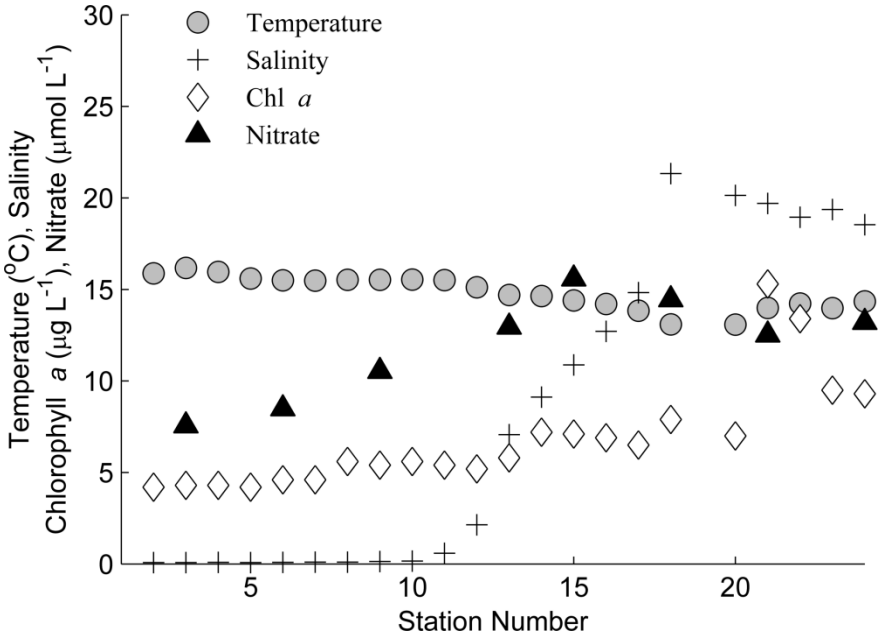

Figure 4.2 Temperature (°C), salinity, nitrate+nitrite (µmol L^{-1}) and chlorophyll *a* (µg L^{-1}) concentrations at each USGS sampling location in San Francisco Bay.

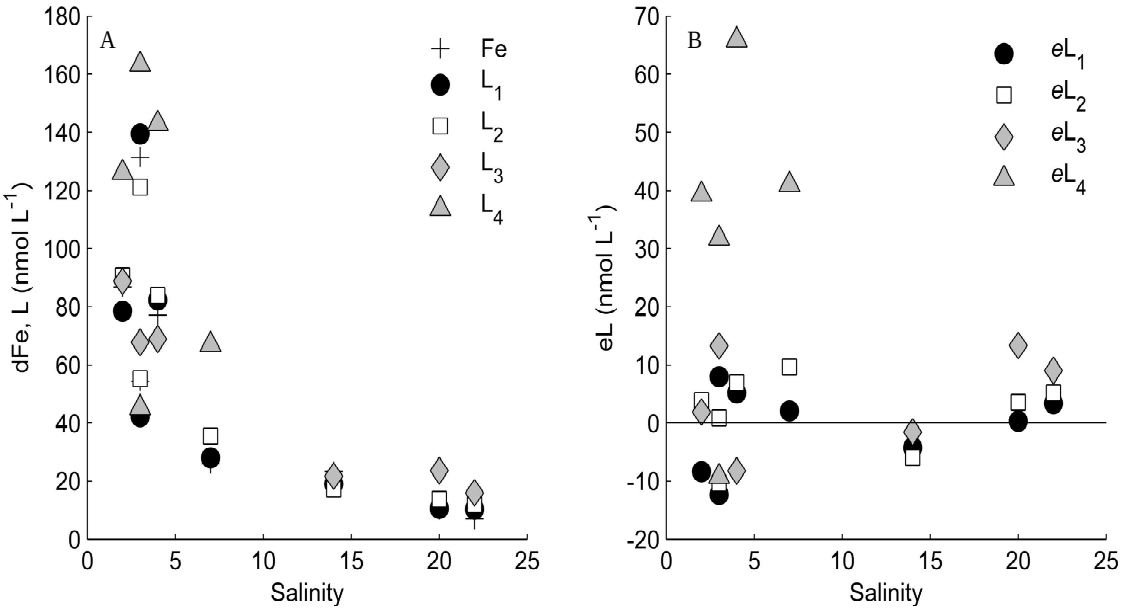

Figure 4.3 (A) Dissolved Fe (nmol L^{-1}), and Fe-binding ligand concentrations (L_1, L_2, L_3 and L_4, nmol L^{-1}) in San Francisco Bay. (B) Excess ligand (*e*L) concentrations ([L_x]-[Fe], nmol L^{-1} where 'x' denotes ligand class, 1-4), at each station versus salinity.

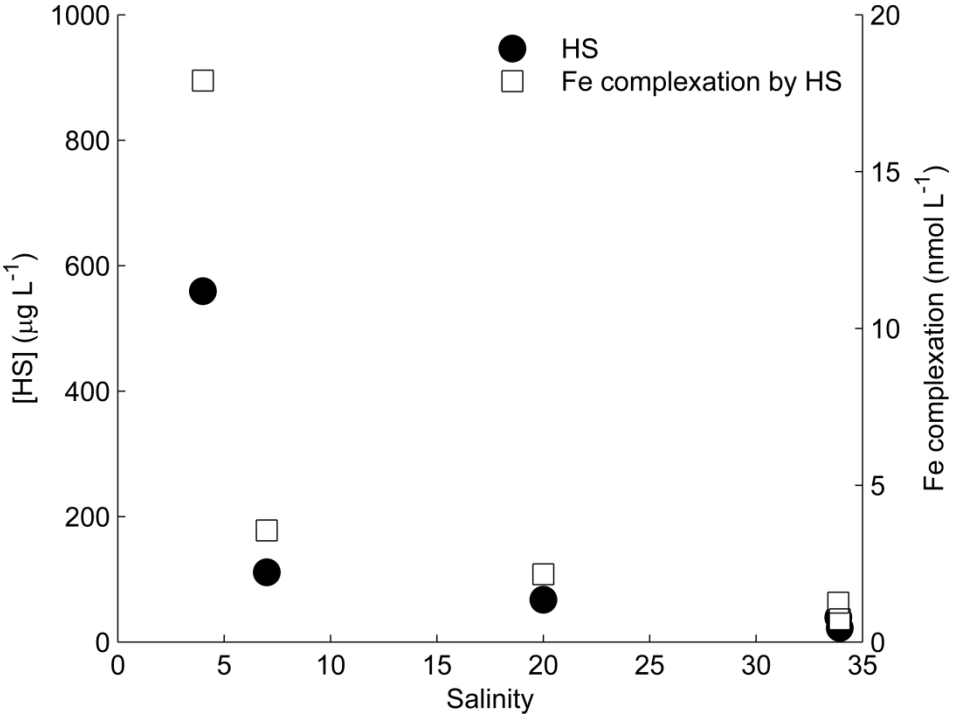

Figure 4.4 Humic-like substances (HS) as measured by CSV in San Francisco Bay and in BBL samples plotted versus salinity. The dissolved iron (Fe) complexation accounted for by HS was based on a binding constant of 32 nmol Fe mg^{-1} HS determined by Laglera and van den Berg (2009).

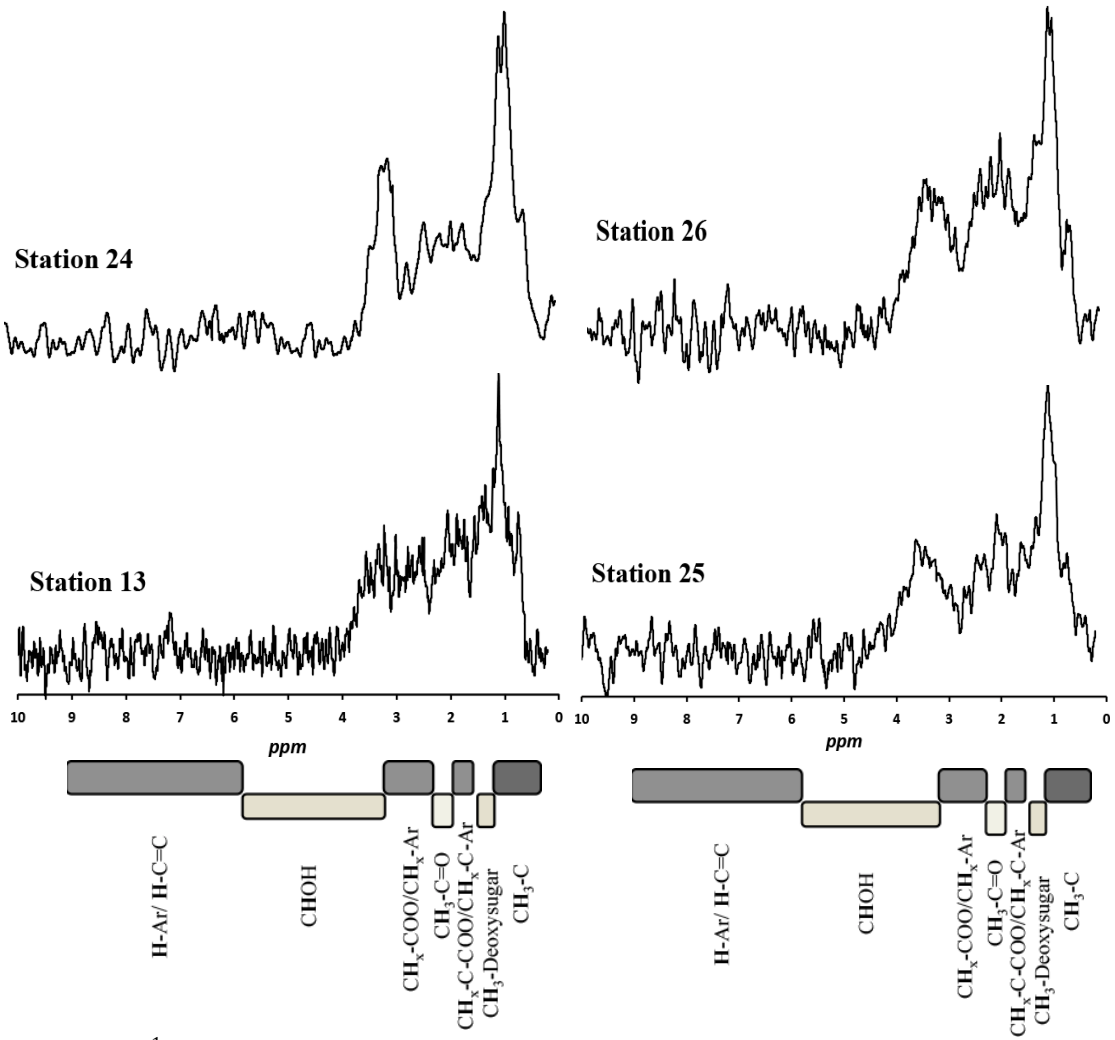

Figure 4.5 ^{1}H-NMR spectra of the San Francisco Bay surface water stations (13 and 24, left panels) and the BBL stations (25 and 26, right panels).

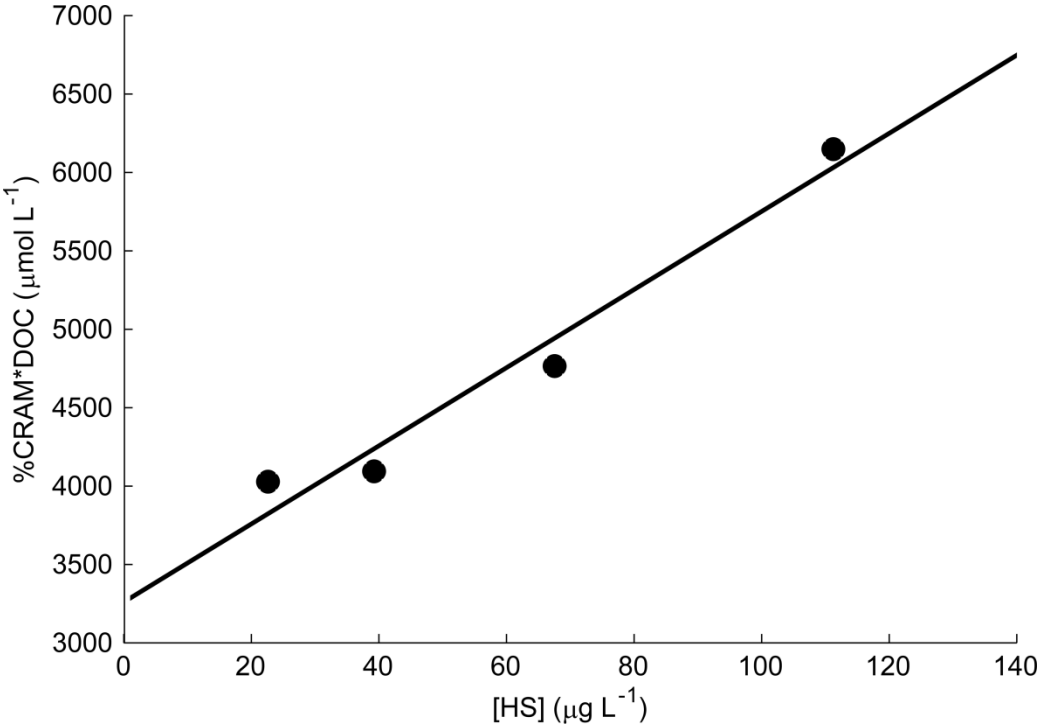

Figure 4.6 Relationship between the humic-like substances (HS) concentration as measured by CSV and the magnitude of CRAM in the samples measured by ^{1}H-NMR and DOC concentration (*y=24.9x+3260, r^2=0.96*).

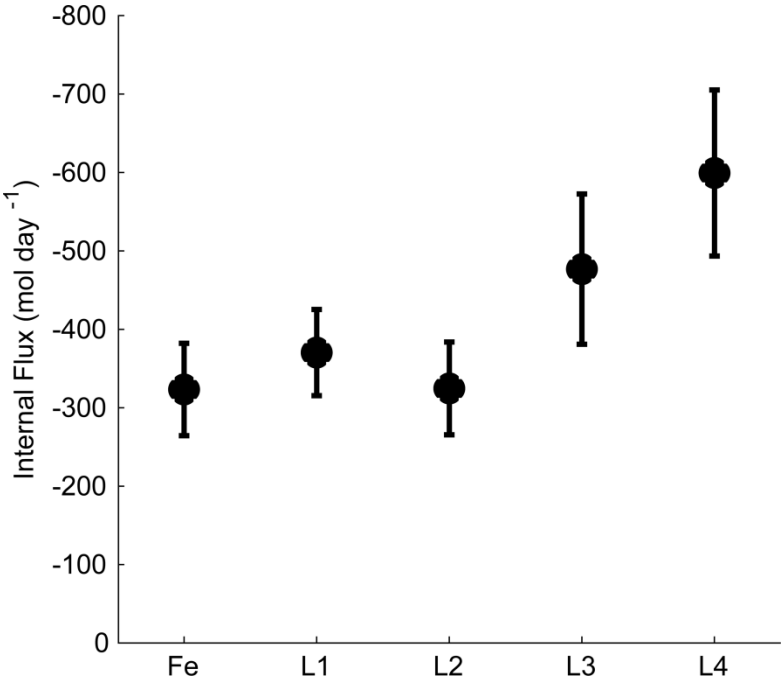

Figure 4.7 Internal flux calculations based on Flegal et al. (1991) for dissolved iron (dFe) and dFe-binding ligands (L_1-L_4). Error bars represent the error propagation of the constituent measurement and in the calculation of .

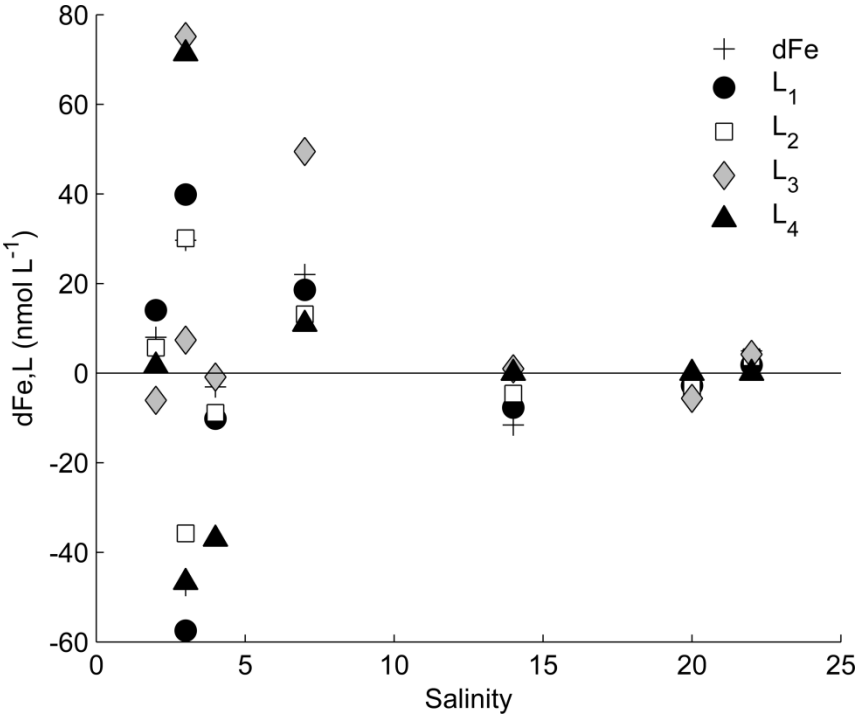

Figure 4.8 Residuals from the best-fit second order polynomial line of constituent versus salinity for each individual dataset of dissolved iron (dFe), and dFe-binding ligands (L_1, L_2, L_3 and L_4) in San Francisco Bay.

Table S4.1 'Overload' titration sensitivities are presented from each sample, along with the deposition time. This sensitivity was used both as the 'initial guess' in the Hudson et al. (2003) protocol comparison (*see* SI-3), and it was used as the sensitivity in each titration following a correction factor, R_{AL}, shown below for the lower detection windows (S4.2).

Station	Overload Sensitivity (nA)	Dep. time (s)
2	18.6	60
4	5.3	60
6	10.4	60
8	10.1	60
13	40.9	60
18	16.2	60
21	17.0	60
24	53.5	60
25	37.2	60
26	40.5	60

Table S4.2 The average [SA] for each analytical window along with the average R_{AL} at each window. The R_{AL} was used to correct the overload sensitivities for the lower analytical window titrations, and was also used in the Hudson et al. (2003) data processing protocol comparison.

Analytical Window	[SA] μmol L^{-1}	AVG R_{AL}
1	32.3±0.0	1.0
2	25.9±1.4	0.7
3	22.1±2.7	0.5
4	17.7±2.3	0.4
5	12.6±2.2	0.2

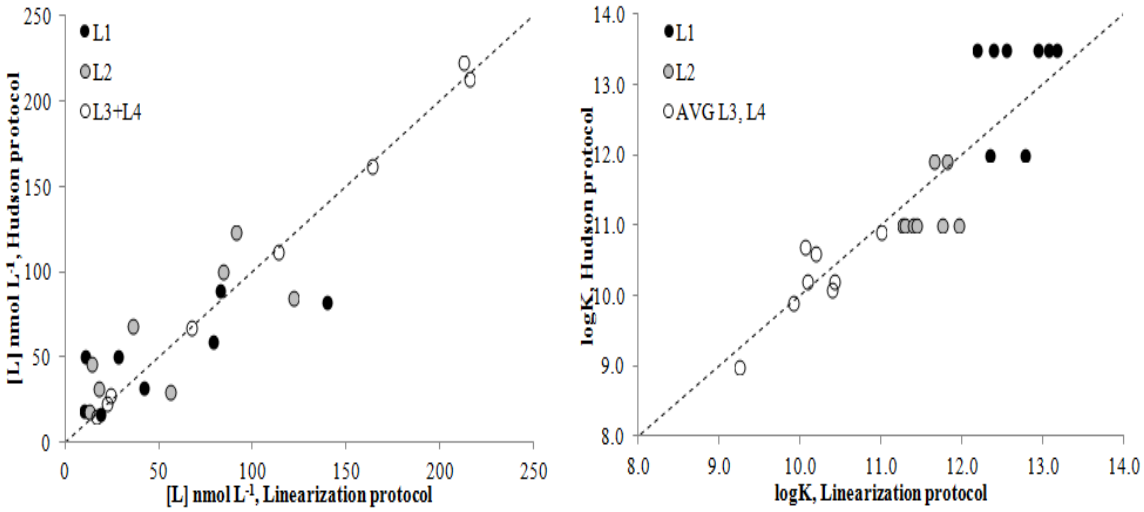

Figure S4.3 The results shown below show the comparison of the data obtained in this study using traditional linearization techniques compared to data obtained using a modified version of the Hudson method (Hudson et al., 2003; Sander et al., 2011) for ligand concentrations (left) and stability constants (right). Only three ligand classes can be measured using the Hudson approach, so the sum of L_3 and L_4 is shown for comparison purposes. Both methods agree very well, with slightly higher logKs calculated in the Hudson method.

7. References

Abdulla, H.A.N., Minor, E.C., Dias, R.F. and Hatcher, P.G., 2010. Changes in the compound classes of dissolved organic matter along an estuarine transect: A study using FTIR and C-13 NMR. Geochimica Et Cosmochimica Acta, 74(13).

Abdulla, H.A.N., Minor, E.C., Dias, R.F. and Hatcher, P.G., 2013. Transformations of the chemical compositions of high molecular weight DOM along a salinity transect: Using two dimensional correlation spectroscopy and principal component analysis approaches. Geochimica Et Cosmochimica Acta, 118: 231-246.

Abualhaija, M.M. and van den Berg, C.M., 2014. Chemical speciation of iron in seawater using catalytic cathodic stripping voltammetry with ligand competition against salicylaldoxime. Marine Chemistry, 164: 60-74.

Aluwihare, L.I., Repeta, D.J. and Chen, R.F., 1997. A major biopolymeric component to dissolved organic carbon in surface sea water. Nature, 387(6629): 166-169.

Aluwihare, L.I., Repeta, D.J. and Chen, R.F., 2002. Chemical composition and cycling of dissolved organic matter in the Mid-Atlantic Bight. Deep-Sea Research Part Ii-Topical Studies in Oceanography, 49(20): 4421-4437.

Batchelli, S., Muller, F.L.L., Chang, K.-C. and Lee, C.-L., 2010. Evidence for strong but dynamic iron-humic colloidal associations in humic-rich coastal waters. Environmental Science & Technology, 44(22): 8485-8490.

Benner, R., Louchouarn, P. and Amon, R.M.W., 2005. Terrigenous dissolved organic matter in the Arctic Ocean and its transport to surface and deep waters of the North Atlantic. Global Biogeochemical Cycles, 19(2).

Benner, R., Pakulski, J.D., McCarthy, M., Hedges, J.I. and Hatcher, P.G., 1992. Bulk chemical characteristics of dissolved organic-matter in the ocean. Science, 255(5051): 1561-1564.

Bertini, I., 2007. Biological Inorganic Chemistry: Structure and Reactivity. University Science Books.

Biller, D.V. and Bruland, K.W., 2012. Analysis of Mn, Fe, Co, Ni, Cu, Zn, Cd, and Pb in seawater using the Nobias-chelate PA1 resin and magnetic sector inductively coupled plasma mass spectrometry (ICP-MS). Marine Chemistry, 130: 50-70.

Biller, D.V. and Bruland, K.W., 2014. The central California Current transition zone: A broad region exhibiting evidence for iron limitation. Progress in Oceanography, 120: 370-382.

Biller, D.V., Coale, T.H., Till, R.C., Smith, G.J. and Bruland, K.W., 2013. Coastal iron and nitrate distributions during the spring and summer upwelling season in the central California Current upwelling regime. Continental Shelf Research, 66: 58-72.

Boyd, P.W., Ibisanmi, E., Sander, S.G., Hunter, K.A. and Jackson, G.A., 2010. Remineralization of upper ocean particles: Implications for iron biogeochemistry. Limnology and Oceanography, 55(3): 1271-1288.

Boyle, E.A., Edmond, J.M. and Sholkovitz, E.R., 1977. Mechanism of iron removal in estuaries. Geochimica Et Cosmochimica Acta, 41(9): 1313-1324.

Bruland, K.W., Rue, E.L. and Smith, G.J., 2001. Iron and macronutrients in California coastal upwelling regimes: Implications for diatom blooms. Limnology and Oceanography, 46(7).

Bruland, K.W., Rue, E.L., Smith, G.J. and DiTullio, G.R., 2005. Iron, macronutrients and diatom blooms in the Peru upwelling regime: Brown and blue waters of Peru. Marine Chemistry, 93(2-4): 81-103.

Buck, K.N. and Bruland, K.W., 2005. Copper speciation in San Francisco Bay: A novel approach using multiple analytical windows. Marine Chemistry, 96(1-2): 185-198.

Buck, K.N. and Bruland, K.W., 2007. The physicochemical speciation of dissolved iron in the Bering Sea, Alaska. Limnology and Oceanography, 52(5): 1800-1808.

Buck, K.N., Lohan, M.C., Berger, C.J.M. and Bruland, K.W., 2007. Dissolved iron speciation in two distinct river plumes and an estuary: Implications for riverine iron supply. Limnology and Oceanography, 52(2): 843-855.

Buck, K.N., Moffett, J., Barbeau, K., Bundy, R.M., Kondo, Y., Wu, J. 2012. The organic complexation of iron and copper: An intercomparison of competitive ligand exchange-adsorptive cathodic stripping voltammetry (CLE-ACSV) techniques. Limnology and Oceanography-Methods, 10: 496-515.

Bundy, R.M., Biller, D.V., Buck, K.N. Bruland, K.W., and Barbeau, K.A. 2014. Distinct pools of dissolved iron-binding ligands in the surface and benthic boundary layer of the California Current. Elsevier, Limnology and Oceanography. 59(3): 769-787.

Byler, D.M., Gerasimowicz, W.V., Susi, H. and Schnitzer, M., 1987. FT-IR spectra of soil constituents - fulvic-acid and fulvic-acid complex with ferric ions. Applied Spectroscopy, 41(8): 1428-1430.

Cabaniss, S.E., 1991. Carboxylic-acid content of a fulvic-acid determined by potentiometry and aqueous fourier-transform infrared spectrometry. Analytica Chimica Acta, 255(1): 23-30.

Chase, Z., Strutton, P.G. and Hales, B., 2007. Iron links river runoff and shelf width to phytoplankton biomass along the U.S. West Coast. Geophysical Research Letters, 34(4).

Cloern, J.E., 1996. Phytoplankton bloom dynamics in coastal ecosystems: A review with some general lessons from sustained investigation of San Francisco Bay, California. Reviews of Geophysics, 34(2).

Cloern, J.E. and Dufford, R., 2005. Phytoplankton community ecology: Principles applied in San Francisco Bay. Marine Ecology Progress Series, 285: 11-28.

Elrod, V.A., Berelson, W.M., Coale, K.H. and Johnson, K.S., 2004. The flux of iron from continental shelf sediments: A missing source for global budgets. Geophysical Research Letters, 31(12).

Elrod, V.A., Johnson, K.S., Fitzwater, S.E. and Plant, J.N., 2008. A long-term, high-resolution record of surface water iron concentrations in the upwelling-driven central California region. Journal of Geophysical Research - Part C - Oceans: C11021 (13 pp.).

Flegal, A.R., Smith, G.J., Gill, G.A., Sañudo-Wilhelmy, S. and Anderson, L.C.D., 1991. Dissolved trace-element cycles in the San-Francisco Bay estuary. Marine Chemistry, 36(1-4).

Giambalvo, E., 1997. A new method for modeling coupled equilibrium and non-equilibrium chemical reactions. M.S. thesis, University of California, Santa Cruz.

Gledhill, M. and Buck, K.N., 2012. The organic complexation of iron in the marine environment: A review. Frontiers in microbiology, 3: 69.

Gledhill, M. et al., 2004. Production of siderophore type chelates by mixed bacterioplankton populations in nutrient enriched seawater incubations. Marine Chemistry, 88(1-2): 75-83.

Gledhill, M. and van Den Berg, C.M.G., 1994. Determination of complexation of iron(III) with natural organic complexing ligands in seawater using cathodic stripping voltammetry. Marine Chemistry, 47(1): 41-54.

Guo, L.D., Santschi, P.H. and Warnken, K.W., 2000. Trace metal composition of colloidal organic material in marine environments. Marine Chemistry, 70(4): 257-275.

Hassler, C.S., Alasonati, E., Nichols, C.A.M. and Slaveykova, V.I., 2011*a*. Exopolysaccharides produced by bacteria isolated from the pelagic Southern Ocean - Role in Fe binding, chemical reactivity, and bioavailability. Marine Chemistry, 123(1-4): 88-98.

Hassler, C.S., Schoemann, V., Nichols, C.M., Butler, E.C.V. and Boyd, P.W., 2011*b*. Saccharides enhance iron bioavailability to Southern Ocean phytoplankton. Proceedings of the National Academy of Sciences of the United States of America, 108(3): 1076-1081.

Hatcher, P.G., Breger, I.A. and Earl, W.L., 1981. Nuclear magnetic resonance studies of ancient buried wood—I. Observations on the origin of coal to the brown coal stage. Organic Geochemistry, 3(1): 49-55.

Hernes, P.J. and Benner, R., 2002. Transport and diagenesis of dissolved and particulate terrigenous organic matter in the North Pacific Ocean. Deep-Sea Research Part I-Oceanographic Research Papers, 49(12): 2119-2132.

Hernes, P.J. and Benner, R., 2006. Terrigenous organic matter sources and reactivity in the North Atlantic Ocean and a comparison to the Arctic and Pacific oceans. Marine Chemistry, 100(1-2): 66-79.

Hudson, R.J.M., Rue, E.L. and Bruland, K.W., 2003. Modeling complexometric titrations of natural water samples. Environmental Science & Technology, 37(8): 1553-1562.

Hutchins, D.A., DiTullio, G.R., Zhang, Y. and Bruland, K.W., 1998. An iron limitation mosaic in the California upwelling regime. Limnology and Oceanography, 43(6): 1037-1054.

Ito, Y., Ishida, K., Okada, S. and Murakami, M., 2004. The absolute stereochemistry of anachelins, siderophores from the cyanobacterium Anabaena cylindrica. Tetrahedron, 60(41): 9075-9080.

Johnson, K.S., V.A. Elrod, S.E. Fitzwater, J. Plant, E. Boyle, B. Bergquist, K. Bruland, A. Aguilar-Islas, K.N. Buck, M. Lohan, G.J. Smith, B. Sohst, K.H. Coale, M. Gordon, S. Tanner, C. Measures, J. Moffett, K.A. Barbeau, A. King, A. Bowie, Z. Chase, J. Cullen, P. Laan, W. Landing, J. Mendez, A. Milne, H. Obata, T. Doi, L. Ossiander, G. Sarthou, P. Sedwick, C.M.G. van den Berg, L. Laglera, J. Wu, Y. Cai, 2007. Developing standards for dissolved iron in seawater. Eos Trans. AGU, 88(11): 131-132.

Jones, M.E., Beckler, J.S. and Taillefert, M., 2011. The flux of soluble organic-iron(III) complexes from sediments represents a source of stable iron(III) to estuarine

waters and to the continental shelf. Limnology and Oceanography, 56(5): 1811-1823.

Kaim, W. and Schwederski, B., 1994. Bioinorganic Chemistry: Inorganic Chemistry in the Chemistry of Life. Wiley, Chichester, UK.

Karlsson, T. and Persson, P., 2010. Coordination chemistry and hydrolysis of Fe(III) in a peat humic acid studied by X-ray absorption spectroscopy. Geochimica Et Cosmochimica Acta, 74(1): 30-40.

King, A.L. and Barbeau, K., 2007. Evidence for phytoplankton iron limitation in the southern California Current System. Marine Ecology-Progress Series, 342: 91-103.

Kogut, M.B. and Voelker, B.M., 2001. Strong copper-binding behavior of terrestrial humic substances in seawater. Environmental Science & Technology, 35(6): 1149-1156.

Krachler, R. et al., 2012. Nanoscale lignin particles as sources of dissolved iron to the ocean. Global Biogeochemical Cycles, 26.

Kung, K.H. and McBride, M.B., 1989. Adsorption of para-substituted benzoates on iron-oxides. Soil Science Society of America Journal, 53(6): 1673-1678.

Laglera, L.M., Battaglia, G. and van den Berg, C.M.G., 2007. Determination of humic substances in natural waters by cathodic stripping voltammetry of their complexes with iron. Analytica Chimica Acta, 599: 58-66.

Laglera, L.M., Battaglia, G. and van den Berg, C.M.G., 2011. Effect of humic substances on the iron speciation in natural waters by CLE/CSV. Marine Chemistry, 127(1-4): 134-143.

Laglera, L.M. and van den Berg, C.M.G., 2009. Evidence for geochemical control of iron by humic substances in seawater. Limnology and Oceanography, 54(2): 610-619.

Lam, B. and Simpson, A.J., 2008. Direct ^{1}H NMR spectroscopy of dissolved organic matter in natural waters. Analyst, 133(2): 263-269.

Leenheer, J.A., Barber, L.B., Amy, G.L. and Chapra, S.C., 1995. Sewage contamination in the upper Mississippi River as measured by the fecal sterol, coprostanol. Water Research, 29(6): 1427-1436.

Liu, X.W. and Millero, F.J., 2002. The solubility of iron in seawater. Marine Chemistry, 77(1): 43-54.

Louchouarn, P. et al., 2010. Analysis of lignin-derived phenols in standard reference materials and ocean dissolved organic matter by gas chromatography/tandem mass spectrometry. Marine Chemistry, 118(1-2): 85-97.

Mantoura, R.F.C. and Riley, J.P., 1975. Analytical concentration of humic substances from natural-waters. Analytica Chimica Acta, 76(1): 97-106.

Mawji, E., Gledhill, M., Milton, J. A., Zubkov, M. V., Thompson, A., Wolff, G. A., and Achterberg, E. P. 2011. Production of siderophore type chelates in Atlantic Ocean waters enriched with different carbon and nitrogen sources. Marine Chemistry, 124(1-4): 90-99.

Moore, R.M., Burton, J.D., Williams, P.J.L. and Young, M.L., 1979. Behavior of dissolved organic material, iron and manganese in estuarine mixing. Geochimica Et Cosmochimica Acta, 43(6): 919-926.

Murray, J.W. and Gill, G., 1978. Geochemistry of iron in Puget Sound. Geochimica Et Cosmochimica Acta, 42(1): 9-19.

Murrell, M.C. and Hollibaugh, J.T., 2000. Distribution and composition of dissolved and particulate organic carbon in northern San Francisco Bay during low flow conditions. Estuarine Coastal and Shelf Science, 51(1): 75-90.

Officer, C.B., 1979. Discussion of the behavior of nonconservative dissolved constituents in estuaries. Estuarine and Coastal Marine Science, 9: 91-94.

Omanović, D., Garnier, C., and Pižeta, I. In review. ProMCC: an all-in-one tool for trace metal complexation studies. Marine Chemistry.

Opsahl, S. and Benner, R., 1997. Distribution and cycling of terrigenous dissolved organic matter in the ocean. Nature, 386(6624): 480-482.

Pearson, Ralph G. 1963. Hard and soft acids and bases. Journal of the American Chemical Society, 85(22): 3533-3539.

Panagiotopoulos, C., Repeta, D. J., and Johnson, C. G., 2007. Characterization of methyl sugars, 3-deoxysugars and methyl deoxysugars in marine high molecular weight dissolved organic matter. Organic Geochemistry, 38(6): 884-896.

Pižeta, I., Sander, S.G, Hudson, R.J.M., Baars, O., Buck, K.N., Bundy, R.M., Carrasco, G., Croot, P., Garnier, C., Gerringa, L.J.A., Gledhill, M., Hirose, K., Kondo, Y., Laglera, L.M., Nuester, J., Omanović, D., Rijkenberg, M.J.A., Takeda, S., Twining, B.S., Wells, M. In review. Intercalibration exercise with simulated titration data as a first step to best practice guide. Elsevier, Marine Chemistry.

Poorvin, L. et al., 2011. A comparison of Fe bioavailability and binding of a catecholate siderophore with virus-mediated lysates from the marine bacterium Vibrio alginolyticus PWH3a. Journal of Experimental Marine Biology and Ecology, 399(1): 43-47.

Repeta, D.J., Quan, T.M., Aluwihare, L.I. and Accardi, A.M., 2002. Chemical characterization of high molecular weight dissolved organic matter in fresh and marine waters. Geochimica Et Cosmochimica Acta, 66(6): 955-962.

Rue, E.L. and Bruland, K.W., 1995. Complexation of iron(III) by natural organic-ligands in the central North Pacific as determined by a new competitive ligand equilibration adsorptive cathodic stripping voltammetric method. Marine Chemistry, 50(1-4): 117-138.

Sander, S.G., Hunter, K.A., Harms, H. and Wells, M., 2011. Numerical Approach to Speciation and Estimation of Parameters Used in Modeling Trace Metal Bioavailability. Environmental Science & Technology, 45(15): 6388-6395.

Santschi, P.H., Hung, C. C., Schultz, G., Alvarado-Quiroz, N., Guo, L., Pinckney, J., and Walsh, I. 2003. Control of acid polysaccharide production and Th-234 and POC export fluxes by marine organisms. Geophysical Research Letters, 30(2).

Sañudo-Wilhelmy, S.A., RiveraDuarte, I. and Flegal, A.R., 1996. Distribution of colloidal trace metals in the San Francisco Bay estuary. Geochimica Et Cosmochimica Acta, 60(24): 4933-4944.

Scatchard, G., 1949. The attractions of proteins for small molecules and ions. Annals of the New York Academy of Sciences, 51(4): 660-672.

Schnitzer, M. and Skinner, S.I.M., 1963. Organo-metallic interactions in soils: 1. Reactions between a number of metal ions and the organic matter of a podzol Bh horizon. Soil Sci, 96(2): 86-93.

Sholkovitz, E.R., Boyle, E.A. and Price, N.B., 1978. Removal of dissolved humic acids and iron during estuarine mixing. Earth and Planetary Science Letters, 40(1): 130-136.

Simpson, F.B. and Neilands, J.B., 1976. Siderochromes in cyanophyceae - isolation and characterization of schizokinen from Anabeana-Sp. Journal of Phycology, 12(1): 44-48.

Sohrin, Y., Urushihara, S., Nakatsuka, S., Kono, T., Higo, E., Minami, T., Norisuye, K. and Umetani, S. 2008. Multielemental determination of GEOTRACES key trace metals in seawater by ICPMS after preconcentration using an

ethylenediaminetriacetic acid chelating resin. Analytical Chemistry, 80(16): 6267-6273.

Stevenson, F.J., 1994. Humus chemistry: genesis, composition, reactions. John Wiley & Sons.

van den Berg, C.M.G., 1995. Evidence for organic complexation of iron in seawater. Marine Chemistry, 50(1-4): 139-157.

Velasquez, I., Nunn, B. L., Ibisanmi, E., Goodlett, D. R., Hunter, K. A., and Sander, S. G. 2011. Detection of hydroxamate siderophores in coastal and Sub-Antarctic waters off the South Eastern Coast of New Zealand. Marine Chemistry, 126(1-4): 97-107.

Vraspir, J.M. and Butler, A., 2009. Chemistry of marine ligands and siderophores. Annual Review of Marine Science, 1: 43-63.

Wang, X., Cai, Y., and Guo, L., 2010. Preferential removal of dissolved carbohydrates during estuarine mixing in the Bay of Saint Louis in the northern Gulf of Mexico. Marine Chemistry, 119(1): 130-138.

Wilhelm, S.W. and Trick, C.G., 1994. Iron-limited growth of cyanobacteria - multiple siderophore production is a common response. Limnology and Oceanography, 39(8): 1979-1984.

Chapter 5

Understanding the sources and sinks of iron-binding ligands in the southern California Current Ecosystem: A mechanistic study

1. Abstract

The distributions of dissolved iron and iron-binding organic ligands were examined in several deckboard incubation experiments and water column profiles in the southern California Current Ecosystem (CCE) along a transition from coastal to semi-oligotrophic waters. Analysis of the iron-binding ligand pool by competitive ligand exchange-adsorptive cathodic stripping voltammetry (CLE-ACSV) using multiple analytical windows (MAWs) revealed three classes of iron-binding ligands present throughout the water column (L_1-L_3), whose distributions closely matched those of dissolved iron and nitrate. Despite significant biogeochemical gradients, ligand profiles were remarkably similar between stations, with surface minima in strong ligands (L_1 and L_2), and relatively constant concentrations of weaker ligands (L_3). A phytoplankton grow-out incubation, initiated from an iron-limited water mass, showed dynamic temporal cycling of iron-binding ligands which were nearly identical between controls and +iron treatments despite drastic differences in phytoplankton biomass. Modeling results were able to capture the patterns of the strong ligands in the incubation relatively well with only the microbial community as a source and sink. An experiment focused on remineralization of particulate organic matter showed production of both strong and weak iron-binding ligands by the heterotrophic community, supporting a mechanism for in-situ production of both strong and weak ligands in the subsurface water column. Photochemical experiments showed a variable influence of natural sunlight on the degradation of natural iron-binding ligands, providing some evidence to explain differences in surface ligand concentrations between stations. Statistical analyses comparing incubation experiments to water column profiles revealed variances in ligand

distributions were primarily related to macronutrient concentrations, suggesting microbial alteration of the ligand pool might dominate on longer time-scales over short-term changes from photochemistry or the phytoplankton community.

2. Introduction

Dissolved iron (dFe) is an essential trace element for phytoplankton and microbial growth in large areas of the ocean (Morel and Price, 2003). High nutrient low chlorophyll regions are especially susceptible to iron (Fe) limitation in surface waters (Martin et al., 1991). Some coastal eastern boundary upwelling regions such as the California Current Ecosystem (CCE) can also exhibit a range of Fe-limiting conditions, from the nearshore continental shelf to the transition zone 10-250 km offshore (Biller and Bruland, 2014; Hutchins et al., 1998; King and Barbeau, 2007; 2011). DFe is important for primary production in the ocean, but it is scarce in seawater and almost always associated with a heterogeneous pool of organic ligands (Rue and Bruland, 1995; Wu and Luther, 1995; van den Berg, 1995). Bacteria and phytoplankton must use an assortment of cellular tools in order to access dFe from this diverse organic matter matrix (Granger and Price, 1999; Hutchins et al., 1999; Maldonado and Price, 1999). The identity and behavior of organic ligands is therefore important for understanding the mechanisms of Fe-acquisition in the ocean. However, the chemical composition and sources and sinks of these ligands are still largely unknown.

It is known that dFe-binding organic ligands can range from highly-specific low molecular weight siderophore-type ligands to large macromolecules with only weak dFe-binding (Gledhill and Buck, 2012). Although dFe-binding ligands can be directly isolated from seawater (*e.g.*, Mawji et al., 2008), ligands have also been detected using indirect electrochemical methods, most commonly competitive ligand exchange-adsorptive cathodic stripping voltammetry (CLE-ACSV). CLE-ACSV methods allow for the identification of dFe-binding ligands based on their concentrations and binding strengths

(*see* review by Gledhill and Buck, 2012), and not their chemical composition. However, the strengths of the strongest ligands identified in the ocean based on electrochemical methods are nearly identical to strong ligands found in culture media and other model ligands, such as siderophores. Strong dFe-binding ligands appear to be largely biologically produced both as a strategy for combating Fe-limitation (Buck et al., 2010; King et al., 2012; Mawji et al., 2011; Maldonado et al., 2002) and for keeping Fe in solution (Reid et al., 1993). The closest link between ligand production and biological growth is associated with the microbial community. Microbes have been shown to produce siderophores both in culture and in the field (Amin et al., 2009; Cabaj and Kosakowska, 2009; Hider and Kong, 2010; Vraspir and Butler, 2009). CLE-ACSV measurements coupled to high performance liquid chromatography (HPLC) methods have also enabled the detection of siderophores associated with natural bacteria assemblages (Gledhill et al., 2004; Mawji et al., 2011). Microbial communities may not be a source of only strong ligands to the water column, as microbial degradation of particulate organic matter has been implicated as a source of weaker ligands to deep waters (Boyd et al., 2010). It appears that bacteria may be a source of strong and weak dFe-binding ligands, but whether there are other factors contributing to changes in dFe-binding ligands is less certain. There have been several lines of evidence which demonstrate the ability of phytoplankton to change the dFe-binding ligand pool, though the mechanism is unclear. Diatom culture studies have identified organic exudates that exhibit some degree of dFe-binding (Urbani et al., 2005; Watt, 1969). Some field studies have also seen ligand production associated with diatom growth (King et al., 2012; Kondo et al., 2008; Rue and Bruland, 1997), particularly when the diatom community

appears to be Fe-limited (Buck et al., 2010). Ligand maxima in the water column are also often associated with the chlorophyll *a* maxima (Boye et al., 2001, 2006; Croot et al., 2004; Ibisanmi et al., 2011; Wagener et al., 2008). It is not clear from field studies however, if the higher ligand concentrations at this depth in the water column are due to active production, or incidental dFe-binding simply due to elevated organic material.

In addition to biological alteration of the ligand pool, photochemistry can also affect the concentration and strength of dFe-binding ligands. Laboratory studies have shown that some siderophores can be degraded by ultra-violet (UV) light when bound to dFe, and their binding strength is subsequently decreased after exposure to light (Barbeau et al., 2001; Barbeau et al., 2003; Barbeau, 2006). This mechanism has been invoked to describe the ligand minima often seen in surface waters (Gledhill and Buck, 2012), as well as the reason for the presence of weaker ligands in surface waters. However, field studies to date have had mixed results with respect to photochemical degradation of natural dFe-binding ligands (Powell and Wilson-Finelli, 2003; Rijkenberg et al., 2006). Despite mixed results in the field, modeling studies routinely invoke a photochemical sink for dFe-binding ligands in surface waters (Jiang et al., 2010; Parekh et al., 2005; Tagliabue et al., 2009; Tagliabue and Voelker, 2011). However, since the identity of dFe-binding ligands is still largely unknown, it is difficult to link laboratory studies on the photochemical reactivity of siderophores with natural ligands measured in the water column.

Siderophores produced by marine bacteria have been shown to include catecholate, carboxylic acid, and/or hydroxamate Fe(III)-binding groups and often exhibit an amphiphilic nature due to the presence of a fatty acid tail (Vraspir and Butler,

2009). Hydroxamate-type siderophores are the only siderophores that have been directly isolated from seawater via solid-phase extraction methods (Gledhill and Buck, 2012), but this bias may be largely methodological. However, the ligands detected in seawater are likely not only siderophores. A spectrum of dFe-binding ligand strengths have been found to exist in seawater, having a range of conditional stability constants (usually expressed as $\log K'^{cond}_{FeL,Fe'}$) from 9.0-14.0, with the weaker ligands often associated with coastal and deep waters, and stronger ligands found in surface waters and regions of high productivity (Gledhill and Buck, 2012; Hunter and Boyd, 2007). Most studies to date have concentrated on measuring one particular ligand class, either strong or weak, often denoted as strong 'L_1' ligands or weaker 'L_2' ligands. Recent studies in our group have focused on measuring several ligand classes in the same sample using CLE-ACSV with multiple analytical windows (MAWs; Bundy et al., 2014; Bundy et al. in review). This approach has shed light on the sources and sinks of both stronger and weaker ligands in surface and benthic boundary layer waters (Bundy et al., 2014) and estuarine-influenced shelf waters off California (Bundy et al., in review). A range of dFe-binding ligands was detected in these studies (L_1-L_4), with the highest concentrations of ligands associated with the coastal environment and declining offshore (Bundy et al., 2014). High weak ligand concentrations were also detected nearshore, with the weakest L_4 ligands only measureable in estuarine-influenced waters (Bundy et al., in review). The measurements thus far using MAWs have been restricted to only surface and benthic boundary layer waters, so the changes in L_1-L_4 with depth in the water column are uncertain.

Although data suggests the presence of strong and weak dFe-binding ligands throughout the water column, the mechanisms linking ligand distributions to sources and

sinks have not been well-studied. This is despite the advent of large-scale projects such as GEOTRACES, which have vastly increased the number and geographic extent of ligand measurements (Buck et al, in review; Sander et al., 2014; Thuróczy et al., 2010; 2011*a*, *b*). An understanding of the processes behind the changes to the ligand pool associated with biogeochemical gradients is important not only for understanding ligand distributions, but also for informing current biogeochemical modeling efforts which are increasingly attempting to incorporate dFe-binding ligands (Archer and Johnson, 2000; Fan, 2008; Moore et al., 2004; Moore and Braucher, 2008; Parekh et al., 2005; Tagliabue et al., 2009; Tagliabue and Voelker, 2011). This study makes the first upper ocean profile measurements of Fe-binding organic ligands utilizing MAW CLE-ACSV, and seeks to link profile data with mechanistic deckboard Fe speciation studies carried out on the same cruise in the southern California Current region, also employing MAW CLE-ACSV. Sources and sinks of different classes of dFe-binding ligands will be inferred from a multi-pronged approach combining both biological and photochemical incubation studies, a zero-dimensional model, and profiles of strong and weak dFe-binding ligands with ancillary profile data. This combination of methods provides a first step in linking ligand source and sink mechanisms to field observations in the same region.

3. Methods

3.1 Sampling region and environmental context

Samples for this study were collected as part of the California Current Ecosystem (CCE) Long-Term Ecological Research (LTER) program (http://cce.lternet.edu/) in the southern California Bight (Figure 5.1) on-board the R/V *Melville* in June-July 2011. This

cruise was a CCE-LTER process cruise, which operated in Lagrangian mode, using drifters to follow distinct water masses (Landry et al., 2009). Each series of stations sampled within the same water mass were denoted as a 'cycle' (Landry et al., 2009). However, only one station from each cycle was sampled in this particular study, so sampling locations will simply be referred to as stations. Each station has been given the same number as the cycle to which it belongs (for example, station 1 was part of cycle 1) in order to compare to other studies from the same cruise (*e.g.*, Brzezinski et al., in prep; Krause et al., submitted).

3.2 Sampling and storage

All trace-metal clean samples were collected either using single Teflon-coated 12 L GO-Flo bottles (General Oceanics) or 5 L X-Niskin bottles (Ocean Test Equipment) mounted on a powder-coated rosette and non-metallic line (Cutter and Bruland, 2012). Sampling depths were determined from a readout on the winch for the GO-Flos, or by pressure triggered by an auto-fire module mounted on the rosette (Seabird Electronics). GO-Flo or Niskin casts were done immediately following a cast by the standard ship CTD rosette, and depths were chosen based on the real-time hydrographic data from the ship's rosette. GO-Flo or X-Niskin sampling bottles were brought inside a Class-100 trace metal clean van upon arriving on deck, and filtered in-line using acid-washed Teflon tubing and Acropak-200 0.2 µm capsule filters (Pall Corporation) pressurized by filtered nitrogen gas. Filtered samples for dFe analysis were placed in 250 mL LDPE bottles, acidified to pH 1.8 (Optima HCl) and stored for at least 3 months until analysis in the lab. Samples collected for dFe-binding ligands were either run immediately (within 3

days) or stored frozen at -20°C until analysis. Results for fresh vs. frozen analyses of dFe-

binding ligands have been shown to be indistinguishable in previous studies (Buck et al., 2012).

Filtered samples for silicate ($Si(OH)_4$), phosphate (PO_4^{3-}), nitrate (nitrate+nitrite; denoted as NO_3^-), and chlorophyll *a* (chl *a*) were taken from the standard CTD rosette cast and on-board incubation experiments. Nutrient samples were collected in 40 ml polypropylene centrifuge tubes (Fisher Scientific) and frozen at -20°C before analysis. Chl *a* and phytoplankton pigment samples were placed in dark bottles and filtered onto GF/F filters (Fisher Scientific). Chl *a* samples were subsequently placed in acetone and analyzed on-board. Pigment samples were placed in cryovials (Nalgene) and stored in liquid nitrogen until analysis in the lab. Microscopy samples for phytoplankton cell counts were collected in 50mL glass vials and stored in 1% tetraborate buffered formalin until analysis.

3.3 Ancillary data analysis

Chl *a* samples from the depth-profiles and incubation experiments were run immediately on-board the ship, after being extracted for 24 hours in acetone at -20°C. Chl *a* samples were analyzed using a Turner Designs 10-AU Fluorometer, fitted with a red-sensitive photomultiplier tube. Phytoplankton pigment samples were stored in cryovials and placed in liquid nitrogen until analysis by HPLC according to (Zapata et al., 2000). Macronutrients from water column profiles and from incubation experiments were analyzed by the Marine Science Institute Analytical Lab at the University of California Santa Barbara (http://msi.ucsb.edu/services/analytical-lab) using a Lachat QuickChem 8000. Samples for phytoplankton cell counts were first adjusted by volume to 60 mL before settling in a 50 mL Utermöhl settling chamber. They were then counted using a

Zeiss phase-contrast inverted light microscope at 200x magnification (UNESCO, 1981; Utermöhl, 1958). Phytoplankton were classified by genera or the following broad categories: *Chaetoceros spp*., *Pseudo-nitzschia spp*., other diatoms (>10 µm), dinoflagellates, flagellates (< 10 µm), and ciliates. Sample volume enumerated ranged from 5.6 to 1.1 mL (1/9 of slide) and detectable cell abundance was between 245 and 1,227 cells/L, depending on volume settled.

3.4 Dissolved iron

DFe was analyzed by flow injection analysis (FIA) after complete reduction of the dFe with sulfite according to King and Barbeau (2007; 2011). This method has been shown to yield accurate results with respect to SAFe (S1 and D2) and GEOTRACES (GS) consensus samples, and has a detection limit of 0.07 nmol L^{-1} (three time the standard deviation of the blank, n = 72). Values obtained for S1 (0.11±0.02 nmol L^{-1}, n = 39), D2 (0.93±0.07 nmol L^{-1}, n = 36), and GS (0.51±0.02 nmol L^{-1}, n = 12) compare well to the most recent consensus values (http://es.ucsc.edu/~kbruland/GeotracesSaFe/kwbGeotracesSaFe.html).

3.5 Dissolved iron-binding ligands

DFe-binding ligands were analyzed using competitive ligand exchange-adsorptive cathodic stripping voltammetry (CLE-ACSV). This method has been used extensively for determining the concentration and binding strengths of dFe-binding ligands in seawater (*see* a recent review by Gledhill and Buck, 2012). The method involves titrating a natural sample with dFe in order to saturate the natural ligands. Then, a well-characterized electroactive ligand is added, in this case salicylaldoxime (SA). The added ligand competes with the natural ligands for dFe, and the $Fe(SA)_x$ complex is deposited on the

mercury drop and analyzed using adsorptive cathodic stripping voltammetry (ACSV) on a hanging mercury drop electrode (BioAnalytical Systems, Incorporated).

The titrations in this study were completed by first adding 50 µl of a 1.5 mol L^{-1} boric acid-ammonium buffer (pH 8.2, NBS scale) to 10 mL aliquots of the sample. Next, 0-25 nmol L^{-1} dFe was added to the 11 separate Teflon vials (Savillex) containing the sample and buffer. The buffer and dFe were left to equilibrate with the natural ligands in the sample for two hours, before adding the appropriate concentration of SA depending on the detection window (17.7, 25.0 or 32.3 µmol L^{-1} SA). The SA was left to equilibrate for 15 minutes before each aliquot was run separately using ACSV with a 150 s deposition time. All electrochemical parameters were the same as have been reported previously (Buck et al., 2007; Rue and Bruland, 1995), and all constants for SA were updated to the most recent calibration reported by Abualhaija and van den Berg (2014). Ligand concentrations and strengths were calculated based on traditional linearization techniques, and are reported as the average between the concentration and strengths determined by a Ružić/van den Berg linearization (Mantoura and Riley, 1975) and Scatchard linearization (Scatchard, 1949). The sensitivity is an important parameter in these data processing methods, and there are several ways to determine the sensitivity. The most traditional method is using an internal sensitivity (S_{IN}) or the slope of the titration curve at the end of the titration where it is assumed all the natural ligands are saturated. The S_{IN} can often be underestimated by this method if all of the ligands have not been titrated, which can especially be a problem in coastal samples (Kogut and Voelker, 2001). However, this is not often a problem in samples with low [dFe] and low ligand concentrations, and other iterative methods can even over-estimate the sensitivity

(Laglera et al., 2013). DFe concentrations were very low in this region (< 1 nmol L^{-1}), and therefore all sensitivities used in this study were S_{IN}. The S_{IN} was consistent between samples analyzed at the same analytical window. S_{IN} was generally greater at lower analytical windows (200-286 nA nmol L^{-1}) compared to the higher analytical window (45-189 nA nmol L^{-1}) as reported by Abualhaija and van den Berg (2014).

The concentration of the added ligand determines the detection window of the method, or the strength of the ligands that can be detected. A higher detection window targets stronger ligands, while a lower window targets weaker ligands. Recently, this method has been used to examine surface and benthic boundary layer samples (Bundy et al., 2014) as well as surface samples along a salinity gradient (Bundy et al., in review), and an updated calibration of SA allows for an even wider range of detection windows to be employed (Abualhaija and van den Berg, 2014). For this study, three different concentrations of SA were used, or three detection windows, in order to examine several distinct ligand classes ([SA] = 17.7, 25.0, and 32.3 µmol L^{-1}). One ligand class was detected at each analytical window, except the lowest detection window ([SA] =17.7 µmol L^{-1}) where two ligand classes were detected. The strongest ligand class (L_1) was determined at the highest detection window (32.3 µmol L^{-1} SA), the next ligand class (L_2) was detected at the middle detection window (25.0 µmol L^{-1} SA) and the weakest ligand classes (L_3 and L_4) were detected at the lowest detection window (17.7 µmol L^{-1} SA).

Currently, there are several methods that have been developed in order to analyze MAW data (Hudson et al., 2003; Omanović et al., in review; Pižeta et al., in review; Sander et al., 2011), but only two of the methods are currently publicly available (Hudson et al., 2003; Omanović et al., in review) and all of these methods to date have

only been tested using copper titration data. However, a recent study tested the use of the Hudson et al. (2003) method modified for dFe organic speciation and found very similar results between the linear techniques used here and the unified data treatment approach, when the initial guesses were set to the values determined by linear techniques (Bundy et al., in review). Since a rigorous intercomparison has not yet been completed for dFe-binding ligand titration data using new numerical methods, traditional linearization approaches were used in this study which we have shown to compare relatively well with unified data processing techniques (Bundy et al., in review).

3.6 Experimental set-up

3.6.1 Biological incubation experiments

Two experiments were conducted in this study to address biological sources of dFe-binding ligands in the CCE, one phytoplankton grow-out experiment (experiment 1) and one remineralization experiment (experiment 2) which immediately followed the termination of the grow-out experiment. Both experiments were conducted at station 3 from water collected at 30 m in the subsurface chl *a* maximum (Figure 5.1). Whole seawater was collected for these experiments and homogenized in a clean 50 L carboy before being aliquoted into acid-cleaned 4 L polycarbonate (PC) bottles. Experiments 1 and 2 contained a set of three unamended controls (Control A, B and C) and three +Fe (5 nmol L^{-1} $FeCl_3$; +Fe A, B and C) bottles. All 6 bottles for experiments 1 and 2 were placed in on-deck flow-through incubators that were screened to 30% light levels. Bottles for experiment 2 were placed in multiple heavy-duty black garbage bags and also placed in the on-deck flow-through incubator. Experiment 1 was terminated after six days, and experiment 2 was terminated after 3 days. Experiment 2 was initiated using the

phytoplankton biomass that had accumulated in the controls and +Fe treatments at the end of experiment 1, and were simply placed in the dark following the termination of the light portion of experiment 1 on day 6.

Samples for chl *a*, macronutrients (NO_3^-, PO_4^{3-}, and $Si(OH)_4$), phytoplankton pigments, phytoplankton cell counts, dFe, and dFe-binding ligands were taken from experiments 1. Experiment 2 was only sampled for dFe and dFe-binding ligands. Samples for chl *a* were taken every day from all six bottles in experiments 1, and macronutrients were sampled every two days from all six bottles. Pigment concentrations and phytoplankton cell counts were sampled on day 0 (initial conditions) and day 6 (final conditions) in all controls and +Fe bottles. DFe and dFe-binding ligands were sampled every day in experiment 1, but only from one bottle from each treatment until day 6, when all bottles were sampled. For example, Control A and +Fe A bottles were sampled on days 1, 4, and 6, Control B and +Fe B were sampled on days 2, 5, and 6, and Control C and +Fe C were sampled on days 3 and 6. DFe and ligands for experiment 2 were only sampled on day 0, and then on day 3 from all treatments.

3.6.2 Photochemical experiments

Photochemical experiments were performed at stations 1, 2, and 6 at the chl *a* maximum. Seawater was collected in X-Niskin bottles or GO Flos and filtered in-line with a 0.2 µm Acropak-200 filter in order to isolate only the effects of light on the dFe-binding ligand pool. Filtered seawater was homogenized in a clean carboy and dispensed into four conditioned quartz flasks with Teflon stoppers (Quartz Scientific). Two of the flasks were wrapped tightly in aluminum foil for the dark controls. All four flasks were placed in a shallow tray coupled to the on-deck flow-through incubators and left in the

natural sunlight for 12 hours. Samples for dFe and dFe-binding ligands were taken randomly from one of the dark flasks for the initial time-point, and from each bottle (Dark A, B and Light A, B) at the end of the 12 hours.

3.7 Modeling

We modified a biological model developed for the Southern Ocean (Jiang et al., 2013) to test the experimental results of incubation experiment 1. The model resolves the classical food web and microbial loop, including three types of nutrients (NO_3^-, $Si(OH)_4$, Fe) and two types of dFe-binding ligands (L_1, L_2). The Fe cycle is simulated with five Fe species including dissolved inorganic Fe (Fe′), dissolved Fe bound to the two stronger ligand classes (FeL_1 and FeL_2), colloidal Fe and particulate Fe. The ligand dynamics include most of the key processes including bio-complexation, thermal dissociation, L_1 ligand production by bacteria during stress conditions, and L_2 ligand production by the remineralization of particulate organic matter. No ligand production due to phytoplankton growth or zooplankton grazing is included (*e.g.* Barbeau, 1996; Sato et al., 2007), and there was no attempt to model the weakest ligand classes (L_3 and L_4). The model had been tested with data from shipboard grow-out incubation experiments and in-situ data during two cruises in the Antarctic Peninsula area, through zero-dimensional and one-dimensional experiments, respectively (Jiang et al., 2013). In this project, some of the model parameters were adjusted to the lower nutrient conditions in the southern CCE. In particular, we assume that the low dFe concentrations do not limit bacterial activity, despite perhaps limiting phytoplankton growth.

3.8 Statistical analyses

A standard principle component analysis (PCA) was used in order to quantitatively compare the experimental data from incubations with the profile data. PCA aims to explain the variance in a dataset by using multiple weighted variables, rather than just simple linear regression. This type of analysis allowed for the comparison of how multiple variables explained the variance between profiles and incubation experiment. Only biological experiment 1 was included in the PCA, due to the lack of ancillary data in experiment 2 and in the photochemical experiments. The PCA was performed using the Statistics Toolbox in Matlab with all ancillary data from CTD profiles and incubation experiment, including the dFe and ligand data. All data categories were normalized by their standard deviation, and missing values were interpolated using a regression with depth for the profile data, or a regression with time for incubation data.

4. Results

4.1 Water column profiles

Each station was loosely grouped as 'nearshore', 'transition' or 'offshore' based on physical characteristics (Krause et al., submitted). Station 4 was classified as a 'nearshore' station, stations 1 and 6 were 'transition' stations, and station 2 was considered 'offshore,' based on defining water mass characteristics in relation to a persistent frontal feature that was sampled in this region as part of the CCE-LTER program. The depth and magnitude of both the chl *a* maximum and nitracline correspond well with these groupings (Figure 5.2). Station 4 (Figure 5.2c) was characterized by a relatively shallow biomass maximum (< 50 m) and nitracline (< 20 m). Very high chl *a* concentrations were observed at station 4 (up to 9 $\mu g\ L^{-1}$), corresponding with almost complete draw down of NO_3^- in surface waters. The transition zone stations (Figure 5.2a,

d) were similar to the nearshore station but had a slightly deeper nitracline (40-50 m) and lower [chl *a*]. The offshore station (station 2, Figure 5.2b) had a much deeper nitracline (> 50 m) and a deep chl *a* maximum.

The [dFe] ranged from < 0.3 nmol L^{-1} in surface waters to approximately 0.8 nmol L^{-1} at 500m in the nearshore station (Figure 5.3c). DFe in the southern CCE is characterized by low concentrations and a deep ferricline, often deeper than 100 m (King and Barbeau, 2011). DFe-binding ligands show a similar pattern to dFe (Figure 5.3). The strongest ligands (L_1, $\log K^{cond}_{FeL_1,Fe'} \geq 12.0$) were present throughout the water column and were still present at 500 m (the deepest depth sampled). Most of the profiles showed a subsurface maxima in L_1 associated with the biomass maxima and then minima, before increasing slightly again at depths below 100 m. Although there were elevated L_1 concentrations at the chl *a* maxima, there were not significantly higher ligand concentrations associated with the large bloom at station 4 (Figure 5.2c, 5.3c). Three of the stations showed a minimum in L_1 in surface water (Figure 5.3a, b, and c), but station 6 had elevated concentrations in the shallowest depth sampled (Figure 5.3d). There is also some evidence at the base of the profiles that L_1 might begin to decline below 500 m, but it is difficult to determine without more sampling depths. For a detailed description of all dFe and ligand data see the supplementary information (S5.1).

L_2 ligands ($\log K^{cond}_{FeL_2,Fe'} = 11.0\text{-}12.0$) were present in slightly higher concentrations than L_1 throughout most of the water column, but had a similar distribution with depth. However, a surface maxima in L_2 was only apparent at station 2 compared to all stations having a subsurface maxima in L_1. There is also some evidence that L_2 began to decrease below 400 m at station 2, but again more sampling depths

would be needed to confirm this pattern in deep waters. The L_2 concentration was greatest at station 1 (ranging from 1.5-4.2 nmol L^{-1}) compared to the other three stations where L_2 did not exceed 3 nmol L^{-1}. This matched the pattern in dFe and other ligand concentrations, perhaps due to enhanced mixing associated with the frontal transition zone at this station (Figure 5.1).

L_3 was relatively distinct from the stronger ligands. [L_3] remained mostly constant throughout the water column with a few exceptions in surface waters (Figure 5.3). The highest concentrations of strong ligands in the upper 100 m were found at the 'transition' stations (stations 1 and 6), and the lowest concentrations of strong ligands were offshore at station 2. On average, this pattern was opposite for the weaker ligands (L_3). There were higher [L_3] in the nearshore station (station 4) and offshore station (station 2) than in the transition zone. No L_4 ligands were detected in any of the profiles at any of the depths sampled.

Statistical analyses of the profiles revealed similar results as the incubation experiments (*see* section 4.3.2), with variances in ligand distributions with depth primarily related to macronutrient concentrations and other parameters which also increase with depth (Supplementary Information, S5.2). These variables mostly all contributed positively to the first principal component (PC), which explains 53.7% of the variance in ligands at different depths. Temperature, oxygen concentrations, particulate organic carbon (POC), particulate organic nitrogen (PON), chl *a*, and fluorescence (which all decrease with depth) all contribute negatively to the first PC. Since the ligand data could be explained predominantly by a combination of several variables that also increase with depth, a cluster analysis was also completed in order to examine differences

in ligands between stations (data not shown). No statistical difference was observed in the ligand distributions between stations, and any differences in clustering was related to biogeochemical patterns alone.

4.2 Biological ligand production experiments

4.2.1 Incubation experiment 1

Experiment 1 was sampled at 30m depth from an aged, upwelled water mass that had likely originated nearshore near Point Conception (Krause et al., submitted). The initial conditions for the experiment started with relatively elevated macronutrient concentrations (11.5 µmol L^{-1} NO_3^-; Figure 5.4c) and dFe (0.54 nmol L^{-1}). Thus, the phytoplankton community was likely not macronutrient limited. Little NO_3^- was drawn down in controls, but significant macronutrient drawdown was observed by day 4 of the experiment in +Fe treatments (Figure 5.4a). The macronutrient drawdown was accompanied by a significant increase in chl *a* biomass in +Fe treatments compared to controls (*t-test*, $p < 0.05$). Although the initial community was relatively diverse (Figure 5.4d), the increase in biomass by day 6 was almost entirely due to an increase in the abundance of diatoms, mostly *Pseudo-nitzschia* spp. (Figure 5.4d). The increase in diatoms was apparent both from cell counts (Figure 5.4d) and from elevated fucoxanthin pigment concentrations compared to initial conditions (data not shown). Although the total biomass was much higher in +Fe treatments, the phytoplankton community structure was very similar between the controls and +Fe treatments (Figure 5.4d). Even though the composition of the phytoplankton community was not significantly different between controls and +Fe treatments, the evolution of NO_3^- compared to dFe (NO_3^-: dFe; µmol L^{-1}: nmol L^{-1}) over the course of the experiment was drastically different in

controls and +Fe bottles (Figure 5.4b). Previous work in this region has shown that μmol L^{-1} NO_3^-: nmol L^{-1} dFe ratios of approximately 10-12 and higher are indicative of Fe limitation of the diatom community (King and Barbeau, 2007). The initial water mass contained a NO_3^-: dFe ratio of 21.5, likely indicating that the diatom community was initially Fe-limited. However, the 5 nmol L^{-1} dFe addition in +Fe bottles appeared to alleviate this Fe-limitation based on the NO_3^-: dFe ratios observed over the course of the experiment (Figure 5.4b) and the increase in biomass by day 6 (Figure 5.4a).

Although the phytoplankton biomass response differed between controls and +Fe treatments, the evolution of dFe-binding ligands was very similar (Figure 5.5). DFe was drawn down in +Fe treatments after day 4 (Figure 5.5a), concomitant with the increase in phytoplankton biomass and decrease in NO_3^-. DFe decreased slightly in controls, likely due to a combination of uptake and scavenging to the walls of the bottles. The strongest ligands (L_1) increased in both controls and +Fe treatments from days 0-1, and then remained relatively constant for the remainder of the experiment (Figure 5.5b). L_2 ligands increased consistently over the 6 days of the experiment (Figure 5.5c). The weaker ligands showed distinct temporal patterns compared to the stronger ligands, with L_3 slowly decreasing during the sampling period and L_4 ligands only appearing on days 4-6 (Figure 5.5d, e). The temporal distributions of each ligand class were not statistically distinct from one another between controls and +Fe treatments over the course of the experiment (ANOVA, $p > 0.05$).

4.2.2 Experiment 2

Experiment 2 was conducted in the dark for three days following the termination of experiment 1 on day 6. Control and +Fe bottles contained different amounts of

phytoplankton biomass initially (Figure 5.4a), but relatively similar dFe and ligand concentrations (Figure 5.6). The goal of this experiment was to assess microbial alteration of the ligand pool in response to distinct amounts of particulate biomass and relative Fe enrichment of the system. Control bottles contained 0.14±0.05 nmol L^{-1} (n = 3) dFe on day 1 of the experiment, and 0.54±0.33 nmol L^{-1} dFe was remineralized by day 3 (n = 3). In +Fe treatments the dFe increased from 0.31±0.07 nmol L^{-1} (n = 3) on day 1 to 1.29±0.21 nmol L^{-1} (n = 3) on day 3. In general, ligands increased more in the controls than in the +Fe treatments (Figure 5.6), though there was high variability between replicate bottles. L_1 ligands increased by 32.6±1.7% on average in controls (n = 3), but they decreased by 1.3±1.2% in +Fe bottles (n = 3). A similar pattern was seen for L_2 ligands, which increased by 29.7±2.1% in control treatments, but decreased by 16.8±2.0% in +Fe bottles (n = 3). L_3 ligands decreased in both treatments, but by a significantly higher percentage (*t-test*, $p < 0.05$) in controls (33.9±2.1%) then in the +Fe case (5.9±2.5%). The weakest ligands (L_4) showed the greatest change between days 1-3 in both treatments, but increased by a significantly (*t-test*, $p < 0.05$) greater percentage in controls (109.1±3.2%) compared to +Fe bottles (32.8±4.9%, n = 3). In general, the average concentration of total ligands (L_1+L_2+L_3+L_4) was higher in controls on day 3 than in +Fe bottles on day 3 (*t-test*, $p < 0.05$).

4.3 Modeling and statistical analyses of incubation experiment 1

4.3.1 Modeling

Numerical experiments using the model developed by Jiang et al. (2013) were performed for incubation experiment 1 in order to investigate biological ligand sources and sinks based on non-measured parameters (*e.g.*, bacterial growth rate and abundance).

Certain rates and other ancillary data were obtained at the same station and depth for experiment 1 as part of the CCE-LTER program (station 3), and were used as the initial values of key parameters in the model, with some adjustments (Table 5.1). Changes in nutrient concentrations over time both in control and +Fe treatments (Figure 5.7a, b, and c) were reasonably reproduced by the model. The corresponding increase in chl *a* was also generally captured by the model (Figure 5.7d). No measurements were made for bacteria or organic matter during the course of experiment 1, but the model results show an increase of both bacteria and organic matter in +Fe treatments (Figure 5.7e, f). The temporal pattern in L_1 was also described relatively well, with the exception of the increase in L_1 ligands from day 0 to day 1 (Figure 5.7g), and the same was true for L_2 ligands (Figure 5.7h). The data indicates there were higher L_1 concentrations in control treatments from days 0-1, while the model results show little difference between the two treatments during the first few days. The differences between treatments in the model become apparent between days 4-6, due to much higher bacterial activity in +Fe treatments (Figure 5.7e, g). Modeled [L_2] is significantly higher in +Fe treatments compared to controls due to degeneration of L_1 and L_2 production from PON (*e.g.*, Boyd et al., 2010). However, the model was unable to account for the peak in L_2 between days 3-5 in +Fe treatments (Figure 5.7h). The model tests suggest that Fe stress is not a significant factor altering bacterial ligand production during incubation experiment 1, because of the similar [L_1] between control and +Fe treatments. Although dFe concentrations were relatively low in control treatments, it is possible that particulate Fe was a significant Fe source (not tested by the model) to the microbial community based on the Fe partitioning in the model. It is also possible that bacteria communities in this

system have been adapted to the low Fe environment in the southern CCE. Similar to Jiang et al. (2013), no direct source of ligands in the model is assumed to come from phytoplankton growth or zooplankton grazing. Thus, the striking differences in biomass between controls and +Fe treatments did not lead to a similar difference in dFe-binding ligand concentrations in the model, which is consistent with observations.

4.3.2 Statistical analyses

Simple linear regression comparing the ligand data to other measured parameters did not explain the temporal variability in ligands in incubation experiment 1 (data not shown). Therefore, in order to analyze the contribution of multiple variables to the variance in ligands over time, a PCA was performed in addition to the modeling study. Approximately 77% of the variance between sampling time points in experiment 1 could be explained by the first three PCs (S5.2). The ligands measured during incubation experiment 1 were primarily correlated with macronutrients and changes in pigments over time. The first PC for the incubation experiments is predominantly explained by macronutrient concentrations, which are negatively correlated with the biological variables measured. This is not surprising, given the variance between samples from different treatments differed significantly in their nutrient concentrations and biomass over time. The second PC however, is dominated by positive contributions from the ligands and dFe, along with the pigments and macronutrients (S5.2). These parameters were negatively correlated with L_3 ligands, and the biological response from the diatoms. This suggests the second PC may have more of an influence on the variances seen in the ligand pool between treatments and over time. The third PC contributes the least to the

percentage of the variance explained (10.9%) and contains strong contributions from a mixture of the parameters measured.

4.4 Photochemical experiments

Each photochemical experiment was completed using water collected from the chl *a* maximum at each station (30m for station 1, 70m for station 2, and 20m for station 6). Filtered seawater was incubated in the dark and light for 12 hours, and dFe and ligands were measured at the beginning and end of each experiment. The first experiment at station 1 contained similar concentrations of strong ligands in the initial conditions and dark treatments, and slightly higher [L_2] were observed in the light treatment (Figure 5.8a), though the differences were not significant (*t-test*, $p > 0.05$). No weaker ligands (L_3) were observed in this experiment in the initial or final conditions. Experiments 2 and 3 from stations 2 and 6, respectively, showed different results (Figure 5.7b, c). Again, the dark bottles contained similar dFe and ligands as initial conditions in both experiment, but light treatments had lower concentrations of L_1 ligands and also contained L_3 ligands, which were absent initially and in the dark treatments (Figure 5.7b, c). The weakest ligands measured in this study (L_4 ligands) were not detected in any of the photochemical experiments.

5. Discussion

5.1 Distribution of multiple classes of iron-binding ligands in the southern California Current system

DFe and ligand profiles in this study were similar to those measured in other oceanic regimes (*see* Gledhill and Buck, 2012), with a minimum in ligands in surface waters and an increase with depth along with dFe (Figure 5.3). Ligand profiles between

stations were also similar, despite the differences in biogeochemical regimes sampled (Krause et al., submitted). Most of the profiles had a surface minimum in L_1 ligands (Figure 5.3), which may be related to photochemical degradation consistent with previous findings of potential photochemical degradation of Fe-binding ligands in near surface waters. This feature can be patchy however, since station 6 for example, had a maximum in L_1 in surface waters (Figure 5.3d). The minimum in L_1 was also sometimes associated with elevated concentrations of L_3, though not at station 1. There appear to be other dynamics affecting [L_1] in the profiles as well, as a maximum in L_1 can be seen at stations 2 and 6 associated with, or near, the chl *a* maximum (Figure 5.2). Other studies have also observed a maximum in strong ligands at or below the biomass maximum (Buck and Bruland, 2007; Boye et al., 2001, 2006; Croot et al., 2004; Gerringa et al., 2006, 2008; Ibisanmi et al., 2011; Rue and Bruland, 1995; van den Berg, 1995, 2006; Wagener et al., 2008). The mechanism leading to this feature is not entirely clear, but one field study done in the Canary Basin showed that 63% of the variance in ligands above or coinciding with the chl *a* maximum was explained by phytoplankton biomass and silicic acid concentrations (Gerringa et al., 2006). L_1 in this study was defined as any ligands with a $\log K^{cond}_{FeL_1,Fe}$, $\geq$ 12.0, and were present at all depths sampled in this study (up to 500 m). Some other studies in the Atlantic Ocean (Cullen et al., 2006) and Southern Ocean (Ibisanmi et al., 2001) have only detected L_1 in near surface waters (< 200 m), though Cullen et al. (2006) used a higher $\log K^{cond}_{FeL_1,Fe}$, cut-off (13.0). In this study, it appears that relatively strong ligands are consistently present in the upper water column in this region. In our previous work examining surface samples in the central and northern CCE we also found that L_1 declined in surface waters offshore (> 200 km)

perhaps due to degradation of the stronger ligand class, or a nearshore source, though only a few samples were measured offshore (Bundy et al., 2014). Other studies have also noted a slight decline in ligand strength from coastal to offshore waters (Sander et al., 2014). All stations sampled in this region were within 200 km of the coast (Figure 5.1), and L_1 was present in surface waters of each station (Figure 5.3). Thus, it is still uncertain whether L_1 is restricted to the upper ocean or within 200 km of the coast in this region. On a GEOTRACES zonal transect in the Atlantic however, recent work has shown L_1-type ligands (average $\log K^{cond}_{FeL_1,Fe'}$ = 12.29±0.31, *n* = 548) present throughout the entire water column, even down to 6000 m (Buck et al., in review). There is likely an in-situ source of strong ligands throughout the water column, especially in the upper ocean where L_1 ligands appear to be a common feature.

L_2 ligand distributions were very similar to the distributions of L_1 in the profiles (Figure 5.3). L_2 ligands, as defined in this study, are generally still considered 'strong' in terms of previous work in the dFe-binding ligand literature (Gledhill and Buck, 2012), and thus may be controlled by similar processes as L_1. Our work in coastal regions has also demonstrated a strong coupling between these two classes of ligands in the stronger ligand pool (Bundy et al., 2014; Bundy et al., in review). A surface salinity transect from San Francisco Bay showed the dFe which survives flocculation in the estuary was tightly coupled to stronger ligands (Bundy et al., in review), but the profiles in the southern CCE show significant excess strong ligand ($[L_{1,2}]$-[dFe])). This is especially true in surface waters, and then strong ligand concentrations start to slowly decline as [dFe] increases (Figure 5.3). This may be evidence of in-situ biological production, even at mid-depths and deeper waters. From the bulk of previous studies measuring dFe-binding ligands, L_2

appears to be a relatively ubiquitous ligand class even in deeper waters (Gledhill and Buck, 2012). Buck et al. (in review) also measured an L_2 ligand class on the zonal Atlantic GEOTRACES transect ($\log K^{cond}_{FeL_2,Fe'}$ = 11.31±0.31, *n* = 427) which was also present down to 6000 m along with L_1. Thus, similar processes affecting the cycling of L_1 may also contribute to the distributions of L_2 in the water column.

The weaker ligands detected in the four profiles (L_3) were slightly distinct from the stronger ligands. L_3 concentrations were almost constant with depth at most stations, with a slight minimum in surface waters at station 1 (Figure 5.3). Evidence from our previous work has shown that L_3 ligands increase in surface samples in a transect from nearshore to offshore in the CCE (Bundy et al., 2014), perhaps due to degradation of the stronger ligand pools. Elevated concentrations of L_3 in the profiles relative to stronger ligands support this preliminary hypothesis. The slight minimum in surface waters might be related to dissolved organic matter (DOC) uptake, if L_3 ligands comprise a portion of the labile organic matter pool utilized by bacteria. The hypothesis that microbial communities are responsible for altering the weaker ligand pool in the deep ocean (Hunter and Boyd, 2007) is also supported by the results from the water column profiles, suggesting an in-situ source of weaker ligands in subsurface waters.

5.2 Iron-binding ligand dynamics in biological incubation studies

Two experiments were performed in this work in order to observe the temporal evolution of the ligand pool during phytoplankton growth (biological incubation experiment 1) and microbial remineralization of particles (biological incubation experiment 2). Each experiment shed light on different possible mechanisms leading to alteration of the ligand pool over time. Incubation experiment 1 examined changes in

dFe-binding ligands over time in an Fe-limited water mass (Figure 5.5). Although there have been links between diatom growth and changes to the ambient ligand pool observed in previous work (Buck et al., 2010; King et al., 2012), incubation experiment 1 showed somewhat different results. Likely some of these differences were related to the characteristics of the initial water mass. For example, experiment 1 was likely initiated under Fe-limiting conditions, as evidenced by the initial NO_3^-:dFe (Figure 5.4b) and the eventual diatom response to Fe addition (Figure 5.4a). Experiment 1 also had elevated strong ligand concentrations initially, which remained relatively constant throughout the experiment (Figure 5.5). It is possible that the elevated concentrations of strong ligands in experiment 1 remained relatively constant over time due to initial Fe-limitation of the planktonic community, in contrast to other incubation studies which were initiated in nutrient replete waters and evolved into Fe-limitation over the course of the incubation (Buck et al., 2010; King et al., 2012).

Overall, the difference in biomass in experiment 1 between controls and +Fe bottles was striking, yet the ligand pools were quite similar. Depending on the source of the strong ligands in these experiments, there may be different mechanisms for the increase in strong ligands in controls versus +Fe treatments. Only a few previous incubation studies have examined dFe-binding ligand production associated with Fe-limited diatoms (Buck et al., 2010; King et al., 2012) or Fe-induced diatom blooms (Kondo et al., 2008). Several studies have also shown a relationship between dFe-binding ligands and diatoms (Buck et al., 2010; Gerringa et al., 2006; King et al., 2012; Rijkenberg et al., 2008; Soria-Dengg et al., 2001; Trick et al., 1983). *Chaetoceros brevis* was one of the dominant diatom species in experiment 1, and may have altered the

natural ligand pool similar to what has been observed in culture media (Gonzalez et al., 2014; Rijkenberg et al., 2008). Other evidence has been found in the field to showing strong ligands are produced associated with large diatom blooms such as those observed during IronEx-II (Rue and Bruland, 1997) and SEEDS II (Kondo et al., 2008). It seems clear from these studies that diatom-dominated phytoplankton blooms can be associated with changes in the strong Fe-binding ligand pool at least on short timescales, but the mechanisms are unclear. The connection between weaker ligands and diatoms is easier to explain based on the available data and some previous studies. Phytoplankton have been shown to release polysaccharides and other cellular material during growth (Myklestad et al., 1989; Myklestad, 1995; Urbani et al., 2005; Watt, 1969) which may explain the increase in weaker ligands observed on days 4-6 in experiment 1 (Figure 5.5d). It is not entirely certain what compounds may comprise the weaker ligand pool in the marine environment, but the decrease in the L_3 ligand class over the duration of experiment 1 along with a slight increase at the termination of the experiment points to perhaps polysaccharides (Hassler et al., 2011) or some other form of labile DOC such as free amino acids (Ducklow et al., 1993). Polysaccharides would fall into the L_3 ligand category in this study based on their conditional stability constant (Hassler et al., 2011), and they are readily consumed by most bacteria as a source of DOC (Arnosti et al., 1994; Zweifel et al., 1993). The L_4 ligand class was only detected on days 4-6 in experiment 1 (Figure 5.5e) which could be partially explained by the release of domoic acid by *Pseudo-nitzschia*, which are known to produce this compound during bloom formation (Rue and Bruland, 2001). Domoic acid has a log $K^{cond}_{FeL,Fe'}$ = 8.6, which falls into the L_4 class as defined in this study (Rue and Bruland, 2001) and experiment 1 was dominated

by *Pseudo-nitzschia*. These ligands may also be comprised of other degraded cellular material, such as viral lysis products (Poorvin et al., 2011), or other high molecular weight (HMW) compounds that have been shown to effectively bind dFe (Abdullha et al., 2010; Laglera et al., 2009). HMW compounds have also been identified associated with diatom growth in culture media containing *T. weiss* and *C. Antigua* (Fuse et al., 1993), suggesting other diatoms in experiment 1 may have contributed to the increase in the weaker ligand pool at the end of experiment 1 (Rijkenberg et al., 2008).

While diatoms must be considered as potentially altering the ligand pool in experiment 1, the production of dFe-binding ligands has also been associated with copepod grazing (Sato et al., 2007). Grazing may be the reason for the initial increase in stronger ligands from day 0-1 (Figure 5.5b,c), since grazing was likely elevated in the incubation bottles compared to in-situ. Grazing may also be an explanation for higher $[L_2]$ on days 3-5 in +Fe treatments in experiment 1 (Figure 5.5c), coinciding with elevated diatom growth on those days. However, due to similarities between controls and +Fe bottles in experiment 1, it is unlikely that phytoplankton grazing was a significant factor affecting ligand concentrations in that experiment. This hypothesis is corroborated by the modeling results for experiment 1, which shows there were potentially significant differences in grazing rates between controls and +Fe treatments during the later days of the experiments (data not shown). This implies there should be differences in ligand concentrations between treatments if zooplankton grazing was a significant source of ligands.

Bacteria were not directly sampled in this study due to volume constraints, but the ability for the natural microbial community to alter the ligand pool in experiment 1 was

analyzed via modeling (Figure 5.7). Modeling results were able to depict the cycling of the stronger ligand pool (L_1 and L_2) reasonably well with only bacteria as biological sources of ligands (Figure 5.7). From the modeling results, it does not appear that the microbial community was Fe-limited in experiment 1, or that the temporal pattern of ligand production was due to different mechanisms in controls and +Fe treatments. If the heterotrophic microbial community was the sole biological source and sink of ligands, this could explain the similar temporal trends in ligands between treatments in incubation experiment 1 (Figure 5.5). Although strong ligands are generally considered to be produced under Fe-limiting conditions as an Fe acquisition strategy, some previous studies have observed siderophore production under nutrient enriched conditions as well (Gledhill et al., 2004; Mawji et al., 2011). The production of strong ligands in the +Fe treatments of experiment 1 may be the result of active microbial production due to nutrient enriched conditions, since these treatments never reached Fe-limiting conditions, even for the phytoplankton community (Figure 5.4b).

The temporal pattern in ligands in incubation experiment 1 was likely the result of several processes, perhaps dominated by microbes. The ability for the heterotrophic community to alter the ligand pool was explicitly tested in incubation experiment 2 (Figure 5.6). Microbial remineralization of organic particles has been examined previously by Boyd et al. (2010) in the Southern Ocean, which found that microbial breakdown of POC produced dFe and L_2 ligands (Boyd et al., 2010). Our incubation study examined microbial remineralization of several ligand classes using MAWs, and found that almost all the ligand classes increased over the incubation period in controls (days 1-3) and the ligand increase was greater in controls than +Fe treatments. It is

possible the strong ligands produced during experiment 2 could be siderophores, especially in control treatments which contained very low [dFe] even after some had been remineralized (Figure 5.6). Siderophores have been shown to be produced by a wide range of marine bacteria (Amin et al., 2009; Vraspir and Butler, 2009), and several siderophores have been found in the marine environment (Haygood et al., 1993, Reid et al., 1993, Martinez et al., 2000, Martinez et al., 2001 and Martinez et al., 2003). L_3 ligands had a different pattern than the other ligand classes in experiment 2, since they decreased slightly from day 1-3, though the differences between the initial and final time points were not significant in either treatment (*t-test*, $p > 0.05$). Similar to experiment 1, it is possible that some form of labile DOC falls into the L_3 ligand category, which may have been consumed during this experiment. In contrast to L_3, L_4 clearly increased during experiment 2. This is consistent with other observations which have shown that HMW organic compounds can increase due to DOC remineralization (Repeta et al., 2002).

5.3 Iron-binding ligand dynamics in photochemical studies

Photochemical experiments done in this region showed mixed results with respect to the effect of natural sunlight on the dFe-binding ligand pool (Figure 5.8). This is similar to other field efforts, where some studies have observed a decrease in the concentration of strong dFe-binding ligands upon exposure to natural sunlight (Powell and Wilson-Finelli, 2003) and others have seen no effect of UV light on ligands found in Dutch estuaries (Rijkenberg et al., 2006) despite elevated ligand concentrations. Thus, it appears not all natural dFe-binding ligands are susceptible to photo-degradation, as has been shown with certain siderophores in laboratory studies (Barbeau et al. 2001, 2003; Barbeau 2006). One reason for this difference in reactivity may be related to the size

class or binding strength of the natural ligands present in the particular environment. For example, natural ligands observed initially in photochemical experiment 1 from this study were slightly weaker (log $K'^{cond}_{FeL,Fe}$= 12.51±0.14), though still strong, than in experiments 2 and 3 (13.70±0.02 and 12.79±0.15, respectively; *t-test*, $p < 0.05$). It is possible that only the strongest ligands were degraded upon exposure to natural sunlight, since the production of L_3 ligands was observed in experiments 2 and 3 at the same time that L_1 ligands slightly decreased (Figure 5.8). Some of the natural dFe-binding ligands in the study conducted by Powell and Wilson-Finelli (2003) had slightly elevated log $K'^{cond}_{FeL,Fe}$ compared to the Rijkenberg et al. (2006) study (log $K'^{cond}_{FeL,Fe}$ of approximately 12 compared to 10.1-11.0), and no degradation of the strong ligands was observed by Rijkenberg et al. (2006). The chemical identity, or size class, of the natural ligands in each study may also be distinct, causing differences in photochemical reactivity. Samples for photochemical experiments in this study were taken from sub-surface chl *a* maxima as opposed to surface waters (Powell and Wilson-Finelli, 2003; Rijkenberg et al., 2006) and therefore, the initial ligands may have had little to no sunlight exposure prior to the experiment. It is notable that no L_3 ligands were detected initially in any of the photochemical experiments, despite the fact that L_3 ligands were detected in the water column at similar depths (Figure 5.3). We speculate that there was some scavenging of L_3 ligands onto the walls of the quartz flasks used in this study, since the initial samples were taken directly from the flasks after filling and we have noted this problem in other experiments with quartz (data not shown). This may be another reason for differences in

field studies examining degradation of natural ligands, if weaker ligands produced from photo-degradation are rapidly scavenged.

Another possible explanation for mixed findings in the field may be related to analytical methods. This study employed MAW analysis, which enabled the detection of both the strongest and weakest dFe-binding ligands ($\alpha_{Fe(SA)_x}$= 74-115). Powell and Wilson-Finelli (2003) employed a low ($\alpha_{Fe(TAC)_2}$= 55) and high ($\alpha_{Fe(TAC)_2}$= 300) analytical window, while Rijkenberg et al. (2006) used only a high window ($\alpha_{Fe(TAC)_2}$= 300). It is possible that the competition strength in the Rijkenberg et al. (2006) study may have been too high to effectively detect some of the weaker dFe-binding ligands. These differences in analytical methods support the utility of using MAWs in the context of mechanistic ligand studies where more than one class of dFe-binding ligand may be detected.

5.4 Sources and sinks of iron-binding ligands in the southern California Current system

To our knowledge, this is the first study to mechanistically link dFe-binding ligand profiles with deckboard incubation experiments on the same cruise, using MAW analysis of the ligand pool. Although only a few profiles were examined in this study, the stations were in biogeochemically distinct sampling regions, and large hydrographic and biological gradients were also sampled vertically. Despite the large gradients however, the ligand profiles were very similar between stations. Station 4, for example, had much higher [chl a] in subsurface waters, but did not show a significant difference in ligands at this depth (*t-test*, $p > 0.05$, Figure 5.2, 5.3). Similarly, biological incubation experiment 1 showed essentially no differences in the ligand pool between an Fe-limited phytoplankton community and an Fe-fertilized phytoplankton bloom (Figure 5.5), despite

the much higher biomass in +Fe bottles (Figure 5.4a). These findings suggest that large changes in phytoplankton biomass in surface waters may have little impact on the overall composition of the dFe-binding ligand pool.

MAW analysis helped to reveal the presence of three ligand classes at almost every sampling depth in the upper 500 m of the southern CCE, suggesting there are ubiquitous in-situ sources of each of these ligand classes, or they have a relatively long residence time. Although no other studies have used MAWs to measure dFe-binding ligand profiles, most studies agree that both strong and weak ligands are present throughout the water column, with perhaps an exceptionally strong ligand class only present in some surface waters (*e.g.*, Cullen et al., 2006). Experimental and statistical evidence from this study suggests a mechanism for the presence of both strong and weak ligands in surface and subsurface waters. Statistical analysis of the profiles revealed that there were no apparent differences between stations that could be explained by the ligand distributions alone; all variances were primarily explained by vertical hydrographic differences. In fact, the variances in the ligand distributions between profiles were primarily explained by macronutrient distributions, which likely points to microbial remineralization as the dominant control on the ligand pool with depth over longer timescales. A field study also found a close link between ligand concentrations in surface waters, DOC and bacterial abundance (Wagener et al., 2008) and microbes are known to be the dominant control on DOC in the ocean. Although some interesting features were also seen in the upper water column that may be related to phytoplankton dynamics, they may function on shorter timescales than microbial remineralization processes altering the ligand pool. Incubation experiment 2, which focused on the ability of the heterotrophic

community to produce dFe-binding ligands from POC remineralization, showed that both strong and weak ligands are produced during this process, in contrast to Boyd et al. (2010) which only explained a mechanism for weaker ligand production in deeper waters. The results from incubation experiment 2 now provide a mechanism for in-situ strong ligand production in subsurface waters as well.

Although L_4 ligands appeared to also be produced during both biological incubation experiments, none were detected in the profiles (Figure 5.3). It may be that these weaker dFe-ligand complexes are scavenged on longer timescales and were therefore not present in the station data, or that L_4 ligands have only a nearshore source such as the benthic boundary layer or San Francisco Bay as seen in our previous work (Bundy et al., 2014; Bundy et al., in review). The conditional stability constants of L_4 ligands are very weak, and may therefore only be present under certain conditions or on certain timescales in the water column. The biological incubation experiments performed in this study suggest that there are, however, in situ sources for these very weak ligands in the oceanic environment.

Subsurface ligand concentrations appear to be largely controlled by the microbial community, but photochemical effects appear to impact near surface waters in this region as well. Evidence from photochemical experiments suggests that photochemical degradation of natural ligands can be variable, and may be restricted to only the strongest ambient ligands. This may provide an explanation for regional differences between studies on photochemical effects (Powell and Wilson-Finelli 2003; Rijkenberg et al. 2006) and the differences between stations in this study (Figure 5.3). Additional explanations for the variable influence of photochemistry on the natural ligand pool will

be important to constrain in future studies, as it appears to be a significant sink for L_1 in CCE surface waters.

6. Conclusions

Experiments and profiles from the CCE point to several variables influencing the distributions of strong and weak dFe-binding ligands. Biological incubation experiments show that strong ligands can be present under both Fe-replete and Fe-limiting conditions, with higher ligand concentrations not necessarily related to higher concentrations of phytoplankton biomass. Modeling results suggest that the temporal evolution of the stronger ligands is closely related to microbial growth rates, and ligand distributions might be similar in different biogeochemical regimes depending on the status of the microbial community. Statistical analyses from incubation experiments and profiles cannot preclude the fact that diatoms may also alter the ambient ligand pool, though a mechanistic understanding of this process is still unclear. Photochemical degradation of natural ligands in sunlight is variable, and findings may depend on the initial strengths of the ambient ligands and the analytical methods employed for their detection. The distribution of macronutrients best explains the variance in dFe-binding ligands between stations and with depth, suggesting microbial alteration of the ligand pool over longer time scales might dominate any short-term changes to the ligand pool due to phytoplankton growth. Overall, a combination of several variables, ranging from chemical to biological, is needed to explain the distributions of strong and weak dFe-binding ligands in the CCE.

7. Acknowledgements

We would like to thank the captain and crew of the *R/V* Melville and the LTER program. We would like to thank Teresa Fukuda for phytoplankton pigment measurements. We also thank Wendy Plante and Shane Hogle for help with sampling. Chapter 5, in full, will be submitted to Marine Chemistry. Bundy, R.M., Barbeau, K.A., Carter, M., Jiang, M. Understanding the sources and sinks of iron-binding ligands in the southern California Current Ecosystem: A mechanistic study. The dissertation author was the primary investigator and author of this paper.

Table 5.1 Ancillary measurements made in the water column as part of the CCE-LTER program for biological experiment 1 and used as initial parameters in the model.

a. The model specifies the initial small phytoplankton and diatom biomass based on the measured chlorophyll using a C/N ratio of 6.625 and C/Chl ratio of 40:1.
b. Model initial Fe concentration for the plus Fe experiment was adjusted because the model was unable to reproduce the initial drop of about 2 nmol L^{-1}.
c. DON was converted from measured DOC (58.4 µmol L^{-1}) using a C/N ratio of 6.625.
d. Bacteria biomass was converted from measured bacteria abundance ($1.07x10^9$ cells L^{-1}) using a biomass to cell ratio 20 $mgC/10^9$ cells (Lee and Fuhrman, 1987) and a Redfield C:N molar ratio of 6.625:1.
e. Initial ligand concentrations were adjusted to account for unknown jumps during the first day of the experiments.

Parameter	Measured Value	Model Initial Value
PAR (µE m^{-2} s^{-1})	263.7	263.7
Temperature (°C)	13.4	13.4
Chlorophyll (mg m^{-3})	0.93	0.93[a]
Dissolved Fe (nmol L^{-1})	0.54 (5.54)	0.54 (3.54)[b]
Nitrate (µmol L^{-1})	11.5	11.5
Silicate (µmol L^{-1})	2.49	2.49
Particulate N (µmol L^{-1})	1.015	1
DON (µmol L^{-1})	8.8[c]	10
Bacterial biomass (µmol L^{-1})	0.27[d]	0.27
L_1 (nmol L^{-1})	1.69	5.5[e]
L_2 (nmol L^{-1})	0.86	3.5[e]

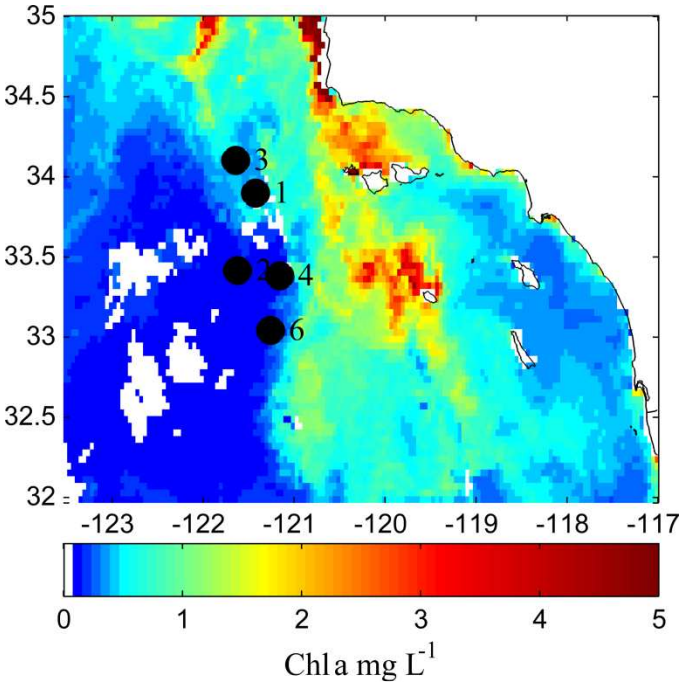

Figure 5.1 Sampling locations for water column profiles and incubation experiments during the June/July 2011 cruise. Stations were sampled in the nearshore (3, 4), transition (1, 6) and offshore (2) side of a distinct frontal feature (Krause et al., in prep) shown as the average in chl *a* from MODIS for the month of July in 2011.

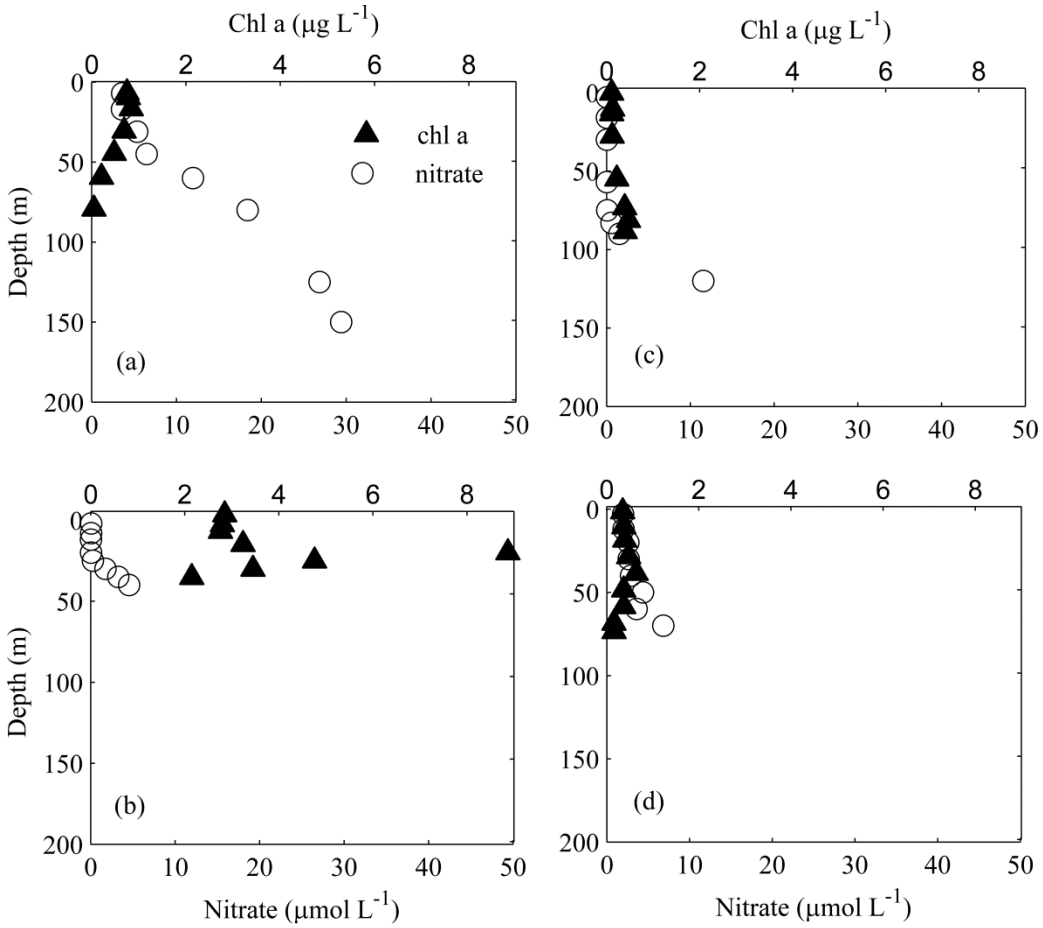

Figure 5.2 Chl *a* and nitrate (nitrate+nitrite) bottle samples for stations 1 (panel a), 2 (panel b), 4 (panel c), and 6 (panel d). Station 4 was classified as 'nearshore', stations 1, and 6 as in the 'transition' zone, and station 2 as 'offshore' according to Krause et al. (submitted).

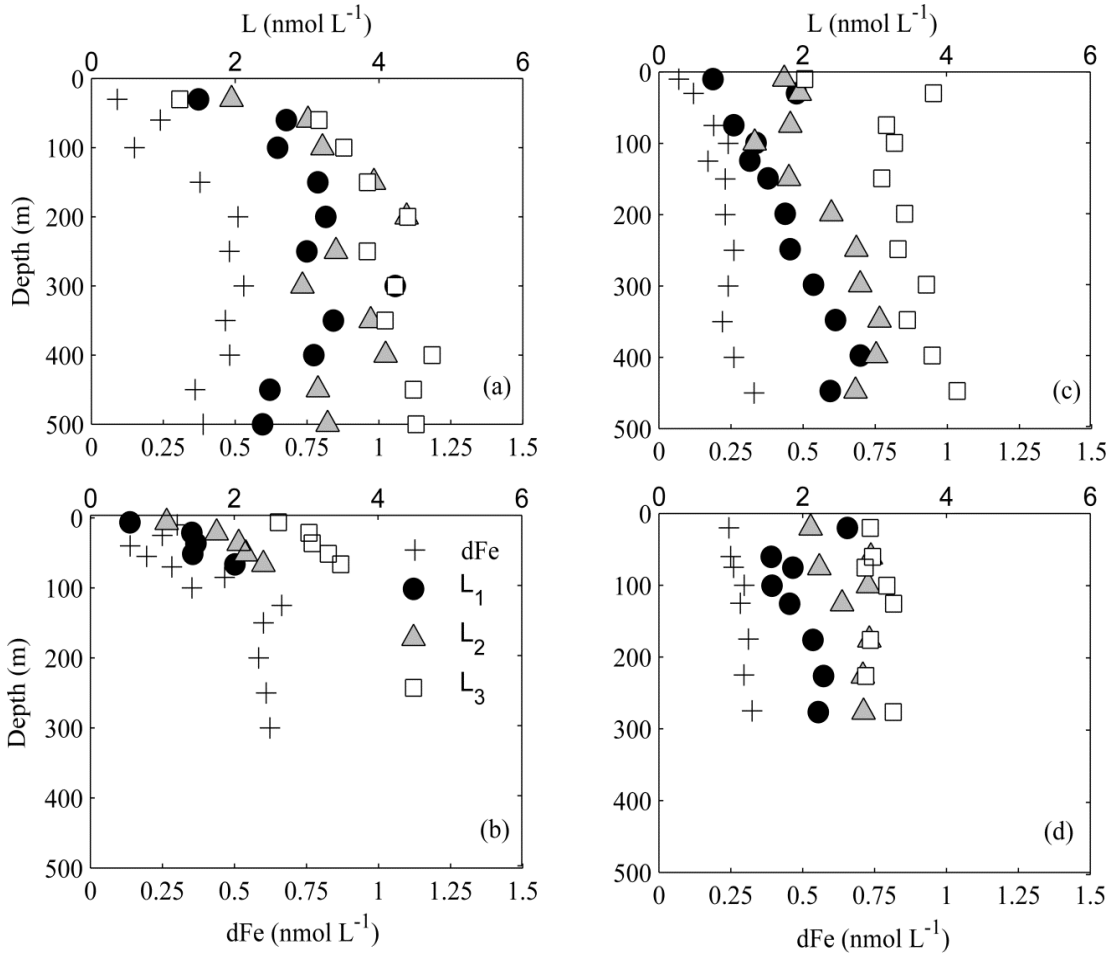

Figure 5.3 DFe (+) and ligand concentrations (L_1 black circles, L_2 grey triangles, L_3 white squares) for stations 1 (panel a), 2 (panel b), 4 (panel c), and 6 (panel d). Station classifications are the same as in figure 5.2.

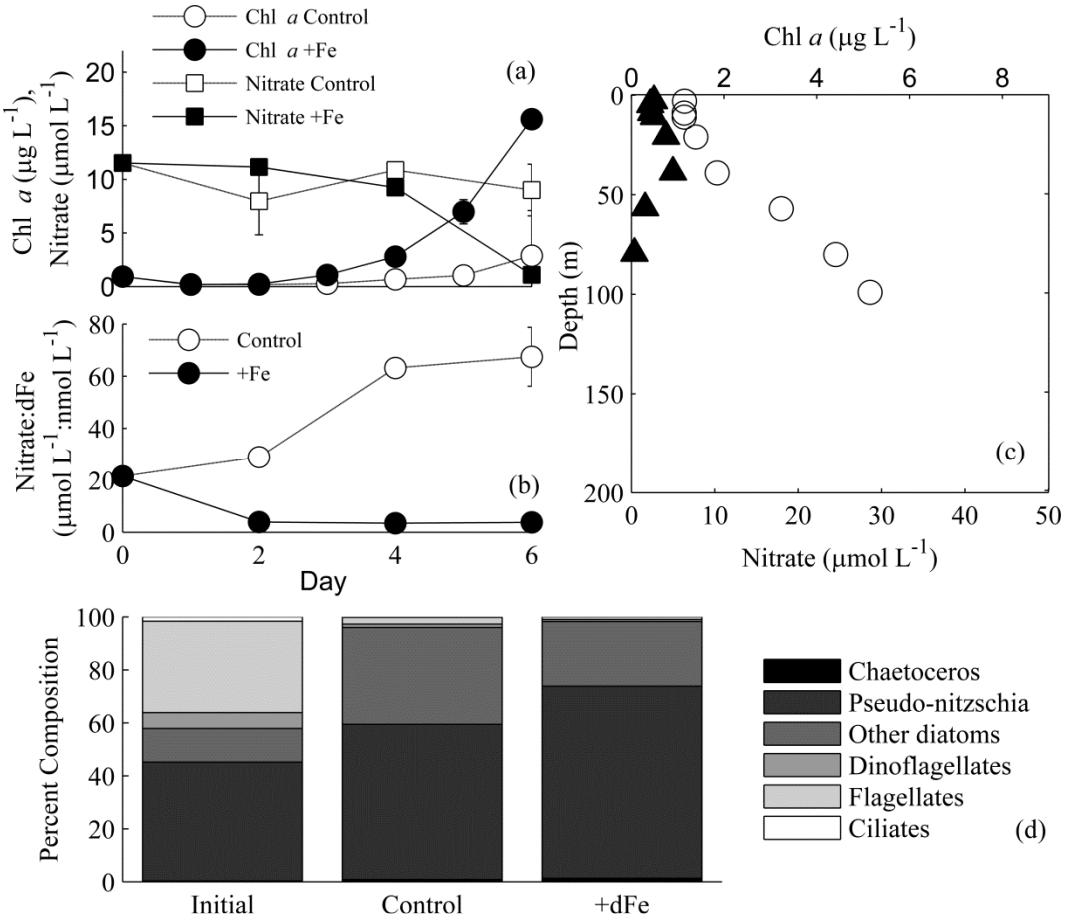

Figure 5.4 Incubation data from biological experiment 1 at station 3. Chlorophyll *a* (chl *a*) and nitrate (nitrate+nitrite) concentrations (a), nitrate:dFe ratios (b), chlorophyll *a* and nitrate distributions in the water column at station 3 (c), and phytoplankton cell counts for controls and +Fe treatments (d). Error bars in panels a, b, d represent the standard deviation from the averages of controls (A, B, C) and +Fe treatments (FeA, FeB, FeC) at each time-point.

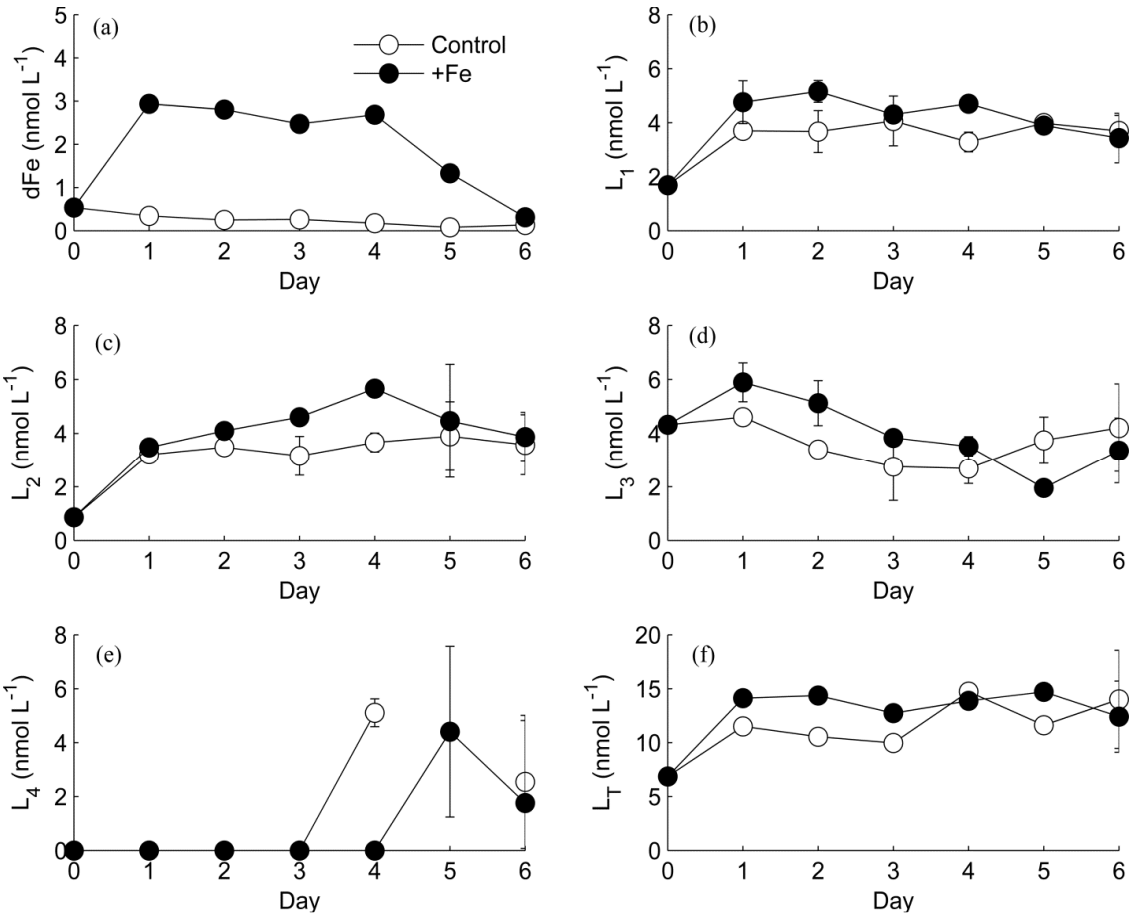

Figure 5.5 DFe (a) and ligand data (b-f) for biological incubation experiment 1 in controls (open circles) and +Fe (closed circles) treatments. Error bars represent the standard deviation between the two linearization techniques employed, except on day 6 when the bars represent the standard deviation from the averages of all control (A, B, C) and +Fe (FeA, FeB, FeC) treatments.

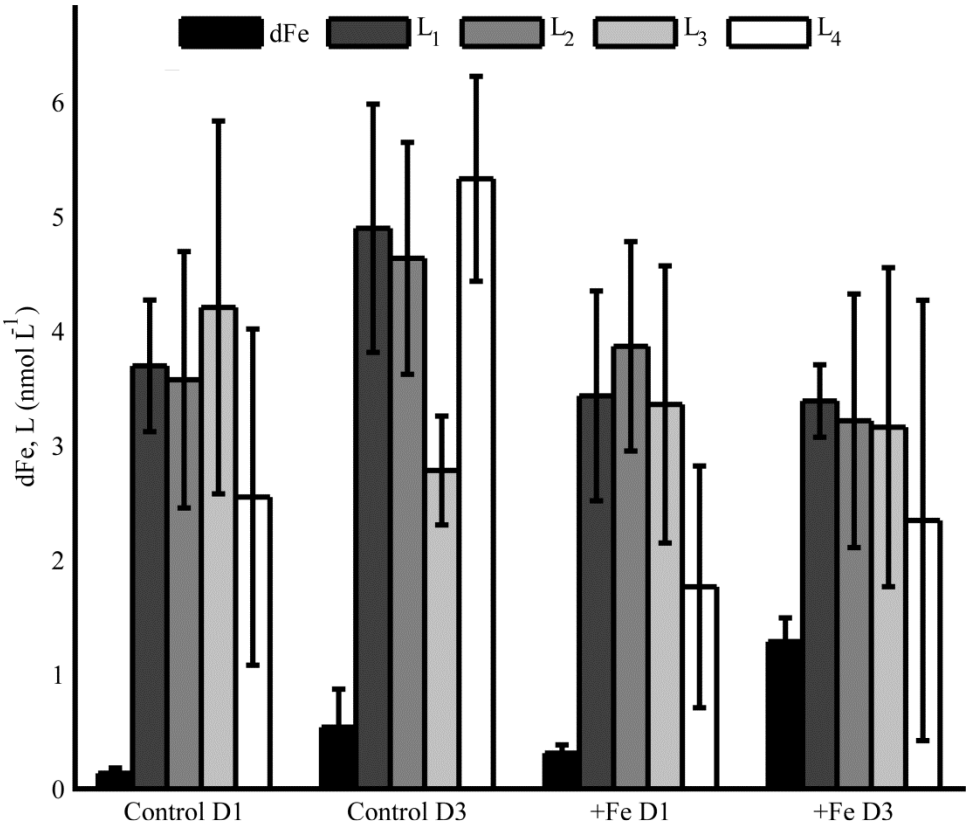

Figure 5.6 DFe (black bars), L_1 (dark grey bars), L_2 (grey bars), L_3 (light grey bars), and L_4 (white bars) ligand concentrations in biological experiment 2 in the dark in controls (left) and +Fe treatments (right) on day 1 (D1) and day 3 (D3). Error bars represent the standard deviation from replicate bottles for the control (A, B, C) and +Fe (FeA, FeB, FeC) treatments.

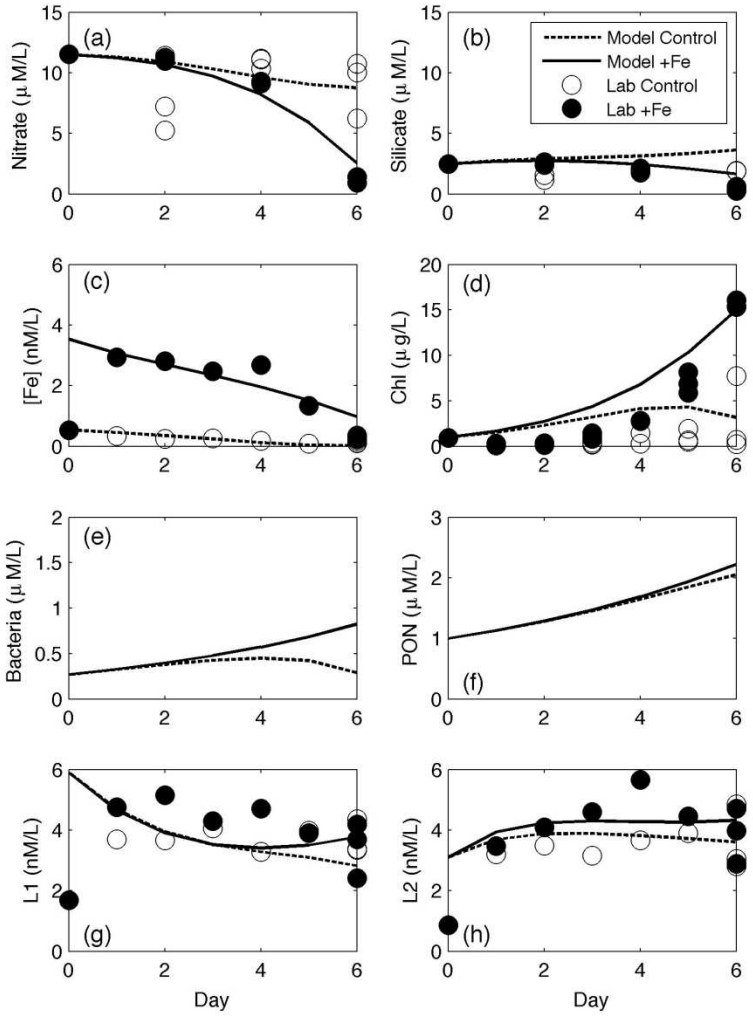

Figure 5.7 Numerical modeling results from biological experiment 1. Results for nitrate (A), silicate (B), [dFe] (C), chl *a* (D), bacteria abundance (E), PON (F), L_1 (G) and L_2 (H) are shown from the model of the controls (dashed line) and +Fe treatments (dark line), along with the data from controls (open circles) and +Fe treatments (closed circles).

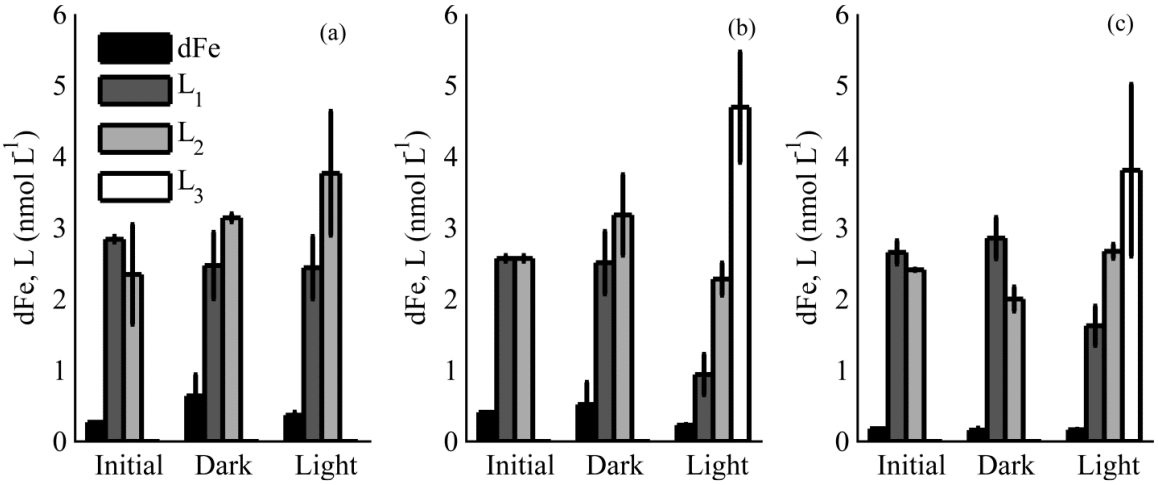

Figure 5.8 DFe (black bars) and ligand concentrations (L_1-L_3) for photochemical experiments 1 (a), 2 (b) and 3 (c) in the initial and final conditions after 12 hours (Dark and Light). Error bars represent the standard deviation between replicate bottles in dark (A, B) and light (A, B) bottles.

Table S5.1 All dFe, and ligand data from each profile sampled, including the station (Sta.), latitude (Lat.), and longitude (Lon.). The '+/-' indicates the standard deviation between replicates. 'Nd' denotes a sample where the ligand class was not determined.

Sta.	Lat. (N)	Lon (W)	Depth (m)	[dFe] nmol L^{-1}	+/-	L_1 nmol L^{-1}	+/-	$logK_1$	+/-	L_2 nmol L^{-1}	+/-	$logK_2$	+/-	L_3 nmol L^{-1}	+/-	$logK_3$	+/-
1	33.90	-121.42	30	0.09	0.01	1.49	0.04	12.42	0.13	1.95	0.11	11.72	0.15	1.23	0.00	10.17	0.01
1	33.90	-121.42	60	0.24	0.04	2.71	0.11	12.68	0.24	3.01	0.30	11.93	0.10	3.17	0.08	10.49	0.06
1	33.90	-121.42	100	0.15	0.01	2.59	0.08	11.93	0.08	3.21	0.04	11.95	0.33	3.51	0.17	10.33	0.07
1	33.90	-121.42	150	0.38	0.01	3.15	0.43	11.90	0.12	3.93	0.01	11.13	0.00	3.84	0.19	10.34	0.09
1	33.90	-121.42	200	0.51	0.03	3.26	0.01	11.93	0.00	4.38	1.04	11.72	0.13	4.40	0.05	10.49	0.01
1	33.90	-121.42	250	0.48	0.02	3.00	0.89	11.91	0.22	3.40	0.03	11.30	0.01	3.84	0.24	10.26	0.25
1	33.90	-121.42	300	0.53	0.06	4.23	0.02	12.08	0.01	2.94	0.53	11.48	0.01	4.23	0.02	10.91	0.27
1	33.90	-121.42	350	0.47	0.02	3.37	0.13	12.45	0.12	3.88	0.01	11.21	0.06	4.08	0.07	10.77	0.17
1	33.90	-121.42	400	0.48	0.01	3.09	0.11	11.98	0.27	4.09	0.11	11.98	0.17	4.74	0.10	10.65	0.03
1	33.90	-121.42	450	0.36	0.01	2.48	0.12	11.92	0.03	3.15	0.08	11.53	0.31	4.48	0.15	10.92	0.03
1	33.90	-121.42	500	0.39	0.00	2.38	0.08	12.11	0.04	3.28	0.03	11.55	0.01	4.52	0.06	10.59	0.13
2	33.41	-121.62	10	0.07	0.06	0.75	0.13	12.03	0.01	1.74	0.11	11.33	0.06	2.03	0.50	10.16	0.10
2	33.41	-121.62	30	0.12	0.02	1.91	0.19	12.46	0.50	1.96	0.87	11.49	0.12	3.82	0.38	10.25	0.22
2	33.41	-121.62	75	0.19	0.01	1.04	0.12	12.88	0.01	1.83	0.08	11.34	0.23	3.17	0.20	10.79	0.32
2	33.41	-121.62	100	0.24	0.02	1.35	0.01	12.84	0.02	1.33	0.02	11.46	0.08	3.28	0.02	10.23	0.08
2	33.41	-121.62	125	0.17	0.01	1.26	0.18	12.19	0.12	nd	nd	nd	nd	nd	nd	nd	nd
2	33.41	-121.62	150	0.23	0.05	1.52	0.07	12.93	0.24	1.81	0.38	11.50	0.06	3.10	0.14	11.09	0.04
2	33.41	-121.62	200	0.23	0.01	1.76	0.16	12.52	0.04	2.40	0.45	11.97	0.08	3.42	0.58	10.46	0.06
2	33.41	-121.62	250	0.26	0.05	1.82	0.22	12.17	0.15	2.75	0.35	11.86	0.05	3.33	0.06	10.12	0.01
2	33.41	-121.62	300	0.24	0.05	2.15	0.03	12.51	0.03	2.80	0.15	11.88	0.03	3.72	0.07	10.83	0.01
2	33.41	-121.62	350	0.22	0.01	2.46	0.18	13.14	0.09	3.07	0.07	11.71	0.01	3.46	0.18	10.94	0.09
2	33.41	-121.62	400	0.26	0.01	2.80	0.36	12.63	0.01	3.02	0.08	11.17	0.01	3.80	0.36	10.53	0.09
2	33.41	-121.62	450	0.33	0.03	2.38	0.06	12.46	1.14	2.73	0.14	11.79	0.11	4.15	0.27	10.96	0.03
4	33.38	-121.16	10	0.30	0.01	0.55	0.00	12.24	0.00	1.06	0.02	11.65	0.02	2.61	1.48	10.01	0.34
4	33.38	-121.16	25	0.25	0.01	1.41	0.20	13.18	0.28	1.76	2.68	11.51	0.32	3.04	3.15	10.89	0.07
4	33.38	-121.16	40	0.14	0.01	1.47	0.19	12.91	0.06	2.06	0.36	11.99	0.00	3.08	0.03	10.12	0.19
4	33.38	-121.16	55	0.20	0.00	1.42	0.02	12.48	0.00	2.16	0.37	11.75	0.10	3.31	0.47	11.08	0.10
4	33.38	-121.16	70	0.28	0.01	2.01	0.02	12.43	0.01	2.41	0.10	11.51	0.01	3.48	0.32	10.41	0.13
6	33.04	-121.26	20	0.24	0.00	2.62	0.03	12.17	0.03	2.11	0.09	11.96	0.00	2.94	0.51	10.63	0.22
6	33.04	-121.26	60	0.25	0.00	1.56	0.08	12.45	0.07	2.95	0.92	11.28	0.26	2.97	0.33	11.04	0.53
6	33.04	-121.26	75	0.26	0.00	1.86	0.14	12.79	0.13	2.23	0.14	11.82	0.11	2.87	0.91	10.22	0.05
6	33.04	-121.26	100	0.30	0.00	1.57	0.59	12.37	0.09	2.91	0.09	11.76	0.01	3.17	0.21	10.30	0.08
6	32.97	-121.27	125	0.28	0.00	1.82	0.06	13.10	0.06	2.55	0.03	11.19	0.13	3.26	0.03	11.09	0.13
6	32.97	-121.27	175	0.31	0.00	2.14	0.15	12.82	0.25	2.93	0.34	11.66	0.01	2.94	0.15	10.62	0.25
6	32.97	-121.27	225	0.30	0.00	2.29	0.01	12.44	0.00	2.84	0.26	11.35	0.13	2.88	0.36	10.26	0.22
6	32.97	-121.27	275	0.32	0.00	2.22	0.04	12.53	0.02	2.85	0.65	11.85	0.06	3.26	0.03	10.50	0.01

Table S5.2 Key variables in the principal components (PC) analysis performed with data from the incubation experiments and water column profiles. The percentage of the variance explained (% Explained) is shown for each PC, along with a description of the variables contributing significantly to that PC ($p < 0.05$). The variables used are: nitrate (NO_3^-), phosphate (PO_4^{3-}), silicate (Si), chlorophyll *a* (chl *a*), dissolved iron (dFe), ligands (L_1-L_4), fucoxanthin (fuc), 19'-hexanoyloxyfucoxanthin (19-hex), 19'-butanoyloxyfucoxanthin (19-but), chlorophyll *b* (chl *b*), divinyl chl *a* (dv chl *a*), zeaxanthin (zea), *Pseudo-nitzschia*, ciliates, other diatoms, particulate organic nitrogen (PON), particulate organic carbon (POC), surface photosynthetically available radiation (SPAR), transmission, fluorescence, temperature, salinity, pressure, oxygen, nitrate:dissolved iron (N:dFe), particulate carbon:particulate nitrogen (C:N) and longitude.

Data Type	PC	% Explained	+ Components	- Components
Incubation experiments	1	37.0	NO_3^-, PO_4^{3-}	chl *a*, all pigments and cell counts
	2	29.2	dFe, L_1, L_2, L_4, NO_3^-, PO_4^{3-}, 19-but, 19-hex, zea, chl b, ciliates	L_3, chl *a*, fuc, dv chl *a*, *Pseudo-nitzschia*, other diatoms
	3	10.9	L_1, L_4, flagellates	dFe, L_3, PO_4^{3-}, Si, chl *a*, 19-hex, chl *b*, dv chl *a*, cell counts
Water Column	1	53.7	pressure, salinity, transmission, all nutrients, N:dFe, all ligands	temperature, oxygen, fluorescence, PON, POC, chl *a*
	2	18.0	SPAR, transmission	longitude, salinity, fluorescence, PON, POC, dFe, L_3, chl *a*
	3	7.6	pressure, temperature, SPAR, fluorescence, PON, POC, N:dFe, chl *a*	longitude, transmission, C:N, L_1, L_2

8. References

Abdulla, H.A.N., Minor, E.C., Dias, R.F. and Hatcher, P.G., 2010. Changes in the compound classes of dissolved organic matter along an estuarine transect: A study using FTIR and C-13 NMR. Geochimica Et Cosmochimica Acta, 74(13).

Abualhaija, M.M. and van den Berg, C.M., 2014. Chemical speciation of iron in seawater using catalytic cathodic stripping voltammetry with ligand competition against salicylaldoxime. Marine Chemistry, 164: 60-74.

Amin, S.A., Green, D.H., Kupper, F.C. and Carrano, C.J., 2009. Vibrioferrin, an Unusual Marine Siderophore: Iron Binding, Photochemistry, and Biological Implications. Inorganic Chemistry, 48(23): 11451-11458.

Archer, D.E. and Johnson, K., 2000. A Model of the iron cycle in the ocean. Global Biogeochemical Cycles, 14(1): 269-279.

Arnosti, C., Repeta, D. and Blough, N., 1994. Rapid bacterial degradation of polysaccharides in anoxic marine systems. Geochimica et Cosmochimica Acta, 58(12): 2639-2652.

Barbeau, K., 2006. Photochemistry of organic iron(III) complexing ligands in oceanic systems. Photochemistry and Photobiology, 82(6): 1505-1516.

Barbeau, K., Moffett, J.W., Caron, D.A., Croot, P.L. and Erdner, D.L., 1996. Role of protozoan grazing in relieving iron limitation of phytoplankton. Nature, 380(6569): 61-64.

Barbeau, K., Rue, E.L., Bruland, K.W. and Butler, A., 2001. Photochemical cycling of iron in the surface ocean mediated by microbial iron(III)-binding ligands. Nature, 413(6854): 409-413.

Barbeau, K., Rue, E.L., Trick, C.G., Bruland, K.T. and Butler, A., 2003. Photochemical reactivity of siderophores produced by marine heterotrophic bacteria and cyanobacteria based on characteristic Fe(III) binding groups. Limnology and Oceanography, 48(3): 1069-1078.

Biller, D.V. and Bruland, K.W., 2014. The central California Current transition zone: A broad region exhibiting evidence for iron limitation. Progress in Oceanography, 120: 370-382.

Boyd, P.W., Ibisanmi, E., Sander, S.G., Hunter, K.A. and Jackson, G.A., 2010. Remineralization of upper ocean particles: Implications for iron biogeochemistry. Limnology and Oceanography, 55(3): 1271-1288.

Boye, M., Aldrich, A., van den Berg, C. M., de Jong, J., Nirmaier, H., Veldhuis, M., Timmermans, K.R. and de Baar, H. J. 2006. The chemical speciation of iron in the north-east Atlantic Ocean. Deep-Sea Research Part I-Oceanographic Research Papers, 53(4): 667-683.

Boye, M., Nishioka, J., Croot, P. L., Laan, P., Timmermans, K. R., and de Baar, H. J. 2005. Major deviations of iron complexation during 22 days of a mesoscale iron enrichment in the open Southern Ocean. Marine Chemistry, 96(3-4): 257-271.

Boye, M., van den Berg, C. M., de Jong, J., Leach, H., Croot, P., and de Baar, H. J., 2001. Organic complexation of iron in the Southern Ocean. Deep-Sea Research Part I-Oceanographic Research Papers, 48(6): 1477-1497.

Buck, K.N., Lohan, M.C., Berger, C.J.M. and Bruland, K.W., 2007. Dissolved iron speciation in two distinct river plumes and an estuary: Implications for riverine iron supply. Limnology and Oceanography, 52(2): 843-855.

Buck, K.N., Moffett, J., Barbeau, K. A., Bundy, R. M., Kondo, Y., and Wu, J., 2012. The organic complexation of iron and copper: an intercomparison of competitive ligand exchange-adsorptive cathodic stripping voltammetry (CLE-ACSV) techniques. Limnology and Oceanography-Methods, 10: 496-515.

Buck, K.N., Selph, K.E. and Barbeau, K.A., 2010. Iron-binding ligand production and copper speciation in an incubation experiment of Antarctic Peninsula shelf waters from the Bransfield Strait, Southern Ocean. Marine Chemistry, 122(1-4): 148-159.

Buck, K.N., Sohst, B. and Sedwick, P.N., In review. The organic complexation of dissolved iron along the U.S. GEOTRACES North Atlantic transect. Elsevier, Deep Sea Research II.

Bundy, R.M., Abdulla, H.A., Hatcher, P., Biller, D.V., Buck, K.N. and Barbeau, K.A., In review. Iron-binding ligands and humic substances in the San Francisco Bay estuary and estuarine-influenced shelf regions of coastal California. Elsevier, Marine Chemistry.

Bundy, R.M., Barbeau, K.A., Biller, D.V., Buck, K.N. and Bruland, K.W., 2014. Distinct pools of dissolved iron-binding ligands in the surface and benthic boundary layer of the California Current. Elsevier, Limnology and Oceanography, pp. 769-787.

Cabaj, A. and Kosakowska, A., 2009. Iron-dependent growth of and siderophore production by two heterotrophic bacteria isolated from brackish water of the southern Baltic Sea. Microbiological Research, 164(5): 570-577.

Croot, P.L., Andersson, K., Ozturk, M. and Turner, D.R., 2004a. The distribution and specification of iron along 6 degrees E in the Southern Ocean. Deep-Sea Research Part Ii-Topical Studies in Oceanography, 51(22-24): 2857-2879.

Croot, P.L., Streu, P. and Baker, A.R., 2004b. Short residence time for iron in surface seawater impacted by atmospheric dry deposition from Saharan dust events. Geophysical Research Letters, 31(23).

Cullen, J.T., Bergquist, B.A. and Moffett, J.W., 2006. Thermodynamic characterization of the partitioning of iron between soluble and colloidal species in the Atlantic Ocean. Marine Chemistry, 98(2-4): 295-303.

Cutter, G.A. and Bruland, K.W., 2012. Rapid and noncontaminating sampling system for trace elements in global ocean surveys. Limnology and Oceanography-Methods, 10: 425-436.

Ducklow, H.W., Kirchman, D.L., Quinby, H.L., Carlson, C.A. and Dam, H.G., 1993. Stocks and dynamics of bacterioplankton carbon during the spring bloom in the eastern North-Atlantic ocean. Deep-Sea Research Part Ii-Topical Studies in Oceanography, 40(1-2): 245-263.

Fan, S.M., 2008. Photochemical and biochemical controls on reactive oxygen and iron speciation in the pelagic surface ocean. Marine Chemistry, 109(1-2): 152-164.

Fuse, H., Takimura, O., Kamimura, K. and Yamaoka, Y., 1993. Marine algae excrete large molecular weight compounds keeping iron dissolved. Bioscience, biotechnology, and biochemistry, 57(3): 509-510.

Gerringa, L.J.A. et al., 2008. Fe-binding dissolved organic ligands near the Kerguelen Archipelago in the Southern Ocean (Indian sector). Deep-Sea Research Part Ii-Topical Studies in Oceanography, 55(5-7).

Gerringa, L.J.A., Veldhuis, M.J.W., Timmermans, K.R., Sarthou, G. and de Baar, H.J.W., 2006. Co-variance of dissolved Fe-binding ligands with phytoplankton characteristics in the Canary Basin. Marine Chemistry, 102(3-4): 276-290.

Gledhill, M. and Buck, K.N., 2012. The organic complexation of iron in the marine environment: a review. Frontiers in microbiology, 3: 69.

Gledhill, M., McCormack, P., Ussher, S., Achterberg, E. P., Mantoura, R. F. C., and Worsfold, P. J., 2004. Production of siderophore type chelates by mixed bacterioplankton populations in nutrient enriched seawater incubations. Marine Chemistry, 88(1-2): 75-83.

Gonzalez, A.G., Santana-Casiano, J.M., Gonzalez-Davila, M., Perez-Almeida, N. and de Tangil, M.S., 2014. Effect of *Dunaliella tertiolecta* Organic Exudates on the Fe(II) Oxidation Kinetics in Seawater. Environmental Science & Technology, 48(14): 7933-7941.

Granger, J. and Price, N.M., 1999. The importance of siderophores in iron nutrition of heterotrophic marine bacteria. Limnology and Oceanography, 44(3): 541-555.

Hassler, C.S., Alasonati, E., Nichols, C.A.M. and Slaveykova, V.I., 2011. Exopolysaccharides produced by bacteria isolated from the pelagic Southern Ocean - Role in Fe binding, chemical reactivity, and bioavailability. Marine Chemistry, 123(1-4): 88-98.

Haygood, M.G., Holt, P.D. and Butler, A., 1993. Aerobactin production by a planktonic marine *Vibrio sp*. Limnology and Oceanography, 38(5): 1091-1097.

Hider, R.C. and Kong, X., 2010. Chemistry and biology of siderophores. Natural Product Reports, 27(5): 637-657.

Hudson, R.J.M., Rue, E.L. and Bruland, K.W., 2003. Modeling complexometric titrations of natural water samples. Environmental Science & Technology, 37(8): 1553-1562.

Hunter, K.A. and Boyd, P.W., 2007. Iron-binding ligands and their role in the ocean biogeochemistry of iron. Environmental Chemistry, 4(4): 221-232.

Hutchins, D.A., DiTullio, G.R., Zhang, Y. and Bruland, K.W., 1998. An iron limitation mosaic in the California upwelling regime. Limnology and Oceanography, 43(6): 1037-1054.

Hutchins, D.A., Witter, A.E., Butler, A. and Luther, G.W., 1999. Competition among marine phytoplankton for different chelated iron species. Nature, 400(6747): 858-861.

Ibisanmi, E., Sander, S.G., Boyd, P.W., Bowie, A.R. and Hunter, K.A., 2011. Vertical distributions of iron-(III) complexing ligands in the Southern Ocean. Deep Sea Research Part II: Topical Studies in Oceanography, 58(21-22): 2113-2125.

Jiang, M., Barbeau, K. A., Selph, K. E., Measures, C. I., Buck, K. N., Azam, F., Mitchell, B.G. and Zhou, M., 2013. The role of organic ligands in iron cycling and primary productivity in the Antarctic Peninsula: A modeling study. Deep Sea Research Part II: Topical Studies in Oceanography, 90: 112-133.

King, A.L. and Barbeau, K., 2007. Evidence for phytoplankton iron limitation in the southern California Current System. Marine Ecology-Progress Series, 342: 91-103.

King, A.L. and Barbeau, K.A., 2011. Dissolved iron and macronutrient distributions in the southern California Current System. Journal of Geophysical Research-Oceans, 116: 18.

Kogut, M.B. and Voelker, B.M., 2001. Strong copper-binding behavior of terrestrial humic substances in seawater. Environmental Science & Technology, 35(6): 1149-1156.

Kondo, Y., Takeda, S., Nishioka, J., Obata, H., Furuya, K., Johnson, W. K., and Wong, C. S., 2008. Organic iron(III) complexing ligands during an iron enrichment experiment in the western subarctic North Pacific. Geophysical Research Letters, 35(12).

Laglera, L.M., Downes, J. and Santos-Echeandia, J., 2013. Comparison and combined use of linear and non-linear fitting for the estimation of complexing parameters from metal titrations of estuarine samples by CLE/AdCSV. Marine Chemistry, 155: 102-112.

Landry, M.R., Ohman, M.D., Goericke, R., Stukel, M.R. and Tsyrklevich, K., 2009. Lagrangian studies of phytoplankton growth and grazing relationships in a coastal upwelling ecosystem off Southern California. Progress in Oceanography, 83(1-4): 208-216.

Lee, S. and Fuhrman, J.A., 1987. Relationships between biovolume and biomass of naturally derived marine bacterioplankton. Applied and Environmental Microbiology, 53(6): 1298-1303.

Maldonado, M.T., Hughes, M.P., Rue, E.L. and Wells, M.L., 2002. The effect of Fe and Cu on growth and domoic acid production by *Pseudo-nitzschia multiseries* and *Pseudo-nitzschia australis*. Limnology and Oceanography, 47(2): 515-526.

Maldonado, M.T. and Price, N.M., 1999. Utilization of iron bound to strong organic ligands by plankton communities in the subarctic Pacific Ocean. Deep-Sea Research Part Ii-Topical Studies in Oceanography, 46(11-12): 2447-2473.

Martin, J.H., Gordon, R.M. and Fitzwater, S.E., 1991. The case for iron. Limnology and Oceanography, 36(8): 1793-1802.

Martinez, J.S., Carter-Franklin, J. N., Mann, E. L., Martin, J. D., Haygood, M. G., and Butler, A., 2003. Structure and membrane affinity of a suite of amphiphilic siderophores produced by a marine bacterium. Proceedings of the National Academy of Sciences of the United States of America, 100(7): 3754-3759.

Martinez, J.S., Haygood, M.G. and Butler, A., 2001. Identification of a natural desferrioxamine siderophore produced by a marine bacterium. Limnology and Oceanography, 46(2): 420-424.

Martinez, J.S., Zhang, G. P., Holt, P. D., Jung, H. T., Carrano, C. J., Haygood, M. G., and Butler, A., 2000. Self-assembling amphiphilic siderophores from marine bacteria. Science, 287(5456): 1245-1247.

Mawji, E., Gledhill, M., Milton, J. A., Tarran, G. A., Ussher, S., Thompson, A., Wolff, G.A., Worsfold, P.J., and Achterberg, E. P., 2008. Hydroxamate Siderophores: Occurrence and Importance in the Atlantic Ocean. Environmental Science & Technology, 42(23): 8675-8680.

Mawji, E., Gledhill, M., Milton, J. A., Zubkov, M. V., Thompson, A., Wolff, G. A., and Achterberg, E. P., 2011. Production of siderophore type chelates in Atlantic Ocean waters enriched with different carbon and nitrogen sources. Marine Chemistry, 124(1-4): 90-99.

Moore, J.K. and Braucher, O., 2008. Sedimentary and mineral dust sources of dissolved iron to the world ocean. Biogeosciences, 5(3): 631-656.

Moore, J.K., Doney, S.C. and Lindsay, K., 2004. Upper ocean ecosystem dynamics and iron cycling in a global three-dimensional model. Global Biogeochemical Cycles, 18(4).

Morel, F.M.M. and Price, N.M., 2003. The biogeochemical cycles of trace metals in the oceans. Science, 300(5621): 944-947.

Myklestad, S., Holm-Hansen, O., Vårum, K.M. and Volcani, B.E., 1989. Rate of release of extracellular amino acids and carbohydrates from the marine diatom Chaetoceros affinis. Journal of Plankton Research, 11(4): 763-773.

Parekh, P., Follows, M.J. and Boyle, E.A., 2005. Decoupling of iron and phosphate in the global ocean. Global Biogeochemical Cycles, 19(2).

Pižeta, I., Sander, S.G, Hudson¸ R.J.M., Baars, O., Buck, K.N., Bundy, R.M., Carrasco, G., Croot, P., Garnier, C., Gerringa, L.J.A., Gledhill, M., Hirose, K., Kondo, Y., Laglera, L.M., Nuester, J., Omanović, D., Rijkenberg, M.J.A., Takeda, S., Twining, B.S., Wells, M., 2014. Intercalibration exercise with simulated titration data as a first step to best practice guide. Elsevier, Marine Chemistry.

Powell, R.T. and Wilson-Finelli, A., 2003. Photochemical degradation of organic iron complexing ligands in seawater. Aquatic Sciences, 65(4): 367-374.

Reid, R.T., Live, D.H., Faulkner, D.J. and Butler, A., 1993. A siderophore from a marine bacterium with an exceptional ferric ion affinity constant. Nature, 366(6454): 455-458.

Repeta, D.J., Quan, T.M., Aluwihare, L.I. and Accardi, A., 2002. Chemical characterization of high molecular weight dissolved organic matter in fresh and marine waters. Geochimica et Cosmochimica Acta, 66(6): 955-962.

Rijkenberg, M.J.A. et al., 2008. Enhancement of the reactive iron pool by marine diatoms. Marine Chemistry, 109(1-2): 29-44.

Rijkenberg, M.J.A. et al., 2006. Iron-binding ligands in Dutch estuaries are not affected by UV induced photochemical degradation. Marine Chemistry, 100(1-2): 11-23.

Rue, E. and Bruland, K., 2001. Domoic acid binds iron and copper: a possible role for the toxin produced by the marine diatom Pseudo-nitzschia. Marine Chemistry, 76(1-2): 127-134.

Rue, E.L. and Bruland, K.W., 1995. Complexation of iron(III) by natural organic-ligands in the central North Pacific as determined by a new competitive ligand equilibration adsorptive cathodic stripping voltammetric method. Marine Chemistry, 50(1-4): 117-138.

Rue, E.L. and Bruland, K.W., 1997. The role of organic complexation on ambient iron chemistry in the equatorial Pacific Ocean and the response of a mesoscale iron addition experiment. Limnology and Oceanography, 42(5): 901-910.

Sander, S.G., 2014. Spatial and seasonal variations of iron speciation in surface waters of the Subantarctic front and the Otago Continental Shelf. In: F. Tian (Editor). Elsevier, Marine Chemistry.

Sander, S.G., Hunter, K.A., Harms, H. and Wells, M., 2011. Numerical Approach to Speciation and Estimation of Parameters Used in Modeling Trace Metal Bioavailability. Environmental Science & Technology, 45(15): 6388-6395.

Sato, M., Takeda, S. and Furuya, K., 2007. Iron regeneration and organic iron(III)-binding ligand production during in situ zooplankton grazing experiment. Marine Chemistry, 106: 471-488.

Soria-Dengg, S., Reissbrodt, R. and Horstmann, U., 2001. Siderophores in marine, coastal waters and their relevance for iron uptake by phytoplankton: experiments

with the diatom Phaeodactylum tricornutum. Marine Ecology Progress Series, 220: 73-82.

Tagliabue, A., Bopp, L., Aumont, O. and Arrigo, K.R., 2009. Influence of light and temperature on the marine iron cycle: From theoretical to global modeling. Global Biogeochemical Cycles, 23.

Tagliabue, A. and Volker, C., 2011. Towards accounting for dissolved iron speciation in global ocean models. Biogeosciences, 8(10): 3025-3039.

Thuróczy, C.E. et al., 2011a. Distinct trends in the speciation of iron between the shallow shelf seas and the deep basins of the Arctic Ocean. Journal of Geophysical Research-Oceans, 116.

Thuróczy, C.E., Gerringa, L.J.A., Klunder, M.B., Laan, P. and de Baar, H.J.W., 2011b. Observation of consistent trends in the organic complexation of dissolved iron in the Atlantic sector of the Southern Ocean. Deep-Sea Research Part Ii-Topical Studies in Oceanography, 58(25-26): 2695-2706.

Thuróczy, C.E., Gerringa, L. J. A., Klunder, M., Laan, P., Le Guitton, M., and de Baar, H. J. W., 2010. Speciation of Fe in the Eastern North Atlantic Ocean. Deep-Sea Research Part I-Oceanographic Research Papers, 57(11).

Trick, C., Andersen, R., Price, N., Gillam, A. and Harrison, P., 1983a. Examination of hydroxamate-siderophore production by neritic eukaryotic marine phytoplankton. Marine biology, 75(1): 9-17.

Trick, C., Andersen, R., Price, N., Gillam, A. and Harrison, P., 1983b. Examination of hydroxamate-siderophore production by neritic eukaryotic marine phytoplankton. Marine biology, 75(1): 9-17.

Trick, C.G., 1989. Hydroxamate-siderophore production and utilization by marine eubacteria. Current Microbiology, 18(6): 375-378.

Trick, C.G. and Kerry, A., 1992. Isolation and purification of siderophores produced by cyanobacteria, *Synechococcus sp* PCC-7942 and *Anabaena-Variabilis* ATCC-29413. Current Microbiology, 24(5): 241-245.

UNESCO, 1981. Background papers and supporting data on the Practical Salinity Scale 1978. UNESCO Technical Papers in Marine Science: 37.

Urbani, R., Magaletti, E., Sist, P. and Cicero, A.M., 2005. Extracellular carbohydrates released by the marine diatoms *Cylindrotheca closterium*, *Thalassiosira pseudonana* and *Skeletonema costatum*: Effect of P-depletion and growth status. Science of the Total Environment, 353(1): 300-306.

Utermöhl, H., 1958. Zur Vervollkommnung der quantitativen Phytoplankton-Methodik. Mitteilungen Internationale Vereinigung fuer Theoretische und Angewandte Limnologie 9, 1–38.

van den Berg, C.M.G., 1995. Evidence for organic complexation of iron in seawater. Marine Chemistry, 50(1-4): 139-157.

van den Berg, C.M.G., 2006. Chemical speciation of iron in seawater by cathodic stripping voltammetry with dihydroxynaphthalene. Analytical Chemistry, 78(1): 156-163.

Vraspir, J.M. and Butler, A., 2009. Chemistry of Marine Ligands and Siderophores. Annual Review of Marine Science, 1: 43-63.

Wagener, T., Pulido-Villena, E. and Guieu, C., 2008. Dust iron dissolution in seawater: Results from a one-year time-series in the Mediterranean Sea. Geophysical Research Letters, 35(16).

Watt, W., 1969. Extracellular release of organic matter from two freshwater diatoms. Annals of Botany, 33(3): 427-437.

Wilhelm, S.W. and Trick, C.G., 1994. Iron-limited growth of cyanobacteria - multiple siderophore production is a common response. Limnology and Oceanography, 39(8): 1979-1984.

Wu, J.F. and Luther, G.W., 1995. Complexation of Fe(III) by natural organic-ligands in the northwest Atlantic-ocean by a competitive ligand equilibration method and a kinetic approach. Marine Chemistry, 50(1-4): 159-177.

Zapata, M., Rodriguez, F. and Garrido, J.L., 2000. Separation of chlorophylls and carotenoids from marine phytoplankton: a new HPLC method using a reversed phase C-8 column and pyridine-containing mobile phases. Marine Ecology-Progress Series, 195: 29-45.

Zweifel, U.L., Norrman, B. and Hagstrom, A., 1993. Consumption of dissolved organic carbon by marine bacteria and demand for inorganic nutrients. Marine Ecology-Progress Series, 101: 23-23.

Chapter 6

Conclusion

1. Introduction

Copper (Cu) and iron (Fe) are important trace nutrients in the ocean, and are needed by phytoplankton and bacteria for basic cellular functions. The dissolved forms of Cu and Fe are predominantly associated with organic ligands in seawater, of various strengths and reactivities. Although the distributions of dissolved Cu and Fe have been studied in several ocean basins, comparatively little data exists for metal-binding ligands. Elucidating the sources and sinks of organic metal-binding ligands in the marine environment however, is important for understanding how these metals cycle in the ocean, and how they interact with the carbon cycle. This is especially pertinent for Fe, where ligand concentrations can significantly affect the overall biologically available Fe inventory and thus, the draw-down of carbon dioxide from the atmosphere via photosynthesis (Tagliabue et al., 2014). Recent global biogeochemical modeling efforts have incorporated Fe-binding ligands, but the sources and sinks of these ligands are understudied compared to metal distributions.

Previous work on metal-binding ligands in seawater has been largely limited to the electrochemical detection of two operationally defined ligand classes, which span several orders of magnitude in ligand strength. This thesis modified existing electrochemical methods in order to enable the detection of several classes of Cu and Fe-binding ligands. The expansion of this method is termed multiple analytical window (MAW) analysis, and allows for the simultaneous detection of both strong and weak ligands on the same sample. Recent advances in the organic metal-binding ligand field have shown that both strong and weak ligands are important for metal bioavailability and cycling in seawater (Hassler et al., 2011). MAW analysis can therefore permit valuable

insights to be gained about metal speciation in the marine environment, by expanding the range of ligands that can be perceived. MAW analysis had only previously been used for Cu-ligand analyses in near-shore high-Cu environments, where a large range of Cu-binding ligands was hypothesized to exist and play an important role in buffering Cu toxicity (Buck and Bruland, 2005; Moffett et al., 1997). It was previously unknown whether a similar range of Cu-binding ligands might exist in the open ocean, and no studies had examined the potential range of Fe-binding ligands that might exist in the marine environment. In this work MAW analysis was applied to studying Cu-binding ligands in an open ocean setting, and was utilized to study Fe-binding ligand distributions for the first time. This thesis added significant contributions to the body of current knowledge about metal-binding ligands in marine systems, and paves the way for future work on ligand sources and sinks.

Chapter 2 expanded upon the use of the MAW electrochemical method to open ocean environments in order to detect a broader spectrum of Cu-binding ligands. A relatively large range of binding strengths were found to exist in waters surrounding the Antarctic Peninsula, and there were distinct ligand classes in the four different water masses sampled. Most interestingly, strong Cu-binding ligands were detected in the Fe-limited waters of the Antarctic Circumpolar Current (ACC), despite low Cu concentrations and low biological activity during the winter sampling time. This was some of the first evidence to suggest there may be other sources of Cu-binding ligands besides active production from bacteria such as *Synechococcus* under Cu-stress conditions. The strong complexation of Cu in this area of the Southern Ocean has

significant implications for some diatoms in the region, as Cu^{2+} levels in this study were approaching concentrations that are limiting for some types of inducible Fe acquisition.

Chapters 3, 4 and 5 expanded MAW analysis to studying Fe-binding ligands in the California Current. Previous hypotheses suggested that only a small range of Fe-binding ligands should exist in seawater, due to the high inorganic side reaction coefficient of Fe. Compared to previous work which only defined an L_1 and L_2 ligand class, this work expanded the detection of electrochemical methods to four ligand classes whose strengths spanned several orders of magnitude. The method was first verified in Chapter 3 in surface and benthic boundary layer waters off central California, which were hypothesized to contain potential endmembers of Fe-binding ligand strengths. Significantly different ligand pools were detected in surface versus benthic boundary layer waters, verifying the method and suggesting different sources and sinks of the ligand pools. Principle component analysis revealed that in fact, variances in the ligand pool in surface waters were predominantly explained by water mass type and variances in the benthic boundary layer pool were mostly explained by the shelf sediment type or the location on the continental shelf. Additional analyses showed that some portion of the ligand pool in the benthic boundary layer was humic substances, hypothesized to originate from San Francisco Bay or other freshwater sources along the coastline.

Chapter 4 extended these analyses to San Francisco Bay to test the hypothesis that estuarine environments are ligand sources to freshwater-influenced shelf regions of the California Current. MAW electrochemical analysis coupled to proton-nuclear magnetic resonance analyses revealed that the ligand pools in the benthic boundary layer outside of estuarine-influenced environments contained similar ligands to those in San Francisco

Bay. In addition, these new electrochemical analyses revealed a mechanism for how some Fe from estuaries survives flocculation in the low salinity end of the estuary. Strong Fe-ligand complexes were found to be the most resistant to flocculation, and the weaker ligand complexes, comprised at least in part by humics, were scavenged at low salinities. This flocculated material is likely deposited on the continental shelf and serves as an important Fe source during spring upwelling events in the region.

Chapter 5 explores Fe-binding ligands in the water column offshore in the southern California Bight, across a frontal feature with a gradient in biological activity. Three of the four ligand classes detected in earlier chapters were found to be present at all sampling depths, with the exception of the weakest ligand class which had only been detected in nearshore environments in Chapters 3 and 4. Mechanistic incubation studies in this chapter revealed that photochemistry is an important process altering the ligand pool in surface waters, but not all natural ligands were photochemically reactive. An Fe-addition grow-out experiment which simulated the growth and decline of a phytoplankton bloom also implicated bacteria as a potential source of ligands, as well as remineralization processes which produced both strong and weak Fe-binding ligands. Overall, several sources and sinks govern the distributions of strong and weak Fe-binding ligands in the California Current.

This study utilized the simultaneous electrochemical detection of stronger and weaker ligands for the first time for Fe speciation, and extended the regions where this method had been applied for Cu speciation studies. Only a few profiles were examined in this study, but future work could provide important insight into the distributions of Fe and Cu ligands in different regions of the oceans, such as suboxic zones or hydrothermal

plumes. Although it is difficult to use MAW analysis on large sample sets due the time intensive nature of the analyses, new data processing tools are beginning to minimize processing time which may facilitate broader application of these methods. Several new numerical methods are currently in development, which would allow the analyst to evaluate the MAW data as a unified dataset, with little to no user input (Hudson et al., 2003; Pižeta et al., in review; Sander et al., 2011). This would significantly lower the time investment needed to process the titration data from MAW analyses, and could allow this method to be applied on a much larger scale such as the international GEOTRACES program. Additional technological advancements such as auto-samplers for metal-binding ligand analyses, would also help to increase sample throughput. These processing methods have so far only been tested for Cu-binding ligand analyses, and have yet to be extended to Fe-binding ligands. The application of MAW analysis on a broad scale would enable a deeper understanding of the processes governing Cu and Fe cycling, and could eventually inform modelers about mechanistic sources and sinks of ligands. Overall, this work significantly increases the number and quality of metal-binding ligand measurements we have in the ocean, and paves the way for future studies to look more closely at the range of ligands that exist in seawater.

2. References

Buck, K.N. and Bruland, K.W., 2005. Copper speciation in San Francisco Bay: A novel approach using multiple analytical windows. Marine Chemistry, 96(1-2): 185-198.

Hassler, C.S., Schoemann, V., Nichols, C.M., Butler, E.C.V. and Boyd, P.W., 2011. Saccharides enhance iron bioavailability to Southern Ocean phytoplankton.

Proceedings of the National Academy of Sciences of the United States of America, 108(3): 1076-1081.

Hudson, R.J.M., Rue, E.L. and Bruland, K.W., 2003. Modeling complexometric titrations of natural water samples. Environmental Science & Technology, 37(8): 1553-1562.

Moffett, J.W., Brand, L.E., Croot, P.L. and Barbeau, K.A., 1997. Cu speciation and cyanobacterial distribution in harbors subject to anthropogenic Cu inputs. Limnology and Oceanography, 42(5): 789-799.

Pižeta, I., Sander, S.G, Hudson, R.J.M., Baars, O., Buck, K.N., Bundy, R.M., Carrasco, G., Croot, P., Garnier, C., Gerringa, L.J.A., Gledhill, M., Hirose, K., Kondo, Y., Laglera, L.M., Nuester, J., Omanović, D., Rijkenberg, M.J.A., Takeda, S., Twining, B.S., Wells, M, Accepted. Intercalibration exercise with simulated titration data as a first step to best practice guide. Elsevier, Marine Chemistry.

Sander, S.G., Hunter, K.A., Harms, H. and Wells, M., 2011. Numerical Approach to Speciation and Estimation of Parameters Used in Modeling Trace Metal Bioavailability. Environmental Science & Technology, 45(15): 6388-6395.

Tagliabue, A., Aumont, O. and Bopp, L., 2014. The impact of different external sources of iron on the global carbon cycle. Geophysical Research Letters, 41(3): 920-926.